



# THE UNIVERSITY *of* EDINBURGH

This thesis has been submitted in fulfilment of the requirements for a postgraduate degree (e.g. PhD, MPhil, DClinPsychol) at the University of Edinburgh. Please note the following terms and conditions of use:

This work is protected by copyright and other intellectual property rights, which are retained by the thesis author, unless otherwise stated.

A copy can be downloaded for personal non-commercial research or study, without prior permission or charge.

This thesis cannot be reproduced or quoted extensively from without first obtaining permission in writing from the author.

The content must not be changed in any way or sold commercially in any format or medium without the formal permission of the author.

When referring to this work, full bibliographic details including the author, title, awarding institution and date of the thesis must be given.

**Immune evasion genes from *Brugia malayi* -  
Functional analyses of *Bm*-SPN-2, the major secreted  
microfilarial product.**



Xuhang Wu

Thesis submitted for the degree of Doctor of Philosophy

The University of Edinburgh

2017



## Abstract

Many parasites have evolved to release products that inhibit host defence mechanisms such as enzymes in the mammalian host, in order to promote and sustain their survival within the host. The human filarial nematode *Brugia malayi* produces larval microfilariae, which circulate in the blood stream. Their most abundant secreted product is a serine protease inhibitor *Bm*-SPN-2. Serine protease inhibitors (Serpins) are reported to be involved in how the nematodes avoid host immune defences, and in the case of *Bm*-SPN-2, the protein was found to specifically inhibit the enzymatic activity of human neutrophil elastase and cathepsin G in a dose-dependent manner. More recently, these two enzymes have been linked to the activation of a major innate cytokine IL-33, which is stored as a full-length 270-aa protein in the cell nucleus, and released as an active C-terminal domain upon stimulation.

As full-length (FL) human and murine IL-33 are not commercially available, soluble murine and human FL-IL-33 were produced in transfected HEK 293T cells, following mutation of the nuclear binding motif. In this form, IL-33 is no longer retained in the nucleus and can be purified as a soluble protein. It was confirmed that once cleaved, recombinant human IL-33 was able to induce significant IL-6 secretion by mast cells. *Bm*-SPN-2 was then shown to block human full-length IL-33 cleavage by inhibiting human neutrophil cathepsin G in a dose dependent manner, supporting the hypothesis that *Bm*-SPN-2 may act *in vivo* to prevent IL-33 activation and the promotion of the TH2 immune response. However, in the *in vivo* setting, it was unexpectedly found that IL-33R (ST2) gene deficiency did not enhance the survival of *B. pahangi* microfilariae. Furthermore, in the absence of IL-33R, murine immune responses to microfilariae were not significantly altered compared to wild-type BALB/c mice, other than in a significant increase in IL-33 expression. Hence while *Bm*-SPN-2 can act *in vitro* to forestall one of the key events in TH2 induction, this has not yet been shown to be crucial to the immune response to the parasite *in vivo*.



## Lay Summary

Many parasites have evolved to release products that inhibit host defence mechanisms in order to promote and sustain their survival within the host. The human filarial nematode *Brugia malayi* produces larval microfilariae, which circulate in the blood stream. Their most abundant secreted product is a serine protease inhibitor *Bm*-SPN-2. *Bm*-SPN-2 was found to inhibit two host enzymes which have recently been linked to the activation of a key host defence system (IL-33) to eliminate the parasite. To study this system, I first produced the individual parasite and host proteins *Bm*-SPN-2 and IL-33. I then verified that recombinant *Bm*-SPN-2 inhibited these two host enzymes. Finally, I investigated whether this inhibitory function is crucial to parasites avoiding host defences by conducting experimental infection with *B. pahangi* *in vivo*.



## Declaration

I declare that this thesis has been composed by myself, describes my own work and that the work has not been submitted towards any other degree.

The experiments of *Alternaria* allergen challenge and design of human and murine mutant FL-IL-33 have been carried out in collaboration with Dr. Henry McSorley. The experiments of human and murine IL-33 cleavage have been carried out in collaboration with Dr. Jean-Philippe Girard and Dr. Corinne Cayrol, the materials were provided by them and the experiments were performed by myself. The experiment of *Brugia pahangi* microfilariae infection of IL-33R deficient mice has been carried out in collaboration with Professor Eileen Devaney and Kerry O' Neill. The microfilariae were provided by them and the infection experiment was performed by myself with the help of Danielle Smyth and Gillian Coakley.

Selected figures from reviews published by other researchers have been used where appropriate; the authors and source are indicated in each case.

Xuhang Wu

August 2017



## Acknowledgements

It has been a great four years for my PhD study, including three years in Edinburgh and a final year in Glasgow, both amazing cities in Scotland in which I have enjoyed study and life. I do feel sad to leave when it comes to an end.

As an international student, and my first abroad study, it was so difficult that both living and studying at the beginning. However, many people have contributed to making sure of that:

First of all: Rick – thank you so much for being the best supervisor I could have wished for, helping me to get here in the first place and then giving me lots of suggestions to develop my project while always encouraging me during my whole PhD, as well as great advice and guidance, sending me to great conferences (Paris and Hydra!), and giving me the freedom to travel to European countries, which I felt meaningful! And finally, thank you so much for support my living cost in the last year in Glasgow, well, have to say that it was a magic coincidence that my husband found a postgraduate study in the University of Strathclyde, like fate! And being so patient revising my chinglish of thesis writing, making sure I could finish my PhD without (too much) panic.

Then the whole rest of lab in Edinburgh- Lab-mama Yvonne, who has saved me countless of times during experiment, teaching me new English word every day and being the one I could talk to; Stephanie, who has saved me when I first started my experiment, guiding me step by step for protein expression; Danielle and Henry, who've helped me with quite a few experiments, especially *Brugia pahangi* microfilariae infection and *Alternaria* administration experiment, respectively, as well as advices and suggestions for solving experimental problems; My office desk and lab-bench neighbour Andrea, who giving me advices on each period of PhD, and Gillian, who helped me to get the mLN in infection experiment, both of you were great conference mates! Natalie, who guided to western blotting; As well as Janice, Kara, James, Elaine, Chris, Simone and David Dresser – all of you taught me so much, be it methods or discussing science, and have made the lab a great place to work in!

My second supervisor Dietmar Zaiss, who has been taking care of me at the last year after Rick moved to Glasgow, and also giving me lots of advice and suggestions. And my postgraduate committee member Joanne Thompson, who giving me advices of planning out the schedule and arranging meeting with supervisors.

In general, the people in Ashworth Labs, I really enjoyed the very collegial atmosphere; special mention here to has to go to a few people who helped me immeasurably, like Amy Buck's lab, Marissa Lear and Jana McCaskill, who helped me to use the Vario Skan machine, the Allen, Taylor and Zaiss labs especially, sharing labs and offices with us, and especially Sharon, Johanna and Carlos for many chats and discussions.

The whole rest of the lab in the last year in Glasgow, Fumi and Stephan, who helped me with the RT-PCR experiment; Maddie, who helped me with FACS trial; Claire, who helped me for mCherry synthesis; Nicola, who always helped me to purchase any reagent; As well as few exchange students Dennis, Ian, Dominik, who helped me to give some suggestions for problem solving.

The collaborators: Jean-Philippe Girard and Corinne Cayrol in France, who have sent the IL-33 RRL samples and mast cell line, which helped making sure the research keeping on going; Professor Eileen Devaney's and Kerry O' Neill, for kindly providing us the *B. pahangi* microfilariae and adult worms; and Dr. Henry McSorley, for providing us the IL-33R deficient mice, together for in vivo infection experiment.

The China scholarship council, who have supported my first three years of living cost; and the University of Edinburgh, who gave me a tuition fee waiver during my PhD.

And finally: my friends and family. There's way too much to write it all, so just: THANK YOU! One thing to mention here though: thank you, Andrea, for giving me your PhD thesis as a template, it probably saved me hours of trying to get the layout right! And my parents, who were always encouraging me even we were thousand miles away; and my husband, who resigned his job to accompany with me during my last two years studying.

## Table of Contents

<b>CHAPTER1</b> .....	<b>1</b>
<b>Introduction</b> .....	<b>1</b>
<b>1.1 Human helminths and filariasis</b> .....	<b>1</b>
1.1.1 Helminths and burden of helminthiases .....	1
1.1.2 Lymphatic filariasis.....	5
<b>1.2 Immune regulation by helminth parasites</b> .....	<b>10</b>
1.2.1 Regulatory T cells in filarial infection.....	11
1.2.2 Immune evolution of helminths parasites.....	13
<b>1.3 Immune evasion genes in filarial nematodes</b> .....	<b>17</b>
1.3.1 Adult surface-associated proteins .....	18
1.3.2 Adult Excretory-Secretory Proteins .....	19
1.3.3 Microfilariae Excretory-Secretory Protein.....	21
<b>1.4 Type 2 immunity and IL-33</b> .....	<b>23</b>
1.4.1 Helminths induce TH2 responses .....	23
1.4.2 IL-33 Initiates Type 2 Immune Responses.....	27
1.4.3 IL-33 .....	29
1.4.4 IL-33 Mature process by proteases.....	29
1.4.5 IL-33/ST2 signaling .....	31
1.4.6 IL-33 and helminth infection .....	32
<b>1.5 Hypotheses and aim of this thesis</b> .....	<b>34</b>
<b>CHAPTER2</b> .....	<b>37</b>
<b>Materials and Methods</b> .....	<b>37</b>
<b>2.1 Cell culture</b> .....	<b>37</b>
<b>2.2 Parasites and Experimental Animals</b> .....	<b>38</b>
2.2.1 Parasites .....	38
2.2.2 Experimental Animals .....	38
<b>2.3 In vivo procedures</b> .....	<b>39</b>
2.3.1 <i>Alternaria</i> Airway allergy model.....	39
2.3.2 Microfilariae infection experiment.....	39

2.3.3 Polyclonal and monoclonal antibody production against <i>Bm</i> -SPN-2	40
<b>2.4 Gene cloning and recombinant protein expression</b>	<b>42</b>
2.4.1 Bacteria expression	42
2.4.2 Mammalian gene expression system	44
2.4.3 Protein concentration measurement	46
<b>2.5 Western blotting</b>	<b>47</b>
2.5.1 Anti-His western blotting	47
2.5.2 Anti- <i>Bm</i> -SPN-2 western blotting	47
2.5.3 Anti-IL-33 western blotting	48
<b>2.6 IL-33 cleavage experiment</b>	<b>48</b>
<b>2.7 Enzyme activity assays</b>	<b>50</b>
<b>2.8 Enzyme-linked immunosorbent assay (ELISA)</b>	<b>50</b>
<b>2.9 Gene expression analysis</b>	<b>51</b>
2.9.1 RNA extraction	51
2.9.2 cDNA preparation	52
2.9.3 Real time PCR	52
<b>2.10 Parasite extract preparation</b>	<b>53</b>
<b>2.11 Accession numbers</b>	<b>54</b>
<b>2.13 Media and buffers</b>	<b>54</b>
<b>CHAPTER3</b>	<b>57</b>
<b>Human and murine IL-33: preparation mutation and testing on mast cells</b>	<b>57</b>
<b>3.1 Introduction</b>	<b>58</b>
<b>3.2 Results</b>	<b>61</b>
3.2.1 Preparation of human wild type full-length IL-33	61
3.2.2 Retention of WT IL-33 within HEK cells	67
3.2.3 Producing mutant human and murine FL-IL-33	67
3.2.4 Stimulation of mast cells with human and murine full length and cleaved IL-33	76
<b>3.3 Discussion</b>	<b>78</b>

<b>CHAPTER4</b> .....	<b>83</b>
<b>Functional analysis of <i>Bm</i>-SPN-2, <i>Brugia malayi</i> microfilariae major secreted product</b> .....	<b>83</b>
<b>4.1 Introduction</b> .....	<b>85</b>
4.1.1 Serine protease inhibitors .....	85
4.1.2 <i>Bm</i> -SPN-2 discovery and disputed functions .....	86
<b>4.2 Results</b> .....	<b>90</b>
4.2.1 <i>Bm</i> -SPN-2 expression and purification .....	90
4.2.2 Full-length IL-33 cleavage by neutrophil cathepsin G and elastase .....	93
4.2.3 Investigating the effects of <i>Bm</i> -SPN-2 on IL-33 cleavage.....	97
4.2.4 Production of mCherry-labelled <i>Bm</i> -SPN-2 .....	104
<b>4.3 Discussion</b> .....	<b>113</b>
<b>CHAPTER5</b> .....	<b>119</b>
<b><i>In vivo</i> studies of the roles of IL-33 and <i>Bm</i>-SPN-2 in responses to microfilariae and allergen challenge</b> .....	<b>119</b>
<b>5.1 Introduction</b> .....	<b>121</b>
<b>5.2 Results</b> .....	<b>124</b>
5.2.1 Making polyclonal and monoclonal antibody against <i>Bm</i> -SPN-2	124
5.2.2 <i>Alternaria/Bm</i> -SPN-2 intranasal <i>in vivo</i> experiment .....	131
5.2.3 <i>Brugia pahangi</i> microfilariae infect IL-33R <sup>-/-</sup> mice .....	133
<b>5.3 Discussion</b> .....	<b>143</b>
<b>CHAPTER6</b> .....	<b>147</b>
<b>Final Discussion</b> .....	<b>147</b>
<b>6.1 <i>In vitro</i> study</b> .....	<b>148</b>
<b>6.2 <i>In vivo</i> study</b> .....	<b>150</b>
<b>6.3 Future work</b> .....	<b>151</b>
<b>References</b> .....	<b>153</b>
<b>Appendices</b> .....	<b>177</b>
<b>1. Human and murine mutant IL-33 gene synthesis</b> .....	<b>177</b>

1.1 Human mutant IL-33 .....	177
1.2 Murine mutant IL-33 .....	181
<b>2. Sequencing result of human and murine mutant FL-IL-33 .....</b>	<b>185</b>
<b>3. Sequencing result of Mini prep product of Bm-SPN-2 .....</b>	<b>187</b>
<b>4.1 Gene synthesis for mCherry .....</b>	<b>190</b>
<b>4.2 Gene synthesis for Bm-SPN-2-mCherry .....</b>	<b>193</b>
<b>4.3 Sequencing result of Mini prep product F of Bm-SPN-2-mCherry .....</b>	<b>200</b>
<b>5.1 Result of ELISA screening for selecting Bm-SPN-2 monoclonal antibody .....</b>	<b>207</b>
<b>5.2 Monoclonal antibody candidate purification trace.....</b>	<b>210</b>

# CHAPTER 1

## Introduction

### 1.1 Human helminths and filariasis

#### 1.1.1 Helminths and burden of helminthiases

Helminths are invertebrate worms that are divided into the two major phyla Platyhelminthes (flatworms) and Nematoda (nematodes), both of which include many important parasites of humans and animals. The Platyhelminthes comprise the Trematodes (also known as flukes) and the Cestodes (tapeworms) (Figure 1.1).

##### 1.1.1.1 Trematodes

Trematodes, which have small flat leaf-like bodies, include parasites such as *Schistosoma haematobium*, *S. mansoni* and *S. japonicum* (blood flukes), *Clonorchis sinensis*, *Fasciola hepatica*, *F. gigantica* and *Opisthorchis viverrini* (liver flukes), *Paragonimus spp.* (lung flukes) and *Fasciolopsis buski* (intestinal flukes). Although most of these are restricted to tropical environments, fascioliasis is a worldwide problem particularly in livestock.

Blood fluke larvae develop into adult schistosomes and form separate sexes, but live conjoined in blood vessels where the female lays eggs in mammals. Eggs from faeces hatch in water and liberate larvae (miracidia) that penetrate the freshwater snail intermediate host. Transmission occurs by cercariae which emerge from snails, penetrating human skin during contact with contaminated water. The above *Schistosoma spp.* cause schistosomiasis in humans, which currently afflicts approximately 207 million humans globally (Hotez et al. 2008).

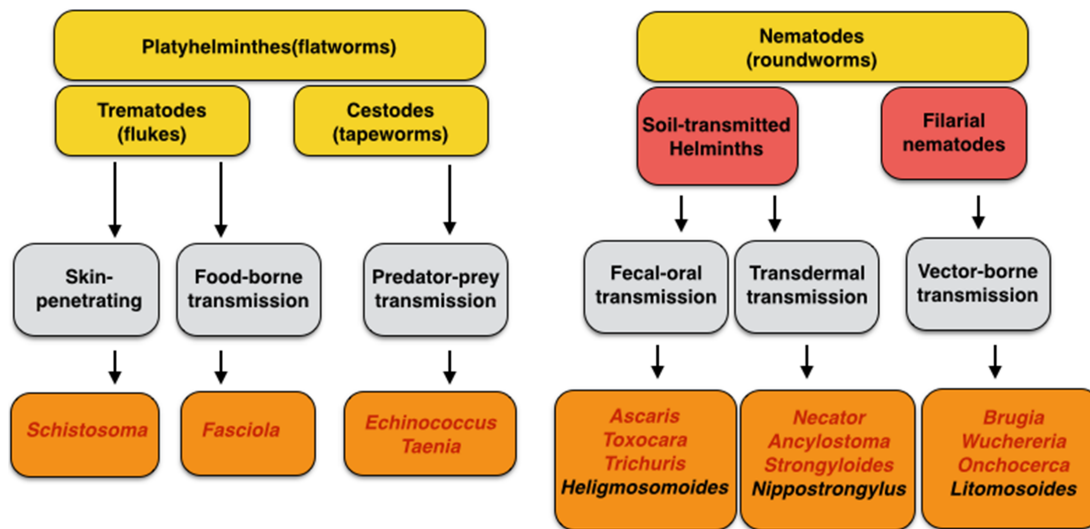


**Figure 1.1 Simplified classification of major helminth parasites by means of transmission.** Top line: taxonomic grouping; second line: route of infection; bottom line: parasite species, parasites causing human disease are in RED and mouse model parasites in BLACK. Adapted from Hewitson and Maizels, 2014.

The life cycle of fascioliasis is complex, involving a final host (particularly livestock) where adult worms live, an intermediate host (water snail) where the larvae develop and a carrier such as water or aquatic plants (Malone 1986). Adult liver flukes live in hepatic bile ducts where they cause hepatic disease in domestic ruminants and humans. Eggs are evacuated into faeces and hatch into larvae that move into the snail. More larvae from the snail are released into the water and swim to attach to the leaves or stems of aquatic plants where metacercariae are formed. Infection occurs when water containing metacercariae is drunk or when uncooked cyst-contaminated aquatic vegetation is eaten. More than 40 million people from more than 75 countries have been reported to have Fascioliasis (Hotez et al. 2008). The World Health Organization (WHO) notably mentioned that no countries can be considered free from the risk of fascioliasis.

#### 1.1.1.2 Cestodes

Cestode life-cycles involve predator-prey transmission between two terrestrial hosts, in which larval metacestodes form cysts in the tissues of herbivores, and subsequently grow into adult tapeworms in the small intestine in carnivores. The larvae of *Taenia spp.* cause cysticercosis in pigs, cattle and humans (0.4 million

cases in Latin America), while those of *Echinococcus* cause hydatid disease in domestic and wild animals, and even humans and lead economic losses in livestock. The definitive carnivore hosts of *Echinococcus* are canids, particularly dogs and foxes.

### 1.1.1.3 Nematodes

The nematodes (also known as roundworms) include the major intestinal worms (soil-transmitted helminths) and the filarial worms that cause lymphatic filariasis (LF) and onchocerciasis (Figure 1.1). Worldwide, more than 2 billion people are infected with soil-transmitted helminths (STH) (Bethony et al. 2006). The main species of STH that infect people are the roundworm (*Ascaris lumbricoides*), the whipworm (*Trichuris trichiura*) and hookworms (*Necator americanus* and *Ancylostoma duodenale*). They are transmitted through soil contaminated with faeces in areas lacking adequate sanitation or hygiene.

*Ascaris* infections involves fecal-oral transmission of infective eggs. Adult ascarids live in the small intestine and feed on intestinal contents, they steal nutrition from the host. A female produces a huge number of eggs (~200,000 eggs per day), excreted with the feces. Freshly-excreted eggs are fertilized for embryonation and become infective in 9-40 days. The eggs' high resistance to external environmental conditions enable them to remain viable in soil for several years. Infections are transmitted by ingestion of infective eggs containing L3 larvae, which hatch in the intestinal tract, and penetrate the mucosal barrier and then systemic circulation to the lung. About 10-14 days after infection, the larvae penetrate the alveolar wall, move up to trachea, ascend the bronchial tree to the throat, and are swallowed down to oesophagus to return to the intestinal tract where they mature as adults, which continues the life cycle. Adult worms can live 1 to 2 years. *Ascaris* infections in humans (1.221 billion in developing regions of Asia, Africa, and Latin America) cause gastroenteritis, protein depletion and malnutrition, poor growth and development in small children. Heavy infections can cause life-threatening gut obstruction that may affect working capacities, and impair physical growth.

Whipworm infection is directly transmitted by oral ingestion of infective eggs. The adult worms (~4cm in length) live in the cecum using their anterior portion to embed into the mucosa epithelium, whereas broader posterior helps female worms

oviposit numerous eggs (3,000 to 20,000 eggs per day). The unembryonated eggs are passed out with the feces become infective in 15 to 30 days. After ingestion of the infective eggs, eggs hatch in the small intestine and mature as adults in the colon, which complete the life cycle. Adult worms can live about 1 year. *Trichuris* infections in humans (795 million cases in developing regions of Asia, Africa and Latin America) cause intestinal manifestations: diarrhoea, abdominal pain, straining, colitis and rectal prolapse (Bethony et al. 2006). *Trichuris* infections have also been reported to compromise cognitive function in children (Nokes et al. 1992).

Hookworm infection is mostly acquired by walking barefoot on contaminated soil via transdermal transmission. The eggs, passed in the stool, hatch in the environment and develop into infective stage L3. These infective larvae migrate to tips of vegetation or soil enabling them to infect passing barefoot mammals by penetrating the skin. Then they migrate through the blood vessel to the heart then to the lungs. Finally, they reach the small intestine and mature into adults after penetrating into the pulmonary alveoli, ascending the bronchial tree to the pharynx and are swallowed. Adult worms can live 1 to 2 years or even longer. Heavy infections by *Ancylostoma* and *Necator* lead chronic intestinal blood loss that results in anaemia in humans, especially children lacking footwear. There are estimated to be 740 million cases in developing regions of Asia, Africa, and Latin America (especially in areas of rural poverty).

The filarial nematode infections are transmitted by arthropod vectors. *Onchocerca* infection is spread by blood-feeding black flies, while lymphatic filariasis by mosquitoes. In addition, *Wuchereria* (the causative agent of lymphatic filariasis) is transmitted by a number of mosquito species mostly from the genera *Mansonia*, *Culex*, *Aedes* (which also transmit Dengue/Yellow/Zika Fever)(Miller and Mitchell 1991), and *Anopheles* (which also spread human Plasmodium causing malaria) (Manguin et al. 2010). Adult filarial worms reside in lymphatic or connective subcutaneous tissues of their hosts. *Onchocerca* infections lead to nodules, skin lesions and river blindness in humans (37 million cases in Sub-Saharan Africa), while those of *Wuchereria* and *Brugia* cause elephantiasis (120 million cases in developing regions of India, southeast Asia, and sub-Saharan Africa).

As this is the filarial parasite studied here, it will be described in more detail in the next section.

### 1.1.2 Lymphatic filariasis

Lymphatic filariasis (LF), a neglected tropical disease, is caused by the nematodes *Wuchereria bancrofti* (which is responsible for 90% of the cases), *Brugia malayi* and *Brugia timori*. *Brugia pahangi* is a closely related filarial nematode that is naturally found in cats, and may also cause clinical infection of humans manifesting as lymphatic filariasis (Tan et al. 2011). The genome of *B. pahangi* was found to have a high similarity to *B. malayi*, with extensive synteny and few genes specific only for one species (Lau et al. 2015).

Lymphatic filariasis can cause a wide variety of clinical symptoms: 1) Some patients show no apparent clinical symptoms; 2) For those who have clinical symptom, acute adenolymphangitis (ADL) is often the first manifestation. It involves high fever, painful, lymph node and lymphatic inflammation (lymphangitis and lymphadenitis), and transient local edema (Nutman and Kazura 2011). 3) Swelling of the upper or lower extremities is the most common chronic manifestation, which causes lymphedema of the arms, legs and even breasts. 4) In many endemic areas, disease of the male genitalia is far more common than that of lymphedema, which cause hydroceles and severe disfigurement of genitalia; 5) Impairment of the renal lymphatics causes a rare but serious manifestation chyluria; 6) A distinct syndrome called tropical pulmonary eosinophilia (TPE) appears in some patients (Nutman and Kazura 2011). It includes paroxysmal cough and wheezing, adenopathy, blood eosinophilia (>3000 eosinophils/ $\mu$ l) and high levels of total serum IgE (10 000-100 000ng/ml). Lymphatic filariasis is closely related to parasites that cause river blindness in humans, and heartworm infections in dogs (Hoerauf et al. 2003, Fu et al. 2012). Thus, the above severe clinical manifestations make LF as one of the leading causes of permanent and long-term disability, reducing worker productivity in many tropical countries, causing massive economic losses (Perera et al. 2007, Nutman and Kazura 2011). Its life cycle (Figure 1.2) involves mosquitoes and humans and a correspondingly complex set of interactions with the human host immune system (Maizels et al. 1993, Molehin, Gobert and McManus 2012).

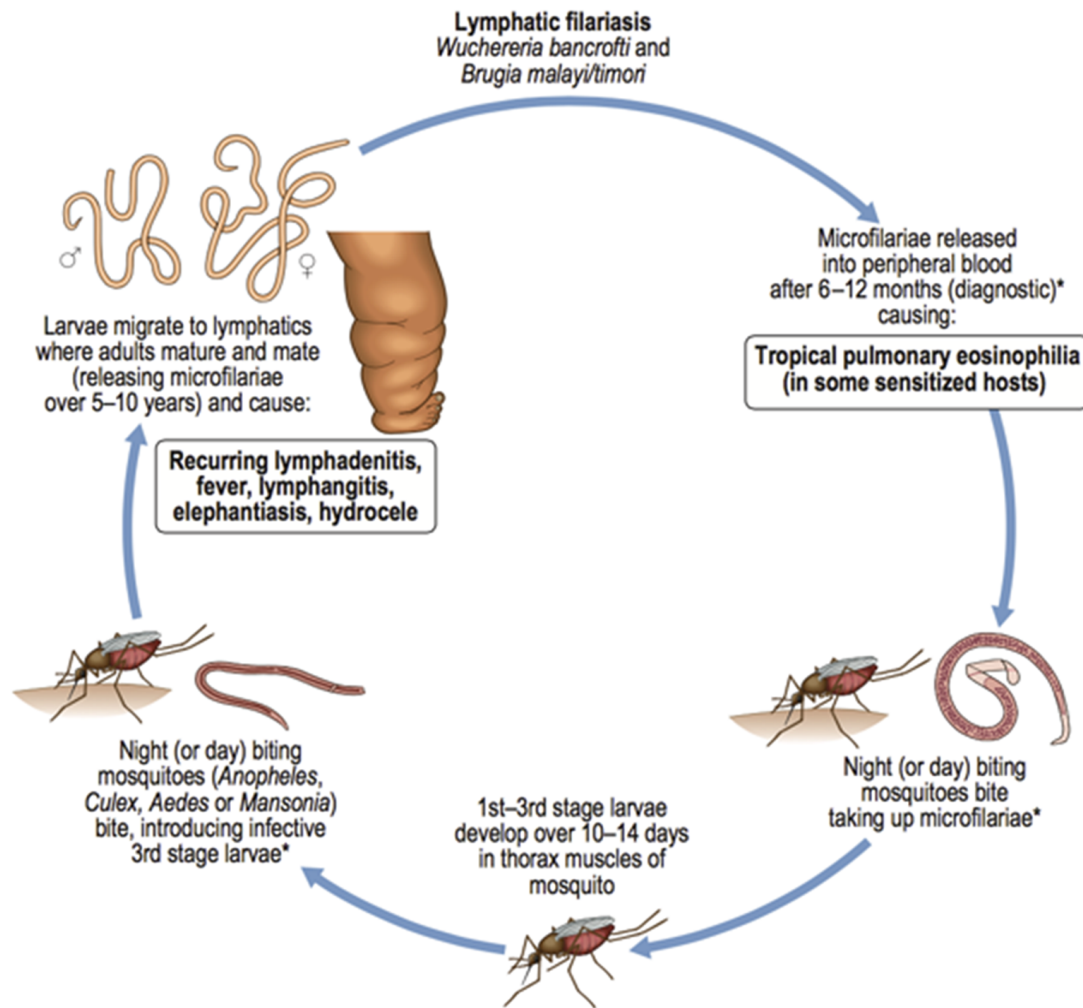


**Figure 1.2: Life cycle of lymphatic filariasis.** During a blood meal on an infected host, a female mosquito takes up microfilariae from the bloodstream. Parasites develop from 1st to 3rd stage larvae (L1-L3) in the thoracic muscles of the mosquito over 10-14 days. During the next blood meal, mosquitoes introduce infective L3 onto the skin of the human host. Larvae penetrate and migrate to the lymphatics where they develop into adults and mate (releasing microfilariae over 5-10 years), causing recurring lymphadenitis, elephantiasis and hydrocoele. Bloodstream microfilariae released by female worms can also cause tropical pulmonary eosinophilia. From Nutman and Kazura, 2011.

### 1.1.2.1 Epidemiology of lymphatic filariasis

At the start of Global Programme to Eliminate Lymphatic Filariasis (GPELF) in 1997, there were an estimated 120 million cases of filariasis infection in both rural and urban areas in about 81 countries (Figure 1.3). The greatest number of *W. bancrofti* infections are in Southeast Asia, sub-Saharan Africa and the western Pacific. The infection is

prevalent in India, Indonesia, Papua New Guinea, the Philippines and several Pacific countries such as parts of Fiji and Tahiti. Infection with *B. malayi* is limited to Asia and several Pacific island groups (Figure 1.3). Fewer than 10 to 20 million persons in these areas are infected with *B. malayi*, which may coexist with *W. bancrofti* (Nutman and Kazura 2011). A smaller number in the Lesser Sunda island archipelago, including Timor and nearby islands, are infected with *B. timori*.

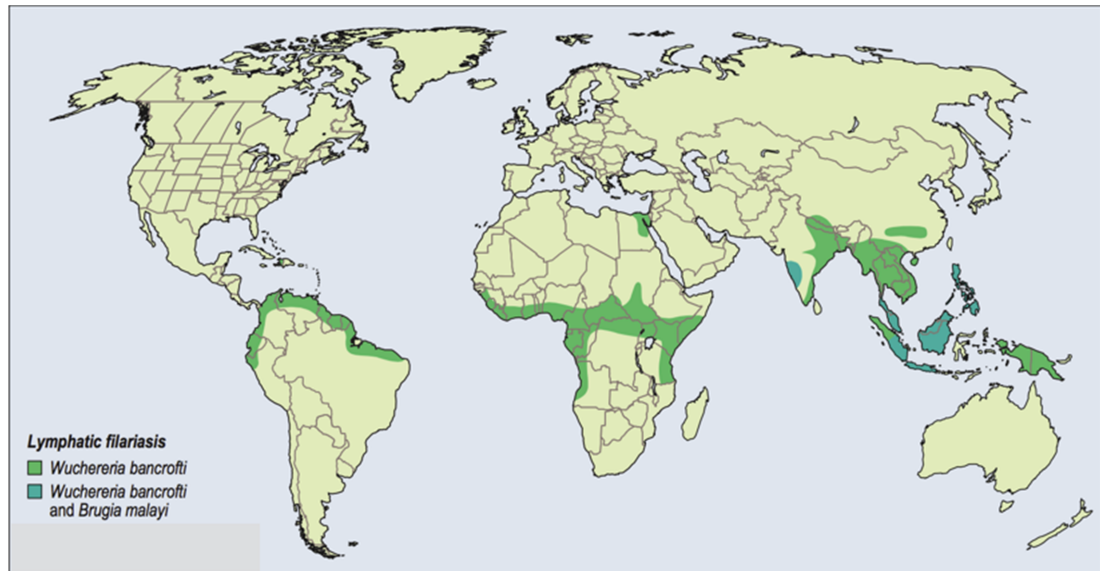


**Figure 1.3: World map of lymphatic filariasis infection.** (Nutman and Kazura 2011).

#### 1.1.2.2 Large-scale treatment and current status

According to GPELF, several control strategies were utilized to interrupt transmission, including mass drug administration (MDA) and vector control. The target of MDA is to reduce the level of microfilaraemia in infected persons to the level that can no longer sustain LF transmission by mosquito to new hosts. The two principal regimens for MDA are: 1) the combinations of two filaricidal medicines given once yearly to entire at-risk population in endemic areas in the following way: Albendazole (400 mg) together with either ivermectin (150–200 mcg/kg) or with diethylcarbamazine citrate (DEC) (6 mg/kg) for 4-6 years (Gyapong et al. 2005); or 2) exclusive use of cooking salt fortified with DEC for 1-2 years (Lammie et al. 2007).

However, the major obstacle to implementing MDA programs is that adverse drug reactions (ADRs) occur after DEC and ivermectin intake. The drug can produce adverse reactions such as arthralgia, drowsiness, epididymitis, fever, headache, lymphangitis, lymphadenitis, nausea, orchitis etc. These reactions are related to the

dose-related chemical toxicity of the drug or, occasionally, with the death of the parasite (Norões et al. 1997), or with the gender of the patients in Brazil (Lima et al. 2012). In Indonesia, moderate reactions (fever, headache and body aches) are manifest in elephantiasis patients with high densities of circulating microfilariae, starting between 2 to 24 hours following DEC intake (Haarbrink et al. 1999). In central Africa, in countries coendemic with *Loa loa*, serious adverse events (including encephalopathy and death) occurs in people with high levels of *Loa* microfilariae in the blood, when treated with ivermectin (Boussinesq et al. 2003).

Without a vaccine, vector-mosquito control remains the only accessible methodology against lymphatic filariasis (Bockarie et al. 2009). The aim of mosquito control is to interrupt the transmission of LF and other mosquito-borne infections. As mentioned above, *Wuchereria* is transmitted by no fewer than 4 disparate mosquito genera including *Mansonia*, *Culex*, *Aedes* (Dengue/Yellow/Zika Fever) (Miller and Mitchell 1991) and *Anopheles* (malaria) (Manguin et al. 2010). Thus, it makes vector control highly problematic. The mosquito-borne Zika virus outbreak in the Americas in 2016 proved that mosquito control has not yet has been successful (Yakob and Walker 2016).

During the first 10 years of GPELF, the number of people receiving MDA treatment, increased from 3 million in 12 countries in 2000, to 500 million in 53 countries in 2011 (Ichimori et al. 2014). However, after 20 years of MDA and vector control, 947 million people in 54 countries worldwide remain threatened by lymphatic filariasis (Modi et al. 2017). To date, there is still no licensed vaccine available and current vaccine candidates only provide partial protection in animal models (Taylor, Hoerauf and Bockarie 2010, Arumugam et al. 2014, Maizels and McSorley 2016, Hartmann et al. 2014). Large-scale treatment with massive drug programmes annually, and mapping all threatened areas worldwide costs a great deal of money and research resources, even though anthelmintic drugs have been donated by three different companies (Ichimori et al. 2014). Potential vaccination could protect humans and animals once and for all. There is also concern that resistance may develop to the limited number of drugs available, and so there is an urgent need to discover new targets for vaccine and drug development. Thus,

understanding the depth of the relationship between filarial parasite and host makes meaningful.

### 1.1.2.3 Available research models for lymphatic filariasis

Although 90% of filariasis cases are due to *W. bancrofti*, this species cannot be maintained in the laboratory, as it only infects primate hosts (Palmieri et al. 1983). Among several mouse models of filariasis, recent studies have focussed on *Litomosoides sigmodontis*, which permits researchers to investigate both the developmental biology and immunology of filarial parasites (Babayan et al. 2010, Taylor et al. 2009). However, it has proven possible to study the human parasite *B. malayi* in the laboratory, as this species will infect the rodent *Meriones unguiculatus* (the Mongolian jird, also a permissive host for *Brugia pahangi* (Ash and Riley 1970a, Ash and Riley 1970b). In the mouse, although infective larvae do not survive for more than a few days, adult worms or microfilariae may be transferred and live for many weeks or months. The laboratory life cycle of *L. sigmodontis*, *B. malayi* and *B. pahangi* are shown in Figure 1.4.

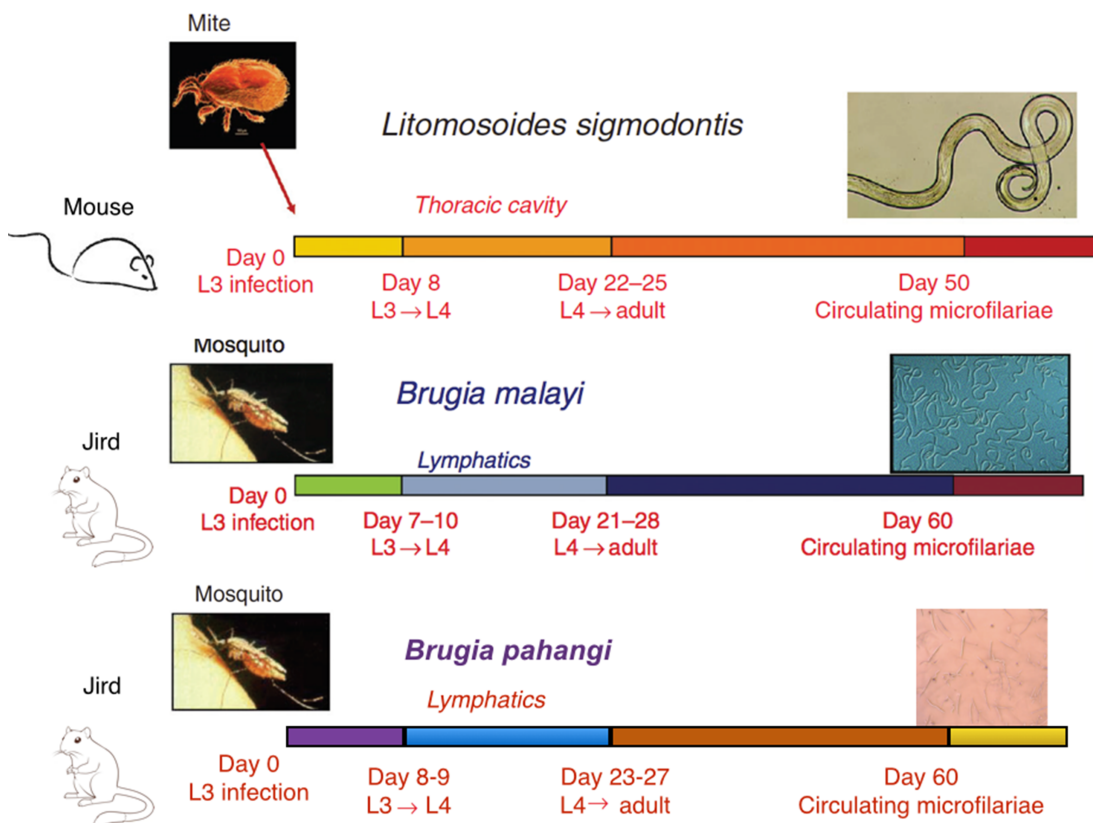


**Figure 1.4: The laboratory life cycle of research models of filariasis.** Adapted from Maizels et al., 2004.

*B. malayi* and *W. bancrofti* are closely related species, and indeed it is not easy to distinguish between clinical diseases caused by these different agents, and they are spread by similar mosquito vector species. At the molecular level, the limited studies on *W. bancrofti* indicate that it is very similar to *B. malayi* (Morgan et al. 1986). Interestingly, *B. malayi* infection is a zoonosis in that there are feline and primate reservoirs, corresponding to its ability to infect some rodent species. Thus, research into *B. malayi* is both logistically feasible and relevant to lymphatic filariasis in general.

## 1.2 Immune regulation by helminth parasites

Parasitic helminths infect more than 2 billion people worldwide, nearly one third of the human population, thus can cause marked disability and morbidity. Helminths are complex eukaryotic pathogens with large genomes, can live for a considerable length of time in the human host (Maizels and Yazdanbakhsh 2003, Muller and Wakelin 2002). Both their extremely high prevalence, and their longevity, indicate that helminth parasites are able to very effectively dampen or block the immune system of their host.

In many helminth infections, a T helper 2 (TH2) immune response is dominant, which is typically marked by the cytokines interleukin-4 (IL-4), IL-5, IL-13, the immunoglobulin E (IgE) isotype, and also high levels of tissue and blood eosinophilia, as well as mucosal mastocytosis and goblet cell hyperplasia in intestinal infections (Maizels and Yazdanbakhsh 2003, Maizels et al. 2004). In general, TH2 responses are considered to be protective by driving a set of type 2 anti-helminth mechanisms, including class-switched antibodies, activated swarms of immune cells; disabling parasites overall fitness and ability to reproduce, degrading parasite integrity and dislodging parasites by making the chosen niche untenable, leading to their destruction or expulsion (Maizels, Hewitson and Smith 2012). TH2 responses against helminths will be described in more detail in the section 1.4.1.

Generally, TH1 cells tend to produce immune responses against intracellular pathogens, such as bacteria and viruses, by producing interferon (IFN)- $\gamma$  and IL-2 (O'Garra and Arai 2000). However, there are a few intriguing cases in which TH1 rather than TH2 cell responses are mounted against helminths. First, it is known that different strains of mice produce TH1 or TH2 cell responses against the nematode

*Trichuris muris*, and where TH1 predominates, mice remain chronically infected (Else et al. 1994). Secondly, the cercarial stage of schistosomes stimulate TH1 cell responses soon after infection is initiated in the mouse model. Subsequently, a TH2 cell response is induced by schistosome egg antigens as infection progresses and eggs are released by adults in the vasculature (Maizels and Yazdanbakhsh 2003, Pearce and MacDonald 2002). Finally, the *B. malayi* microfilarial stage is also a notable exception to the pattern of TH2 induction by helminths. In this case, the microfilarial stage of *B. malayi* promotes TH1 cell responses in BALB/c mice, although adult filarial worms, especially female worms, exert polarization of the TH2-cell response (Pearlman et al. 1993, Lawrence et al. 1994).

### 1.2.1 Regulatory T cells in filarial infection

Dating back to 1980, it has been found that suppressor cells can cause specific immunologic unresponsiveness to microfilarial antigens in patients with patent Brugian filariasis (Piessens et al. 1980). Based on the in vitro study of peripheral blood mononuclear cell (PBMC) isolated from microfilaremic individuals in Indonesia, these suppressor cells have been discovered to be the regulatory T cells (Tregs) which are functional in suppressing proliferation and possibly TH2 cytokine responses to *B. malayi* adult worm antigen, proving Tregs is a key element of TH2 suppression and a key feature of filarial infection (Taylor, van der Werf and Maizels 2012, Wammes et al. 2012).

In the light of the respective roles of TH1, TH2 and Tregs in infection, it was proposed that according to the balance of these subsets, three different outcomes of specific immune response could be produced by host upon exposure to helminth parasites (Figure 1.5) (Maizels and Yazdanbakhsh 2003). In the first outcome, individuals susceptible to long-term infection display “Modified T helper 2 (TH2)-cell responses”, with ineffective TH2 cell responses and low levels of TH1 cells, but developing strong regulatory T (Treg)-cell activity by expressing high levels of IL-10; the antibody response is dominated by IgG4 with little IgE. Secondly, in cases of more severe pathology, there is an uncontrolled inflammatory (TH1) response developed against parasites, whereas there is a low level of Treg-cell activity (low IgG4 vs. high IgE). Thirdly, if individual was resistant to parasite infection, they present with

restrained Treg-cell activity and balanced TH1 and TH2 cell responses described as “balanced TH1/TH2” (with similar IgG4 and IgE isotypes).

This model is well illustrated by human cases of filariasis. In lymphatic inflammation, there are strong type-1 (and TH17) immune responses comprising both IgE and IgG4, which lead to pathological changes such as elephantiasis (Babu et al. 2009). In contrast, highly infected microfilarial patients have high levels of IgG4, but lower levels of IgE (Kurniawan et al. 1993). During filarial infection, the TH2 cells are differentiated into a hyporesponsive state that is well demonstrated, the modified TH2 cell response. In human infection with *Onchocerca volvulus*, it has been shown that T cell in vitro immune responsiveness could be restored by the addition of exogenous IL-2 (Gallin et al. 1988). It has also been shown that significant impairment of both TH1 and TH2 immune responses identified by diminished corresponding cytokine responses of PBMC from filariasis patients to live *B. malayi* microfilariae or larvae, as further evidence for the development of T cell hyporesponsive state (Babu et al. 2006). In addition, using the laboratory mouse model of filariasis infection with *L. sigmodontis*, effector CD4<sup>+</sup> T cells isolated from the infection site were shown to lose the capacity to proliferate and produce TH2 cytokines in response to antigen. In contrast, mice in which regulatory T cell activity was ablated by combined antibody treatment against CD25 and glucocorticoid-induced TNF receptor family-related gene (GITR), were able to reverse hyporesponsiveness and overcome an established infection, leading to clearance of filarial parasites (Maizels and Yazdanbakhsh 2003, Taylor et al. 2005). However, neutralization of IL-10 receptor or depletion of Foxp3 CD25 Treg cells alone were unable to restore the ability of the immune system to expel parasites (Taylor et al. 2005, Taylor et al. 2007). Cytotoxic T lymphocyte antigen 4 (CTLA4) blockade in human PBMC cultures switches the unresponsive state, increases TH2 cytokine production and reduces anergy-inducing factors expression in filariasis patients (Babu et al. 2006). Thus, these data suggest that during chronic helminth infection, CD4<sup>+</sup> T cells develop both intrinsic antigen specific hyporesponsiveness/ tolerance, and expanded regulatory T cell activity, in both human and mouse models, thereby mediating two levels at which filarial parasites suppress host immunity.

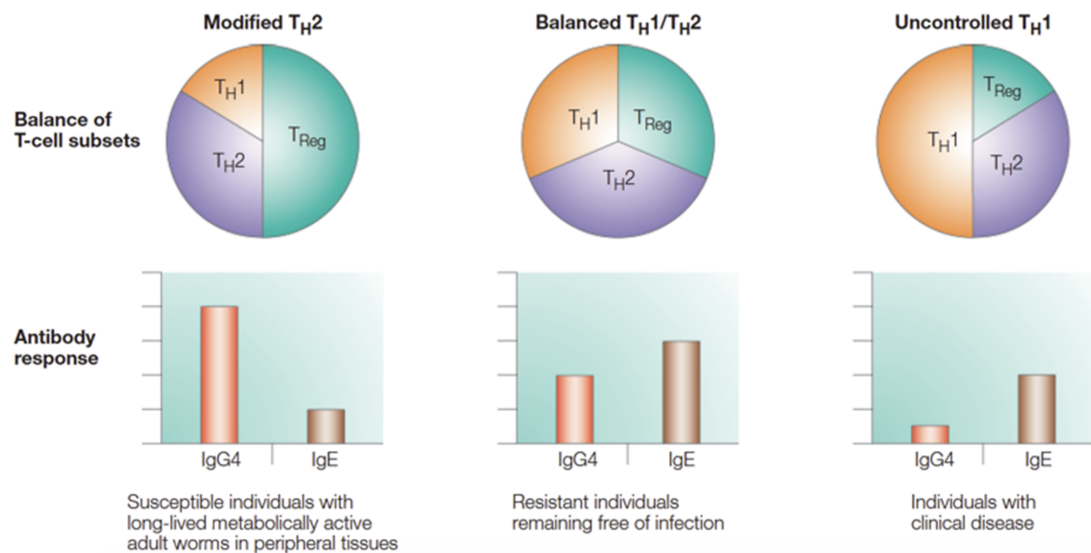


**Figure 1.5: Immunology of human infections with helminth.** From Maizels and Yazdanbakhsh, 2003.

## 1.2.2 Immune evolution of helminths parasites

In order to protect themselves from elimination, long-lived helminth parasites have thus proved to be strong selective forces for immune evolution and to be able to (1) modify the bystander immune responses and also (2) downregulate the host immune system (Maizels and McSorley 2016).

### 1.2.2.1 Modifying the bystander immune responses

It has been noted since 1968 that autoimmune disorders, such as rheumatoid arthritis, are much less frequent in developing countries due to the immunological disturbance by parasite infection (Greenwood 1968). It has been shown in the follow-up studies that mice and rats infected with rodent malaria were protected from autoimmune disease (Greenwood and Voller 1970, Greenwood, Herrick and Voller 1970). More recently, children infected with *S. haematobium* were detected to have lower levels of skin reactivity to allergen house-dust mite (HDM) than uninfected children (van den Biggelaar et al. 2000). Furthermore, it has been shown in the follow-up study that atopic reactivity to HDM increased in those schoolchildren who have reduced *Ascaris* and/or *Trichuris* infections after taking anthelmintic drugs (van den Biggelaar et al. 2004). Exposure to helminth immune modulation can even begin before birth, as it was reported that maternal helminth infections during gestation reduced infants' allergen skin prick test reactivity to perennial allergens (Clark et al. 2016).

Cases such as these are consistent with the so-called “Hygiene Hypothesis”, which was first postulated in 1989 (Strachan 1989), that increased exposure to microorganisms protected children from the development of allergy. Although Strachan considered only virus and bacterial infections, many subsequent commentators extended the “Hygiene Hypothesis” to postulate that helminth infections in low-income countries would reduce the development of allergic and autoimmune diseases (Versini et al. 2015). Using the paradigm proposed in the 1990s of opposing TH1 and TH2 lymphocyte populations in the immune response (Mosmann and Coffman 1989) and the recognition that viral and bacterial infections induce a TH1 response, it was first thought that early-life exposure to virus and bacterial infections protected younger siblings in larger families from developing allergies such as hay fever (Strachan 1989, Strachan 2000). Thus, the young immune system may be “educated” away from excessive and allergy-promoting IgE mediated TH2 responses (Maizels, McSorley and Smyth 2014). It is difficult with this model to explain how helminth infection reduce allergy, as helminth infections generally drive the TH2 responses. However, it might be an answer that some autoimmune diseases are driven by TH1 responses, or by TH17 cells, such as Type I diabetes, multiple sclerosis and Crohn’s disease. Following the principal that infectious agents can dampen inflammation in the mature immune system, helminth therapy is proposed to protect against autoimmune diseases (Maizels et al. 2014). Versini et al. 2015 summarized a list of the experimental and clinical studies utilizing live parasites or parasite antigen for various autoimmune diseases including Crohn’s disease, inflammatory bowel disease (IBD), multiple sclerosis (MS), rheumatoid arthritis (RA) and other diseases in either human or mouse (Versini et al. 2015). For long term research, it may be more effective to identify the specific immunosuppressive molecule from these parasites. For example, the filarial-derived glycoprotein ES-62 has been characterized to be the most effective molecule in mouse models of RA (Pineda et al. 2014). However, such helminth-derived molecules have yet been used in RA clinical trials (Versini et al. 2015).

Parasite helminths also alter immune responses to other agents. To take co-infections with human filariasis as an example, filariae mediate immunomodulatory mechanisms and also change the protective immune responses to other parasites (e.g. malaria) and infectious microbes (e.g. tuberculosis) (Taylor et al. 2010). Filarial

infections suppress the cytokine response specifically against *Plasmodium falciparum*, reducing resistance to malaria in an IL-10-dependent manner (Metenou et al. 2009), and they diminish *M. tuberculosis*-specific TH1 and TH17 responses (Babu et al. 2009). In addition, intestinal helminth infections are considered to potentially indirectly influence the immune response through the effects on the composition of the intestinal microbiome (Leung 2013). It has been shown that chronic infection with *H. polygyrus* favors specific types of commensal bacteria, especially members of the Lactobacillaceae family (Walk et al. 2010). Furthermore, it has been found interestingly that intestinal microbiota provide a platform for *T. muris* hatching eggs (Hayes et al. 2010), suggesting intestinal helminths might alter resident microbes (Mishra et al. 2014).

In addition, helminth infections compromise disease prevention efforts, as they reduce vaccine responses. This has been shown, for example, in maternal parasitic infections with schistosomes, filarial worms and malaria during pregnancy can impair later immune responses by infants to childhood vaccinations (LaBeaud et al. 2009). Mice with *S. mansoni* infections (Elias et al. 2005) have decreased responses to BCG vaccination, humans with schistosomiasis (Sabin et al. 1996) or onchocerciasis (Cooper et al. 1998) have impaired tetanus-specific responses following tetanus toxoid vaccination.

#### 1.2.2.2 Downmodulation of host immunity

It is worth mentioning that helminths have co-evolved with their hosts for centuries; their goal is to survive as long as possible by dampening host immunity but not to kill their host. To accomplish this, helminths are able to finely down-modulate the function of various effector cell populations of host immunity to prevent recognition or activation that may lead to their elimination, while not creating too profound an immunosuppression which would lead to host death from infection. Currently, filarial parasites are thought to interfere in at least three different ways:

- 1). Interference with antigen processing: Using the fluorogenic substrate preferentially cleaved by asparaginyl endopeptidase (AEP), the recombinant *B. malayi* cysteine protease inhibitor-2 (*Bm*-CPI-2) was found to inhibit the cysteine proteases AEP, which are required for antigen presentation (Manoury et al. 2001). Filarial

parasites also interfere with innate cell recognition through toll receptors (Semnani et al. 2008).

2). Cytokine mimicry: A homologue of the endogenous immunosuppressive cytokine TGF- $\beta$  was found to be expressed by the filarial nematode *B. malayi* and was the first helminth cytokine discovered to interact functionally with host cytokine receptors (Gomez-Escobar, Gregory and Maizels 2000). Another set of helminth cytokines are the macrophage-migration inhibitory factors (MIFs). *Bm*-MIF-2 was shown to have extremely similar structure to human MIF, and to induce similar responses from mammalian macrophages (Zang et al. 2002, Falcone et al. 2001, Prieto-Lafuente et al. 2009). A related activity was found with the *B. malayi* abundant larval transcript-2 (ALT-2) protein that is secreted by infective larvae, and shown to activate SOCS1 (suppressor of cytokine signaling-1), an inhibitor of IFN $\gamma$  signalling (Gomez-Escobar et al. 2005).

3). Blocking efferent immune mechanisms and effector cells (Figure 1.6): Many of the other secreted products of filarial parasites are likely to modulate effector cells and their products. For example, it has been shown that the serpin secreted from bloodstream microfilariae of *B. malayi*, SPN-2, inhibits the enzymatic activity of the neutrophil proteases elastase and cathepsin G, encoded by the human host (Zang et al. 1999, Maizels and Yazdanbakhsh 2003). Adult parasites of the same species secrete a wide range of proteins that have been identified (Hewitson et al. 2008) including galectin and triose phosphate isomerase.

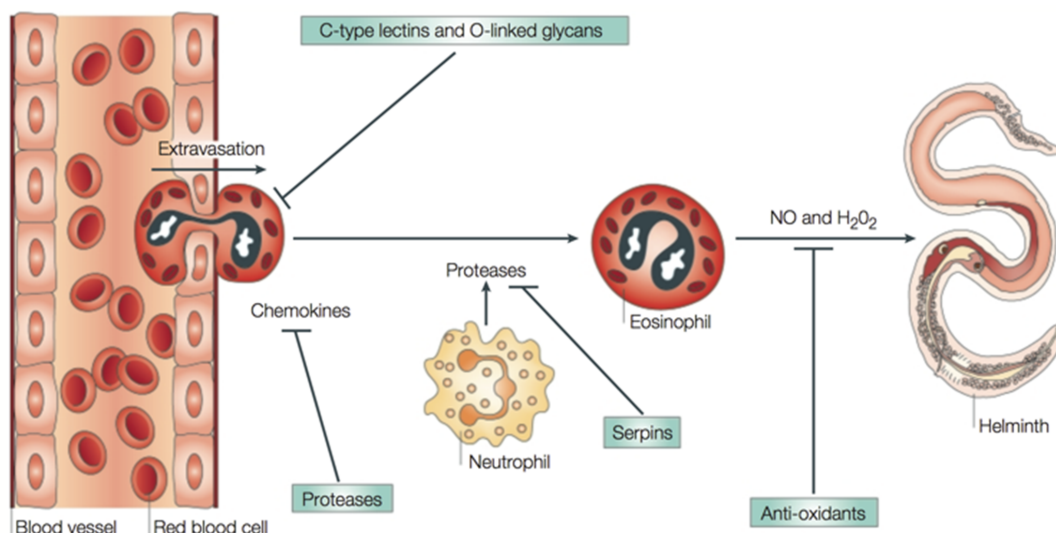


**Figure 1.6: Blocking efferent immune mechanisms.** From Maizels and Yazdanbakhsh, 2003.

### 1.3 Immune evasion genes in filarial nematodes

Because living nematode parasites do not replicate but are established for many months or years, it is presumed that immune evasion is accomplished by products which they express on their surface and/or which they release *in vivo*. Such released products may be modelled *in vitro* by cultivating live parasites and collecting their excretory-secretory products. The term “Excretory-Secretory (ES) products” is a long-standing parasitological term describing the assortment of molecules that parasitic helminths excrete or secrete into their hosts (Lightowers and Rickard 1988). The stage- and gender-specific ES products of helminths also include components such as digestive enzymes produced from the intestine by adult worms, or uterine contents released along with eggs, larvae or microfilariae by female worms. In addition, it has recently been established that along with soluble proteins and other macromolecules, many parasitic helminths release exosome-like extracellular vesicles (EVs) (Buck et al. 2014, Coakley, Maizels and Buck 2015). Extracellular vesicles can be released both by the intracellular parasites (either by endocytic pathways or are directly released from the plasma membrane), including *Leishmania spp.* and *Trypanosoma cruzi* (Gonçalves et al. 1991, Silverman et al. 2010), and also by extracellular pathogens, which providing a mechanism for the import of parasite cargo into host cells, including virulence factors from diverse protozoan parasites, such as *Trypanosoma brucei* and *Trichomonas vaginalis* (Szempruch et al. 2016, Twu et al. 2013). In the case of extracellular parasites, including helminths, the vesicles represent a previously unsuspected pathway by which the pathogens can influence the intracellular milieu of the host cells to which the vesicles are targeted. Each of these products may be associated with immune evasion strategies against the corresponding host (Hewitson, Grainger and Maizels 2009).

Technically, researchers developed simple methods to collect the excretory-secretory ES products for study, generally using serum-free medium with few supplements to avoid introducing extraneous components (such as serum proteins) into the preparation. However, parasites vary dramatically in their ability to survive in such simple media, with adult filarial worms living no more than 1 week (Hewitson et al. 2008). In contrast, it was found the intestinal nematode *H. polygyrus* survives for at least 3 weeks, as maintained in the Maizels laboratory (Johnston et al. 2015).

### 1.3.1 Adult surface-associated proteins

In 2001, Maizels et al. summarized information on the major surface and secreted proteins from different stages the adult, microfilariae and larval of filarial *Brugia* parasites, based on techniques such as surface labelling, molecular cloning and antibody immunoprecipitation (Maizels et al. 2001). Subsequently, high-throughput research technologies including secretome proteomics, mass spectrometry and transcriptome sequencing have been combined to mine potential diagnostic or vaccine candidates, as well as immune modulators in *Brugia* (Hewitson et al. 2008, Moreno and Geary 2008, Bennuru et al. 2009). An extensive list of secreted proteins has now been revealed for deeper understanding of how these parasites and each of their stages survive in their particular host.

The major surface-associated proteins of adult *B. malayi* are *Bm*-GPX-1 (glutathione peroxidase) and *Bm*-SOD (superoxide dismutase); both carry out important anti-oxidant functions. *Bm*-GPX-1 is also designated as gp29 because the major component is a 29kDa glycoprotein (Maizels et al. 1989). GPX may protect parasite lipid by neutralizing reactive oxygen intermediate attack, or modifying and removing host immunomodulatory lipids (Bennuru et al. 2009). *Bm*-GPX-1 was identified in ES from both female and male adult worms as well as microfilariae, but was revealed to be of much higher abundance in adults compared to the Mf stage, suggesting a more important role in adult survival (Moreno and Geary 2008).

Superoxide dismutase (SOD), which is similarly involved in immune evasion of free oxygen radicals, was reported to be present in variable amounts among different stages. Moreover, two forms of *B. malayi* SOD were reported: a cytoplasmic form and an extracellular form (Ou et al. 1995). It was found that extracellular protein was detected at higher levels in adult male worms, whereas the cytoplasmic form was present to a similar degree in all stages. According to the protein fold and the metal cofactor, SOD is divided into three major families: the Cu/Zn type (binds both copper and zinc), Fe and Mn types (bind either iron or manganese), and the Ni type (binds nickel). *B. malayi* copper/zinc superoxide dismutase (Cu/Zn-SOD), the recombinant enzyme of which has 32kDa (Lee et al. 2005), appeared similar abundance in ESP among all stages from Moreno and Geary 2008 (Moreno and Geary 2008), whereas a

greater abundance was found in microfilariae than adult in Bennuru et al., 2009 (Bennuru et al. 2009).

### 1.3.2 Adult Excretory-Secretory Proteins

The recent proteomic studies of the ‘secretome’ of adult *B. malayi* has revealed a wider range of potential immunomodulatory molecules. Among these are galectins, triose phosphate isomerase (TPI), leucine aminopeptidase (LAP) and macrophage migration inhibitory factor (MIF).

Galectins are a family of evolutionarily conserved carbohydrate-binding proteins with many potential roles as regulators of immune cell homeostasis and host-pathogen interactions (Rabinovich et al. 2002a, Rabinovich, Rubinstein and Toscano 2002b). *Bm*-GAL-1 (*Bm*1\_24940) was identified as a Galectin (galactoside-binding lectin, PF00337) which is one of the most abundant proteins in *B. malayi* adult excretory–secretory products (BES) (Hewitson et al. 2008). Blastp analysis of the *Bm*-GAL-1 sequence showed high homologues to *Loa loa*, *O. volvulus* and *Dirofilaria immitis*, with 98%, 96% and 97% identity, respectively. It was also found that 89.42%, 32.56% and 31.95% identity against *Toxascaris leonina* galectin, human galectin 9 (*Hs*-GAL-9) and galectin 4 (*Hs*-GAL-4), respectively. *Hs*-GAL-9 was reported to suppress the generation of TH17, and promote the induction of regulatory T cells (Seki et al. 2008). Moreover, Li et al. identified that N- and C-terminal CRD of Gal-9 have different functions, Gal-9-C was more potent in inducing T cell death while Gal-9-N was more potent in activating DCs, by inducing higher TNF- $\alpha$  and IL-6 production/greater phosphorylation of p38 and AKT (Li et al. 2011). Zhu et al. proposed that murine Gal-9 binds to murine Tim-3 and Gal-9 is the ligand for Tim-3 (Zhu et al. 2005, Zhu, Anderson and Kuchroo 2011). However, Leitner et al. obtained a contrasting conclusion that Gal-9 is NOT the ligand for Tim-3 (Leitner et al. 2013). Hewitson et al. found that *Bm*-GAL-1 is able to bind to host immune cells in a carbohydrate dependent manner. Both N- and C- terminal domains bind host cells through canonical CRD sites. Monoclonal antibody B37 blocks binding of the N-terminal domain of *Bm*-GAL-1. *Bm*-GAL-1 potentiates TGF- $\beta$ -dependent induction of Foxp3 (unpublished data), which potentially drive regulatory T cells in the host, helping parasites avoid the host immune response.

The glycolytic enzyme triose phosphate isomerase (*Bm-TPI*, EC 5.3.1.1) has been revealed to be the most abundant ES protein of adult *B. malayi*, predominantly from female worms (Hewitson et al. 2008). TPI was also found in moulting L3 larvae early in infection by stage specific proteomic sequencing (Bennuru et al. 2009). It has been shown that polyclonal sera against TPI results in little inhibition of catalytic activity although TPI is a prominent target of the antibody response to infection. The follow-up study by Hewitson et al. demonstrated that two of twenty-three anti-TPI monoclonal antibodies produced in the laboratory were able to block TPI enzymatic activity. It has been further shown that immunization of jirds with *Bm-TPI* was not able to induce neutralising antibodies. However, passive transfer of neutralising mAb to mice before adult *B. malayi* implantation lead to 60-70 % reductions in the number of microfilariae produced by female worms, suggesting TPI plays an important role in the transmission cycle of *B. malayi* and is considered to be a potential drug target against filarial infections (Hewitson et al. 2014).

Leucine aminopeptidase (LAP; also named as ES-62) was identified to be an abundant phosphorylcholine containing glycoprotein, secreted by *Acanthocheilonema viteae* adult worms (Harnett et al. 1999). A homolog in *B. malayi* is detected to be secreted by L3s molting to L4s and also by adult worms (Hewitson et al. 2008, Bennuru et al. 2009). Interestingly, it has been demonstrated that ES-62 in *A. viteae* is heavily decorated with phosphorylcholine (PC) (Harnett, McInnes and Harnett 2004), while the ES-62 homologue in *B. malayi* is not conjugated to PC. This was demonstrated by western blotting with anti-PC monoclonal antibody, the *B. malayi* molecule was designated PC-free ES-62 (Hewitson et al. 2008). PC is a pathogen-associated molecular pattern (PAMP) expressed by a wide range of disease-causing agents, including bacteria, fungi and protozoa, as well as gastrointestinal and filarial nematodes (Harnett and Harnett 1999). Despite the fact that it enables recognition of pathogens by the host (via antibodies or C-reactive protein), it can also help pathogen survival by modulating host immunity (Harnett, Melendez and Harnett 2010). However, so far, no studies have shown PC from *Brugia* is playing a role in immune evasion.

Macrophage migration inhibitory factor (MIF) from filarial parasites has been discovered with striking structural similarities to the mammalian cytokine (Maizels et al. 2001). In *B. malayi* the two homologues are *Bm-MIF-1* and -2. *Bm-MIF-1* is present

in all 3 stages of worms and both genders, whereas MIF-2 is detected in the ES of the moulting L3 and also in the adult stage (Moreno and Geary 2008, Bennuru et al. 2009).

### 1.3.3 Microfilariae Excretory-Secretory Protein

In two proteomic studies of the microfilarial ES products, endochitinase and serpin were both reported to be abundant proteins at this developmental stage (Moreno and Geary 2008, Bennuru et al. 2009). Chitinases are essential for chitin degradation during moulting of larval filariae and hatching of microfilariae (Moreno and Geary 2008, Tachu et al. 2008) and have been suggested as candidate vaccine antigens (Fuhrman et al. 1992, Raghavan et al. 1994). The serine protease inhibitor (serpin) *Bm*-SPN-2 was also found to be specifically secreted by the microfilarial stage (Zang et al. 1999, Moreno and Geary 2008). Serpins expressed by parasitic nematodes are thought to help parasites avoid host immune defenses. Zang and Maizels and Molehin et al. have summarized the parasite serpins and smapins (Zang and Maizels 2001, Molehin et al. 2012) (Table 1.1).

Moreno and Geary suggested that the function of many microfilariae secreted proteins would be to regulate enzyme activity (Moreno and Geary 2008). Notably, many Mf secreted proteins are associated with protease inhibition, and in addition Mf secrete a different set of protease inhibitors compared to adults. For example, as well as SPN-2, Mf secrete more cysteine protease inhibitor-2 (*Bm*-CPI-2) than adults (Bennuru et al. 2009), and this product inhibits activities of multiple cysteine proteases required for antigen presentation, found in the endosomes/lysosomes of human B lymphocyte lines (Manoury et al. 2001). The release of protease inhibitors may be related to the ability of filarial nematodes to dampen host immunity (Hewitson et al. 2008, Hartmann and Lucius 2003), and differential expression by life cycle stages is most likely due to the different anatomical location between adult worms and microfilariae (lymph vs. blood).

**Table 1 Serine protease inhibitors from parasitic helminths**

Species	Serpins/ smapins	Molecular weight	type	Stage and/or localization	Target or closet mammalian	Reference/GenBank Accession number
<b>Nematode Serpins</b>						
<i>Ascaris suum</i>	<i>As</i> -SPN				Human antithrombin III	AW165870
<i>B.malayi</i>	<i>Bm</i> -SPN-1	44kDa	Secretory	All life cycle	Unknown	(Yenbutr and Scott 1995)
<i>B.malayi</i>	<i>Bm</i> -SPN-2	47.5 kDa	Secretory	Microfilariae	Neutrophil elastase.	(Zang et al. 1999)
<i>Haemonchus contortus</i>	<i>Hc</i> -serpin	63 kDa	Intracellular	Adult/gastrointestinal tract epithelial cells	Anticoagulant/	(Yi et al. 2010)
<i>Onchocerca volvulus</i>	<i>Ov</i> -SPN-1				Mouse neuroserpin	(Lizotte-Waniewski et al. 2000)
<i>Onchocerca volvulus</i>	<i>Ov</i> -SPN-2				Porcine elastase inhibitor	AA625018
<i>Onchocerca ochengi</i>	<i>Oo</i> -SPN				Mouse neuroserpin	AI363545
<i>Trichostrongylus spiralis</i>	<i>Ts</i> 11-1	42 kDa	Intracellular	Muscle larvae	Trypsin	(Nagano et al. 2001)
<i>Trichostrongylus vitrinus</i>	<i>Tv</i> SERP	42 kDa	Intracellular	All life cycle	Elastases, trypsin,	(MacLennan, McLean and Knox 2005)
<b>Trematode serpins</b>						
<i>S. haematobium</i>	<i>Sh</i> serpin	46.2 kDa	Surface	Adult worm	Unknown	(Blanton, Licate and Aman 1994)
<i>S. mansoni</i>	<i>Smpi</i> 56	56 kDa		Adult worms	Neutrophil and pancreatic	(Ghendler, Arnon and Fishelson 1994)
<i>S. mansoni</i>	Contrapsin	68 kDa	Surface and	Male adult worms	Trypsin	(Modha and Doenhoff 1994)
<i>S. japonicum</i>	<i>Sj</i> serpin	45.2 kDa	Surface	Intestinal/epithelium of adult worms and cercariae	Unknown	(Yan et al. 2005)
<i>S. japonicum</i>	<i>Sj</i> B6	60 kDa	secretory	intra-mammalian stage of the parasite	Unknown	(Molehin et al. 2014)
<i>Clonorchis sinensis</i>	<i>Cs</i> proSERPIN	42.2 kDa	Intracellular	Metacercariae	Unknown	(Yang et al. 2009)
<i>Clonorchis sinensis</i>	<i>Cs</i> SERPIN	44 kDa	Intracellular	All life cycle	Chymotrypsin	(Kang et al. 2010)
<i>Paragonimus westermanni</i>	<i>Pw</i> SERPIN	43 kDa	Intracellular	All life cycle	Human neutrophil	(Hwang et al. 2009)
<b>Cestode serpins</b>						
<i>Echinococcus multilocularis</i>	Serpinemu	45 kDa	Intracellular	Oncospheres	Trypsin and elastase	(Merckelbach and Ruppel 2007)
<i>Echinococcus granulosus</i>	Antigen B	12 kDa	Secretory	Protoscolex	Porcine elastase	(Shepherd, Aitken and McManus 1991)
<b>Nematode Smapins</b>						
<i>Anisakis Simplex</i>	<i>ASPI</i> -1				Elastase	(Lu et al. 1998, Nguyen et al. 1999)
<i>Anisakis Simplex</i>	<i>ASPI</i> -2				Elastase	(Lu et al. 1998, Nguyen et al. 1999)
<i>Ancylostoma caninum</i>	<i>Ac</i> AP5				Factor Xa, XIa	(Stassens et al. 1996)
<i>Ancylostoma caninum</i>	<i>Ac</i> AP6				Factor Xa	(Stassens et al. 1996)
<i>Ancylostoma caninum</i>	<i>Ac</i> APc2				Factor VIIa/TF	(Stassens et al. 1996)
<i>Ascaris suum</i>	ICE1				Chymotrypsin, elastase	(Huang et al. 1994)
<i>Ascaris suum</i>	ICE2-5				Chymotrypsin, elastase	(Huang et al. 1994)
<i>Ascaris suum</i>	ITR1				Trypsin	(Grasberger, Clore and Gronenborn 1994)
<i>Ascaris suum</i>	ITR2				Trypsin	(Grasberger et al. 1994)
<i>Onchocerca volvulus</i>	<i>Ov</i> -SPI-1					(Lizotte-Waniewski et al. 2000)
<i>Onchocerca volvulus</i>	<i>Ov</i> -SPI-2					AA618955, OVAA94747,
<i>Trichuris suis</i>	<i>Ts</i> -CEI				Chymotrypsin, elastase, chymase, cathepsin G	(Rhoads et al. 2000a)
<i>Trichuris suis</i>	<i>Ts</i> -TCI				Chymotrypsin, trypsin	(Rhoads, Fetterer and Hill 2000b)

## 1.4 Type 2 immunity and IL-33

### 1.4.1 Helminths induce TH2 responses

Epithelial cells (ECs) provide the very first barrier in the host against environmental pathogens, as well as commensal bacteria and inhaled or ingested antigens (Figure 1.7). ECs can recognize these via a number of different mechanisms. They can express pattern recognition receptors (PRRs) such as Toll-like receptors (TLRs) (Abreu 2010) to respond to not only type-1 associated ligands, but also type-2-cell-mediated stimuli (Hammad and Lambrecht 2015). Thanks to the expression of protease-activated receptors (PARs), they can also recognize proteases produced by pathogens to gain entry into host tissues (Chiu et al. 2007, Park et al. 2011). PARs belong to a subfamily of G protein-coupled receptors, including four members PAR-1, PAR-3, and PAR-4 (activated by thrombin) and PAR-2 (activated by trypsin) (O'Brien et al. 2001, Macfarlane et al. 2001). It was suggested that PAR2 is a recognition receptor for the *N. brasiliensis* proteases, trypsin and trypsin-like enzymes (Devlin, Gasser and Cocks 2007). Experiments with PAR2 deficient mice has shown that *T. spiralis* infection could not evoke TH2 responses characterized by markedly low level of TH2 cell-secreted cytokines IL-4, IL-5, and IL-13 (Park et al. 2011).

Barrier ECs mount a set of prototypical innate cytokines such as interleukin-1 (IL-1), IL-25, IL-33, and thymic stromal lymphopoietin (TSLP), as well as the danger-associated molecular patterns (DAMPs) or alarmins, uric acid (UA), ATP, High Mobility Group Box 1 (HMGB1), and S100 family proteins, that activate a range of target cell populations, including dendritic cells (DCs) to promote adaptive TH2 cell immunity (Hammad and Lambrecht 2015).

Type 2 innate lymphoid cells (ILC2s), previously named “nuocytes”, are another innate cell population discovered to respond *in vivo* by expansion after administration of IL-25, IL-33, and TSLP (Fallon et al. 2006, Neill et al. 2010, Saenz, Noti and Artis 2010, Salimi et al. 2013). ILC2s have been shown to be required for the induction of type 2 immune responses, producing IL-5 and IL-13 long before TH2 cells (Fallon et al. 2006). IL-33 and IL-25 can induce different types of ILCs. It has been shown that IL-33 can induce ILC2s while IL-25 prefers to elicit multi potent progenitor (MPP) type 2 cells (Saenz et al. 2010). However, ILC2s

and TH2 cells interact repeatedly in promoting type 2 immune responses and contributing to helminth expulsion, reflecting an ongoing dialogue between the innate and adaptive arms of the immune system (Oliphant et al. 2014, Huang et al. 2015).

Multiple effects occur subsequently in response to IL-4, IL-5 and IL-13 produced by ILC2s and TH2 cells (Figure 1.7). In the intestinal and airway smooth muscle, IL-33 can cause hyper-contractility of the smooth musculature. In the gut, IL-13 promotes goblet cell differentiation and enhance mucin secretion, which is crucial for intestinal nematode rejection (Hasnain et al. 2011, Allen and Maizels 2011). The intestinal epithelium also produces resistin-like molecule- $\beta$  (RELM $\beta$ ), which is an innate protein with direct anti-helminth activity that impairs the function of the worm chemosensory apparatus (Artis et al. 2004). IL-4 and IL-13 also drive the alternative activation of macrophages (AAM) for immunity to parasites as demonstrated by their ability to trap tissue larvae of *H. polygyrus* (Anthony et al. 2006). In the infected gut, mucosal mast cells expand and release mast cell proteases that can degrade tight junctions, increasing fluid flow as part of the “weep and sweep” response that aids in parasite expulsion (Allen and Maizels 2011).

In the non-mucosal tissues, basophils produce high levels of IL-4 and significantly amplify type 2 responses during helminth infection (Ohnmacht et al. 2010). In tissues such as the lung and intestinal lamina propria, IL-4R $\alpha$ -dependent alternative activation of macrophages induces the production of arginase 1, chitinase 3-like proteins 3 (YM1) and 4 (YM2) and RELM $\alpha$ . While the function of YM-1/YM-2 and RELM $\alpha$  is less clear, the latter has been reported to mediate a feedback inhibition of TH2 responses *in vivo* (Chen et al. 2016).

In humoral immunity, TH2 cells and the type 2 cytokines are integral to the induction of the antibody class switch to IgG1, IgE and IgG4 (in humans) isotype antibodies in B cells (Xu et al. 2012).

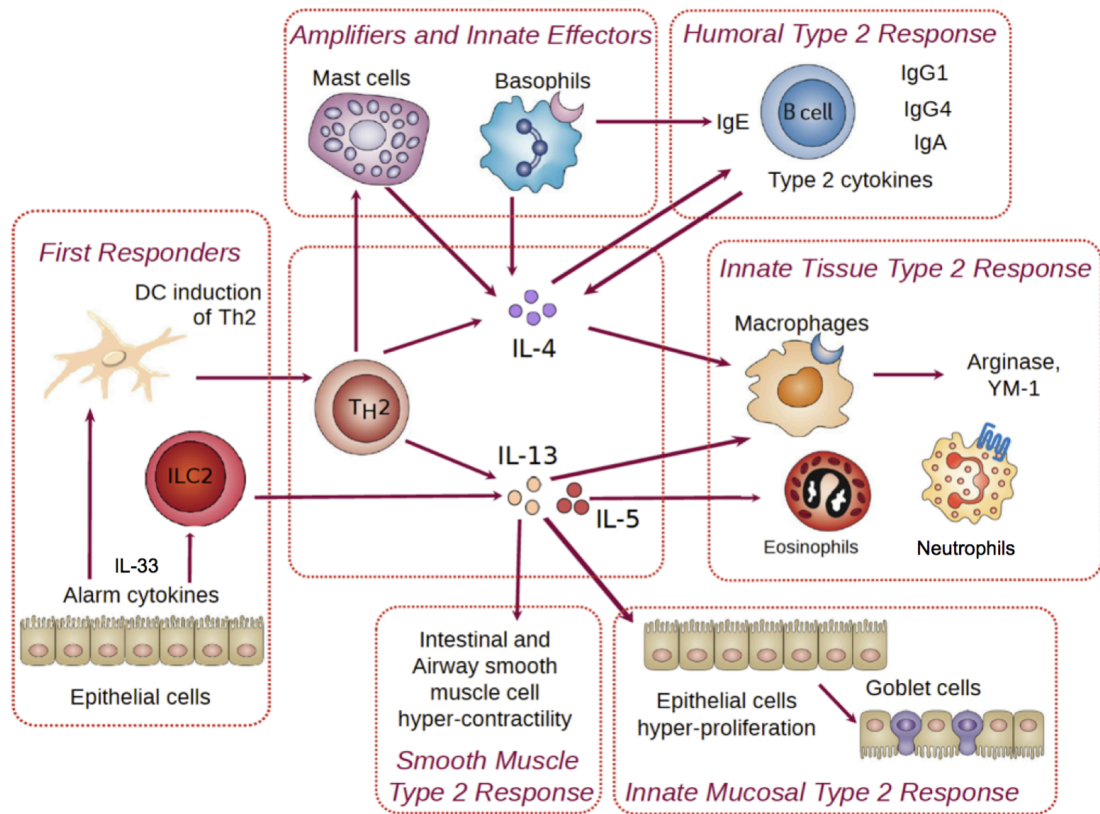


**Figure 1.7: Type 2 immune response induced by helminth.**

Upon helminth infection, the host immune system is activated, alarmin cytokines like IL-33 induce ILC2s and DCs to initiate TH2 cell differentiation. The type 2 immune response activates a range of diverse cell types, including mast cells, eosinophils, basophils, neutrophils and macrophages, which differentiate into alternatively activated macrophages. In humoral immunity, the class switch of B cells to IgG1, IgG4 or IgE is induced. In addition, the airway and intestinal smooth muscle cells and the mucosa are activated to help expulsion of parasites. Ig, immunoglobulin; IL, interleukin; ILC2: Type 2 innate lymphoid cell; DC: Dendritic Cell; YM-1, chitinase-like secreted protein (adapted from Allen and Maizels, 2011 and Kemter PhD thesis).

The main function of IgE is immunity against helminth parasites (Erb 2007) such as *Trichinella spiralis* (Watanabe, Bruschi and Korenaga 2005) and *Fasciola hepatica* (Pfister et al. 1983). IgE is able to kill schistosome larval stages via antibody-dependent cellular cytotoxicity mechanisms (Fitzsimmons et al. 2007), and is involved in vaccine-mediated protection against larval *Onchocerca volvulus* in mice (Abraham et al. 2004). IgE is also utilized during immune responses against a few protozoan parasites such as *Plasmodium falciparum* (Duarte et al. 2007).

Moreover, IgE plays an essential role in type I hypersensitivity (Gould et al. 2003), which manifests in a wide range of allergic diseases: allergic asthma, food allergies and atopic dermatitis and so on. Beside this, IgE also plays an important role in responses to allergens.

#### 1.4.1.1 Mast cells

Mast cells originally develop in the bone marrow, then migrate as immature precursors to peripheral tissues, especially skin, intestine and airway mucosa where they mature. Mast cells are considered to play at least three important roles in host defense. First, their location close to body surfaces allows them to recruit swarms of cells both pathogen-specific (such as antigen-specific lymphocytes) and nonspecific effector cells (such as neutrophils, macrophages, basophils and eosinophils) to sites where infectious agents are most likely to enter. Secondly, the flow of lymph (from sites of antigen deposition to the regional lymph nodes) is increased by the inflammation they cause, activating naive lymphocytes as soon as possible. Thirdly, mast cell products are able to trigger muscular contraction, contributing to the physical expulsion of pathogens from the lungs or the gut (Murphy and Weaver 2016).

Mast cells and IgE can work together and enhance host resistance to parasites (Galli and Tsai 2010). It was demonstrated that both mast cells and intact IgE are required for better resistance to a secondary infection of the skin of WBB6 F1-W/W<sup>v</sup> mice with larval *Haemaphysalis longicornis* ticks (Matsuda et al. 1990). Mast cells also play a role in the clearance of intestinal parasites by the accumulation of mast cells in the intestine, known as mastocytosis, that accompanies helminth infection. The W/W<sup>v</sup> mutant mice, which have a profound mast-cell deficiency caused by a mutation in the gene c-kit, show impaired clearance of the intestinal nematodes *Trichinella spiralis* (Knight et al. 2000) and *Strongyloides species* (Abe and Nawa 1987, Lantz et al. 1998).

Mouse mast cells, enhanced by TH2 cells, constitutively express ST2 (IL-33 receptor). Mast cell secreted proteases can cleave human and murine IL-33 into mature forms, and this will be discussed in more detail in section 1.4.4.

#### 1.4.1.2 Eosinophils

Eosinophils are enhanced by TH2 cells. During the defense against certain types of multicellular parasites, particularly helminths, host immunity is strongly associated with IgE production and the presence of many eosinophils (eosinophilia) in blood and tissues. Depletion of eosinophils in mice using polyclonal anti-eosinophil serum enhances the severity of infection with *Schistosoma mansoni* (Mahmoud, Warren and Peters 1975). In some cases, eosinophils induced by IL-5 play an important role in the termination of the parasites too large to be engulfed and seem to be directly responsible for helminth expulsion: examination of infected tissues shows accumulated and degranulated eosinophils adhering to helminthes larvae (Moqbel 1980, Lange et al. 1994), and *in vitro* experiments have shown that “fully activated” eosinophils can kill *S. mansoni* in the presence of anti-schistosome IgG (IgG1 and IgG3) antibodies (Khalife et al. 1989). However, eosinophils are suggested to preserve parasite growth and survival (e.g. *Trichinella spiralis*) by promoting accumulation of TH2 cells and preventing macrophage and neutrophil induction of NO synthase (Gebreselassie et al. 2012).

#### 1.4.1.3 Neutrophils with helminths infection

Neutrophils, formed from stem cells in the bone marrow, are the most abundant type of granulocytes and the most numerous type of white blood cells, and with a short lifespan of only 6–8 hours (L Makepeace et al. 2012). Neutrophils are known to be involved in “Type 3” responses characterized by the actions of group 3 ILCs (ILC3), TH17 cells, opsonizing IgG isotypes and responding mainly to extracellular bacteria and fungi. However, back in 2000, neutrophils were found to mediate worm control in murine filariasis and this neutrophil accumulation was IL-5 dependent (Al-Qaoud et al. 2000). Recently, two further studies have shown that neutrophils are involved in helminth expulsion (Chen et al. 2014, Sutherland et al. 2014). It has also been suggested that neutrophils can sense the size of pathogens and could release neutrophil extracellular traps (NETs) upon large pathogens, enabling neutrophils to help catch and kill them (Branzk et al. 2014).

#### 1.4.2 IL-33 Initiates Type 2 Immune Responses

IL-33, is an alarmin cytokine, it is stored in the nucleus of endothelial cells and epithelial cells. During programmed cell death (apoptosis), IL-33 is cleaved by

caspases into an inactivated form, whereas in contrast it is released as an active full-length (FL) protein during necrosis. Serine proteases, cathepsin G and elastase secreted by recruited neutrophils, are able to cleave FL-IL-33 resulting in a mature product with approximately 10-fold higher bioactivity. Mature bioactive IL-33 then initiates a type 2 and/or inflammatory response from a range of target cell populations expressing the IL-33R (in mice designated as T1/ST2) in Figure 1.8 (Lefrançais and Cayrol 2012).

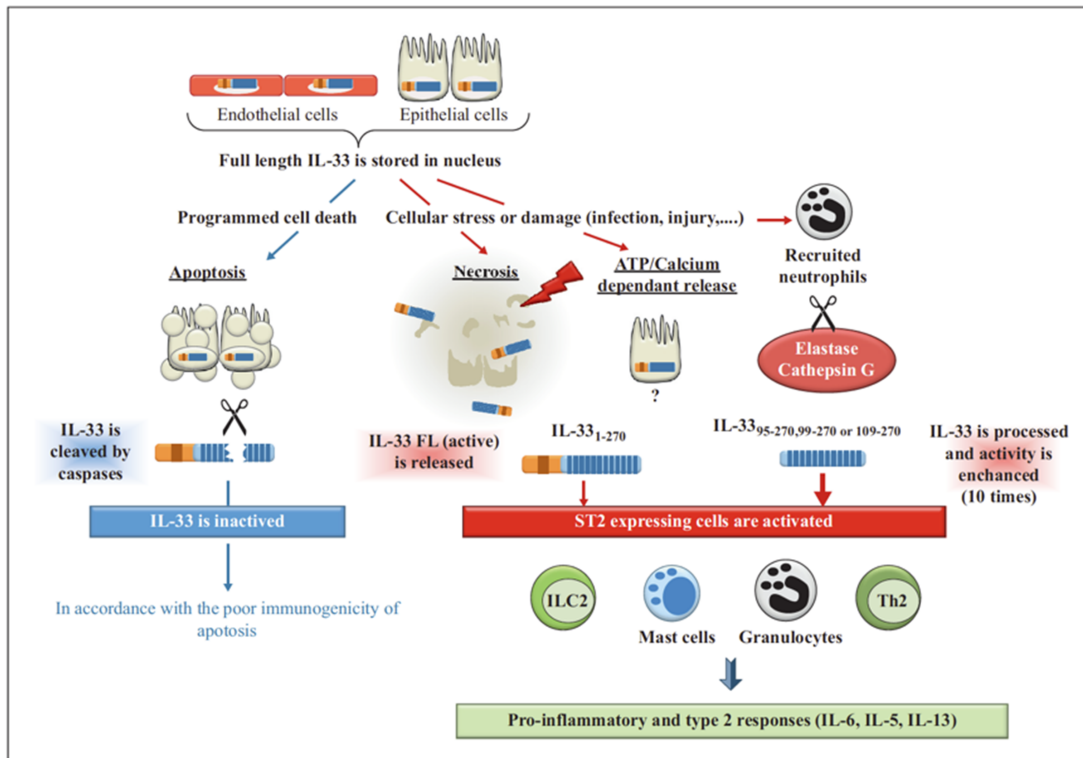


**Figure 1.8: Type 2 immune response initiation by IL-33.** From Lefrançais and Cayrol, 2012.

### 1.4.3 IL-33

Interleukin-33 is the latest member of the IL-1 cytokine family, discovered originally as a nuclear factor present in endothelial cells, and first designated NF-HEV (nuclear factor from high endothelial venules)(Girard et al. 2003). Two years later, it was re-identified as the extracellular ligand for the prominent orphan IL-1 receptor ST2, and named IL-33 (Schmitz et al. 2005). Healthy mice and human share constitutive IL-33 expression, primarily in nuclei of non-hematopoietic cells (Schmitz et al. 2005), most abundant in epithelial and endothelial cells (Moussion, Ortega and Girard 2008, Pichery et al. 2012). The major target cells of IL-33 are the innate lymphoid cells type 2 (ILC2) which are involved in the initiation of T helper cell 2 (TH2) immune responses, but many other immune system cells from macrophages to memory TH2 cells express ST2 and can respond to IL-33 (Lefrançois and Cayrol 2012).

### 1.4.4 IL-33 Mature process by proteases

Full-length murine and human IL-33 are transcribed from seven coding exons, which express an approximately 32-kDa protein of 266 and 270 amino acids, respectively (Molofsky, Savage and Locksley 2015). Exons 1–3 encode the N-terminal domains (amino acids 1-109 in mouse; 1-95 in human) required for IL-33 nuclear localization, whereas exons 4–7 (amino acids 109–266 in mouse, 95-270 in human) encode the C-terminal IL-1-like cytokine domain, which binds to the IL-33 receptor ST2, thus facilitating recruitment of IL-1RAcP to induce the canonical NF- $\kappa$ B signalling pathway(Carriere et al. 2007).

Other members of the IL-1 family such as IL-1 $\beta$  and IL-18 have to be cleaved from their pro-forms by caspases in order to be active and to initiate signalling via IL-1/IL-18R. Interestingly, IL-33 is a divergent member of the IL-1 family as other members are cleaved and activated by caspase-1 while the N-terminal portion of IL-33 does not require cleavage by caspase 1 for release from the cell nucleus or to bind to their receptor (Cayrol and Girard 2009). In contrast, if the C-terminal IL-1- like domain of IL-33 is processed by apoptotic caspase-3 and caspase-7, the result is to inactivate IL-33, and ablate its ability to bind the ST2 receptor (Cayrol and Girard 2009, Lüthi et al. 2009).

IL-33 is also distinct from other members of the IL-1 family, as it is reported that full-length human IL-33<sub>1-270</sub> is active (unlike IL-1 $\beta$  and IL-18) (Cayrol and Girard

2009) but activity is greatly enhanced when cleaved by inflammatory cell neutrophil serine proteases cathepsin G and elastase (Lefrançois et al. 2012). Using a combination of *in vitro* and *in vivo* approaches, Lefrançois et al. demonstrate that full-length human IL-33<sub>1-270</sub> is cleaved into mature forms IL-33<sub>95-270</sub>, IL-33<sub>99-270</sub>, and IL-33<sub>109-270</sub> approximately 18 and 21 kDa in size, processed by these two neutrophil serine proteases. These forms have a 10-fold higher potency than full-length IL-33 in cellular assays or to activate ST2. They found murine neutrophil cathepsin G and elastase can also cleave full-length murine IL-33 into mIL-33<sub>102-266</sub> with 20kDa, and detected both full-length and cleaved endogenous IL-33 in the bronchoalveolar lavage fluid (BAL) in an *in vivo* model of acute lung injury associated with neutrophil infiltration. Furthermore, they suggested that independently active full-length IL-33 might act as an endogenous danger signal or alarmin to alert cells of the innate immune system to tissue damage during trauma or infection (Cayrol and Girard 2009, Lefrançois et al. 2012).

It is worth noting that the central cleavage domain of IL-33 (amino acids 66–111) might act as an important functional domain. It has been further studied that serine proteases, chymase and tryptase, secreted by activated mast cells cleave central domain of IL-33 for potent activation of group-2 innate lymphoid cells. *Ex vivo* experiments demonstrated that the mature forms of IL-33 produced by mast cell proteases were 30-fold more effective than FL-IL-33 for activation of ILC2s. By characterizing the level of IL-5 and IL-13 *in vivo*, it has been shown that these mature forms of IL-33 induced a strong expansion of ILCs and eosinophils. In addition, Lefrançois et al. demonstrated that mast cell tryptase also cleaves murine FL-IL-33 and IL-33-dependent allergic airway inflammation was reduced by a tryptase inhibitor *in vivo* (Lefrançois et al. 2014). Table 2 summarizes, for human and mouse IL-33, the relevant enzymes, their cleavage fragments and the activity of different fragments.

**Table 2. Human and mouse IL-33 and their cleavage by different enzymes**

Full-length IL-33	Enzymes	Cleavage fragments	Activity	Reference
Human IL-33 1-270	Caspase-1	112-270	Inactivated	Schmitz et al. 2005
	Caspase-1 & 3	1-178, 179-270	Inactivated	Cayrol and Girard,2009; Martin and Martin,2016
	Cathepsin G (neutrophils)	95-270 & 109-270	10 fold	Lefrancais et al. 2012
	Elastase (neutrophils)	99-270	10 fold	
	Chymase (mast cells)	95-270 & 109-270	30 fold	Lefrancais et al. 2014
	Tryptase (mast cells)	107-270,79-270 & 72-270	30 fold	
	Granzyme B (mast cells)	111-270	Not known	
Mouse IL-33 1-266	Caspase-1 & 3	176-266	Not known	Cayrol and Girard, 2009
	Neutrophil Cathepsin G	102-266	Not known	Lefrancais et al. 2012
	Neutrophil Elastase	102-266 & 109-266	Not known	
	Tryptase (mase cells)	Not known	Not known	Lefrancais et al. 2014

#### 1.4.5 IL-33/ST2 signaling

The IL-33 receptor ST2, expressed by T helper 2 (TH2) cells and mast cells, has two forms including a soluble form (sST2) and a longer membrane-bound receptor form (ST2L) (Molofsky et al. 2015). IL-33 is a nuclear cytokine *in vivo*, which is always found in the nucleus of cells expressing the protein in both human and mouse tissues (Pichery et al. 2012, Moussion et al. 2008, Cayrol and Girard 2014). During cell damage or mechanical injury associated with necrosis or necroptosis (a form of “programmed necrosis”, a new model of cell death, shown the morphological

features of necrosis but highly regulated by an intracellular protein platform like apoptosis (Vandenabeele et al. 2010), biologically active full-length IL-33 is released from the nucleus into the extracellular environment. Once released into the extracellular spaces, full-length IL-33 can be further processed by serine proteases, such as neutrophil cathepsin G, elastase and mast cell chymase and tryptase into mature bioactive forms. sST2 binds free IL-33, decreases the concentration of IL-33 and restricts its availability for ST2L binding. Both full-length and cleaved mature IL-33 bind to ST2L in combination with the IL-1 receptor accessory protein (IL-1RAcP) on target cells, to activate NF- $\kappa$ B and mitogen-activated protein kinase (MAPK) signalling pathways leading to cellular activation and proliferation (Figure 1.9). The myeloid differentiation factor 88 (MyD88) and downstream TNF receptor-associated factor 6 (TRAF-6) are both required for intact IL-33 signaling (Kakkar and Lee 2008, Molofsky et al. 2015).

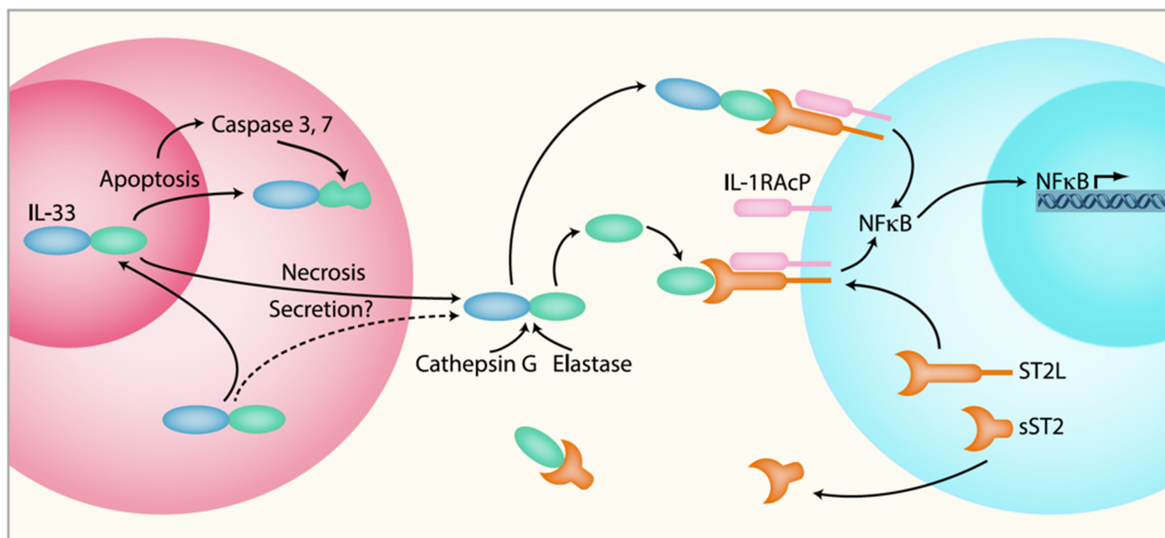


**Figure 1.9: IL-33/ST2 signalling.** From Molofsky et al, 2015.

#### 1.4.6 IL-33 and helminth infection

Previous findings show IL-33 is critically involved in developing the initial TH2 response to helminth infections, and peak expression was observed at early time points, indicating that prompt release of the alarmin cytokine IL-33 is a potent signal for type 2 response initiation.

In the mouse, infection with *Nippostrongylus brasiliensis* (Moro and Koyasu 2010), *S. mansoni* (Townsend et al. 2000) and *T. muris* (Humphreys et al. 2008) each cause IL-33 release and activation of ILC2s and TH2 cytokine production. Using IL13-eGFP reporter mice in the absence of IL25 and IL33 signaling, nuocytes were unable to expand, leading to a defect in expulsion of *N. brasiliensis* (Neill et al. 2010); In IL-4 and IL-13 reporter mice, lineage-negative innate cells, which arise during type 2 immunity or in response to IL-25 and IL-33 *in vivo*, expand robustly in response to exogenous IL-25 or IL-33 and after infection with *N. brasiliensis* (Price et al. 2010), suggesting that IL-33 might cooperate with the parasite-induced TH2 cells or other epithelial cytokines, including IL-25, to mediate helminth worm expulsion. ST2 deficiency but not MyD88 deficiency in mice significantly alter larval burdens in the muscle tissue after *T. spiralis* infection, which suggests IL-33 signaling limited worm encystation in muscle (Scalfone et al. 2013).

Administration of exogenous IL-33 leads to worm expulsion of *H. polygyrus* (Yang et al. 2013), *N. brasiliensis* (Bouchery et al. 2015), *Strongyloides venezuelensis* (Yasuda et al. 2012), and *T. muris* (Humphreys et al. 2008). Exogenous IL-33 treated mice were successful at expelling worms, expulsion of which was associated with the development of a protective TH2 response with increased expression of TH2 cytokines IL-4, IL-9, and IL-13, elevated goblet cell numbers, and increased levels of serum IgE (Humphreys et al. 2008).

Further studies utilizing IL-33R-deficient mice supported the role for IL-33 in the promotion of TH2 cytokine responses. IL-33R-deficient mice (ST2<sup>-/-</sup> mice), which lack the extracellular domain common to both the soluble sST2, the membrane-bound form ST2L and thus lack the IL-33 signaling pathway.

Townsend et al. demonstrated that ST2<sup>-/-</sup> mice failed to induce a TH2 response *in vivo* and form granulomas after intravenous injection of *S. mansoni* eggs (Townsend et al. 2000). Mice lacking the IL-33 signaling pathway were observed to have a defect in the induction of type 2 responses to helminth parasites and are more susceptible to infection with *L. sigmodontis* (Ajendra et al. 2014), *N. brasiliensis* (Hung et al. 2013), and *T. spiralis* (Scalfone et al. 2013). Using *L. sigmodontis* infected mice, the absence of ST2 was proven to lead to significantly increased levels of peripheral

blood microfilariae, the filarial progeny, whereas adult worm burdens were not affected (Ajendra et al. 2014).

Thus the IL-33 signaling pathway is likely to be a primary target for parasitic helminth immunomodulation, to allow continuous infection and re-infection. In fact, it was recently demonstrated that the excretory/secretory products of *H. polygyrus* (HES) significantly inhibit the IL-33 pathway, both by suppressing IL-33 release (McSorley et al. 2014) and by suppressing expression of the IL-33 receptor IL1RL1/ST2 (Buck et al. 2014) resulting in decreased type 2 cytokine responses and ablated inflammation in a mouse model of asthma. Further studies revealed that the functional parasite secreted protein Hp-ARI (Alarmin Release Inhibitor) was able to profoundly inhibit IL-33, by binding both mouse IL-33 and human IL-33, and tethering it within the cell, preventing release (Osbourn et al. 2017). Whether these pathways of immunomodulation are common to numerous parasitic helminths, or unique to the chronically infective *H. polygyrus*, remains to be researched (Maizels and McSorley 2016).

## 1.5 Hypotheses and aim of this thesis

### Can *Bm*-SPN-2 block IL-33 cleavage processed by neutrophil cathepsin G and elastase?

It is mentioned above that full-length human IL-33<sub>1-270</sub> is cleaved into 10-fold higher activity mature forms IL-33<sub>95-270</sub>, IL-33<sub>99-270</sub>, and IL-33<sub>109-270</sub> processed by neutrophil serine proteases cathepsin G and elastase, as well as mouse IL-33. Furthermore, independently active full-length IL-33 might act as an endogenous danger signal or alarmin to alert cells of the innate immune system to tissue damage during trauma or infection (Cayrol and Girard 2009, Lefrançois et al. 2012).

Based on all of the aforementioned information, the proposed hypothesis is that the function of *Bm*-SPN-2 is to inhibit human and murine full-length IL-33 cleavage into mature active IL-33 processed by murine and human neutrophil serine proteases (cathepsin G and elastase), thereby inhibiting the host alarm signal.

### Can *Bm*-SPN-2 inhibit TH2 initiation?

It was reported by two independent laboratories that injecting live Mf intraperitoneally into mice first induces a TH1 immune response; splenocytes restimulated with parasite

antigen showed enhanced IFN- $\gamma$  production and reduced quantities of the TH2-type cytokines IL-4 and IL-5 (Pearlman et al. 1993, Lawrence et al. 1994). Also, a TH1 response to intravenously administered Mf has been reported ((Lawrence, Allen and Gray 2000). On the contrary, a TH2-dominated response elicited when adult parasites were implanted. This pattern is unusual as most helminths - including adult *B. malayi* - are the prototypic inducers of TH2 responses (Allen and Maizels 2011).

As the most abundant protein in ES of Mf, *Bm*-SPN-2 might play a role in boosting the TH1 immune response. The Maizels group revealed that mice infected with *B. malayi* Mf mounted a strong, but short-lived *Bm*-SPN-2-specific TH1 response with significant increases in IFN- $\gamma$  production, but this was replaced by a TH2-dominated response to other Mf antigens after 28 days (Zang et al. 1999, Zang et al. 2000).

Considering that *Bm*-SPN-2 drives TH1 responses in mice and IL-33 drives TH2 response (Schmitz et al. 2005), we infer that *Bm*-SPN-2 could inhibit TH2 initiation by blocking IL-33 cleavage.

### Can Mf number enhance in ST2 deficient mice?

Using *L. sigmodontis* infected mice, a recent paper reported that in the absence of ST2, the IL-33-specific subunit of the IL-33 receptor, led to significantly increased levels of peripheral blood microfilariae, the filarial progeny, whereas adult worm burden was not affected (Ajendra et al. 2014). This study demonstrated that ST2 is required to control the number of microfilariae but was not essential for the TH2 immune response.

Considering that ST2 is the receptor for IL-33, it is interesting to repeat this experiment using wild type (WT) and IL-33R-deficient mice infected with *B. pahangi* microfilariae instead of *L. sigmodontis*. The number of microfilariae between WT and ST2 deficient mouse groups is counted. It is hypothesized that IL-33R deficiency will enhance the number of microfilariae compared to the WT group.

### Aim of this thesis

In this study, we aim to further understanding of the relationship between parasites and their host and the mechanisms by which microfilariae avoid host immune responses. The ultimate aim of this study is to evaluate if *Bm*-SPN-2 is a strong candidate for drug or vaccine development, on the basis of its immune function.



# CHAPTER 2

## Materials and Methods

### 2.1 Cell culture

Human alveolar basal epithelial cells (A549 cells, a human lung cancer cell line, was first established in 1972 by D. J. Giard et al.) (Giard et al. 1973) were kindly provided by Henry McSorley, and cultured in Dulbecco's Modified Eagle Medium DMEM containing 10% FBS.

Human embryonic kidney 293T (HEK 293T) cells were obtained from liquid nitrogen stocks of the Maizels lab. Cells were maintained in complete Dulbecco's Modified Eagle Medium DMEM high glucose containing 10% FBS (Thermo Scientific Hyclone No.: 30014.03), 5 ml Pen/Strep (stock 10,000 I.U. Penicillin and 10,000 mg/ml streptomycin) Thermo Scientific Hyclone No.: SV30010) 5 ml L-glutamine (stock 200 mM L-Glutamine, final concentration 1 mM) (Thermo Scientific Hyclone No.:SH30034.01)

SP2 cells were also obtained from liquid nitrogen stocks of the Maizels lab, originally purchased from The European Collection of Authenticated Cell Cultures (ECACC). SP2 cells were growing in complete Roswell Park Memorial Institute (cRPMI) 1640.

cRPMI=500ml RPMI+5ml L-Glutamine+5ml Penicillin/Streptomycin+50ml FBS.

Hybridoma cells were cultured in complete hybridoma media:

- 500ml RPMI with 20% special FCS (Hyclone Fetalclone 1 SH30080.03)
- 5ml Penicillin/Streptomycin and 5ml L-Glutamine
- HAT (hypoxanthine-aminopterin-thymidine medium): Hypoxanthine 6.8 mg; Aminopterin 0.088 mg; Thymidine 1.94 mg for 500ml culture media.

• OPI Media Supplement Hybri-Max™: 0.15 g oxaloacetate, 0.05 g pyruvate, and 0.0082 g insulin. Reconstitute contents of vial with 10 mL sterile water. Use 5ml for 500ml culture media to make a final working concentration: 1 mM oxaloacetate, 0.45 mM pyruvate, 0.2 U/ml insulin.

**Note:** For monoclonal antibody purification from cells grown in flasks, hyclone special FCS in the medium was replaced with ultra low IgG fetal bovine serum (Thermo Scientific).

The mast cell line MC/9 ATCC (CRL-8306) was kindly provided by Lefrançois et al. Cells were grown up in Dulbecco's Modified Eagle's Medium DMEM (ATCC 30-2002) with 4 mM L-glutamine adjusted to contain 4.5 g/L glucose and 1.5 g/L sodium bicarbonate and supplemented with 2 mM L-glutamine, 0.05 mM 2-mercaptoethanol, 10% Rat T-STIM (Becton Dickenson Catalog No. 354115) and 10% fetal bovine serum (FBS 30-2021).

For mast cell stimulation experiment, cleaved or full-length IL-33 was mixed with  $1$  or  $2 \times 10^5$  cells (in 96-wells plates, 200  $\mu$ l/well) and incubated for 24h at 37°C. Supernatant was then harvested for IL-6 ELISA.

All cells were grown at 37°C with 5% CO<sub>2</sub> and 95% humidity. All cells were counted on a haemocytometer under Leica DM2000 LED microscope.

## 2.2 Parasites and Experimental Animals

### 2.2.1 Parasites

*Brugia pahangi* microfilariae were kindly provided by Professor Eileen Devaney, University of Glasgow. Jirds (*Meriones unguiculatus*) were infected with 250 *Brugia pahangi* L3; microfilariae (Mf) were recovered from the peritoneal cavity of infected jirds 4 months later. Microfilariae were washed extensively in Hanks' Balanced Salt Solution (HBSS). Histopaque-1077 (Sigma) was used to purify Mf from host cells by density centrifugation at 1,000 RCF for 15 mins without brake (Osborne 1997). Mf were then resuspended in HBSS and counted.

### 2.2.2 Experimental Animals

Wild-type BALB/c mice and Sprague/Dawley rats were bred in house at the University of Edinburgh and accommodated according to Home Office regulations. Eight-week-old female BALB/c mice were utilized for the *Alternaria* airway allergy

model (see Section 2.3.1). Two male Sprague/Dawley Rats and two female BALB/c mice were immunized with *Bm*-SPN2 protein to generate polyclonal and monoclonal antibodies, respectively.

T1/ST2 (IL-33 receptor, abbreviated to ST2) deficient mice (Townsend et al. 2000) were bred and maintained at the University of Edinburgh animal facilities, kindly provided by Henry McSorley, University of Edinburgh. ST2-deficient mice and BALB/c mice were used for *Brugia pahangi* microfilariae infection experiments.

## 2.3 *In vivo* procedures

### 2.3.1 *Alternaria* Airway allergy model

: To test the effects of *Bm*-SPN-2 on allergy, *in vivo* experiments delivered *Alternaria alternatus* antigen (Greer) with or without *Bm*-SPN-2 by the intranasal route.

Mice were lightly anaesthetised using isoflurane. 50 µl PBS containing 40 µg LPS-depleted *Bm*-SPN-2 protein or 50 µl PBS alone was administered intranasally 0.5 hour prior to PBS containing 50 µg *Alternaria* or 50 µl PBS alone (Figure 5.5A). 1 hour later, mice were culled by cervical dislocation, and lungs were taken for further experimentation, including release of IL-33 measured by ELISA (section 2.8) and anti-IL-33 western blotting (section 2.5.3).

### 2.3.2 Microfilariae infection experiment

ST2-deficient and BALB/c mice were injected intraperitoneally (i.p.) with 150,000 *Brugia pahangi* microfilariae (Mff). Uninfected ST2<sup>-/-</sup> and BALB/c mice were set as controls. Mice infected with microfilariae were sacrificed by terminal anaesthesia with CO<sub>2</sub> on day 1 and day 6 post infection, uninfected mice were culled on day 6 (the experimental plan is shown in Figure 5.8A). Peritoneal lavage of each mouse was performed by injecting 5 ml 4°C HBSS immediately after cull, the first three 5ml peritoneal lavage were harvested for the Mff counting and ELISA analysis. Mesenteric lymph nodes (mLN) were collected into 1 ml RNAlater (Qiagen) and spleens were weighed, followed by cytokine ELISA of peritoneal lavage, real-time PCR of mLN and comparison of spleen weight. Microfilariae were harvested, purified and counted from peritoneal lavage to assess the effect of ST2 receptor deficiency on Mff infection. An in-house made glass chamber was used to count live

microfilariae from 20 µl samples.

### 2.3.3 Polyclonal and monoclonal antibody production against *Bm*-SPN-2

#### 2.3.3.1 Polyclonal antibody preparation

Two rats were each immunized with 100 µg of *Bm*-SPN-2 in alum by intraperitoneal (i.p.) injection. In order to prepare antigen in Alum, 15ml Falcon was used. An amount of 200 µg *Bm*-SPN-2 was added into 1ml PBS. Step by step, 1ml of 9% alum and 2 drops of phenol red were added and mixed. Next, drops of 1M NaOH were added and mix well by vortex each time until colour is pretty luminous pink. The whole mix sample was placed onto a rotating mixer at room temperature for 30 minutes. Finally, sample mix in 15ml falcon tube was centrifuged at 3000 x g for 10 minutes and washed three times with PBS. The pellet was made up to 1ml with PBS, 0.5ml mixture was injected per rat by i.p. Rats were boosted with 20 µg *Bm*-SPN-2 in alum i.p. 28 days later. A second boost was given with 20µg *Bm*-SPN-2 in alum i.p. one week later. Rats were bled out after another week. Blood was left in fridge overnight and allowed to coagulate. Sera was taken by directly collecting the fluid phase from the coagulated blood and stored at -80°C until use.

#### 2.3.3.2 Monoclonal antibody screening

Two BALB/c mice were immunized by i.p. injection with 200 µl PBS containing 50 µg of *Bm*-SPN-2 in Alum prepared as above. After 6 weeks, mice were boosted with *Bm*-SPN-2 without adjuvant by intravenously injection (i.v.) for 3 consecutive days with 200 µl PBS containing 1 µg *Bm*-SPN-2. Two days after the final injection, brachial bleeds were taken for polyclonal antisera and following euthanasia, spleens were recovered (workflow of injection is shown in Figure 5.1A). Immediately, spleens were mashed through a 70µm cell strainer using the plunger of a 1ml syringe and washed through with 10mls of culture media. Culture media contains: 500ml Roswell Park Memorial Institute RPMI (Gibco) 50ml FCS Gibco) 5ml L-glutamine Gibco) 5ml Pen-strep (Gibco) 50µl β-mercaptethanol (500mM stock). Cells were washed three times in 50 ml RPMI-1640 media with 0.5ml Penicillin-Streptomycin (P/S) at 350xg for 8mins each time. Cells were resuspended in 2mls of red blood cell lysis buffer (Sigma, #11814389001) and left to lyse for 3-5 minutes at RT. Cells were

then washed again with 50 ml RPMI, resuspended in 10ml RPMI and counted on a haemocytometer.

In parallel, the mouse myeloma cell line Sp2/0-Ag14 (ATCC® CRL-1581™) (SP2) was cultured in cRPMI media; cells from T75 flasks were centrifuged at 350xg for 8mins and resuspended in 20 ml cRPMI and counted on a haemocytometer. For the fusion, immunized spleen cells and SP2 cells were mixed in 1:1 ratio, with  $4 \times 10^7$  of each. A traditional method of making hybridoma cells was applied, the whole strategy and workflow is shown in Figure 5.1. Polyethylene glycol (PEG) was added for cell fusion. 1ml of warmed 50% PEG 1500(w/v) PEG was added drop-wisely over a period 1 min whilst turning tube by vortex to achieve thorough mixing. Then 1ml of RPMI was added by the same way. The total volume was brought up to 20ml with RPMI. Fused cells were centrifuged for 5 min at 500 xg. Cells were resuspended with 200ml complete hybridoma media (See section 2.1) 20% FBS and HAT selection medium and plate 150  $\mu$ l of cell suspension to ten 96-well plates. Multiple hybridoma colonies were then incubated in 96-well plate at 37°C with 5% CO<sub>2</sub>. After 10–14 d postfusion, hybridoma colonies can be observed in the 96-well plates. Wells may contain a single hybridoma colony or multiple hybridoma colonies derived from different independently fused B-lymphocyte/myeloma cells. ELISA screen against r *Bm*-SPN-2 was performed to select the desired well from the 96 wells, and limiting dilution desired wells with complete hybridoma media was followed to obtain clonal population x2 (takes ~2 weeks each). Another two ELISA screens against r*Bm*-SPN-2 were performed to select the final desired well. mAb isotype was determined by ELISA. ELISA was performed by coating r*Bm*-SPN-2 and using mAb candidate as primary antibody and different secondary antibody IgG1-HRP, IgG2a-HRP, IgM-HRP, IgA-HRP or IgE-HRP, with sera from naïve mice as negative control and polyclonal antibody sera as positive control.

### 2.3.3.3 IgG monoclonal antibody purification

Hybridoma cell lines which secreted ELISA-positive monoclonal antibodies were expanded into larger cultures in cRPMI (complete Roswell Park Memorial Institute 1640 =500ml RPMI+5ml L-glutamine+5ml penicillin/streptomycin+50ml ultra low IgG foetal bovine serum) containing ultra low IgG foetal bovine serum (Thermo Scientific) in T175 flasks. Supernatants were harvested, filtered using a Thermo

Scientific™ Nalgene™ Rapid-Flow™ 75mm Filter Unit (0.2µm) and 1:1 diluted into 2x PBS binding buffer. A total of 250ml supernatant was loaded onto a HiTrap Protein G HP 5ml column (GE Healthcare) using a Minipuls 2 peristaltic pump (Anachem). 2ml fractions were eluted with 100% 0.1M glycine Elution buffer and collected into the neutralization buffer 1M Tris base pH9.0 using an AKTA Prime (GE Healthcare, Wisconsin, USA) together with the UNICORN software. Monoclonal antibody purification was confirmed by SDS-PAGE using NuPAGE® 4-12% Bis-Tris Gels and NuPAGE® MES SDS running buffer (Novex®, Life Technologies) and visualized by InstantBlue™ (expedion). In addition, Mff extract and *Bm*-SPN-2 were loaded on a gel and transferred onto blot, the western blotting was then visualized by mAb candidates as primary antibody and polyclonal antibody sera as positive with 1:2000 dilution and also anti-mouse immunoglobulins (P0260 by Dako) as secondary antibody.

## 2.4 Gene cloning and recombinant protein expression

### 2.4.1 Bacteria expression

#### 2.4.1.1 Expression of *Bm*-SPN-2 and *Bm*-SPN2-mCherry

*Bm*-SPN-2 was expressed in (plasmid – pET29) that had been inserted with restriction enzymes *Nde*I and *Xho*I; for the work in this thesis Zang's original protocol and plasmid were used (Zang et al. 1999). This construct used the initiator ATG of the *Nde*I site and omitted the signal peptide sequence of *Bm*-SPN-2 (Amino acid sequence and the structure of *Bm*-SPN-2 is shown in Figure 4.2A).

mCherry-labelled *Bm*-SPN-2: Signal peptide depleted *Bm*-SPN-2 and mCherry were connected with three restriction enzymes *Nde*I at N-terminal, *Not*I and *Xho*I. Sequence was codon optimized for expression in *Escherichia coli* (*E. coli*) and synthesized by GeneArt (See Figure 4.4A). Inserts were reacquired by restriction enzyme double digestion using corresponding restriction enzymes according to the following protocol at 37°C over night.

#### *Nde*I and *Xho*I Digest

dH <sub>2</sub> O	14 µl
DNA	1 µg or 10 µl
CutSmart Buffer	3 µl
restriction enzymes	1.5 µl each

The expression vectors pET29T, pET29c and pET29a vector (Invitrogen) are each linked to six histidine residues for nickel column purification and a kanamycin resistance gene for selection, was digested using the same protocol. Digested insert and vector were purified by DNA gel electrophoresis and the QIAquick<sup>®</sup> Gel Extraction Kit, and ligated by T4 DNA ligase (NEB) over night at 16 °C.

*E. coli* bacterial cell line JM109 cells (Agilent Technologies) were transformed with the above corresponding plasmids by heat shocking 42°C for 45 seconds before adding plasmid, and grown for one hour at 37 °C in 0.9 ml of S.O.C medium (Invitrogen). Colonies were grown overnight on LB agar containing 50 µg/ml of kanamycin, then were expanded into 10ml LB containing the same concentration of antibiotic at 37°C. Plasmid purification was performed by Qiagen miniprep kit, primers for vector T7 promoter and T7 terminator (T7 promoter primer and T7 terminator primer are pET29a vector primer. The sequence of T7 promoter primer: 5'TAATACGACTCACTATAGGG3'; the sequence of T7 terminator reverse primer: 5'GCTAGTTATTGCTCAGCGG3') were used for insert sequencing by The Gene pool, Universtiy of Edinburgh (<http://genepool.bio.ed.ac.uk>) and eurofins (<http://www.eurofins.com>).

BL21(DE3) *E. coli* (Novagen<sup>®</sup>) were then transformed with these plasmids in the above method. Colonies were grown overnight on kanamycin agar plates before expansion into 500 ml LB medium. To determine bacterial growth was in the exponential phase, regular OD600 readings were measured from 1 ml samples of the culture using a photometer (BioPhotometer Eppendorf, Hamburg, Germany). 0.5 ml of 1M inducer IPTG (isopropyl-1--D-galactopyranoside; Melford laboratories, Ipswich, UK) was added when OD600 reached 0.6. Bacterial cultures were then grown for three hours at 37 °C until further experiment.

### 2.4.1.2 Purification of recombinant protein

Large culture pellets were resuspended in BugBuster<sup>™</sup> Protein Extraction Reagent (Novagen). Cells were resuspended in 5 ml BugBuster per gram of wet cell paste. Resuspended cells were incubated on a rotating mixer for 20 min at room temperature. Supernatants were harvested by centrifugation 16,000 xg for 20 min at 4°C, filtered and then loaded onto a 1ml HiTrap<sup>™</sup> Chelating HP column (GE Healthcare) by a Minipuls 2 peristaltic pump (Anachem). The protein was eluted

with 100% His elution buffer using Akta Prime. The protein contents of each 1ml eluted fraction were determined by SDS-PAGE (section 2.3.3.3). One gel was directly stained by InstantBlue™ (expedon) for 1 hour at room temperature. The other gel was then used to transfer separated proteins onto a nitrocellulose membrane (Bio-Rad) with NuPAGE® Transfer Buffer (20X), then the membrane was blocked with blocking reagent (Qiagen) and protein detected using anti-Penta-His HRP Conjugate (Qiagen). Bands were visualized with a FluorChem™ SP (Alpha Innotech) and PXi/PXi Touch Fluorescent & Chemiluminescent Imaging System from SYNGENE. Fractions containing protein of interest with little contamination were selected and dialysed in 5 L PBS using Slide-A-Lyzer Dialysis Cassettes (Thermo Scientific) for 48 hours. The solution was then sterile filtered and concentration determined using the Bradford assay (section 2.4.3.1) and NanoDrop 2000 (Thermo Scientific). More dilute fractions (<100 µg/ml) were concentrated using Vivaspin columns (5 kDa molecular weight cut-off; Sartorius Stedim Biotech, Aubagne, France).

#### 2.4.1.3 Depletion of endotoxin from *E. coli* expressed protein

Endotoxin was depleted using Triton X-114 as previously described (Liu et al. 1997). Briefly, 5 µl Triton X-114 was added to 500 µl protein solution at a final concentration of 1%, and the sample rotated for 45 minutes at 4°C to allow Triton binding to LPS. Samples were then heated to 37°C for 10 minutes to allow formation of Triton-LPS micelles. The aqueous layer was then harvested after centrifugation at 13,000 xg at room temperature, and the whole procedure repeated another 2 times to further deplete LPS. The final protein concentration was determined also by the Bradford assay and Nanodrop. The Limulus Amebocyte Lysate (LAL) assay was used to measure the remaining endotoxin level.

### 2.4.2 Mammalian gene expression system

#### 2.4.2.1 Cloning of WT hIL-33, mutant hIL-33 and mL-33

The coding sequences for the target proteins were acquired from the human and mouse database NCBI (<https://www.ncbi.nlm.nih.gov>). Primers were designed for human wild type IL-33 (Primer position is shown in Figure 3.2A):

Forward primer (nt 1-30, starting at Gly-1, AscI GGCGCGCC was added at the 5' end) 5'-GGCGCGCCAAGCCTAAAATGAAGTATTC-3' and Reverse primer

(nt 821-797, starting at Gly-273, *ApaI* GGGCCC was added at the 5' end) 5'-GGGCCCAGTTTCAGAGAGCTTAAAC-3'. The A549 cell line was cultured for a substrate for mRNA to amplify the IL-33 coding sequence.

To make mutant human and mouse IL-33, chromatin binding site amino acids L47, R48, S49 ('LRS') were each mutated to alanine residues ('AAA'). The entire coding sequences were codon optimized for expression in mammalian system, flanked with restriction sites, using the GeneArt GeneOptimizer® tool (ThermoFisher Scientific) and synthesized by GeneArt. Inserts were extracted by restriction enzyme double digests using *AscI* and *ApaI*.

#### *AscI* and *ApaI* Digest

dH <sub>2</sub> O	14 µl
DNA	1 µg or 10 µl
CutSmart Buffer	3 µl
restriction enzymes	1.5 µl each

The mammalian expression plasmid vector pSecTag2a with ampicillin resistance was digested also by *AscI* and *ApaI*; digestion products were purified and ligated at 16°C overnight, catalyzed by NEB T4 DNA ligase (M0202). JM109 cells were transformed (section 2.4.1.1) with recombinant plasmid and selected by overnight culture on ampicillin agar plates, followed by colony screen PCR using T7 promoter primer and BGH reverse primer (T7 promoter primer and BGH primer are pSectag vector primer. The sequence of T7 promoter primer: 5'TAATACGACTCACTATAGGG3'; the sequence of BGH reverse primer: 5'TAGAAGGCACAGTCGAGG3'). Positive colonies were subjected to DNA extraction and sequencing of insert. Clones of the verified insert were grown up in 100 ml LB medium containing ampicillin and plasmid DNA extracted using the QIAfilter™ Plasmid Midi Kit (Qiagen), and stored at -20°C until HEK-293 cell transfection.

#### 2.4.2.2 Transfection into HEK-293 cells

The day before transfection, HEK-293T cells were counted and plated out at  $8 \times 10^5$  cells per tissue culture dish (100 mm) in 10 ml complete growth medium (complete Dulbecco's Modified Eagle Medium DMEM High Glucose containing 10% FBS (Thermo Scientific Hyclone No.: 30014.03), 5 ml Pen/Strep (stock 10,000 I.U.

Penicillin and 10,000 mg/ml streptomycin) Thermo Scientific Hyclone No.: SV30010) 5 ml L-Glutamine (stock 200 mM L-Glutamine, final concentration 1 mM) (Thermo Scientific Hyclone No.:SH30034.01). Three hours before transfection, spent media was replaced. Five plates of cells were prepared for transfecting each construct. For each 100 mm plate, 20 µg DNA was first mixed well with dH<sub>2</sub>O (the volume of dH<sub>2</sub>O differs because different concentration of DNA batches), then 62 µl 2M CaCl<sub>2</sub> was added to a total volume of 500µl, and mixed again. In a tissue culture hood, this mixture was drop-wise added to 500 µl 2x HEPES-buffered saline (Sigma) while vortexing gently. After 30min incubation at room temperature, the transfection solution was vortexed briefly and the 1 ml volume distributed drop-wise across each plate. Plates were then returned at 37°C CO<sub>2</sub> incubator for 24 hours before rinsing them twice and replacing with fresh complete growth medium. 72 hours after transfection, cells were transferred into tissue culture T25 flasks with selective medium (10% FBS DMEM containing 100 µg/ml Zeocin™ (Invitrogen)). Stable cells that were successfully transfected were selected for 1 month, with biweekly medium exchange, after which cells were cultured in serum-free medium to produce recombinant proteins. Supernatants of stably transfected HEK 293T cells in serum-free medium were harvested and dialysed with 1x PBS three times for 24 hours. Next, 45-60ml of supernatant was loaded onto a HiTrap column after applying 1x binding buffer (more details see section 2.4.1.2).

### 2.4.3 Protein concentration measurement

#### 2.4.3.1 Bradford assay

The Bradford protein assay, a spectroscopic analytical procedure, based on an absorbance shift of the dye Coomassie Brilliant Blue G-250, used to measure the concentration of protein in a solution. Serial doubling dilutions of bovine serum albumin (BSA) were made and 10 µl of each added to 190 µl of Coomassie Plus Protein Assay Reagent (Thermo Scientific), providing a standard curve. 10 µl of sample was similarly added to Coomassie Plus. After 5-10 minutes, ELISA plates were then read using an Emax precision microplate reader (Molecular Devices) under 595nm and concentrations calculated using the SoftMax®Pro software (Molecular Devices).

### 2.4.3.2 Qubit® Protein Assay Kit (Life technologies)

Compared to the Bradford assay, the Qubit® Protein Assay Kit could quantitate samples ranging from 12.5 µg/ml to 5 mg/ml and exhibits low protein to protein variation by using between 1 and 20 µl of sample. Qubit® working solution was prepared by diluting the Qubit® protein reagent 1:200 in Qubit® protein Buffer. Assay tubes were prepared as the following table. The mixture was vortexed for 2-3 seconds and incubated at room temperature for 15 min. A Qubit® 2.0 Fluorometer was used to calibrate with standards and read the samples.

Volume	Standards	Samples
Working solution	190 µl	190 µl
Standard (from kit)	10 µl	--
Sample	--	10 µl

## 2.5 Western blotting

### 2.5.1 Anti-His western blotting

To detect proteins bearing the hexa-histidine tag, 20 µl of protein mixed with 5µl of 4x loading buffer was loaded on the SDS-PAGE gel using NuPAGE® 4-12% Bis-Tris Gels and MES SDS Running Buffer (Novex®, Life Technologies). Gel-separated proteins were transferred onto nitrocellulose membrane in NuPAGE® transfer buffer (25X) at 35 Volts for 80 min. The membrane was blocked with blocking reagent (directly provided in the kit, Qiagen) before incubating with 50pg anti-Penta-His HRP Conjugate in prepared solution at RT for 1hour (Qiagen), a sensitive detection of recombinant proteins carrying His tags without the need for secondary antibodies, and proceeding to detect proteins by addition of ECL 2 Western Blotting Substrate A:B (1:40) at RT for 5 min (Thermo Scientific™ Pierce™, 80196).

### 2.5.2 Anti-*Bm*-SPN-2 western blotting

To verify monoclonal antibody candidates against *Bm*-SPN-2, recombinant serpin protein or Mff or adult extract was loaded onto SDS-PAGE gel. Following transfer to nitrocellulose as described above, the membrane was visualized by mAb candidates

as primary antibody and polyclonal antibody sera as positive with 1:2000 dilution 4°C over night and also anti-Mouse Immunoglobulins (P0260 by Dako) as secondary antibody at RT for 1 hour.

### 2.5.3 Anti-IL-33 western blotting

In order to measure the IL-33 from bronchoalveolar lavage after *Alternaria* intranasal administration by WB, 20 µl of the BAL sample with 5µl of the loading buffer 4x was loaded on the gel. Gel was transferred onto nitrocellulose membrane (Amersham GEHealthcare Life Science) in NuPAGE<sup>®</sup> transfer buffer (25X) at 35Volts for 80 min. The membrane was then blocked with 5% non-fat milk diluted in TBST (TBS-Tween 0.1%), for 30 min at RT. Blot was revealed by primary antibody goat anti-mouse IL-33 (R&D systems AF3626) 4°C over night and secondary antibody Donkey anti-goat-HRP V8051 (Promega A16005) at RT for 1 hour.

## 2.6 IL-33 cleavage experiment

Human and murine full-length IL-33 proteins, produced in rabbit reticulocyte lysate (RRL), were kindly provided by Corinne Cayrol, the French National Center for Scientific Research.

On ice, 5 µl RRL (HsIL-33<sub>1-270</sub> or MmIL-33<sub>1-266</sub>) was mixed with Elastase (0.01 mU/µl) or Cathepsin G (Calbiochem<sup>®</sup>, 0.25 mU/µl). The volume was made up to 15 µl with PBS (containing Ca<sup>2+</sup>/ Mg<sup>2+</sup>). The mixtures of full-length IL-33 were incubated for 30 min for Elastase and 1 h for Cathepsin G at 37°C (workflow see Figure 4.5A and 4.6A).

At the end of this incubation, 5µl of 4x loading buffer (containing 5% β-mercaptoethanol) was added, heated 5 min at 95°C, and loaded onto the SDS-gels immediately (to avoid excess cleavage even after boiling). In order to clearly see the 2 bands resulting from Cathepsin G cleavage of full-length IL-33, 13.5% SDS polyacrylamide gels were made as the following protocol.

Separating gel	8 ml	4% Stacking gel	5 ml
ddH <sub>2</sub> O	3.1ml	ddH <sub>2</sub> O	3.1ml
1.5M Tris PH8.8	2ml	0.5M Tris PH6.8	1.25ml
40% Acrylamide	2.7ml	40% Acrylamide	0.5ml
10% SDS	80μl	10% SDS	50μl
10% APS	80μl	10% APS	50μl
TEMED	8μl	TEMED	5μl

As migration control, 1μl of the HsIL-33<sub>95-270</sub> and HsIL-33<sub>109-270</sub> was comigrated for the human blot, and MmIL-33<sub>102-266</sub> for the mouse blot. Samples were run into the 4% stacking gel at 35mA for 30 min and then the separating gel at 45mA for 40 min. Gel was transferred onto nitrocellulose membrane (Amersham GEHealthcare Life Science) in NuPAGE<sup>®</sup> transfer buffer (25X) at 35 Volts for 80 min. The membrane was then blocked with 5% non-fat milk diluted in TBST (TBS-Tween 0.1%), for 30 min at RT. Then the membrane was incubated with the primary antibody (anti HsIL-33 305B from Adipogen, diluted 1/1500 in TBST 2% milk or goat anti-mouse IL-33, R&D systems AF3626, diluted 1/750 in TBST 2% milk) overnight at 4°C. The membrane was washed 6 times 5 min with TBST, at RT, and then incubated with the secondary antibody (“anti mouse-HRP” diluted 1/10,000 in 2% TBST for the human blot and Donkey anti-goat-HRP V8051, Promega A16005, diluted 1/5000 in 2% TBST for the mouse blot) for 1 hour at RT. The membrane was washed 6 times 5 min with TBST, at RT. Antibody-bound proteins were then detected by adding ECL 2 Western Blotting Substrate (Thermo Scientific™ Pierce™, 80196).

To test the inhibitory function of *Bm*-SPN-2 to neutrophil proteases, different concentrations of *Bm*-SPN-2 were pre-incubated with the neutrophil elastase and CatG at 37°C for 10 min. Then the above IL-33 cleavage experiment was continued with *Bm*-SPN-2 incubated proteases. The workflow of investigating *Bm*-SPN-2 acts on human and murine IL-33 cleavage is shown in Figure 4.7A and 4.8A, respectively.

## 2.7 Enzyme activity assays

To further verify the ability of *Bm*-SPN-2 to inhibit cathepsin G, cathepsin G activity colorimetric assay kit (K146-100, BioVision) was employed according to each manufacturer's instructions. Briefly, neutrophil elastase, cathepsin G was pre-incubated with *Bm*-SPN-2 at 37°C for 20 min. Cathepsin G with or without pre-incubation with *Bm*-SPN-2, were mixed with corresponding enzyme substrates. The substrate can be cleaved by the cathepsin G into a colorimetric product. As appropriate, absorbance (at 405nm) was measured in kinetic mode at 37 °C every one minute for 60 min. Each sample reading was then converted according to standard curves prepared at the same time.

## 2.8 Enzyme-linked immunosorbent assay (ELISA)

To measure different cytokines present in the peritoneal lavage after microfilariae infection of ST2-deficient and BALB/c mice, enzyme-linked immunosorbent assay (ELISA) of IFN- $\gamma$ , IL-4, IL-5, IL-13, IL-33 and Relm $\alpha$  was performed. To compare mast cell stimulation by full-length and cleaved IL-33, IL-6 secretion from mast cell supernatants was measured by ELISA. Also to select monoclonal antibodies against *Bm*-SPN-2, an ELISA screen was performed.

In each assay, 96-well flat bottomed plates (NUNC Maxisorp) were coated with 50  $\mu$ l/well capture antibody in carbonate buffer at corresponding working dilution (see Table 2.1 for concentrations) overnight at 4°C. For *Bm*-SPN-2 monoclonal antibody ELISA screen, 1 $\mu$ g/ml of r*Bm*-SPN-2 was made for coating. The next day, plates were washed 4 times with ELISA wash buffer (0.05% TBS-T) and blocked with 150  $\mu$ l/well of ELISA blocking buffer (1% BSA in ELISA wash buffer) and incubated for 2 hours at 37°C. After removing the blocking buffer, relevant wells were incubated with standards and samples overnight at 4°C. On day 2, plates were emptied, washed 4 times with wash buffer and incubated 1 hour at 37°C with 50  $\mu$ l/well biotinylated detection antibodies at the optimal concentration (concentrations see Table 2.1). The plates were then washed another 4 times before adding extravidin alkaline phosphatase (1/10,000) in 50  $\mu$ l blocking buffer per well, followed by 4 further washes with wash buffer, twice with distilled water and incubation with 100  $\mu$ l p-Nitrophenyl phosphate (Sigma) made up from tablets

according to the manufacturer's instructions, until colour development allowed measurement to take place. For the ELISA screen for monoclonal antibody, wells were incubated with polyclonal rabbit anti-mouse immunoglobulins HRP (P0260, Dako) 1:4000, followed by incubation with 50  $\mu$ l detection reagent ABTS® Peroxidase Substrate System until reading. ELISA plates were then read using an Emax precision microplate reader (Molecular Devices) under 405nm and concentrations calculated using the SoftMax®Pro software (Molecular Devices).

**Table 2.1: Antibodies used for ELISA**

Specificity	Clone	Capture	Standard	detection
IL-4	BD	1/1000	1/250	1/8000
IL-5	BD	1/4000	1/500	1/1000
IL-6	BD	1/250	1/200	1/1000
IFN- $\gamma$	BD	1/1000	1/200	1/250
IL-13	BD	1/125	1/500	1/1000
IL-33	BD	1/125	1/32.5	1/60
Relm $\alpha$	BD	1/400	1/100	1/400
extravidin alkaline phosphatase	BD			1/10000
anti-mouse immunoglobulins HRP	Dako			1/4000

## 2.9 Gene expression analysis

### 2.9.1 RNA extraction

RNA was extracted from mesenteric lymph nodes of ST2-deficient and BALB/c mice at day 1 and day 6 post-microfilariae infection as well as uninfected mice. mLNs were collected in 1 ml RNA later (Qiagen) until being transferred into new tissue lysis Eppendorf tubes, with a steel ball in 700  $\mu$ l Qiazol, then disrupted in Tissue Lyser for 1min at a frequency of 25. In the meantime, gradient centrifugation of peritoneal lavage cells was performed using Histopaque, the white cell layer was collected and resuspended in 700  $\mu$ l Qiazol. After transfer into an RNase-free 2ml tube, 140  $\mu$ l chloroform was added and the mixture shaken vigorously for 15s and incubated 5 min at room temperature. Following centrifugation (12,000 x g, 15 min, 4°C), the aqueous phase was transferred into a new RNase-free 1.5ml tube, and mixed thoroughly with 1.5 volumes of 100% ethanol. To get rid of any contaminated

DNA, RNA was then cleaned further using DNase 1 (Qiagen) and the RNeasy® Mini Kit (Qiagen), a developed kit for fast purification of high-quality RNA.

### 2.9.2 cDNA preparation

RNA concentration was measured by determination of optical density at 260 nm (OD<sub>260</sub>) using a NanoDrop 2000 (Thermo Scientific). For reverse transcription, 1 µl qScript RT reverse transcriptase (20x) was added to 250 ng RNA in 15 µl RNase-free water, followed by addition of 4 µl of qScript Reaction Mix (5x) (Quanta qScript cDNA kit). The reaction was performed in a thermocycler with the following program.

1 cycle	22°C	5 min
1 cycle	42°C	30 min
1 cycle	85°C	5 min
	4°C	hold

Note: In order to clone human WT IL-33, this protocol was also used for RNA extraction and cDNA preparation from A549 cells.

### 2.9.3 Real time PCR

To perform RT-PCR, cDNA was diluted 1/5 and a 1-5 µl of each sample pooled for use as top standard. Standards were serially diluted 1/5 to obtain six standard concentrations. 3 µl of sample or standard and 9.5 µl of master mix (see below) were added to each well. Samples and standards were used in triplicate for each primer; experiments were performed using 384-well plates and the QuantStudio™ 7 Flex (Thermo Scientific) using the following cycling conditions.

PCR products was analyzed by agarose gel electrophoresis and results analysed using delta CT method.

#### **Master mix for 384 well PCR plates**

6.25µl Perfecta SYBR Green SuperMix, Low ROX (2X)

0.25µl forward primer

0.25µl reverse primer

2.75µl Nuclease free water

Template 3µl

Final volume 12.5µl

### **Cycling conditions**

95°C 2:30 minute

40 cycles

95°C 15 seconds (Denature)

60°C 45 seconds (Anneal)

### **Mouse gene expression primer list**

GAPDH forward	5' ATG ACA TCA AGA AGG TGG TG 3'
GAPDH Reverse	5' CAT ACC AGG AAA TGA GCT TG 3'
RPL13a Forward	5' CCC TCC ACC CTA TGA CAA GA 3'
RPL13a Reverse	5' GCC CCA GGT AAG CAA ACT T 3'
IL-4 Forward	5' GAG AGA TCA TCG GCA TTT TGA 3'
IL-4 Reverse	5' TCT GTG GTG TTC TTC GTT GC 3'
IFN-γ	5' TGA ACG CTA CACACT GCA TCT TGG 3'
IFN-γ	5' CGA CTC CTT TTC CGCTTC CTG AG 3'
IL-33 Forward	5' GAC ACA TTG AGC ATC CAA GG 3'
IL-33 Reverse	5' AAC AGA TTG GTC ATT GTA TGT ACT CAG 3'
Arginase 1 Forward	5' GTC TGT GGG GAA AGC CAA T 3'
Arginase 1 Reverse	5' GCT TCC AAC TGC CAG ACT GT 3'
Relmα Forward	5' TAT GAA CAG ATG GGC CTC CT 3'
Relmα Reverse	5' GGC AGT TGC AAG TAT CTC CAC 3'

## 2.10 Parasite extract preparation

Microfilarae and adult worms of both *B. malayi* and *B. pahangi* were obtained from liquid nitrogen stocks of the Maizels lab and Eileen group, respectively. 500µl cold PBS was added to parasites, then 50 µl protease inhibitor cocktail solution was added. The protease inhibitor cocktail solution was prepared by dissolving one tablet of cOmplete™, Mini, EDTA-free Protease Inhibitor Cocktail (Cat.No.04693159001, Roche) into 1ml PBS. After mixing, adult worm samples were transferred to a glass homogenizer (Jencons H103/32/423 with a ground glass barrel), and repeated strokes used to break up macroparasites. Sonication using a Soniprep 150 (MSE) was performed on microparasites (microfilariae) for 3 min at 6 µm on ice, keeping the samples cold at all times. Suspensions were then placed on ice for 60 min, agitating occasionally. Centrifugation was performed at 10,000 g, 30 min, 4 °C. Supernatants

were harvested and then passed through a Millex 0.2 µm filter. Protein concentrations were measured and stored at -80 °C until use.

## 2.11 Accession numbers

The accession number of *Bm*-SPN-2 is AF009825.

To make human fl-IL-33, the primers were designed based on the *Homo sapiens* (*Hs*) IL-33 mRNA with the accession number of NM\_0033439.2.

## 2.12 Software and statistics

Statistical analysis was performed using GraphPad Prism 8. Depending on the data set, multiple t-tests, one or two-way ANOVAs were used, with significance thresholds of: \*:  $p \leq 0.05$ ; \*\*:  $p \leq 0.01$ ; \*\*\* :  $p \leq 0.001$ .

## 2.13 Media and buffers

### **His-tag Binding buffer (8x) (mM: milli molar)**

40 mM Imidazole	2.72 g
4 M NaCl	233.76 g
160 mM Tris-HCl	25.22 g
pH7.9	1 Litre

### **His-tag Elute buffer (8x)**

4 M Imidazole	272.3 g
2 M NaCl	116.8 g
80 mM Tris-HCl	12.61 g
pH 7.9	1 Litre

### **His-tag Charge buffer (8x)**

400 mM Nickel sulphate NiSO <sub>4</sub>	105.12g/L
--	-----------

### **His-tag Strip buffer (8x)**

400mM EDTA	37.22g
2M NaCl	29.22g

80mM Tris HCL                    3.15g  
 pH 7.9                                250 mL

**Carbonate coating buffer**

Buffer A     8.5 g NaHCO<sub>3</sub> in 100 ml H<sub>2</sub>O (1M)  
 Buffer B     10.6 g Na<sub>2</sub>CO<sub>3</sub> in 100 ml (1M)  
 Add 45.3 ml of A to 18.2 ml of B and 936.5 ml H<sub>2</sub>O  
 pH to 9.6  
 10µl 10% sodium azide

**cRPMI**

500 ml RPMI                                (Gibco)  
 5ml L-Glutamine                            (Gibco)  
 5ml Penicillin/Streptomycin            (Gibco)  
 50 ml FCS                                    (Gibco)

**ELISA wash buffer (TBS-T)**

5 L TBS  
 2.5 ml Tween® 20

**ELISA blocking buffer:** 1% BSA in ELISA wash buffer

**Protein G column purification buffers**

Binding buffer 2 x PBS     20mM Sodium phosphate pH7.0  
 Elution buffer                0.1M Glycine-HCl pH2.7  
 Neutralisation buffer        1M Tris HCl pH9.0

**[13.5% SDS PAGE gel]**

**1.5M Tris PH8.8**

Tris base     90.82g  
 HCL            adjust to pH 8.8  
                   Up to 500 ml

**0.5M Tris PH6.8**

Tris base     30.27g  
 HCL            adjust to pH 6.8  
                   Up to 500 ml

**10% SDS**

SDS 5.0g/50ml

**10% Ammonium persulphate (APS)**

Ammonium persulphate 0.1g/ml

**Western Blot washing buffer**

1L TBS

1ml Tween® 20

**Silver Stain Developing**

6.25g Sodium carbonate

0.05ml Formaldehyde (37%)

fill up to 250ml with dH<sub>2</sub>O

**Silver Stain Fixation**

100ml Ethanol

25ml Acetic acid

fill up to 250ml with dH<sub>2</sub>O

**Silver Stain Sensitizing**

75ml Ethanol

0.5g Sodium thiosulfate

17g Sodium acetate

fill up to 250ml with dH<sub>2</sub>O

**Silver Stain silver reaction reagent**

0.1g Silver nitrate

40ml d H<sub>2</sub>O

**Silver Stain Stop solution**

3.65g EDTA Na<sub>2</sub>·2H<sub>2</sub>O

fill up to 250ml with dH<sub>2</sub>O

# CHAPTER 3

## Human and murine IL-33: preparation mutation and testing on mast cells

### ABSTRACT

The most abundant secreted product from the *Brugia malayi* microfilarial stage, serine protease inhibitor-2 (*Bm*-SPN-2), was found to specifically inhibit the enzymatic activity of human neutrophil elastase and cathepsin G in a dose-dependent manner. More recently, these two enzymes have been linked to the activation of a major innate cytokine IL-33, which is stored as a full-length 270-aa protein in the cell nucleus, and released as an active C-terminal domain upon stimulation. In order to verify the hypothesis that *Bm*-SPN-2 blocks full-length (FL) IL-33 cleavage by inhibiting neutrophil elastase or cathepsin G, FL-IL-33 is required for this study. It was found that only C-terminal human and murine IL-33, and not FL IL-33 from either species are commercially available. In addition, recombinant wild-type FL-IL-33 was unable to be secreted directly into the supernatant of transfected HEK 293T cells. It was possible, however, to produce soluble murine and human FL-IL-33 in HEK 293T cells, following mutation of the nuclear binding motif. In this form, IL-33 is no longer retained in the nucleus and can be purified as a soluble protein. Furthermore, it was confirmed that once cleaved, but not by caspase, human IL-33 was able to induce significant IL-6 secretion by mast cells.

### 3.1 Introduction

Many parasites have evolved to release products that interfere with host defence mechanisms such as enzymatic activation pathways in the mammalian host, in order to promote and sustain their survival. The human filarial nematode *Brugia malayi* produces larval microfilariae, which circulate in the blood stream. Their most abundant secreted product is a serine protease inhibitor with sequence homology to mammalian serpins, termed *Bm*-SPN-2 (Hewitson et al. 2008). Serine protease inhibitors are reported to be involved in how nematodes avoid host immune defences, and in the case of *Bm*-SPN-2, the protein was found to specifically inhibit the enzymatic activity of human neutrophil elastase and cathepsin G in a dose-dependent manner (Zang et al. 1999). More recently, it was reported that these two enzymes are also linked to the activation of a major innate ‘alarmin’ cytokine IL-33, which is stored as a full-length 270-aa protein in the cell nucleus, and released as an active C-terminal domain upon stimulation (Lefrançois et al. 2012).

A role for IL-33 in parasitic infection was first suggested by the discovery that *Leishmania major*-infected BALB/c mice showed a switch in T cell response polarity from TH2 cell response to a protective TH1-type response, upon the administration of an ST2 (IL-33 receptor)-specific blocking antibody (Xu et al. 1998). As summarized in the general introduction (Chapter 1.4.6) it is now recognised that IL-33 is critically involved in developing the initial TH2 response to helminth infections, including *Nippostrongylus brasiliensis* (Moro and Koyasu 2010), *Schistosoma mansoni* (Townsend et al. 2000) and *Trichuris muris* (Humphreys et al. 2008). Furthermore, peak IL-33 expression was observed at early time points (Humphreys et al. 2008), indicating that prompt release of this alarmin cytokine is a potent signal for type 2 response initiation.

Based on the above information, as *Brugia malayi* is a human filarial parasite, the hypothesis is proposed that the function of *Bm*-SPN-2 is to inhibit the cleavage of human full-length IL-33 into the mature active form processed by human and neutrophil serine proteases (cathepsin G and elastase). Such an effect would directly inhibit the host alarm signal, and could be key to understanding both the host and parasite relationship and the parasite immune evasion strategy. As human and mouse IL-33 are 55% identical at the amino acid level (Schmitz et al. 2005), this hypothesis

may also be extended to infections in mice as well.

In order to verify this hypothesis, human and murine full-length IL-33 are required. As commercial sources proved to only provide the cleaved, activated C-terminal form, it was necessary to produce full-length IL-33 in our own laboratory.

In previous work, it has been demonstrated using real-time PCR by Schmitz et al. that human and murine IL-33 mRNA are expressed in a wide range of tissues and cell types (Schmitz et al. 2005). In mice, IL-33 mRNA is expressed in activated macrophages, epithelial cells and purified dendritic cells and it was also confirmed that its expression was much higher in stomach, lung, brain, spinal cord and skin tissues. However, human IL-33 mRNA expression follows a somewhat different pattern is found in activated dermal fibroblasts, bronchial smooth muscle cells and small airway epithelial cells, various resting epithelial cells and pulmonary artery smooth muscle cells (Schmitz et al. 2005). Thus, with the sequences of full length cytokines from both human (IL-33<sub>1-270</sub>) and murine (IL-33<sub>1-266</sub>) available from NCBI, it was feasible to produce human and murine recombinant full-length IL-33 in the laboratory, as described in this section.

Most recently, it was also reported that the processing of IL-33 into mature bioactive IL-33 can also be mediated by mast cell serine proteases, namely chymase and tryptase (Lefrançais et al. 2014). As discussed in the General Introduction (Chapter 1.4.1.1), mast cells are involved in many instances of parasite expulsion (Murphy and Weaver 2016). Upon infection with *Strongyloides* species, the TH2 cytokines, IL-3 and IL-9, stimulate mast cell growth and degranulation, increasing smooth muscle contraction (Maizels and Holland 1998). For example, athymic nude mice, which have no thymus-dependent T cells, expel *Strongyloides ratti* following repetitive administration of IL-3 (mast cell growth factor) (Abe et al. 1992). In addition, IL-3-deficient mice show delayed expulsion of *Strongyloides venezuelensis* (Lantz et al. 1998). Overproduction of IL-9, which functionally activates mast cells and augments IgE and IgG1 production, enables mice to rapidly expel *T. spiralis*. Using antibodies against c-kit receptor, which normally acts to promote mast cell maturation, impedes mouse mucosal mastocytosis and parasite expulsion (Faulkner et al. 1997). In the intestinal setting, mast cell products are thought to promote fluid egress through relaxing tight junctions, and to trigger muscular contraction, hence

### Chapter 3. Human and murine IL-33 preparation

underpinning the “weep-and-sweep” response. For instance, upon infection with gastrointestinal helminths (*H. polygyrus bakeri* and *Trichuris muris*), mast cell-deficient mice had dramatically reduced TH2 cytokine production and increased parasite burdens (Hepworth et al. 2012a). In the tissues and skin, mast cells work together with IgE to cause rejection of parasites including ticks and helminths. Notably, it has been shown that IL-33 is a potent activator of mast cells and can induce their degranulation, maturation, and production of pro-inflammatory cytokines, like IL-6 (Allakhverdi et al. 2007, Iikura et al. 2007). IL-9 can stimulate IL-6 production, which is considered to be a crucial cytokine for mast cell maturation (Conti et al. 2002), from certain mast cell lines and also promote the expression of mast cell proteases (Hültner et al. 1990, Faulkner et al. 1997). Very recently, it was shown by Shimokawa et al., 2017 that mast cells are a potent source of IL-33, crucial for ILC induction and clearance of *H. polygyrus* (Shimokawa et al. 2017). Thus, it is interesting to investigate how IL-33 and mast cells work together.

## 3.2 Results

### 3.2.1 Preparation of human wild type full-length IL-33

In initial experiments to determine the optimal amount of IL-33 for antibody detection on Western blots, Western blotting was performed with a range of amounts (100ng, 10ng, 1ng, 0.1ng) of rIL-33 purchased from a commercial supplier (R&D). Although the antibody used in these experiments successfully detected the target cytokine, it was found that the size of detected IL-33 was ~20-kDa, representing the proteolytically cleaved form of IL-33 (Figure 3.1). It thus transpired that the IL-33 protein sold by R&D was actually the cleaved form, which although having 10 times greater biological activity than FL-IL-33, was not suitable for experiments testing inhibition of cleavage. However, the result did clearly indicate that the amount of IL-33 needed for Western blotting detection was in the order of 10ng.

In order to test the hypothesis that *Bm*-SPN-2 inhibits the cleavage of full-length IL-33 by neutrophil cathepsin G or elastase, another strategy was required to obtain human and murine FL-IL-33. It was therefore necessary to produce full-length IL-33 in our laboratory, starting from a template of cDNA for IL-33 obtained from human and mouse cells.

A number of reports indicated potential sources for IL-33 mRNA. For example, both transcript and protein for human IL-33 have been reported to be widely expressed in various cell types such as adipocytes, bronchial, dendritic cells, endothelial cells, fibroblasts, intestinal epithelial cells, macrophages, osteoblast and smooth muscle cells (Schmitz et al. 2005). Also, it was reported that IL-33 is expressed in primary human monocytes (Nile et al. 2010). To amplify the corresponding cDNA, the human IL-33 sequence was first obtained from Genbank as Reference Sequence NM\_033439.3. Using an online Eurofins oligo analysis tool, primers were then designed for human full-length IL-33 as detailed in Figure 3.2B.

In the previous attempt to amplify IL-33, human peripheral blood mononuclear cells were isolated from a volunteer's blood. Unfortunately, under the conditions used in this study, IL-33 cDNA was not able to be amplified from the isolated human PBMCs.

As it was reported by Moussion et al., that IL-33 is constitutively expressed in epithelial cells (Moussion et al. 2008), it was then decided to isolate IL-33 cDNA

Chapter 3. Human and murine IL-33 preparation from human alveolar basal epithelial cells (A549 cell line). In this instance, IL-33 cDNA was successfully amplified from the A549 cell line (Figure 3.3A). The PCR product containing IL-33 cDNA was ligated into pGEMT holding vector, sequenced and verified to be error-free. The insert was then excised with restriction enzymes AscI and ApaI to be ligated into the pSecTag expression vector (Figure 3.3B and 3.3C), followed by HEK293T cell transfection.

Although cells were successfully transfected with the IL-33-pSecTag construct, no IL-33 was detected in the HEK cell supernatant by western blotting, after transfection of IL-33 into HEK cells (data not shown). According to the manufacturer's instruction, cell lysates of stable IL-33-transfected HEK293T cell lines were then prepared with mammalian cell lysis buffer (Cat.# G9381, promega) and the cell lysate supernatant was harvested. Subsequently, both anti-His and anti-IL-33 Western blotting of the cell lysate supernatant were carried out (Figure 3.4). The anti-His Western blot revealed a strong band around 60-kDa, which may be fetuin within the Foetal Calf Serum (FCS) added to the cell growth media (Figure 3.4A). However, specific anti-IL-33 Western blotting showed an approximately 40-kDa band, consistent with the expected size of human full-length IL-33 (Figure 3.4B).

Unfortunately, efforts to purify wild-type FL-huIL-33 protein by nickel-chelating AKTA column purification were not satisfactory (protein purification trace was shown in Figure 3.5A). Although by anti-IL-33 Western blotting, a band of ~40-kDa corresponding to human full-length IL-33 was clearly visible in fractions 15-18 (Figure 3.5C), multiple other proteins were detected in these fractions by silver staining (Figure 3.5B). The high level of contamination with other proteins rendered these fractions problematic for experiments with proteolytic enzyme activity.

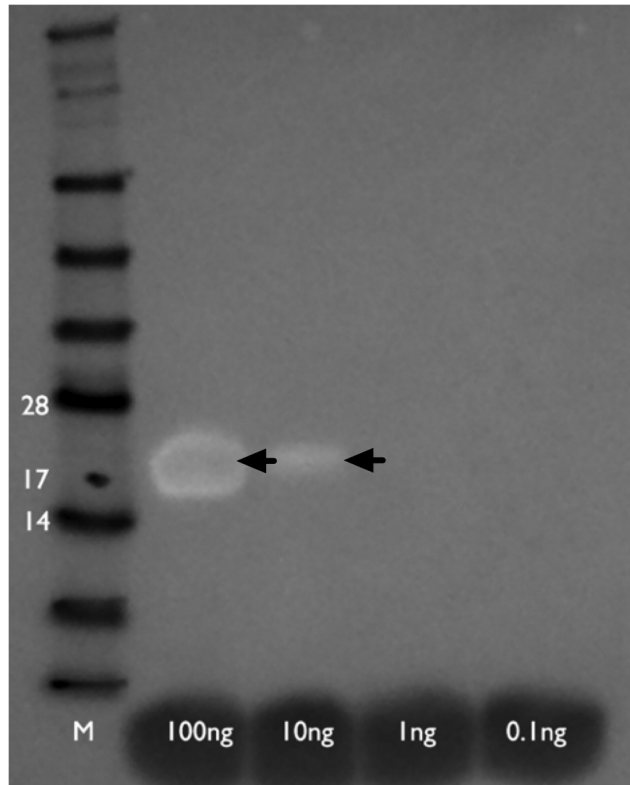


**Figure 3.1: Western blotting of a range of quantities of rIL-33.** Recombinant IL-33 (R&D) with the stock concentration of 100 $\mu$ g/ml were used to prepare the range of quantities of rIL-33, 1/10 serial dilution from 100ng, 10ng and 1ng to 0.1ng, then loaded onto the gel. IL-33 biotinylated antibody (R&D) with the working concentration of 0.2 $\mu$ g/ml, was prepared from the stock concentration of 36 $\mu$ g/ml. ExtrAvidin HRP (1:4000) and ECL Plus Western blotting substrate (Cat. #PI80196) were used for detection. The bands and the marker were captured individually by FluorChem®SP Superior Performance Imaging System, this image was the merged version (The images of the bands and marker were taken separately, and were merged together). “M” stands for marker: SeeBlue® Plus2 Pre-stained Protein Standard. 100ng and 10ng of IL-33 were detected in western blotting. The detected band were cleaved IL-33 with the size of ~20 kDa (black arrow).

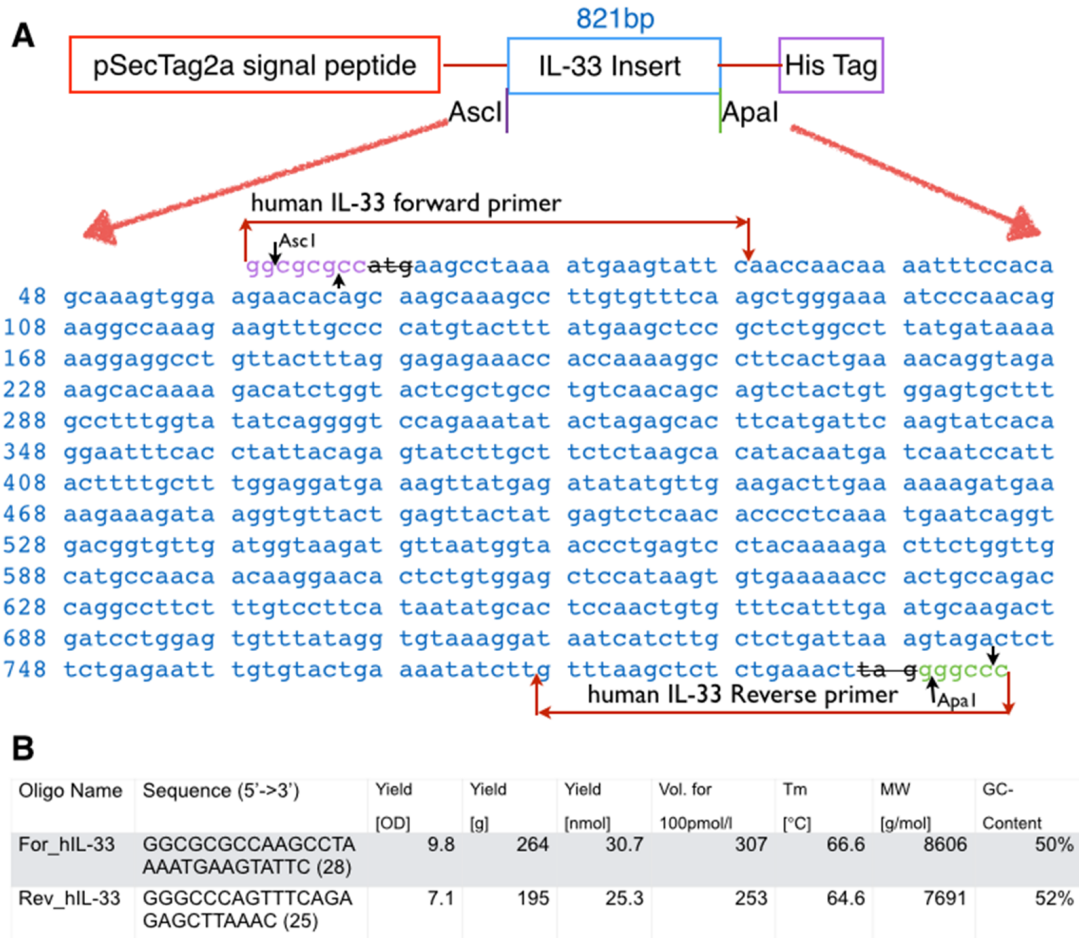


**Figure 3.2: Primer design and construct design for human full-length IL-33.**

(A) Schematic of the proteins produced, with vector sequences in red and restriction sites used indicated. Ascl (GGCGCGCC) shown in purple and Apal (GGGCC) shown in green. The start codon (ATG) and the stop codon (TAG) were deleted when the primer was designed. The forward and reverse primer for human IL-33 are shown at the beginning and the end of the IL-33 insert, respectively. A total of 821 bp should be the size of the PCR product.

(B) Primer information for human full-length IL-33. Reference sequence NM\_033439.3 from Genbank.

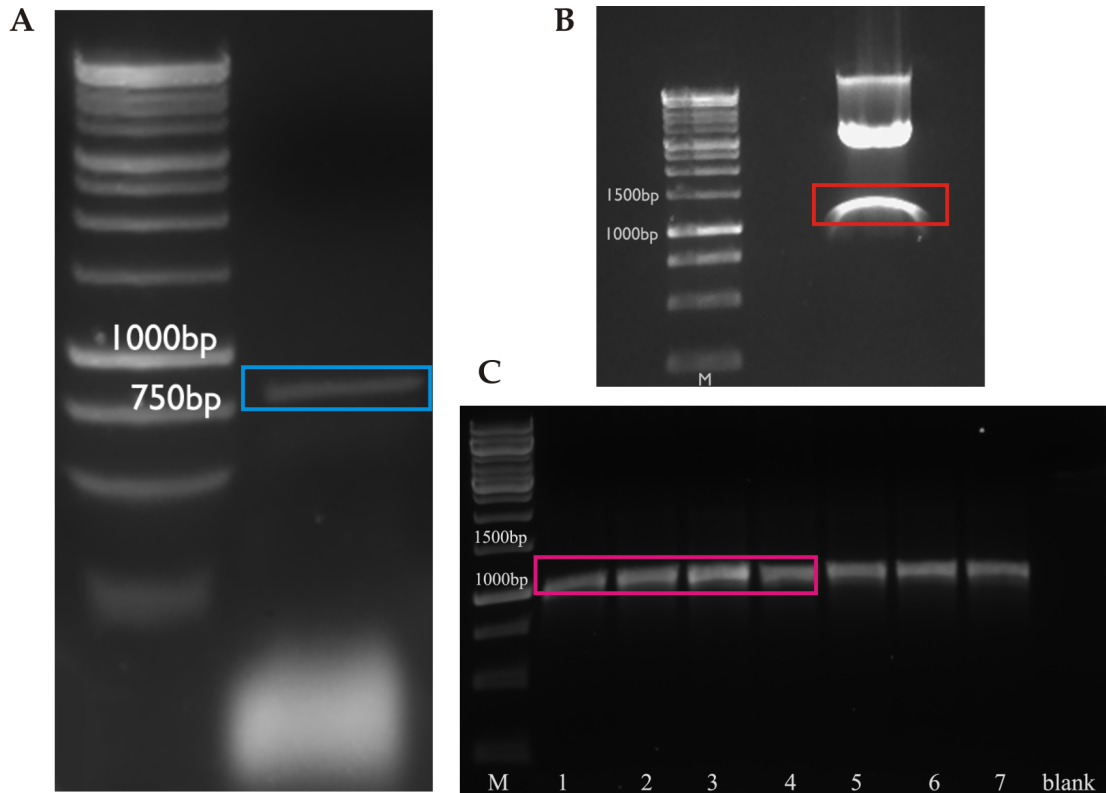


**Figure 3.3: IL-33 cDNA cloning from A549 cell line and ligation into pSecTag.**

(A) Agarose gel of IL-33 PCR product with the size of 821bp from A549 cell line cDNA using the primers shown in figure 3.2B.

(B) Digestion products from pGEMT holding vector with IL-33 following digestion with *Apa*I/*Asc*I restriction enzymes; gel extraction of the shortest band (IL-33 insert) was followed by ligation into the pre-cut pSecTag expression vector.

(C) T7 promoter primer (primer for pSecTag vector, sequence is shown in Section 2.4.2.1) and IL-33 specific reverse primer were used to perform colony screens, colonies 1-4 were first chosen for sequencing and proved to contain correct sequences. “M” stands for marker: GeneRuler™ 1 kb DNA Ladder.

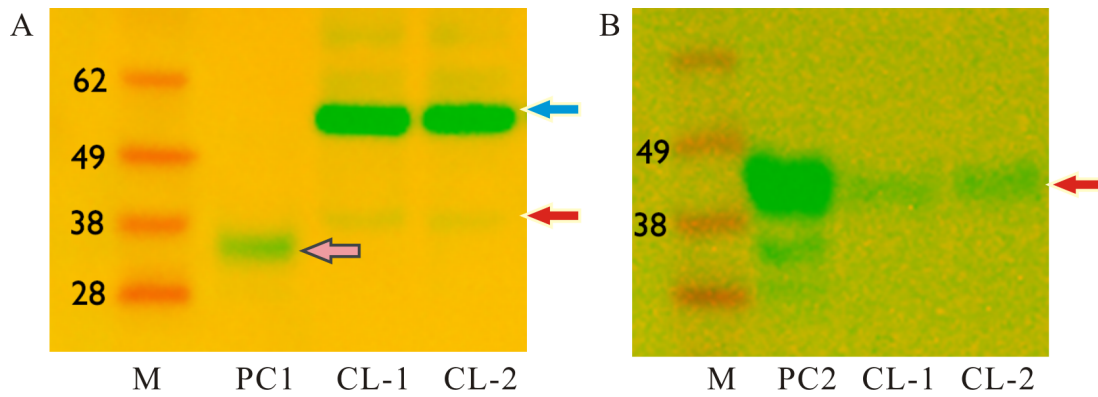


**Figure 3.4: Anti-His-tag and anti-IL-33 detection of products in IL-33 transfected HEK cell lysates.** CL-1 and CL-2 were sample replicates of IL-33 transfected HEK293 T cell lysate. 20  $\mu$ l of cell lysate were loaded into each lane. “M” stands for marker: SeeBlue® Plus2 Pre-stained Protein Standard. The blots were visualised by FluorChem®SP Superior Performance Imaging System, ladder and bands were captured individually, then were emerged together.

(A) Anti-His western blotting. “PC1” was NSP-4, a His-tagged protein transfected in HEK293 T cells made in our laboratory, as the positive control for anti-His western blotting. Pink arrow with blue frame shows the band of the positive control. Blue arrow points out the band about 60kDa might be the fetuin within the Foetal Calf Serum added to the cell growth media. Red arrow directs the weak band of IL-33 around 40kDa.

(B) Anti-IL-33 western blotting. “PC2” stands for positive control for IL-33 western blotting, was the cell lysate which proved to have IL-33 during the previous experiment. Red arrow points out the band of FL-IL-33 about 40kDa.

### 3.2.2 Retention of WT IL-33 within HEK cells

The retention of IL-33 within the cell body, and the inability to export it into the supernatant of HEK293T cells, can be attributed to an important biological feature of this alarmin. Previously, Carriere et al. defined a non-conserved domain, in IL-33, absent from other IL-1 family members, aa 1-65, which was identified as a chromatin and mitotic chromosome association domain (Carriere et al. 2007). Further, using deletion mutagenesis, Roussel et al. have demonstrated that IL-33 residues 40–58 are sufficient to tether N- or C-terminal green fluorescent protein (GFP) to mitotic chromatin in living human embryonic kidney (HEK) 293T cells (Roussel et al. 2008). Using alanine scanning mutagenesis, human IL-33 residues 43–54 were individually mutated to alanine (A) within the IL-33 chromatin binding motif (CBM). Six of these residues were found to be essential for chromatin binding: M45, L47, R48, S49, G50 and I53. The same authors further verified that a triple alanine mutation within the IL-33 CBM, IL-33<sub>40–58</sub> (47AAA49) abrogated chromosome association. It was confirmed in the context of full-length IL-33 (IL-33FL) that GFP-IL-33FL(47AAA49) and GFP-IL-33FL(R48A) mutants were found not to associate with chromatin. It was also shown that the IL-33 CBM is conserved in murine IL-33 (Roussel et al. 2008), as shown in the sequence alignment between human and murine IL-33 and its chromatin binding motif in Figure 3.6.

### 3.2.3 Producing mutant human and murine FL-IL-33

To produce a soluble, secreted form of FL-IL-33 which would not be retained within the cell by chromatin binding, the cDNAs for human and mouse IL-33 were mutated to alanine ‘AAA’ at positions 47–49, in accordance with the previous finding (Roussel et al. 2008). Mutant human and murine FL-IL-33 gene sequences were synthesized and inserted into the pMA-T vector, flanked with AscI and ApaI restriction endonuclease sites, by GeneArt (Gene synthesis details see appendix 1A and 1B). The amino acid alignment of mutant and WT human and murine FL-IL-33 are shown in Figure 3.7.

The synthesized mutant human and murine FL-IL-33 were excised from the pMA-T vector by double digestion with restriction enzymes AscI and ApaI, then ligated into the pSectag expression vector. The sequential steps of gel extraction of

### Chapter 3. Human and murine IL-33 preparation

hIL-33, mIL-33 and pSectag2a products used for the ligation are shown in Figure 3.8A. Following transformation of *E. coli* colonies were screened (Figure 3.8B) and sequenced (sequence results are shown in Appendix 2), followed by transfection of HEK293T cells with the verified plasmids.

From culture of these transfected cells in serum-free media, it was possible to purify secreted mutant human and murine full-length IL-33, with sizes of 34.1kDa and 33.3kDa, respectively. As both human and murine FL-IL-33 were predicted to have N-glycosylation sites, the sizes of the proteins were somewhat greater than expected (see Figure 3.9C and 3.10C). The schematic of the proteins produced is shown in Figure 3.9A, the human mutant IL-33 inset with the size of 821bp was flanked with the restriction enzymes *AscI* and *ApaI*. The UV trace, anti-IL-33 western blotting and silver staining of the purified fractions of human IL-33 are shown in Figure 3.9B, 3.9C and 3.9D. The insert of murine mutant IL-33 is 809bp. Similar results of murine mutant IL-33 are shown in Figure 3.10 A, B, C and D.

Figure 3.9 C and D shown the purified fraction B4 of human mutant IL-33, according to the IL-33 western blotting, there is a band for IL-33 at a mol wt of 40 kDa, whereas the silver staining shows a predominant band of a smaller size in this fraction. In order to ascertain the purity of these five fractions, they were sent for analysis by mass spectrometry (MS). The MS result shows that there are many other peptides in these fractions. However, MS result has shown that human IL-33 amino acid was detected in the Fraction 4 and Fraction 5. The amino acid sequences detected by MS were “VDSSENLCTENILFK”, “VLLSYYESQHPNSNESGDGVDGK” and “CEKPLPDQAFFVLHNMHSNCVSFECK” in fraction 4; whereas “TDPGVFIGVK” in the fraction 5 (the alignment with human mutant IL-33 is shown in Figure 3.11).

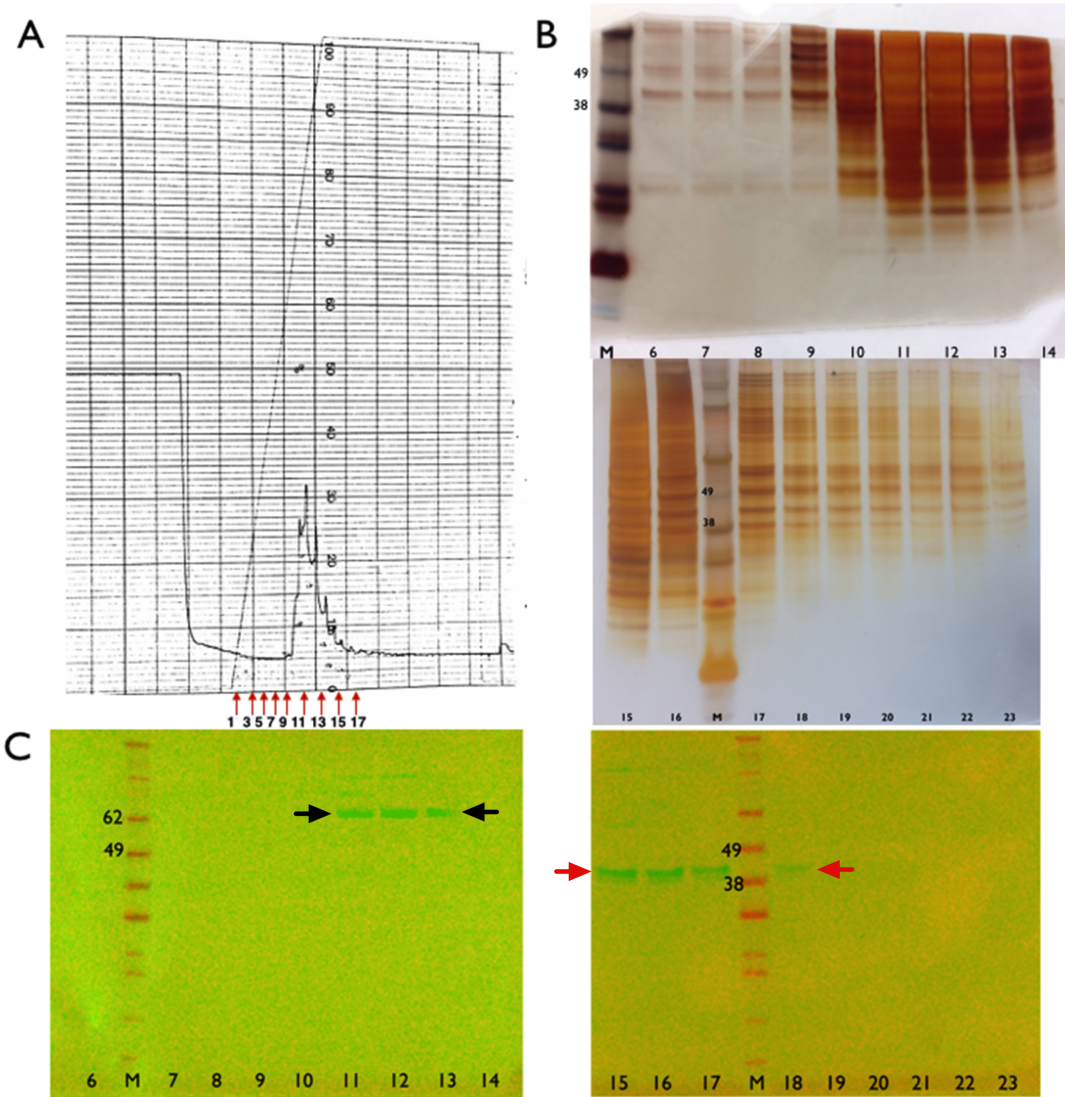


**Figure 3.5: AKTA purification fractions of WT human FL-IL-33 transfected HEK293T cell lysate.** “M” stands for marker: SeeBlue® Plus2 Pre-stained Protein Standard. “6-23” stand for “Fractions 6-23”.

(A) Purification trace of the purified fractions. 0%-100% gradient of the Elution buffer was used to elute the protein. Fractions are collected in Eppendorf tubes. Red arrows indicate each fraction 1, 3, ..., 17 etc.

(B) Silver staining of purified fractions 6-23.

(C) Anti-IL-33 western blotting of purified fractions 6-23. Fraction 11-13 shows a band about 60kDa (black arrow) might be the fetuin within the Foetal Calf Serum added to the cell growth media. Fraction 15-18 shows a band of about 40kDa (red arrow) which is likely to be the FL-IL-33.

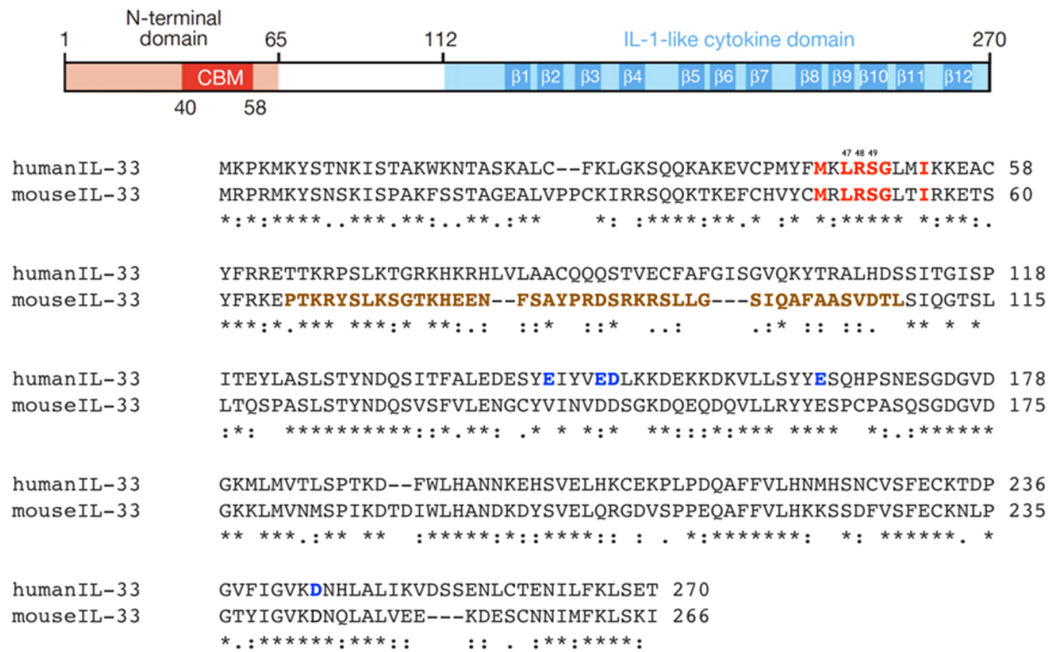


**Figure 3.6: Sequence alignment between human and murine IL-33 and their chromatin binding motif (CBM).** CBM was located close to the N-terminal domain. Red = residues required for chromatin binding; Brown = region which binds to (and inhibits) NF-kappa-B; Blue = residues which, when mutated, ablate ST2 binding of human IL-33.



**Figure 3.7: The amino acid alignment of wild type and mutant human and murine full-length IL-33.** The site of the triple mutation from LRS to AAA is shown in red. The flanking sequences showing in Blue are the pSectag vector sequence. Six hexahistidine-tags are shown in Green.

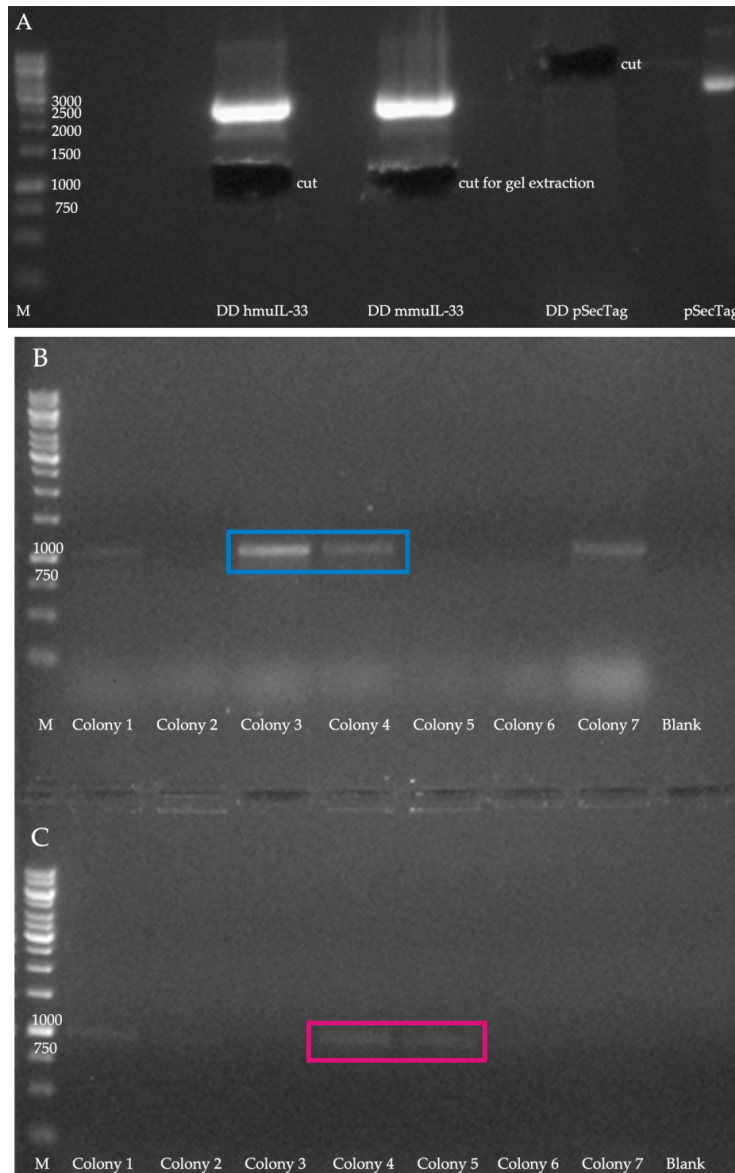


**Figure 3.8. Mutant human and mouse IL-33 insert into pSectag2a vector.**

(A) Human and mouse mutant IL-33 as well as pSectag2a vector were double digested with Apa1/Asc1, gel extraction was followed (the areas cut for gel extraction are visible on the image).

(B) and (C) T7 promoter primer and BGH reverse primer (vector primers for pSectag) were used to screen colonies; colonies 3 and 4 in blue frame were chosen for human mutant IL-33 sequencing, whereas colonies 4 and 5 in pink frame were chosen for mouse mutant IL-33. “M” means marker, GeneRuler™ 1 kb DNA Ladder. “DD” stands for Double digested by AscI and ApaI. “hmuIL-33” refers to human mutant IL-33. “mmuIL-33” means mouse mutant IL-33.

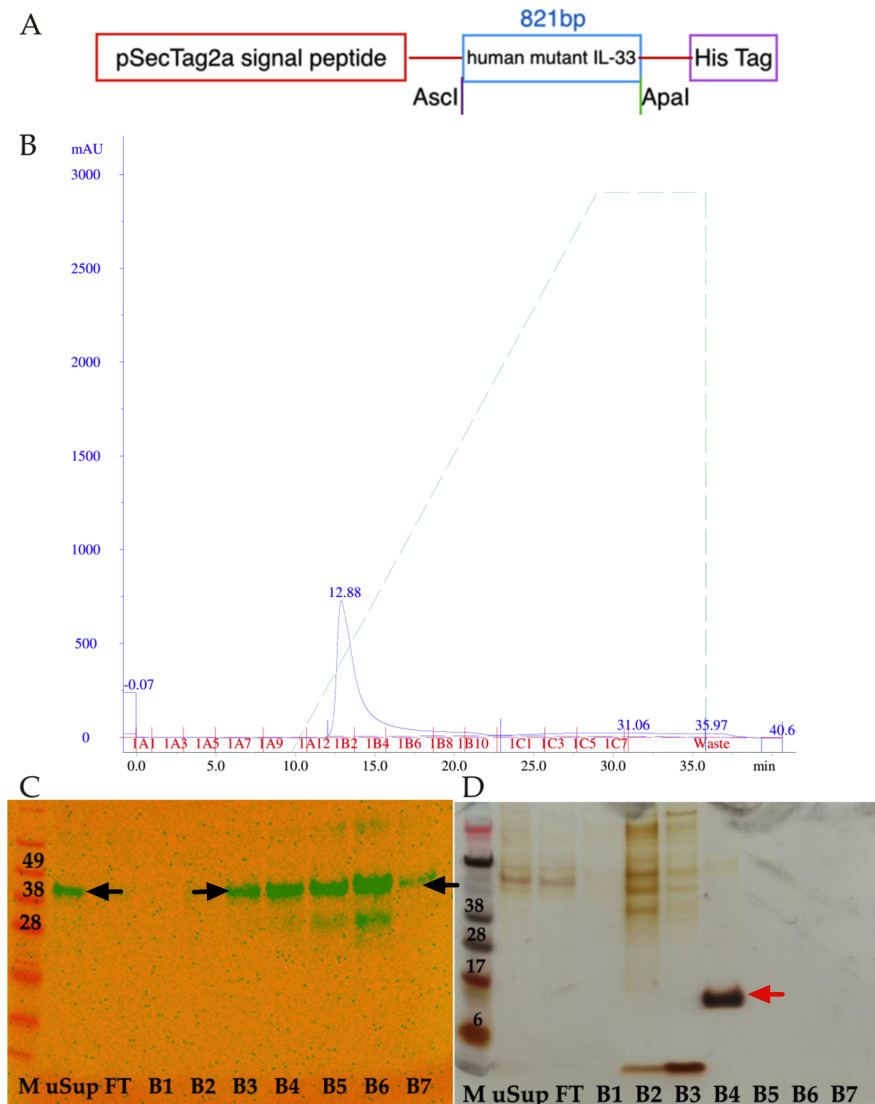


**Figure 3.9: Human mutant full-length IL-33 purification from transfected HEK293T cell supernatant by AKTA FPLC.**

(A) Schematic of the proteins produced, with vector sequences in red and restriction sites used indicated. The insert is 821bp.

(B) The UV trace of purified fractions from human mutant IL-33 (black arrow indicates the purified IL-33). The elution gradient of imidazole is indicated on each trace with a gradient from 0% to 100% of Elution buffer. Fractions are collected by 96 wells plates, then fractions order are shown as A1, A2,...,A12; B1,B2...B12 and C1,...C12.

(C) Anti-human IL-33 Western blotting of purified fractions following chelating column chromatography of supernatants of HEK cells expressing human mutant IL-33. (D) Silver staining of purified fractions of human mutant IL-33. Red arrow points to an unknown band in purified fraction 4. “uSup” is the un-purified supernatant, “FT” stands for flow through.

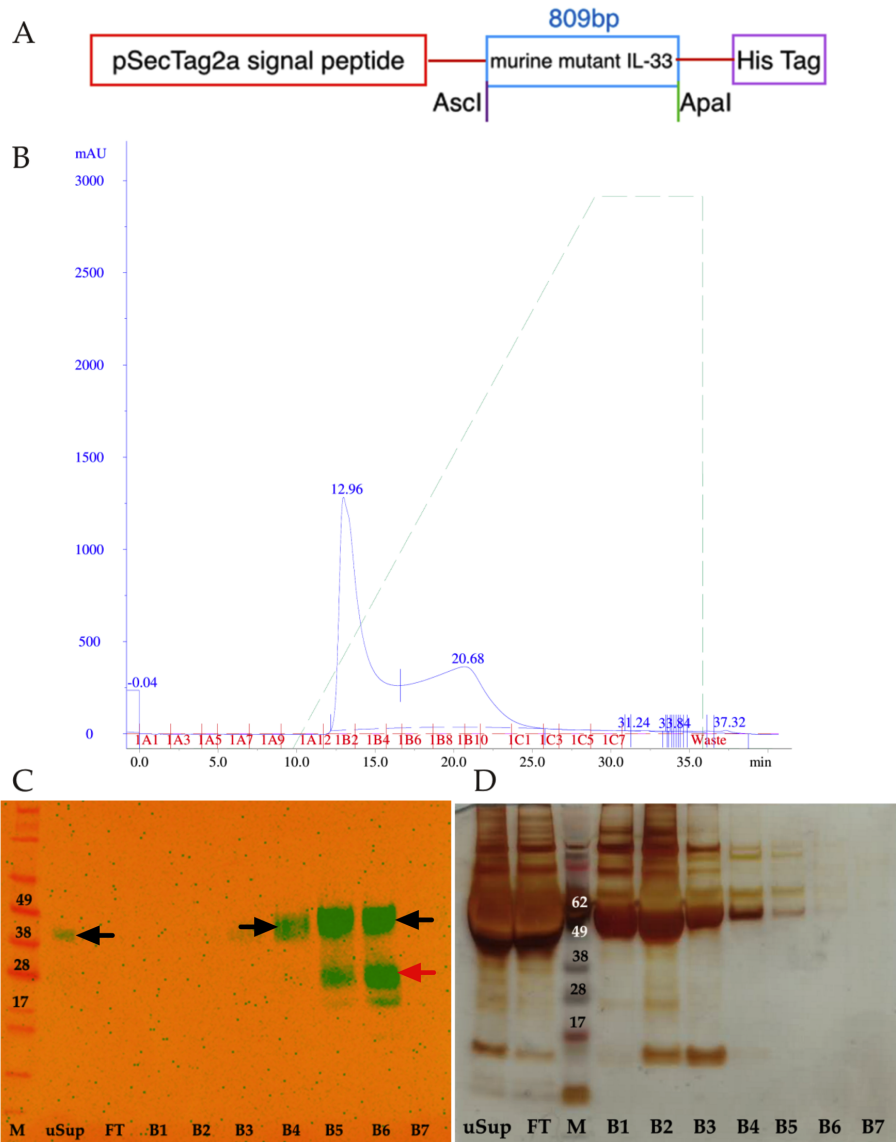


**Figure 3.10: Mouse mutant full-length IL-33 purification from transfected HEK293T cell supernatant by AKTA FPLC.**

(A) Schematic of the proteins produced, with vector sequences in red and restriction sites used indicated. The insert is 809bp.

(B) The UV trace of purified fractions from mouse mutant IL-33. The elution gradient of imidazole is indicated on each trace with a gradient from 0% to 100% of Elution buffer. Fractions are collected by 96 wells plates, same way as human mutant IL-33.

(C) Anti-mouse IL-33 Western blotting of purified fractions following chelating column chromatography of supernatants of HEK cells expressing mouse mutant IL-33 (Black arrow indicates the purified murine full-length IL-33; red arrow shows the cleaved IL-33).

(D) Silver staining of purified fractions of mouse mutant IL-33. “uSup” is the un-purified supernatant, “FT” stands for flow through.

```

hmuIL-33      METDTLLLWVLLLWVPGSTGDAAPARRAKPKMKYSTNKISTAKWKNTASKALCFKLGKS 60
hmuIL-33      QQKAKEVCPMYFMKAAAGLMIKKEACYFRRETTKRPSLKTGRKHKRHLVLAACQQQSTVE 120
hmuIL-33      CFAFGISGVQKYTRALHDSSITGISPITEYLASLSTYNDQSITFALEDESYEIYVEDLKK 180
hmuIL-33      DEKDKVLLSYYESQHPSNESGDGVDGKMLMVTLSPTKDFWLHANNKEHSVELHKCEKPL 240
MS result     VLLSYYESQHPSNESGDGVDGK                                     CEKPL
               *****                                             *****

hmuIL-33      PDQAFFVLHNMHSNCVSFECKTDPGVFIGVKDNLALIKVDSSENLCTENILFKLSETGP 300
MS result     PDQAFFVLHNMHSNCVSFECKTDPGVFIGVK                             VDSSENLCTENILFK
               *****                                             *****

hmuIL-33      EQKLISEEDLNSAVDHHHHHH- 321
  
```

**Figure 3.11: Mass spectrometry result of human mutant IL-33 purified fractions, aligned with mutant IL-33.**

Amino acid sequence showing in blue are the pSectag vector sequence. 6 His tags present in green at the end of the vector. “AAA” showing in red are the mutant DNA binding motif of IL-33. Sequences in purple are the detected amino acid from the purified fraction 4, whereas the sequence in brown is the detected amino acid from the purified fraction 5.

### 3.2.4 Stimulation of mast cells with human and murine full length and cleaved IL-33

It has been reported previously that full-length IL-33 significantly induced IL-6 secretion by cells of the MC/9 mast cell line, whereas following degradation by caspase-1, there was no effect (Cayrol and Girard 2009). In contrast, it was also shown that incubation of full-length IL-33 with neutrophil elastase and cathepsin G resulted in a more potent induction of IL-6 secretion by mast cells, compared with cells treated with full-length IL-33 alone (Lefrançois et al. 2012).

To better understand how IL-33 interacts with mast cells, a collaborative experiment was undertaken with the group of Cayrol et al. MC/9 cells were grown up and cultured with rabbit reticulate lysate full-length and Cathepsin-G cleaved IL-33, 24 hours prior to assaying cell supernatants for IL-6 release by ELISA (Figure 3.12A). It was confirmed that human cleaved IL-33<sub>95-270</sub> significantly increased IL-6 secretion by mast cells, compared with cells treated with human full-length IL-33<sub>1-270</sub> alone (Figure 3.12B).

In further experiments, a similar result was obtained with mouse IL-33; Here was a modest induction of IL-6 from mast cells with full length IL-33 compared to very significantly increased IL-6 from mast cells stimulated with cleaved mouse IL-33<sub>106-266</sub> (Figure 3.12C). Hence the same relationship between IL-33 and mast cells was found for both the human and mouse cytokines, and also that the murine mast cell line MC/9 is a sensitive readout for human IL-33 bioactivity. As very limited quantities of murine cleaved IL-33 were available to us, the murine IL-33 stimulation experiment was only performed once. Further experiments are still needed to verify this conclusion.

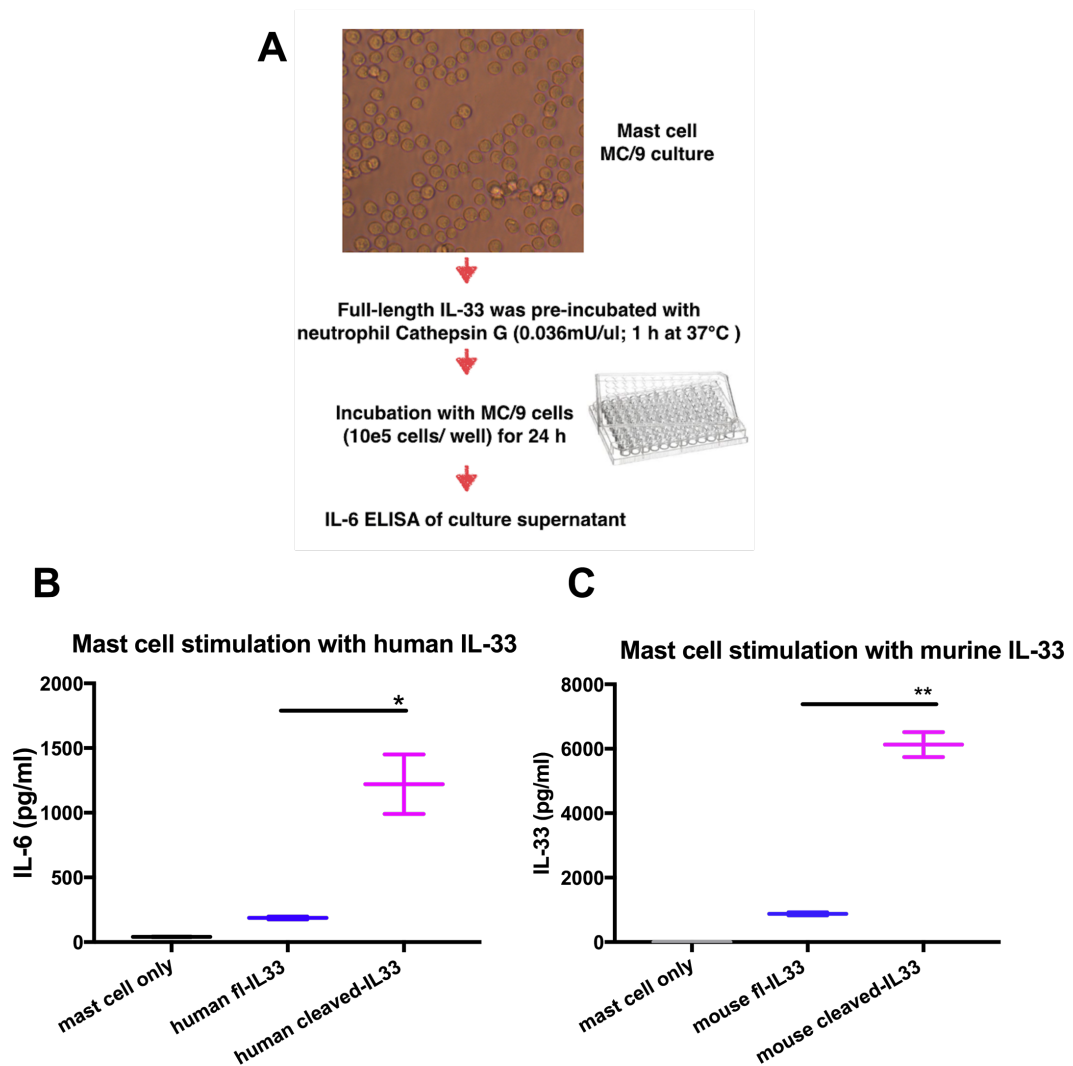


**Figure 3.12: IL-6 induction by human and murine IL-33 stimulation of mast cells.**

(A) Experimental protocol for mast cell incubation and stimulation.

(B) IL-6 secretion after human full-length IL-33<sub>1-270</sub> and cleaved IL-33<sub>109-270</sub> stimulation of the MC/9 murine mast cell line. Cleaved human IL-33<sub>109-270</sub> significantly increased IL-6 secretion.

(C) Mouse full-length IL-33<sub>1-266</sub> and cleaved IL-33<sub>106-266</sub> stimulation of MC/9 cells, using 10<sup>6</sup> mast cells/well. Cleaved murine IL-33<sub>106-266</sub> shows significantly increasing IL-6. 2μl of IL-33 rabbit reticulocyte lysate RRL was added to each well. IL-6 was measured by ELISA after 24 hours incubation. Human IL-33 stimulation was repeated twice, whereas murine IL-33 stimulation was performed only once.

### 3.3 Discussion

At the outset of this study, neither human nor mouse full-length IL-33 was available, as it transpired that the commercial products were the cleaved bioactive IL-33 form. It was therefore apparent that the only way of obtaining full-length IL-33 was to produce recombinant IL-33 in the laboratory.

In carrying out this work, results were not consistent with the previous finding that IL-33 messenger RNA is expressed in human monocytes (Nile et al. 2010). Although IL-33 cDNA could not be cloned from human isolated PBMCs, it was possible to take advantage of gene expression data from the first screening of IL-33 expression among various tissue and cell types (Schmitz et al. 2005). It had been observed that there was abundant expression of the endogenous IL-33 protein in epithelial cells from tissues exposed to the environment, and in fibroblastic reticular cells (FRCs) of lymphoid organs (Moussion et al. 2008, Pichery et al. 2012). Furthermore, IL-33 cDNA has been cloned from adenocarcinomic human alveolar basal epithelial cells (A549 cell line). Hence, after an initial setback, full length human IL-33 was successfully cloned.

In addition, it was confirmed that both human and murine wild type IL-33 are not secreted into the supernatant of transfected HEK293T cell cultures, as they are retained in the cell nucleus through the chromatin binding motif located in the N-terminal sequence of the IL-33 full-length protein (Roussel et al. 2008). Several reports suggest that IL-33 is a nuclear cytokine *in vivo*, which is always found in the nucleus of cells expressing the protein in both human and mouse tissues, with no evidence for cytoplasmic or extracellular localization (Moussion et al. 2008, Pichery et al. 2012, Cayrol and Girard 2014). It was summarized by Cayrol and Girard 2014 that (i), in the homeostatic state, IL-33 localizes in the nucleus of epithelial cells, with no ST2-dependent cytokine activity and inflammation; and (ii), during the programmed cell death, cleavage of IL-33 within the IL-1-like cytokine domain by caspases 3 and 7, abolishes its cytokine activity and consequent inflammation. It was concluded that IL-33 is thought to function as an 'alarmin', which is released

following cell necrosis to alert the immune system to tissue damage or stress (Miller 2011). Cayrol and Girard also proposed that during cell damage or mechanical injury associated with necrosis or necroptosis (a form of “programmed necrosis”, a new model of cell death, showing the morphological features of necrosis but highly regulated by an intracellular protein platform like apoptosis) (Vandenabeele et al. 2010), biologically active full-length IL-33 (the IL-1-like cytokine domain) is released from the nucleus into the extracellular environment followed by the cleavage of IL-33 in the central domain (Molofsky et al. 2015). This somewhat explains the reason for retention of full-length IL-33 in cells.

So far, the nuclear role(s) of IL-33 remains unclear. However, IL-33 can be involved with chromatin by tethering to histones H2A/H2B, via a short chromatin-binding motif, located in its N-terminal nuclear domain (Carriere et al. 2007, Roussel et al. 2008). It has recently been shown that deletion of this chromatin-binding nuclear domain result in constitutive extracellular release of the protein, ST2-dependent multi-organ inflammation and death of the organism (Bessa et al. 2014). Thus, nuclear localization (retention) is a fundamental property of IL-33, which is crucial for regulation of its cytokine activity (Cayrol and Girard 2014).

Notably, after mutating residues 47-49 of chromatin binding motif of both human and mouse full-length IL-33, soluble human and mouse FL-IL-33 were successfully purified from the supernatant of the transfected HEK293T cells, with the theoretical size of 34.1kDa and 33.3kDa, respectively. Because of both of human and murine FL-IL-33 are predicted to be N-glycosylated, the actual band size in Figure 3.9C and Figure 3.10C is greater than the computational size.

Although it is understood that a human full-length IL-33 protein was commercially available in the year of 2017 by Abnova (Cat No. H00090865-P01), it is a recombinant protein expressed *in vitro* in a wheat germ extract system, and has a size of 57.2kDa. However, in the construct reported here, the chromatin-binding motif-mutated human full-length IL-33 is codon optimized to this mammalian expression system and expressed in human embryonic kidney cells 293 (HEK293T cells) with 34.1kDa, indicating a lower degree of post-translational modification and arguably providing a final product closer to the natural human protein.

Mast cells (MCs) belong to the white blood cell lineage, however, they reside in peripheral tissues and are well situated to respond immediately to invasive agents (Anthony et al. 2007). MCs are involved in many instances of parasite expulsion (Murphy and Weaver 2016). Upon infection with *Strongyloides* species, the TH2 cytokines, IL-3 and IL-9, stimulate mast cell growth and degranulation, increasing smooth muscle contraction (Maizels and Holland 1998). Antibodies against c-kit receptor, which normally acts to promote mast cell maturation, impedes mouse mucosal mastocytosis and parasite expulsion (Faulkner et al. 1997). Previously, a role for mast cells in helminth immunity had also been shown in *Trichinella spiralis*, in which it was reported, using W/W<sup>v</sup> mice or stem-cell factor (SCF)-specific antibodies that impair mast-cell function, that SCF is required for mucosal mastocytosis and effective helminth expulsion (Grencis et al. 1993, Newlands et al. 1995). Interestingly, it was shown that mouse mast cell protease 1 (mMCP-1; also known as Mcpt1 and  $\beta$ -chymase)-deficient mice are unable to expel *T. spiralis*; however, mMCP-1 deficiency has little effect on *N. brasiliensis* host resistance (Knight et al. 2000, Anthony et al. 2007). Furthermore, it was inferred by Anthony et al. 2007 that mMCP-1 might function to impair epithelial-cell barriers by degrading the tight junction protein occluding, increasing luminal fluid flow (McDermott et al. 2003, Pennock and Grecis 2006). In the intestinal setting, mast cell products are thought to promote fluid egress through relaxing tight junctions, and to trigger muscular contraction, hence underpinning the “weep-and-sweep” response. For instance, upon infection with gastrointestinal helminths (*H. polygyrus bakeri* and *Trichuris muris*), mast cell-deficient mice had dramatically reduced TH2 cytokine production and increased parasite burdens (Hepworth, Maurer and Hartmann 2012b), demonstrating a novel role for gastrointestinal mast cells in the early events that lead to the generation of TH2 immunity to helminth infection (Hepworth et al. 2012b). However, MCs do not appear to have a key role in schistosomiasis, although they might contribute to the immune response at early stages of infection when the cercariae penetrate the skin (Gerken, Vaz and Mota-Santos 1990). Thus, it would be interesting to know whether MCs play a role in adult or microfilariae *Brugia malayi* infection, as the adult of this species live in the lymphatics whereas the microfilariae live in the blood stream of the host, like the schistosomes.

As mentioned in the introduction, mast cells work together with IgE to cause rejection of parasites including ticks and helminths in the tissues and skin (Murphy and Weaver 2016). Notably, it has been shown that IL-33 is a potent activator of mast cells and can induce their degranulation, maturation, and production of pro-inflammatory cytokines, like IL-6 (Allakhverdi et al. 2007, Iikura et al. 2007). Most recently, it was also reported that the processing of IL-33 into mature bioactive IL-33 can also be mediated by mast cell serine proteases, namely chymase and tryptase (Lefrançois et al. 2014). Very recently, it was shown by Shimokawa et al., 2017 that mast cells are a potent source of IL-33, crucial for ILC induction and clearance of *H. polygyrus* (Shimokawa et al. 2017). However, the important question remains of whether mast cells are important in protecting non-intestinal nematodes, and is subject to ongoing investigation.

Another clear finding was that cleaved human IL-33<sub>95-270</sub> significantly increased IL-6 secretion by mast cells compared to the full-length protein. Cleavage of the full-length IL-33 can either inactivate the cytokine (Schmitz, et al. 2005 and Cayrol and Girard, 2009), or generate a C-terminal fragment of greater activity. Thus caspase-1 cleaves FL-IL-33 into two different bands IL-33<sub>179-270</sub> and IL-33<sub>1-178</sub>, neither of which retain biological activity (Cayrol and Girard 2009). In contrast, a number of proteases can cleave human full-length IL-33 into a more active form. In addition to neutrophil elastase and cathepsin G which cleave human full-length IL-33<sub>1-270</sub> into IL-33<sub>95-270</sub> and IL-33<sub>109-270</sub> (Lefrançois et al. 2012), the mast cell proteases, tryptase and chymase, cleave FL-IL-33 into IL-33<sub>95-270</sub>, IL-33<sub>107-270</sub>, and IL-33<sub>109-270</sub>, which were 30-fold more potent than full-length human IL-33<sub>1-270</sub> for activation of ILC2s ex vivo (Lefrançois et al. 2014).

Thus, based on current knowledge, at least four enzymes including neutrophil elastase, cathepsin G, mast cell chymase and tryptase can cleave human full-length IL-33<sub>1-270</sub> into active fragments such as IL-33<sub>95-270</sub>. It is then inferred that the full-length human IL-33<sub>1-270</sub> is firstly cleaved by neutrophil cathepsin G and elastase into cleaved human IL-33<sub>95-270</sub>, IL-33<sub>95-270</sub> then enhances IL-6 secretion by mast cells. As IL-6 release represents mast cell activation, more proteases could then be secreted from mast cells, in particular chymase and tryptase. To amplify the cycle, these proteases then could cleave more full-length IL-33 into mature active IL-33<sub>95-270</sub>, to

### Chapter 3. Human and murine IL-33 preparation

maximise the TH2 immune response stimulated in the host. This is consistent with the very recent finding that mast cells play a role as a crucial source of IL-33, which can activate ILC2 responsible for parasite expulsion in the early phase, following infection with the intestinal helminth, *H. polygyrus* ((Bouchery and Harris 2017, Shimokawa et al. 2017).

There have been a couple of reports suggesting that IL-6 plays an important role in helminth infection. It was demonstrated using IL-6 deficient mice that IL-6 promotes host susceptibility following helminth infection (*H. polygyrus*) by impeding TH2 responsiveness and altering regulatory T (Treg) cell phenotype (characterized by lower expression of Foxp3, Helios and GATA3, and increased production of IL-2 and IL-17). Moreover, restoration of normal Treg cell function decreased the TH2 cell response to *H. polygyrus*. This suggests that IL-6 stabilizes Treg cells during helminth infection (Smith and Maizels 2014). As described earlier, IL-6 release also triggers mast cell activation, and it would therefore be important to further investigate the role of IL-6 and mast cells in helminth infection.

# CHAPTER 4

## Functional analysis of *Bm*-SPN-2, *Brugia malayi* microfilariae major secreted product

### ABSTRACT

The most abundant secreted product from *Brugia malayi* microfilaria stage, serine protease inhibitor-2 (*Bm*-SPN-2) was found to specifically inhibit the enzymatic activity of human neutrophil elastase and cathepsin G in a dose-dependent manner. Subsequently, however, another group had reported that *Bm*-SPN-2 is a non-inhibitory member of the serpin family. More recently, these two neutrophil enzymes have been linked to the activation of the major innate cytokine IL-33 and its release as an active C-terminal domain following stimulation. Thus, the hypothesis was proposed that *Bm*-SPN-2 blocks full-length (FL) IL-33 cleavage by inhibiting neutrophil elastase or cathepsin G. Here, recombinant *Bm*-SPN-2 was expressed into *E. coli* and soluble *Bm*-SPN-2 was purified. Furthermore, using western blotting, it was confirmed that human neutrophil cathepsin G cleaves human full-length IL-33 into two major bands Hs IL-33<sub>95-270</sub> and Hs IL-33<sub>109-270</sub>, whereas neutrophil elastase cleaves human full-length IL-33 into one major product IL-33<sub>99-270</sub>. It was also shown that neutrophil CG cleaves murine full-length IL-33<sub>1-266</sub> into a major band mIL-33<sub>102-266</sub>, whereas neutrophil elastase cleaves mIL-33<sub>1-266</sub> into two different products mIL-33<sub>102-266</sub> and mIL-33<sub>109-266</sub>. It was then found that using a commercial enzyme activity assay, *Bm*-SPN-2 did not show any inhibitory function against

#### Chapter 4. Functional analysis of *Bm*-SPN-2

human neutrophil cathepsin G. However, utilizing Western blotting, it was demonstrated that *Bm*-SPN-2 could inhibit human IL-33 cleavage by inhibiting this enzyme in a dose-dependent manner. Finally, *Bm*-SPN-2-mCherry construct was synthesized and cloned into pET29a vector for future fluorescent binding studies.

## 4.1 Introduction

### 4.1.1 Serine protease inhibitors

The term ‘serpin’ (serine proteinase inhibitor) was originally coined as a superfamily of structurally conserved proteins (Pfam No. PF00079) (Huntington, Read and Carrell 2000). They are typically 350–500 amino acids in size (Silverman et al. 2001) with corresponding molecular weights of 40-60 kDa (van Gent et al. 2003), and those with inhibitory activity employ a suicide substrate-like mechanism: The structure of the reactive centre loop (RCL) is a critical feature for serpin to undergo the conformational change, including the permanent loss of 37% of the structure and overall distortion of the protease, necessary for inhibitory activity (Huntington et al. 2000, Irving et al. 2000, van Gent et al. 2003). It was shown by Huntington et al. (2000) that the permanent loss of the protease structure is a direct consequence of the limited length of the serpin RCL, which causes the ‘plucking away’ of the protease ester-linked serine from its catalytic partners, hence the name ‘suicide’ substrate inhibitors (Molehin et al. 2012, Huntington et al. 2000). Over 1000 serpins have now been identified in species as diverse as bacteria, fungi, viruses, plants, insects, birds, and mammals. In humans, serpins have evolved to be a predominant family of protease inhibitors with 36 recognised members (Huntington et al. 2000).

Smapins (small serine protease inhibitors) are small proteins distinct from serpins and comprise no more than 100 amino acid residues. These inhibitors appear to be unique to nematodes, with no recognizable relatives from any other organism (Molehin et al. 2012, Zang and Maizels 2001).

In mammals, serpins play an important role in the regulation of many fundamental processes, including blood coagulation, complement activation, cell development and inflammation (Potempa, Korzus and Travis 1994, Knox 2007). Some serpins are uniquely involved in more diverse functions such as the control of chromatin folding and Toll signalling (Grigoryev, Bednar and Woodcock 1999, Levashina et al. 1999).

Serpins are also expressed by parasitic nematodes, and thought to help parasites avoid host immune defences (Molehin et al. 2012). The likely nematode serpin and smapin genes have been summarized in Zang and Maizels, 2001 and Molehin et al. 2012, with eight serpin genes (*Ce*-SPN-1, ...*Ce*-SPN-8) being identified in the model

organism, *Caenorhabditis elegans*, and four in a range of parasitic nematode species, including *Ascaris suum*, *B. malayi*, *Onchocerca volvulus* and *Trichostrongylus vitrinus*, as well as in trematode *Schistosoma spp.* and the cestodes *Echinococcus multilocularis* and *E. granulosus*. In addition, nematode smapins have been identified in *Anisakis simplex* (Kobayashi et al. 2007), *A. suum* (Grasberger et al. 1994), *Ancylostoma caninum* (Duggan, Dyson and Wright 1999), *O. volvulus* (Ford et al. 2005) and *Trichuris suis* (Rhoads et al. 2000b, Rhoads et al. 2000a) (Table 1.1).

The metastable conformation of serpins is required for their inhibitory activity (Zang and Maizels 2001). The serpins consist of a conserved tertiary structure comprising nine alpha helices and three beta sheets A, B and C (Silverman et al. 2001). Key features include a serpin motif, a reactive site loop (the functional domain near the C-terminus) and a serpin signature sequence (Knox 2007). The functional domain ‘reactive site loop’ is exposed on the surface and contains a scissile bond which acts as a cleavable bait to trap the target proteinase, inducing a profound change in its conformation and thus inhibiting proteases (Huntington et al. 2000).

A total of 14 serpins have been predicted in the *B. malayi* genome, but only two - *Bm*-SPN-1 and *Bm*-SPN-2 - have been characterized to be secretory (Zang et al. 1999, Molehin et al. 2012, Ballesteros et al. 2016). Phylogenetic analysis shows that *Bm*-SPN-1 and -2 have low homology and are not closely related, sharing only 27.8% identity (110/395) at the amino acid level but showing conserved ‘motif’ and ‘signature’ sequences (Zang and Maizels 2001). *Bm*-SPN-1 is detected in all life cycle stages, but little is known about its target protease(s) (Yenbutr and Scott 1995). Neither *Bm*-SPN-1 nor any of the other serpins appear to be secreted from adult worms, as no serpin was detected in adult *B. malayi* “excretory-secretory” (BES) proteins (Hewitson et al. 2008). *Bm*-SPN-2 was subsequently confirmed as specific for the microfilarial stage, by both proteomic analysis and transcriptome sequencing (Moreno and Geary 2008, Bennuru et al. 2009, Li et al. 2012, Ballesteros et al. 2016). *Bm*-SPN-2 will be described in the following section.

#### 4.1.2 *Bm*-SPN-2 discovery and disputed functions

In order to identify prominent antigens from bloodstream *B. malayi* microfilariae (Mf) proteins that might be recognized by the host immune system’s T lymphocytes, previous research in the Maizels lab isolated a fraction from Mf proteins of 35-55

kDa which potently stimulated antigen-specific T-cell proliferation and cytokine production (Zang et al. 1999). A clone encoding a native serine proteinase inhibitor protein, with a molecular mass of 47.5 kDa, was then identified as a major T cell antigen and isolated by immunoscreening of an Mf cDNA library (Zang et al. 1999). It was designated as *Bm*-SPN-2 because of the similarity to the previously described *Bm*-SPN-1 by Yenbutr and Scott (1995) (Yenbutr and Scott 1995).

Through the following studies, *Bm*-SPN-2 was demonstrated to be the most abundant protein only secreted by the *B. malayi* microfilarial stage. Using first-strand cDNA from a range of *B. malayi* stages (L3, adult female, adult male, Mf) as templates, transcription of *Bm*-SPN-2 by 2 gene-specific primers was only detected in blood-dwelling microfilariae. As stated above, no serpin was detected from *B. malayi* “excretory-secretory” (BES) proteins from adult worms (Hewitson et al. 2008). *Bm*-SPN-2 was further confirmed as specific and one of the most abundant proteins for the microfilarial stage by proteomic analyses and transcriptome sequencing in independent laboratories (Moreno and Geary 2008, Bennuru et al. 2009, Li et al. 2012, Ballesteros et al. 2016).

In the original studies, the open reading frame encoding *Bm*-SPN-2 lacking the signal peptide was subcloned into the pET-29 *E. coli* expression vector, permitting expression of recombinant *Bm*-SPN-2 as a fusion protein containing a C-terminal hexahistidine-tag for affinity purification, with molecular weight of 52 kDa (Zang et al. 1999).

When tested for its ability to inhibit a panel of mammalian serine proteases with differing substrate specificity and function, *Bm*-SPN-2 protein was found to specifically inhibit the enzymatic activity of human neutrophil elastase and cathepsin G in a dose-dependent and highly specific manner (Zang et al. 1999). In that study, human neutrophil cathepsin G or elastase was incubated with *Bm*-SPN-2. After 10 minutes of incubation at room temperature, a corresponding peptidyl-p-nitroanilide substrate solution was added to the mixture, and the residual enzyme activity was measured by monitoring the absorbance change at 405nm with time. The enzymes and their substrates used in the tests were human neutrophil cathepsin G (1 µg/µL, Athens Research & Technology, Inc) and N-succinyl-Ala-Ala-Pro-Phe-p-nitroanilide (Sigma); human neutrophil elastase (1 µg/µL, Athens Research & Technology, Inc) and N-

succinyl-Ala-Ala-Pro-Leu-p-nitroanilide (Sigma) (Zang et al. 1999, Jiang and Kanost. 1997). This specificity of inhibition was confirmed by the fact that *Bm*-SPN-2 showed no inhibitory activity with bovine pancreatic  $\alpha$ -chymotrypsin or porcine pancreatic elastase, two enzymes which hydrolyze the same substrates as human neutrophil cathepsin G and elastase, respectively (Zang et al. 1999, Molehin et al. 2012).

However, Stanley and Stein disputed this result by analyses which concluded that *Bm*-SPN-2 is a non-inhibitory serpin, which has no effect on the activity of neutrophil cathepsin G or elastase (Stanley and Stein 2003). This group also expressed the *Bm*-SPN-2 protein in *E. coli*, and characterized its structural and functional properties. Comprehensive sequence alignment, phylogenetic analysis, and susceptibility to cleavage by proteases suggested that the *Bm*-SPN-2 shared the conserved tertiary structure of the serpin family, including a reactive centre loop (Irving et al. 2000). However, they found that the protein had no effect on the activity of neutrophil cathepsin G or elastase and did not undergo the characteristic stressed to relaxed transition required for protease inhibition by serpins. As in the study by Zang et al., Stanley and Stein determined proteinase inhibition by measuring the release of p-nitroanilide at 405 nm at 37°C, using a different substrate N-methoxysuccinyl-Ala-Ala-Pro-Val-p-nitroanilide for elastase, but the same substrate N-succinyl-Ala-Ala-Pro-Phe-p-nitroanilide for cathepsin G. The absorbance was measured on a Shimadzu UV-1601 spectrophotometer at 405 nm at 25 °C (Stanley and Stein 2003). These authors concluded that *Bm*-SPN-2 was a new non-inhibitory serpin. Therefore, it was thought worthwhile to re-assess the previous conclusion about the function of *Bm*-SPN-2 and its ability to inhibit the neutrophil cathepsin G and elastase.

A further question is whether *Bm*-SPN-2 influences the host-parasite relationship *in vivo*. Mice infected with *B. malayi* microfilariae mount a strong but short-lived *Bm*-SPN-2-specific TH1 response with significant increases in IFN- $\gamma$  production (Zang et al. 1999, Zang et al. 2000). Human filariasis patients displayed a potent humoral response to *Bm*-SPN-2 but primarily in both IgG1 and IgG4 antibody subclasses, which are promoted by TH2 cytokines, hence if there is also a TH1 response to *Bm*-SPN-2 in humans, it may also be short-lived (Zang et al. 2000). Overall, *Bm*-SPN-2 was suggested to play an important role in neutralizing the

immunostimulatory properties of the host neutrophils proteases and contributing to the longevity of Mf in the host bloodstream (Molehin et al. 2012).

It is interesting now to ask whether *Bm*-SPN-2 interacts with the IL-33 pathway. Analysis of tissue mRNA isolated from mice treated with IL-33 each day by Schmitz et al. demonstrates that IL-33 drives the TH2 immune response by inducing the expression of IL-4, IL-5, and IL-13, as measured by quantitative PCR, and leads to severe pathological changes in mucosal organs (Schmitz et al. 2005). More recently, it was reported by Corinne et al. that both full-length human and murine IL-33 are processed into mature bioactive IL-33 by the two human neutrophil proteases, cathepsin G and elastase (Lefrançais et al. 2012), that Zang et al found to be targeted by *Bm*-SPN-2 (Zang et al. 1999).

Based on these findings, we hypothesized that *Bm*-SPN-2, as the most abundant product secreted specifically from microfilariae stage, could impede IL-33 cleavage into mature bioactive forms by inhibiting the activity of these two enzymes, then block TH2 initiation, helping microfilariae avoid the protective arm of the host immune response. Testing this hypothesis was the aim of the work described in this chapter.

## 4.2 Results

### 4.2.1 *Bm*-SPN-2 expression and purification

To express recombinant *Bm*-SPN-2, the plasmid pET29-*Bm*-SPN-2-His, previously constructed by Zang et al. (Zang et al. 1999), was used for transformation of JM109 *E. coli* cells. The Mini-Prep product of pET29-*Bm*-SPN-2-His was sequenced to verify the nucleotide sequence of the insert, with the result presented in Appendix 3. To determine the optimal conditions of Isopropyl  $\beta$ -D-1-thiogalactopyranoside (IPTG) induction, four groups were designed for expression as set out in Figure 4.1A, with the results presented in Figure 4.1B. Notably, clear expression of the recombinant protein was found in all protocols, with the best induction condition for protein expression found to be 0.1mM IPTG for 3 hours. *Bm*-SPN-2 with the size of about 52kDa was purified on a chelating Nickel Column on the AKTA Prime machine. The original *Bm*-SPN-2 was encoded by 428-aa, (the protein structure of recombinant *Bm*-SPN-2 is shown in Figure 4.2A,) with the signal peptide deleted and restriction enzymes NdeI and XhoI added at the both end of the insert. The trace of purified fractions is shown in Figure 4.2B, and the coomassie blue staining of the purified fractions in Figure 4.2C. Protein concentrations are estimated based on OD 280 using a Nanodrop ND-1000 Spectrophotometer or using Bradford assay. After purification, we obtained a total of 9.778 mg *Bm*-SPN-2 protein with the concentration of 1.8mg/ml, which was stored at -80°C until use.

**A**

conditions groups	IPTG concentration	Induction duration	Incubate temperature & RPM	sample collecting	OD600 value
Group1	1mM (500μl/ 500mL)	3hr	37°C; 265	un-induced; 1hr; 2hr; 3hr	0.616
Group2	0.1mM (50μl/500mL)	3hr	37°C; 265	un-induced; 1hr; 2hr; 3hr	0.636
Group3	1mM (500μl/ 500mL)	3hr	20°C; 200	un-induced & 3hr	0.610
Group4	1mM (500μl/ 500mL)	16hr	20°C; 200	un-induced & 16hr	0.608

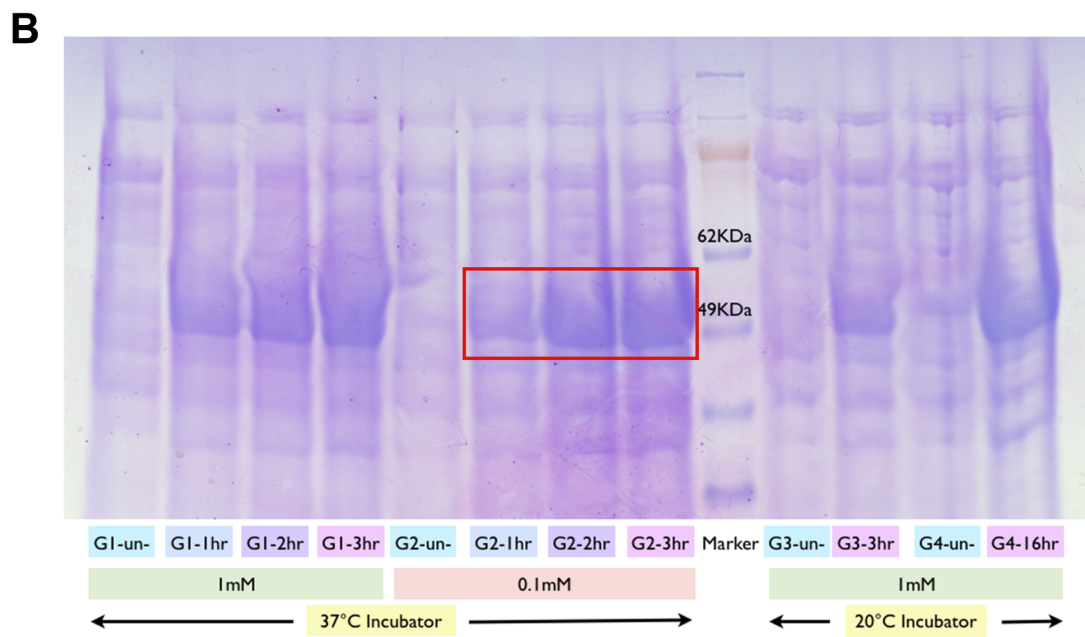


**Figure 4.1: Different conditions of IPTG Induction for *Bm*-SPN-2 expression.**

(A) Table of different conditions tested for IPTG induction of *Bm*-SPN-2 protein expression. (B) Coomassie blue staining of SDS-PAGE gel from each IPTG induction group. “kDa” means “molecular weight in kilodaltons”. “G1-un-“ stands for “Group 1 un-induced”, “G1-1hr” “G1-2hr” and “G1-3hr” represent “Group 1 post-induced 1 hour”, “Group 1 post-induced 2 hours” and “Group 1 post-induced 3 hours”. “1mM” and “0.1mM” are the concentration of IPTG. Group 1 and 2 were incubated at 37°C, while Group 3 and 4 were incubated at 20°C.

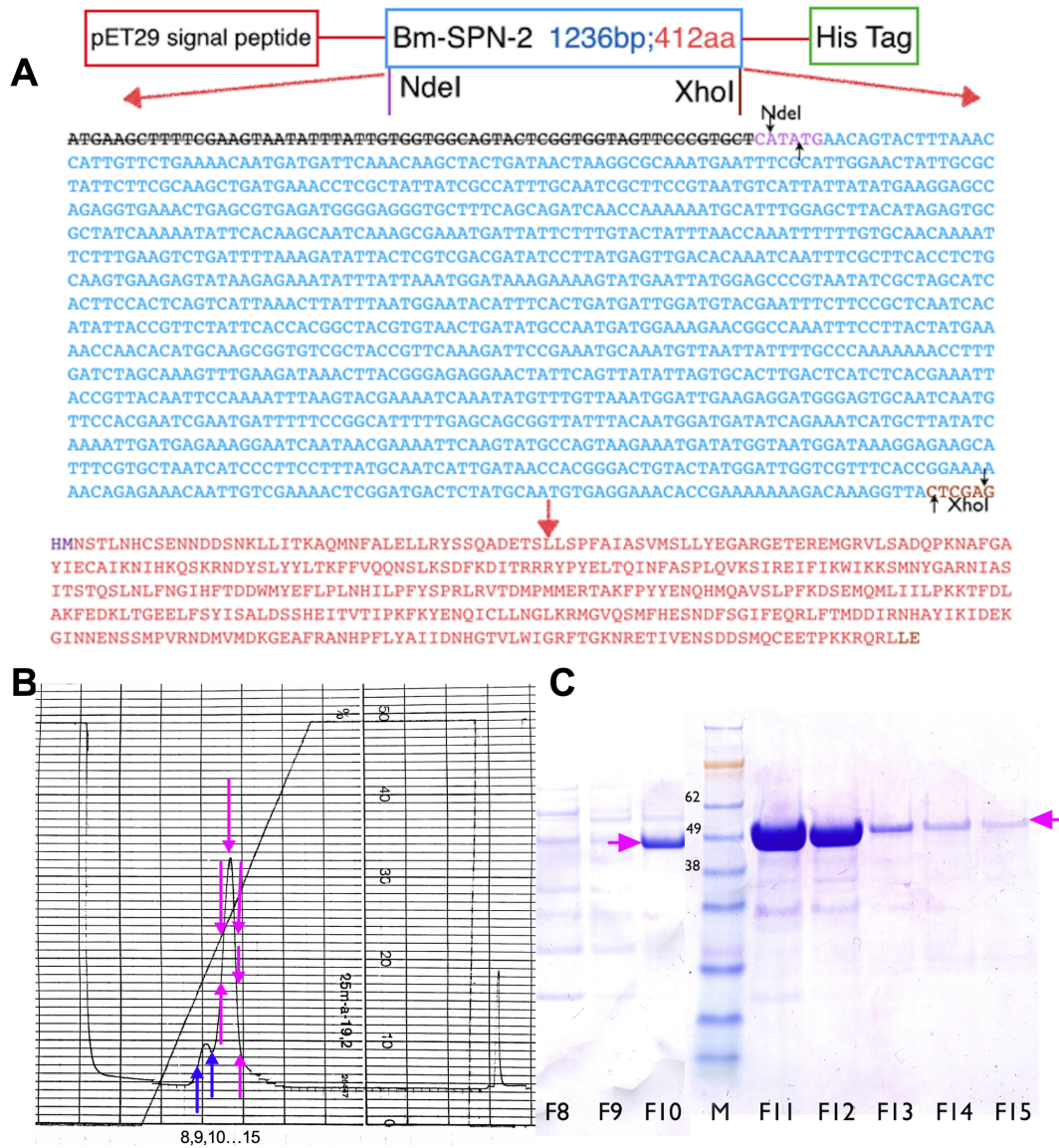


**Figure 4.2: Recombinant *Bm*-SPN-2 structure and purification.**

(A) Schematic of the *Bm*-SPN-2 produced, with vector sequences in red and restriction sites used indicated. Signal peptide of *Bm*-SPN-2 was deleted. *NdeI* (CATATG) in purple and *XhoI* (CTCGAG) in brown were placed either side of the *Bm*-SPN-2 insert and a 6-Histidine tag inserted at the C-terminal end. The insert has a total size of 1236 bp and 412aa.

(B) The UV trace of purified fractions from *Bm*-SPN-2. The elution gradient is indicated on each trace with a gradient from 0% to 50% of Elution buffer with 4M imidazole. Fractions were collected in Eppendorf tubes. Blue and purple arrows direct fraction 8 and 9, and fractions 10-15, respectively.

(C) SDS-PAGE of the purified fractions of *Bm*-SPN-2 by Coomassie Blue Staining. “M” stands for marker: SeeBlue® Plus2 Pre-stained Protein Standard. Fractions 10-12 have a clean and strong band about 52kDa, fractions 13-15 also have a clear band (purple arrow).

#### 4.2.2 Full-length IL-33 cleavage by neutrophil cathepsin G and elastase

Previously, Lefrançois et al., demonstrated that neutrophil serine proteases cathepsin G and elastase can cleave full-length human IL-33<sub>1-270</sub> and generate mature forms IL-33<sub>95-270</sub> and IL-33<sub>109-270</sub>, and IL-33<sub>99-270</sub>, respectively. Murine full-length IL-33 is also cleaved by these two enzymes (Lefrançois et al. 2012). In order to verify whether *Bm*-SPN-2 blocks IL-33 cleavage via western blotting, it was first confirmed that neutrophil cathepsin G and elastase can cleave full-length human and mouse IL-33 into cleaved forms in our own laboratory.

Using human and murine full-length IL-33 provided by Cayrol et al and commercial human neutrophil cathepsin G (Calbiochem®, Cat: 219373-100MIU) and elastase (Calbiochem®, Cat: 324681-50UG), these collaborative experiments were undertaken with the group of Cayrol et al.

For human IL-33 cleavage, 2µl of full-length IL-33<sub>1-270</sub> was incubated with human neutrophil Cathepsin G (0.025mU/µl) for 1 hour at 37°C or for 30 minutes with human neutrophil Elastase (0.01mU/µl). Following incubation, proteases were inactivated by heating 95°C 5 minute and samples loaded immediately onto SDS-PAGE gel. Western blotting was then performed with anti-human IL-33, using Hs IL-33 (305B) monoclonal antibody from Adipogen as primary antibody and anti-mouse HRP from Promega as secondary antibody (the workflow of human IL-33 cleavage experiment is shown in Figure 4.3A). As the western blotting shown in Figure 4.3B, human neutrophil Cathepsin G (0.025mU/µl) cleaves human full-length IL-33<sub>1-270</sub> into two major products: Hs IL-33<sub>95-270</sub> of about 21kDa and Hs IL-33<sub>109-270</sub> of around 18kDa. In addition, human neutrophil elastase (0.01mU/µl) less efficiently cleaves human full-length IL-33<sub>1-270</sub> into one major product Hs IL-33<sub>99-270</sub> with the size of ~20 kDa (in the right-hand panel of Figure 4.3B), which is consistent with the previous finding of Lefrançois et al, although it was not showing relatively weak cleavage (Lefrançois et al. 2012), suggesting higher concentration of neutrophil elastase is needed. Proteins were comigrated on SDS-PAGE with 1µl in vitro-translated Hs IL-33<sub>95-270</sub> and Hs IL-33<sub>109-270</sub>.

For murine full-length IL-33 cleavage experiment, a similar procedure was performed as human IL-33, followed by anti-mouse IL-33 western blotting and revealed by primary antibody goat anti-mouse IL-33 (R&D systems AF3626) and secondary antibody donkey anti-goat-HRP V8051 (Promega A16005) (the workflow of mouse IL-33 cleavage experiment is shown in Figure 4.4A). It is shown in Figure 4.4B that compared to the concentration of 0.005mU/ $\mu$ l, 0.025mU/ $\mu$ l of neutrophil Cathepsin G could completely cleave 2 $\mu$ l murine IL-33<sub>1-266</sub> into a major cleavage product: Mm IL-33<sub>102-266</sub> with the size of ~20 kDa, whereas 0.05mU/ $\mu$ l of neutrophil Elastase could fully cleave murine IL-33<sub>1-266</sub> into a similar major cleavage product Mm IL-33<sub>102-266</sub> and a second minor product Mm IL-33<sub>109-266</sub> (~18 kDa), which is also consistent with the previous findings of Lefrançois et al (Lefrançois et al. 2012). Proteins were comigrated on SDS-PAGE with 1 $\mu$ l *in vitro*-translated murine IL-33<sub>102-266</sub> (~20 kDa).

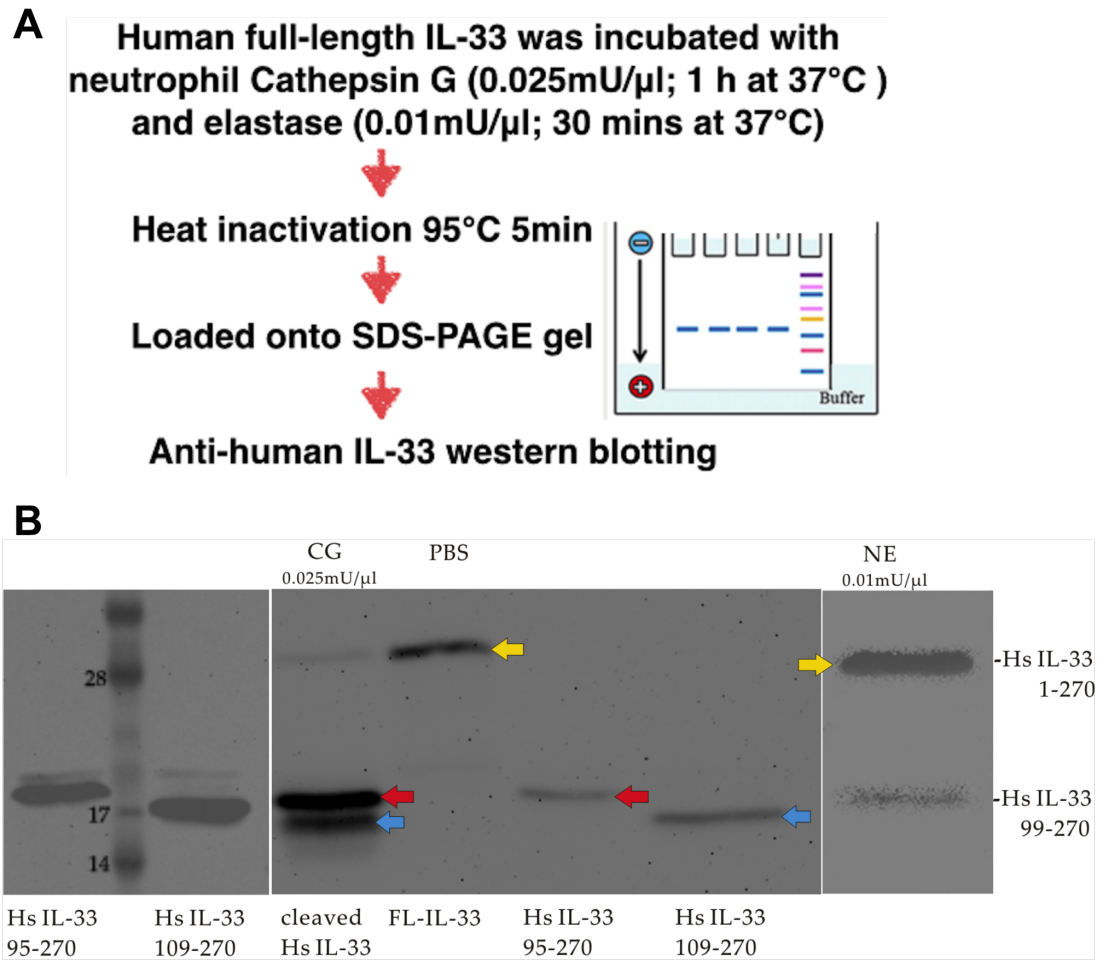


**Figure 4.3: Human neutrophil cathepsin G (CG) or neutrophil elastase (NE) cleaves human full-length IL-33 into cleaved forms.**

(A) Workflow of human IL-33 cleavage experiment by CG or NE.

(B) PBS, CG (0.025mU/ $\mu$ l) or NE (0.01mU/ $\mu$ l) were incubated with 2 $\mu$ l human full-length IL-33<sub>1-270</sub>. Human FL-IL-33 (yellow arrow) was cleaved into two major bands by CG: Hs IL-33<sub>95-270</sub> (red arrow at the left) and Hs IL-33<sub>109-270</sub> (blue arrow at the left), whereas one major band Hs IL-33<sub>99-270</sub> was observed after cleavage by NE. Proteins were comigrated on SDS-PAGE with in vitro-translated Hs IL-33<sub>95-270</sub> (red arrow at the right) and Hs IL-33<sub>109-270</sub> (blue arrow at the right) and revealed by western blot with primary antibody Hs IL-33 (305B) monoclonal antibody from Adipogen and secondary antibody mouse HRP from Promega.

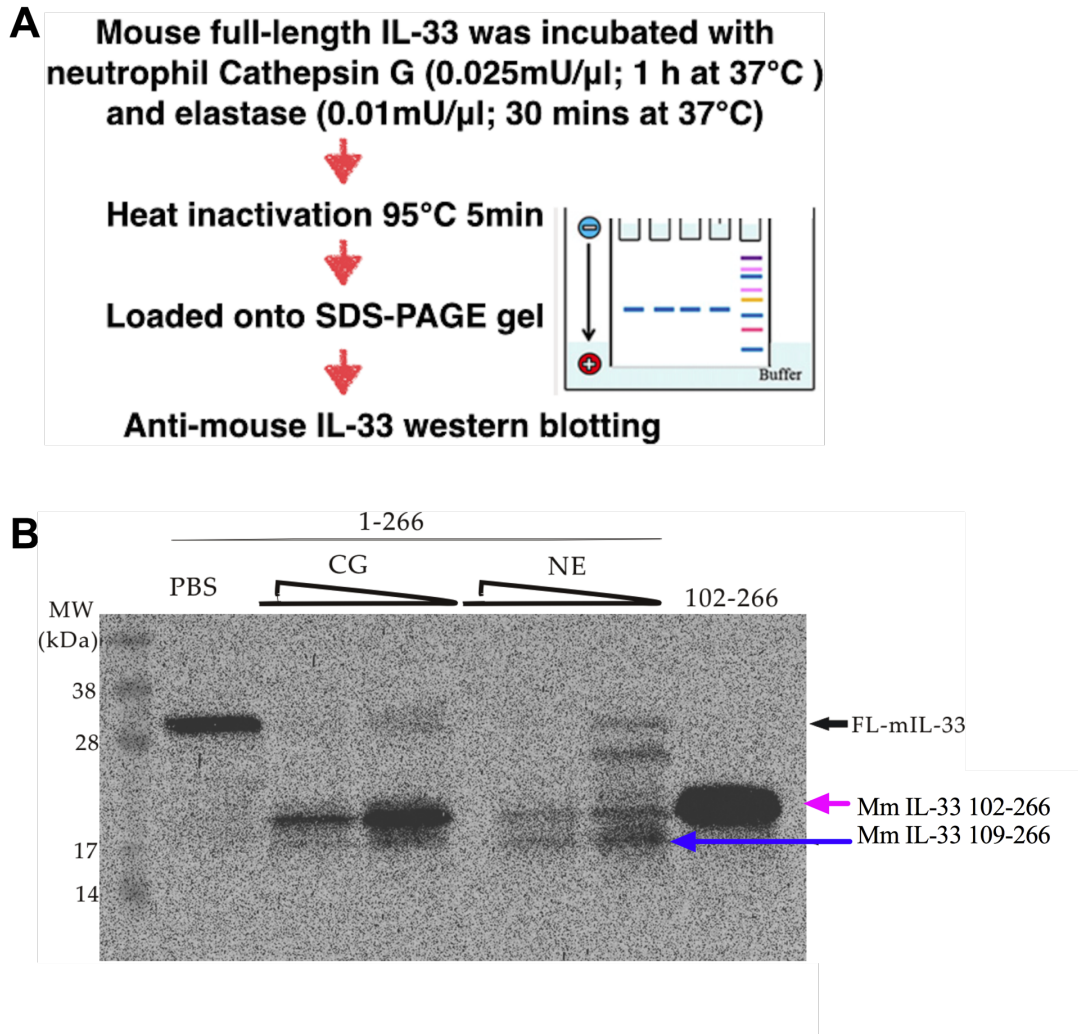


**Figure 4.4: Murine full-length IL-33 cleavage processed by human neutrophil cathepsin G (CG) and elastase (NE).**

(A) Workflow of murine IL-33 cleavage experiment by CG or NE.

(B) PBS, CG (0.025mU/μl and 0.005mU/μl) or NE (0.05mU/μl and 0.005mU/μl) were incubated with 2μl murine full-length IL-33<sub>1-266</sub>. Proteins were comigrated on SDS-PAGE with 1 μl in vitro-translated murine IL-33<sub>102-266</sub> (~20kDa) and revealed by western blot with primary antibody goat anti-mouse IL-33 (R&D systems AF3626) and secondary antibody Donkey anti-goat-HRP V8051 (Promega A16005). Mouse FL-IL-33 was cleaved into one major band by human neutrophil CG: Mm IL-33<sub>102-266</sub> (purple arrow) with the size of about 20kDa, whereas one major band Mm IL-33<sub>102-266</sub> and a second minor band MmIL-33<sub>109-266</sub> (blue arrow) were observed after cleavage by human neutrophil NE.

### 4.2.3 Investigating the effects of *Bm*-SPN-2 on IL-33 cleavage

#### 4.2.3.1 Testing *Bm*-SPN-2 for its ability to block IL-33 cleavage

In order to verify whether *Bm*-SPN-2 blocks human and murine full-length IL-33 cleavage by inhibiting the enzyme activity of human neutrophil cathepsin G or elastase, different concentrations of *Bm*-SPN-2 were pre-incubated with human neutrophil Cathepsin G (0.025mU/ $\mu$ l) or elastase (0.01mU/ $\mu$ l) for 10 minutes at 37°C, prior to adding 1 or 2 $\mu$ l of human or murine full-length IL-33. Similar steps were then performed as in the IL-33 cleavage experiments above, followed by anti-human or murine IL-33 western blotting, respectively (the workflow is shown in Figure 4.5A).

To test whether *Bm*-SPN-2 blocks human IL-33 cleavage, as shown in Figure 4.5B, 0, 1, 2, 3 and 4  $\mu$ g/ $\mu$ l of *Bm*-SPN-2 was pre-incubated with 0.025mU/ $\mu$ l cathepsin G or heat treated (95°C 5 minutes) CG prior to adding 2 $\mu$ l of full-length human IL-33 protein produced in rabbit reticulocyte lysate (RRL). (kindly provided by the group of Cayrol et al.) In order to reveal the expected cleaved bands of human IL-33, a 13.5% SDS-PAGE gel was made for western blotting. Proteins were comigrated on SDS-PAGE with 1 $\mu$ l *in vitro*-translated human IL-33<sub>95-270</sub> and Hs IL-33<sub>109-270</sub>. In addition to visualising protein migration on the gel (Figure 4.5B), the band intensities of human full-length and cleaved IL-33 were quantified as in Figure 4.5C. The results showed that with increasing concentrations of *Bm*-SPN-2, the band signal of full-length IL-33 increased correspondingly, whereas the band signal of lower band of cleaved IL-33 (109-270) decreased. However, in this experiment *Bm*-SPN-2 was not able to fully block the cleavage of IL-33.

An additional experiment was then conducted, to evaluate increasing the concentration of *Bm*-SPN-2 up to 6 $\mu$ g/ $\mu$ l while reducing the full-length IL-33 down to 1 $\mu$ l, directly using the human RRL IL-33 from the previous paper of Lefrançois et al., (Lefrançois et al. 2012) without measuring the concentration of IL-33. According to this paper, Lefrançois et al. mapped the cathepsin G cleavage sites at F94 and L108 in the human IL-33 sequence. Surprisingly, the upper band of cleaved IL-33<sub>95-270</sub> but not the lower band of cleaved IL-33<sub>109-270</sub> were detected after western blotting.

This finding might be due to there being very little FL-IL-33 and a higher amount of *Bm*-SPN-2 protein blocking the CG cleavage site L108 of the FL-IL-33. It was also found that inhibition is significantly increased at 6µg/µl of *Bm*-SPN-2, which can almost completely block the cleavage of the human IL-33 (Figure 4.5D). The quantification of the band intensity of full-length and cleaved IL-33 were analysed in Figure 4.5E, showing that there is almost no signal for the cleaved IL-33 when using 6µg/µl of *Bm*-SPN-2. However, it was not possible to obtain any evidence that *Bm*-SPN-2 blocks the cleavage of human IL-33 by human neutrophil elastase.

To test whether *Bm*-SPN-2 also blocks murine IL-33 cleavage by inhibiting these two enzymes, a similar workflow was performed as shown in Figure 4.6A. It was demonstrated that *Bm*-SPN-2 does show some ability to block mouse IL-33 cleavage by inhibiting neutrophil elastase in a dose-dependent manner (see Figure 4.6B). However, even the highest concentration of *Bm*-SPN-2 (6µg/µl) could not completely inhibit the function of neutrophil elastase to cleave mouse full-length IL-33. In contrast, heat-treated neutrophil elastase could no longer cleave murine full-length IL-33. Unfortunately, unlike the human IL-33 cleavage experiment (Figure 4.5), it was not possible to analyse western blotting of mouse IL-33 cleavage (Figure 4.6) accurately on the LI-COR® Image Studio Lite software, due to resolution and background problems. However, interestingly, *Bm*-SPN-2 shows slight inhibitory function against Cathepsin G cleavage of mouse IL-33 but did not to do so in a dose-dependent manner (see Figure 4.6C). As each of the Western blotting experiments with both human and murine full-length IL-33 were performed only once (due to the sample of FL-IL-33 being very limited), any firm conclusions must await repeats being done.

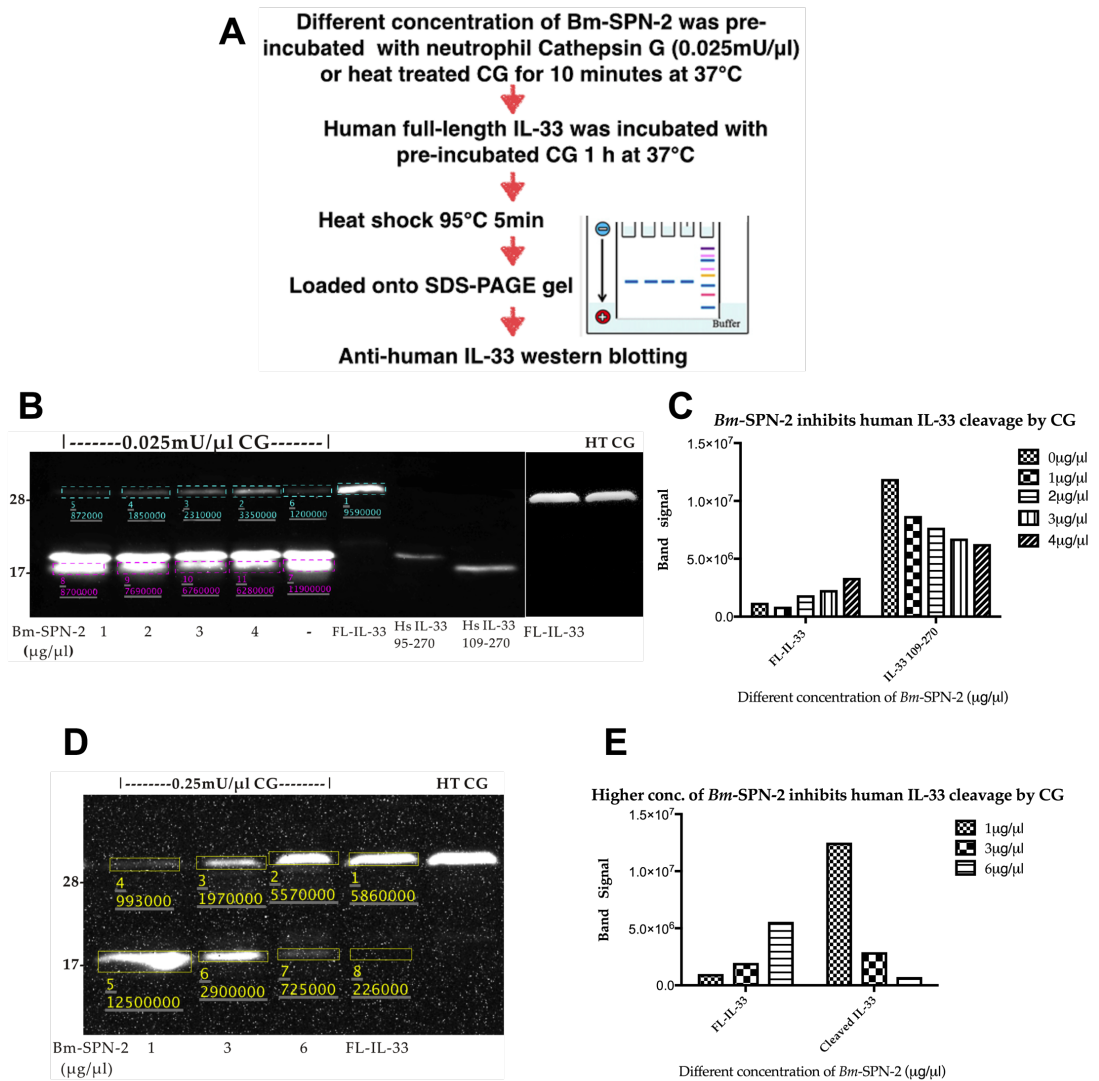


**Figure 4.5** *Bm*-SPN-2 inhibits human full-length IL-33 cleavage by human neutrophil CG in a dose-dependent manner.

(A) Workflow of human IL-33 cleavage inhibition test by *Bm*-SPN-2.

(B) Western blotting of human IL-33 following cleavage by human neutrophil cathepsin G in the presence of *Bm*-SPN-2. 0, 1, 2, 3, 4 μg/μl of *Bm*-SPN-2 were pre-incubated with 0.025mU/μl CG or heat treated (HT) CG. 2μl of human full-length IL-33 protein produced in rabbit reticulocyte lysate (RRL) was used. 13.5% SDS-PAGE gels were used to reveal cleaved bands. Proteins were comigrated on SDS-PAGE with in vitro-translated Hs IL-33<sub>95-270</sub> and Hs IL-33<sub>109-270</sub> and revealed by western blot with primary antibody Hs IL-33 (305B) monoclonal antibody from Adipogen and secondary antibody mouse HRP from Promega.

(C) Quantification of the human full-length and lower mol.wt cleaved IL-33 bands from the western blot shown in Panel B.

#### Chapter 4. Functional analysis of *Bm*-SPN-2

(D) Western blotting of human IL-33 following cleavage by neutrophil cathepsin G in the presence of higher concentrations of *Bm*-SPN-2. 1, 3, 6  $\mu\text{g}/\mu\text{l}$  of *Bm*-SPN-2 were pre-incubated with 0.025mU/ $\mu\text{l}$  CG or heat treated (HT) CG. 1 $\mu\text{l}$  of human full-length IL-33 proteins produced in rabbit reticulocyte lysate (RRL) was used here.

(E) Quantification of the human full-length and cleaved IL-33 bands from the western blot shown in Panel D. Western blotting of different amounts of human FL-IL-33 was only performed once, as the sample of FL-IL-33 is very limited. Western blot quantification was analyzed by software LI-COR® Image Studio Lite.

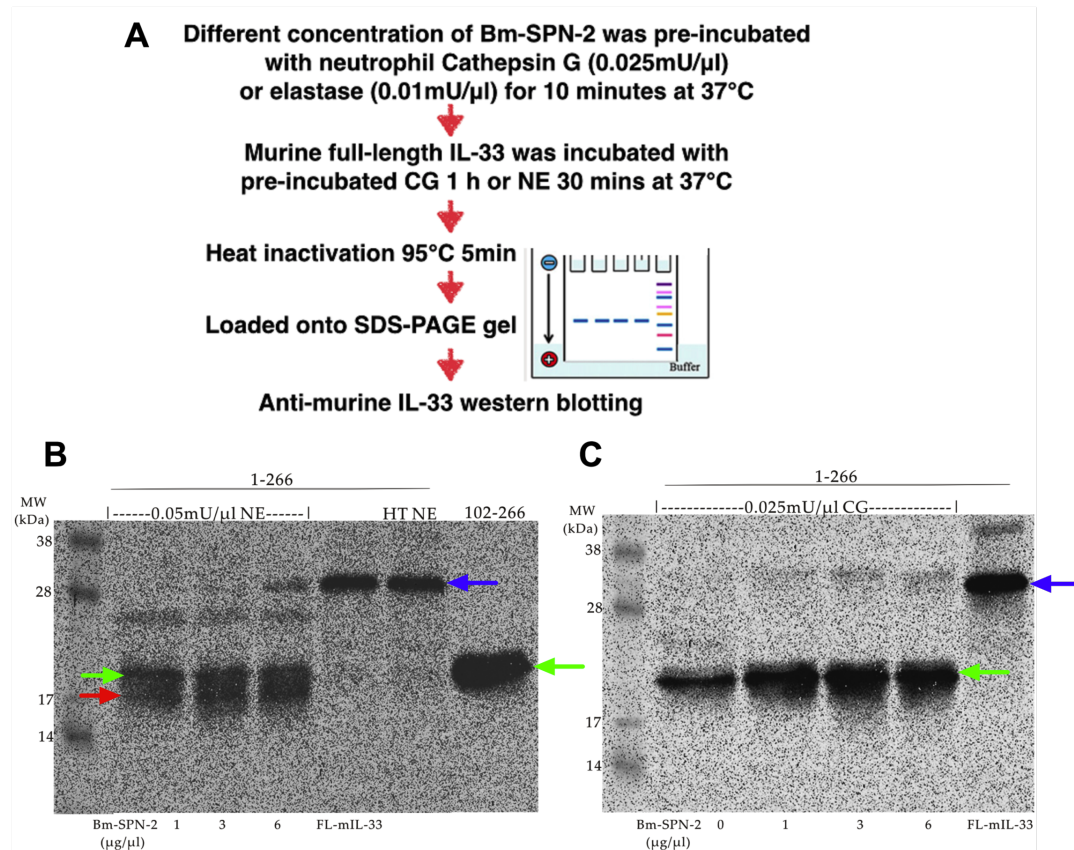


**Figure 4.6: Inhibitory functional test of *Bm*-SPN-2 in a murine IL-33 cleavage experiment with neutrophil cathepsin G or elastase.**

(A) Workflow of murine IL-33 cleavage inhibition test by *Bm*-SPN-2.

(B) *Bm*-SPN-2 inhibitory function test on murine IL-33 cleavage by neutrophil elastase. 1, 3, 6  $\mu$ g/ $\mu$ l of *Bm*-SPN-2 were pre-incubated with 0.05mU/ $\mu$ l NE prior to adding 2 $\mu$ l murine full-length IL-33. “HT NE” stands for heated treated neutrophil elastase. Heat treated NE can no longer cleave IL-33.

(C) *Bm*-SPN-2 inhibitory function test through murine IL-33 cleavage by neutrophil CG. 0, 1, 3, 6  $\mu$ g/ $\mu$ l of *Bm*-SPN-2 were pre-incubated with 0.025mU/ $\mu$ l CG prior to adding 2 $\mu$ l murine full-length IL-33. Blue arrow indicates the murine full-length IL-33, green arrow shows the murine IL-33 (102-266) and red arrow indicates the murine IL-33 (109-266) fragment. Western blotting with the murine FL-IL-33 was performed only once, as the sample of FL-IL-33 was very limited.

#### 4.2.3.2 Testing *Bm*-SPN-2 inhibitory function by enzyme activity assay

Based on the previous result that *Bm*-SPN-2 blocks human IL-33 cleavage by inhibiting human neutrophil Cathepsin G in a dose-dependent manner, it was decided to verify this inhibitory function utilizing a commercial enzyme activity assay kit. Thus, the Cathepsin G activity colorimetric assay kit purchased from BioVision (Cat No. K146) was used to perform this experiment. In this assay kit, Cathepsin G cleaves the substrate and releases the dye group, pNA (4-Nitroaniline), which can be detected in the visible wavelengths at 405 nm.

A range of different concentrations of *Bm*-SPN-2, as well as the corresponding concentrations of bovine serum albumin (BSA) as controls, cathepsin G inhibitor or phosphate-buffered saline (PBS) were incubated with human neutrophil cathepsin G for 20 minutes at 37°C. Next, the pre-incubated samples were directly diluted into the Assay Buffer, to take volumes up to 50 µl/well in a 96-well plate. Background controls added 10 µl Assay Buffer alone to one test sample, and 10 µl diluted Cathepsin G inhibitor to another. Next, substrate solution was added to each sample well and mixed. Finally, absorbance was measured at 405nm at 37°C at time zero and 1 hour later on an ELISA plate reader (the workflow of the cathepsin G activity assay kit is shown in Figure 4.7A).

As shown in Figure 4.7B and 4.7C, however, no inhibitory activity could be detected. This was determined with two independent batches (A and B) of different concentration (1, 2.5 and 5µg/µl) of *Bm*-SPN-2, with no conditions showing inhibitory function against neutrophil cathepsin G, whereas CG inhibitor could inhibit the activity of Cathepsin G. Although the OD values of samples including *Bm*-SPN-2 were higher than those with CG alone, this may be accounted for a low level of intrinsic absorbance by *Bm*-SPN-2 itself (as shown in Figure 4.7C).

In parallel, a fluorometric neutrophil elastase activity assay kit (Cat No. K383 by Biovision) was also used to test the inhibitory function of *Bm*-SPN-2 against elastase. However, it proved unsuccessful to obtain a clear result due to problems with variability with the standard curve stable (data not shown).

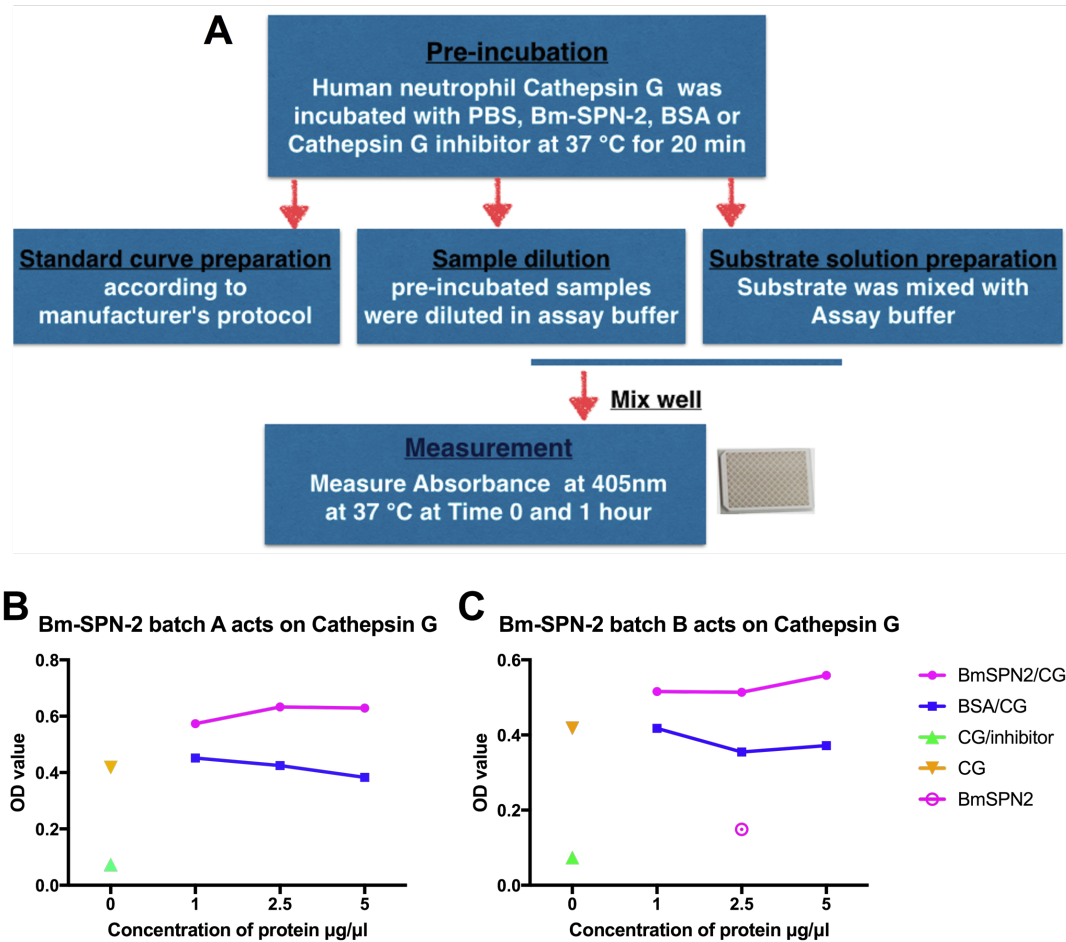


**Figure 4.7: Testing the inhibitory function of *Bm*-SPN-2 by enzyme activity assay kit of Cathepsin G.**

(A) Workflow of investigating the inhibitory function of *Bm*-SPN-2 by Cathepsin G Activity Colorimetric Assay Kit.

(B) 1, 2.5 and 5 µg/µl of *Bm*-SPN-2 batch A (pink round solid) or BSA (blue square), or cathepsin G inhibitor (Green triangle) was incubated with 0.5mU/µl of human neutrophil cathepsin G, or CG only (Brown triangle).

(C) Similar incubation as (B) of *Bm*-SPN-2 batch B and *Bm*-SPN-2 alone (pink circle).

#### 4.2.4 Production of mCherry-labelled *Bm*-SPN-2

mCherry is a fluorescent protein used in biotechnology as a tracer to follow the flow of fluids, or as a marker for specific molecules and cell components. mCherry, derived from a protein isolated from *Discosoma* sp., is a monomeric fluorescent construct with peak absorption/emission at 587 nm and 610 nm, respectively. It is resistant to photobleaching and is relatively stable (Shaner et al. 2004).

In *Brugia malayi*, two serpin proteins have been described, *Bm*-SPN-1 (Yenbutr and Scott 1995) and *Bm*-SPN-2 (Zang et al. 1999). Although both *Bm*-SPN-1 and *Bm*-SPN-2 were characterized to be secretory (Zang et al. 1999, Molehin et al. 2012), *Bm*-SPN-2 (GenBank: AF009825.1) shows very low similarity (53.4%, 197/369) and identity (27.9%, 103/369) to the previously described *Bm*-SPN-1 (GenBank: U04206.1) at the amino acid level; however conserved ‘motif’ and ‘signature’ sequences can be recognized (Zang and Maizels 2001) (Figure 4.8). After mapping the protein sequence of *Bm*-SPN-2 against WormBase ParaSite website, it was shown to have 99.8 % identity with *B. timori* serpin and 96.7% identity with *B. pahangi* serpin (Figure 4.9). As reported by Zang et al. compared to homologues from other species such as *Caenorhabditis elegans*, *Bm*-SPN-2 has not only acquired a signal peptide but also an extra N-terminal tract (Figure 4.10) (Zang et al. 1999), which might be the crucial for interacting with host cells. In order to investigate any potential binding or uptake of *Bm*-SPN-2 with host cells such as human neutrophils to carry out its potential inhibitory function detected by the Western blotting, it was necessary to develop an m-Cherry labelled construct of *Bm*-SPN-2. Considering that we already had *Bm*-SPN-2 construct in pET29 vector, the first strategy was to insert the mCherry open reading frame into the previous construct at the site of restriction enzyme “*Xho*I”, at the 3' end of the *Bm*-SPN-2 coding sequence as shown in Appendix 4.1. An insert encoding mCherry was designed with *Xho*I and *Not*I restriction sites at the both ends and codon optimized for *E. coli* for gene synthesis in the pMK vector (bacterial resistance against kanamycin) by GeneArt®, as shown in Appendix 4.1. Terminal *Not*I sites were included to allow the insert a more flexible use for any subsequent construct in the lab.

As this strategy necessitated insertion into a single site in the coding sequence, it was not directional and equally the synthesized mCherry insert

contained the same restriction enzymes at both ends. Hence, there would be only a 50% chance of insertion in the correct orientation of mCherry sequence into the existing *Bm*-SPN-2 construct pET29T vector. Because the cut *Bm*-SPN-2 plasmid could reanneal at the single *Xho*I restriction site, calf-intestinal alkaline phosphatase (CIP) was applied to the *Xho*I digested *Bm*-SPN-2 construct to catalyze the removal of phosphate groups from the 5' end of DNA strands (Sambrook, Fritsch and Maniatis 1989), thereby preventing recircularization of linearized vector DNA, and this step was expected to improve the yield of vector containing the appropriate insert (Ullrich et al. 1991). As the insert is relatively short (737 bp) compared to the *Xho*I-digested vector (6558bp), a range of different ratios of vector and insert were applied 1:5, 1:10, 1:20, 1:50 etc. Unfortunately, using these materials and the methods to hand, and despite a number of attempts, inserting the mCherry into the previous construct *Bm*-SPN-2 was not successful.

An alternative strategy was then adopted to express full-length *Bm*-SPN--mCherry fusion protein in the pET29 vector. The full nucleotide sequence of the desired *Bm*-SPN-2-mCherry protein was codon optimized for *E. coli* and gene synthesised by Invitrogen "GeneArt" Thermo Fisher Scientific; the insert was provided cloned into in pMA-T vector (containing an ampicillin resistance gene) with the structure shown in Figure 4.11A (Gene synthesis documents see Appendix 4.2). As the pET29a vector encodes resistance against kanamycin, the vector and synthesized *Bm*-SPN-2-mCherry pMA-T were transformed into JM109 cells onto kanamycin and ampicillin agar plates, respectively. Plasmid minipreps of both insert and vector were double digested with restriction enzymes *Nde*I and *Xho*I, with an additional CIP treatment of the vector in case of incomplete cleavage permitting recircularization. The *Nde*I/*Xho*I digestion products from pET29a and *Bm*-SPN-2-mCherry in pMA-T were analyzed by DNA gel (Figure 4.11B).

Gel extraction of the lower mol wt band depicted in pink (*Bm*-SPN-2-mCherry insert) was followed by ligation into the pre-cut pET29a (in blue frame) expression vector (Figure 4.11B). In order to maximise the chance of a large insertion (1953bp) into the pre-cut vector, very low amounts (down to 15.5ng) of vector and a range of different insert: vector ratios (such as 10:1; 20:1 and 50:1) were used for the ligation at 16°C overnight, catalyzed by NEB T4 DNA ligase (M0202).

Following the ligation, transformation and plating of bacterial cells, new colonies were screened. The T7 promoter primer and T7 terminator reverse primer (specific primers for pET29a vector, primer sequences see section 2.4.2.1) were used to perform colony screens, colonies A, D, F, K, M and S were first chosen for sequencing and colony F proved to contain correct sequence (See Figure 4.11C, sequencing result see appendix 4.3).

Next, the plasmid from the validated colony F was used to express the *Bm*-SPN-2-mCherry fusion protein in *E. coli*. Purified plasmid was used to transform BL21 (DE3) chemically competent *E. coli* cells, which were then grown in 500ml cultures in the presence of 1mM IPTG for protein expression. Following 3 hours induction, bacteria were centrifuged and the BugBuster® protein Extraction Reagent was then used for extracting proteins into a soluble supernatant. The schematic of the proteins produced is shown in Figure 4.12A, showing the *Bm*-SPN-2-mCherry insert with the size of 1953bp being flanked with sites for the restriction enzymes *Nde*I and *Xho*I, and as a fusion protein containing a C-terminal hexahistidine-tag for affinity purification.

*Bm*-SPN-2-mCherry protein was then purified by nickel chelating chromatography. The UV trace of purification is shown in Figure 4.12B, with material starting to elute from the fraction A8 and ending at fraction B5. It was striking to see that these fractions are visibly pink in colour, reflecting the presence of the mCherry component of the fusion protein.

SDS-PAGE and anti-His western blotting of the purified fractions of *Bm*-SPN-2-mCherry were then carried out, as shown in Figure 4.12C, 4.12D and 4.12E. By protein staining, a faint band can be observed with the molecular weight of *Bm*-SPN-2-mCherry of about 75 kDa (Figure 4.12C). Western blotting with anti-His antibodies confirms the presence of the recombinant protein at this position, as pointed out in Fig 4.12D by a pink arrow. A lower mol.wt band around 26kDa is also observed (blue arrow), which corresponds to the mCherry portion of the protein resulting from cleavage during heating prior to gel analysis. In this instance, proteins were heated to 62°C for 5 minutes, rather than 95°C which would cause more extensive breakdown and release of mCherry (data not shown). Anti-His western blotting of purified fractions A8-B3 can also be captured by Alexa Fluor 488 at

610nm using PXi/PXi Touch Fluorescent & Chemiluminescent Imaging System from SYNGENE (see Figure 4.12E), with similar results, confirming that mCherry is successfully expressed together with the recombinant *Bm*-SPN-2.

```

CLUSTAL O(1.2.4) multiple sequence alignment

Bm-SPN-2      MK--LFEVIFIVVAVLGGSSRANSTLNHCSENDDSNKLLITKAQMNFALELLRYSSQAD
Bm-SPN-1      MKNQTITAI FVLVAS----AQFVF-----ILGQISLTERAQLDFAVSL LQNVAESD
                **   : .**:**      : :                .: *  :***:**.**: :**

Bm-SPN-2      ETSLLSPFAIASVMSLLYEGARGETEREMGRVLSADQPKNAFGAYIECAIKNIHKQSKRN
Bm-SPN-1      KSSVLSPFVSVSTSLFIAYLAADGETKQQLQSVLGDASISEFRLHFAKQLAYIARAGS-R
                **:***:**: : : * . * **::: : ** . * . * : : : * : . . .

Bm-SPN-2      DYSLYYLTKFFVQQ--NSLKSDFKDITRRRYPYELTQINFASPLQVKSIREIFIKWIKKSM
Bm-SPN-1      NYTLTVANRLYVREGLSVKESFQRVLSFYYSDDLHKFSFGQ---RNRLVQQINNWISSKT
                **: * . :***: : **..* : : * * : : . . : : : : : **..

Bm-SPN-2      NYGARNIA---SITSTQSLNLFNGIHFTDDWMEFLPLNHILP-FYSPRLRVTDMPMMER
Bm-SPN-1      NNKVRNIITRSITEDTRMLLMNAIHFKGTWTWVQFIDFATKQKQFHISENEVKLVPMMSK
                * .***   ** . : **.***.. * **: :      * : . . * . :***:

Bm-SPN-2      TAKFPYYENQHMQAVSLPFKDSMQMLIILPKKTFDLAKFEDKLTGEELFSYISALDSSH
Bm-SPN-1      SDTVPYYEDDAVKVIKLPYIGDEVEMVIIIPRRRFGLSDVLENLSGEKLLKYVNEAT-NR
                : ..***: : : .** : ..*::***: : *.. . : : **:**. * . . .

Bm-SPN-2      EITVTIPKFKYENQICLLNGLKRMGVQSMFHESNDFSGIFEQRL-FTMDDIRNHAYIKID
Bm-SPN-1      SVSIKLPFRFKVEEKRNLNSALQAIGITDAFSGNANSEELFNNSLPISIGKIIHAGFIEVN
                .: : : ** * : : * ..* : : * . * . : . : * : * : : . . * : : ** : :

Bm-SPN-2      EKGINNENSSMPVRNDMVMKGEAFRANHPFLYAIIDNHGTVLWIGRFTGKNRETIVENS
Bm-SPN-1      EKGTESAAATI-IELEDRMGSSRNFNADQPFLFAIVKDLKTVLFLGQYVK-----
                *** : . : : : : : * . . . * . : : ** : : : : : ** : : : :

Serpin motif Reactive-site loop Serpin signature

Bm-SPN-2      DDSMQCEETPKKRQRL
Bm-SPN-1      -----
    
```

**Figure 4.8: *Bm*-SPN-1 and *Bm*-SPN-2 alignment.**

*Bm*-SPN-1 and 2 stands for *Brugia malayi* serine protease inhibitor 1 and 2. *Bm*-SPN-1 refers to GenBank: U04206.1 whereas *Bm*-SPN-2 refers to GenBank: AF009825.1. Serpin motif, reactive-site loop and serpin signature were labelled with three different colour.

Chapter 4. Functional analysis of *Bm*-SPN-2

```

>>EMBOSS_001 (428 aa)
Waterman-Eggert score: 2731; 669.8 bits; E(1) < 4.4e-197
96.7% identity (99.1% similar) in 428 aa overlap (1-428:1-428)

      10      20      30      40      50      60
Bm-SPN-2 EMBOS MKLFEVIFIVVAVLGGSSRANSTLNHCSENNDDSNKLLITKAQMNFALELLRYSSQADET
      .....
Bp-SPN EMBOS MKLFEVIFIVVAVLGGSSRANSTLNHCSENNDDSNKLLITKAQMNFALELLRYSSQADEA
      10      20      30      40      50      60

      70      80      90      100     110     120
Bm-SPN-2 EMBOS SLLSPFAIVSVMSLLYEGARGETEREMGRVLSADQPKNAFGAYIECAIKNIHKQSKRNDY
      .....
Bp-SPN EMBOS SLLSPFAIVSVMSLLYEGARGETEREMGRVLSADQPKNAFGAYIECAIKNIHKQSKRNDY
      70      80      90      100     110     120

      130     140     150     160     170     180
Bm-SPN-2 EMBOS SLYYLTKFPVQQNSLKSDFKDITRRRYPYELTQINFASPLQVKSIREIFIKWIKKSMNYG
      .....
Bp-SPN EMBOS SLYYLTKFPVQQNSLKSDFKDITRRRYPYELTQINFASPLQVKSIREIFIKWIKKSMNYG
      130     140     150     160     170     180

      190     200     210     220     230     240
Bm-SPN-2 EMBOS ARNIASITSTQSLNLFNGIHFTDDWMEFLPLNHLPPFYSRLRVTTIPMMERTAKFPYY
      .....
Bp-SPN EMBOS ARNIASMVSTQSLNLFNGIHFTDDWMEFLPLNHMSPFYSRLRVTTIPMMERTAKFPYY
      190     200     210     220     230     240

      250     260     270     280     290     300
Bm-SPN-2 EMBOS ENQHMQAVSLPFKDSEMQLIILPKKTFDLAKFEDKLTGEELFSYISALDSSHEITVTIP
      .....
Bp-SPN EMBOS ENQHMQAVSLPFKDSEMQLIILPKKTFDLAKFEDKLTGEELFSYISALDSSHEITVTIP
      250     260     270     280     290     300

      310     320     330     340     350     360
Bm-SPN-2 EMBOS KFKYENQICLLNGLKRMGVQSMFIESNDFSGIFEQRLFTMDDIRNHAYIKIDEKGINNEN
      .....
Bp-SPN EMBOS KFKYENQICLLNGLKRMGVQSMFIESNDFSGIFEQRLFTMDDIRNHAYIKIDEKGINNKN
      310     320     330     340     350     360

      370     380     390     400     410     420
Bm-SPN-2 EMBOS SSMPVRNDMVMKGEAFRANHPFLYAIIDMNGITVLWIGRFTGKNRETIVENSDDSMQCEE
      .....
Bp-SPN EMBOS SIMPVRNDMVMKGEAFRANHPFLYAIIDMNGITVLWIGRFTGKNRETIVENSDDSMQCEE
      370     380     390     400     410     420

Bm-SPN-2 EMBOS TPKKRQRL
      .....
Bp-SPN EMBOS TPKKRQRL

```

**Figure 4.9:** *Bm*-SPN-2 mapping against *Brugia pahangi* (PRJEB497) via the parasite wormbase.

*Bm*-SPN-2 stands for *Brugia malayi* serine protease inhibitor 2. Red frame shows the unmatched amino acids.

## Chapter 4. Functional analysis of *Bm*-SPN-2

CLUSTAL O(1.2.4) multiple sequence alignment

```

Bm-SPN-2  MKLFVIFIVVAVLGGSSRANSTLNHCSENNDDSNKLLITKAQMNFALELLRYSSQADET
Ce-SPN     -----MALLQSETFDGLGLLRQQN-ISES
           N-terminal signal peptide      Extra N-terminal      *: ::: :*.* *** .. .*:

Bm-SPN-2  SLLSPFAIASVMSLLYEGARGETEREMGRVLSADQPKNAFGAY--IECAIKNIHKQSK-
Ce-SPN     LAFSPLSIALALSLVHVAAGETRDQIREALVKGSTDEQLEQHFANISAALLAAERGTVEV
           **:*** .:*::: .:****. ::..* .. .: : : *..* : : :

Bm-SPN-2  RNDYSLYYLTKFFVQQNSLKSDFKDITRRRYPYELTQINFASPLQVKSIREIFIKWIKKS
Ce-SPN     KLANHVFTTRAGFK-----IKQSYLDDVKKLYNAGASSLDFDNKEATA--EAINNFVREN
           : : : * :*..* * .: : * : : : * . . * : : : :

Bm-SPN-2  MNYGAR--NIASITSTQSLNLFNGIHFDDWMEFLPLNHIL-PFYSPRLRVTDMPM-M
Ce-SPN     TGDHIKKIIGSDSINSDLVAVLTNALYFKADWQNKFKKDFSTFKSEFFSSADSKREIDFLH
           . : . *..* * * : : * . * : : * * : : :

Bm-SPN-2  ERTAKFPYYENQHMQAVSLPFKDEMQMLIILPKKTFDLAKFEDKLTGEEFSYISALDS
Ce-SPN     ASSVSRDYAENDQFVLSLPYKDNFALTIFLPKTRFGLTESLKTLDSATIQHLLSN-VS
           :.. * * : : : : * : : * : : * . * : : * * : : *

Bm-SPN-2  SHEITVTIPKFYENQICLLNGLKRMGVQSMFHESNDFSGIFEQRLFTMDDIRNHAYIKI
Ce-SPN     STSVNVQIPWKIETKLGLEALQSLGIKKAFDNDADLGNMADGLY--VSKVTHKALIEV
           * . : * * : : * * : : * : : * : : * . : . * : : : : * : :

Bm-SPN-2  DEKGINNENSS--MPVRNDMVMDKGEAFRANHPFLYAIIDNHGTVLWIGRFTGKNRETIV
Ce-SPN     DEDGTVAVAATRCSIERCRKKMKENIEFHAEHPFFFILH-HGTSYIFLGVFTG-----
           **.* : : * * . : . * : : * : : : : : : * * *

Bm-SPN-2  ENSDDSMQCEETPKKRQL
Ce-SPN     -----

```

**Figure 4.10: *Bm*-SPN-2 and *Ce*-SPN alignment.** N-terminal signal peptide is shown in the blue box, and the red box shows the additional N-terminal sequence unique to *Bm*-SPN-2. *Ce*-SPN is serpin from *Caenorhabditis elegans*, GenBank: CCD68323.1.

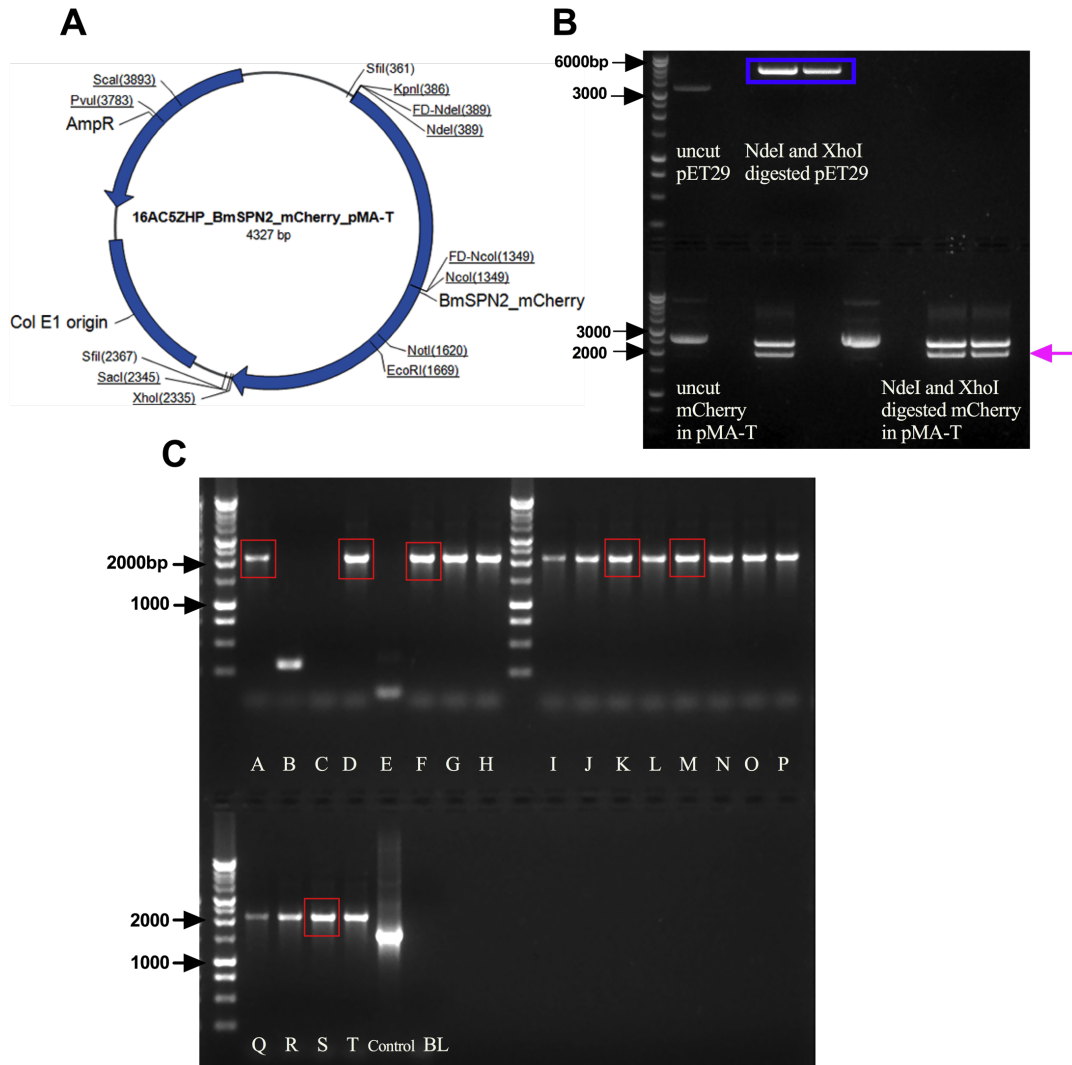
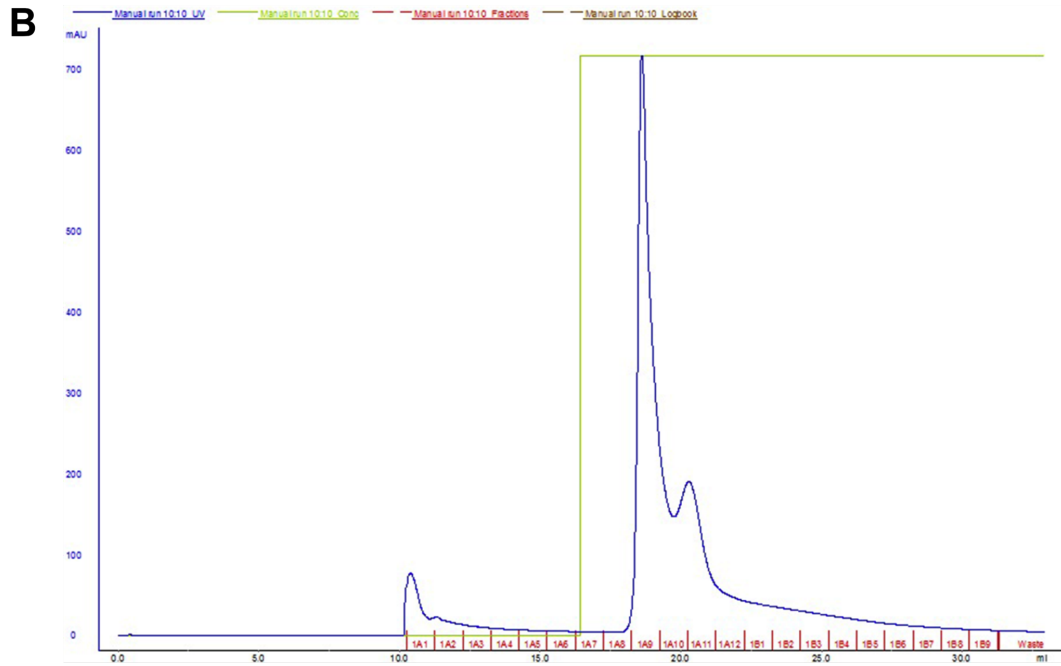
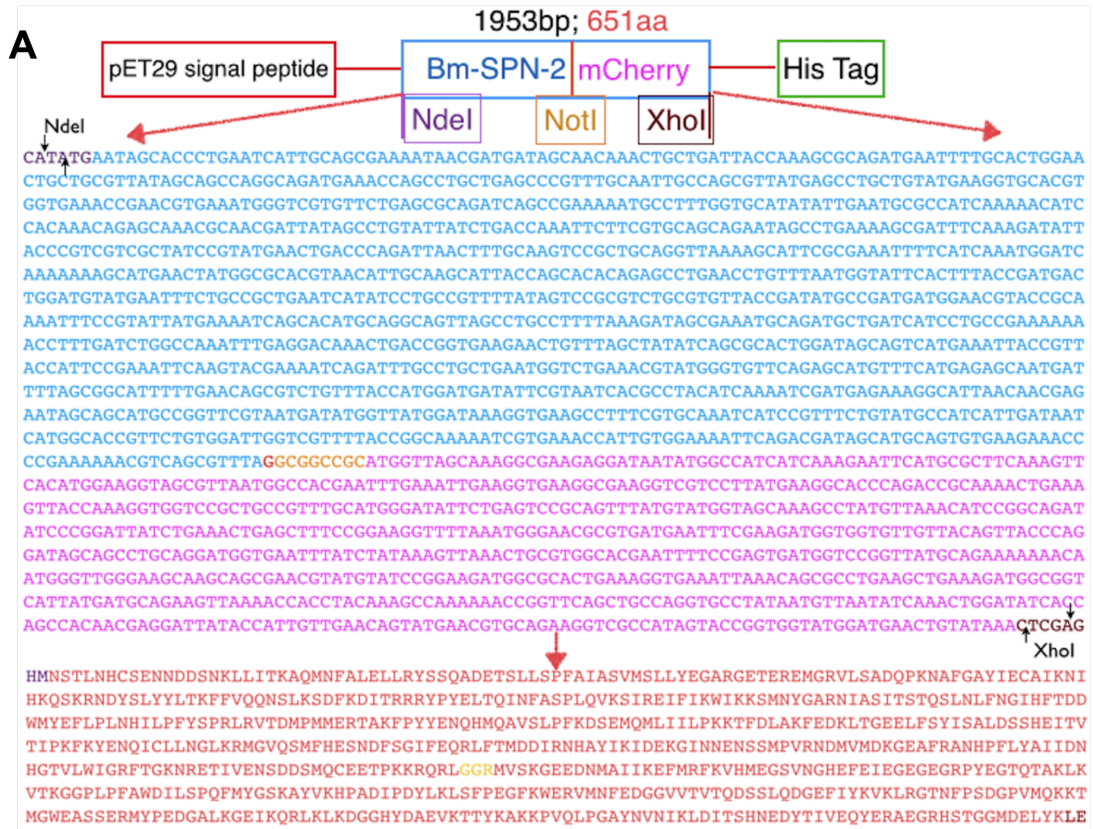


**Figure 4.11: mCherry labelling *Bm*-SPN-2 synthesis, ligation and sequencing.**

(A) Structure of gene synthesized to express *Bm*-SPN-2-mCherry fusion protein.

(B) Digestion products from pET29a vector and mCherry *Bm*-SPN-2 in pMA-T vector and following digestion with *NdeI/XhoI* restriction enzymes; gel extraction of the shorter band indicated with a pink arrow (mCherry *Bm*-SPN-2 insert of 1953bp) was followed by ligation into the pre-cut pET29a expression vector (blue box).

(C) T7 promoter primer (primer for pET29a vector, sequence is shown in Section 2.4.2.1) and T7 terminator reverse primer were used to perform colony screens, colonies A, D, F, K, M and S were first chosen for sequencing and colony F was proven to contain correct sequences. The GeneRuler™ 1 kb DNA Ladder was used. "Control" is plasmid from the previously constructed *Bm*-SPN-2.



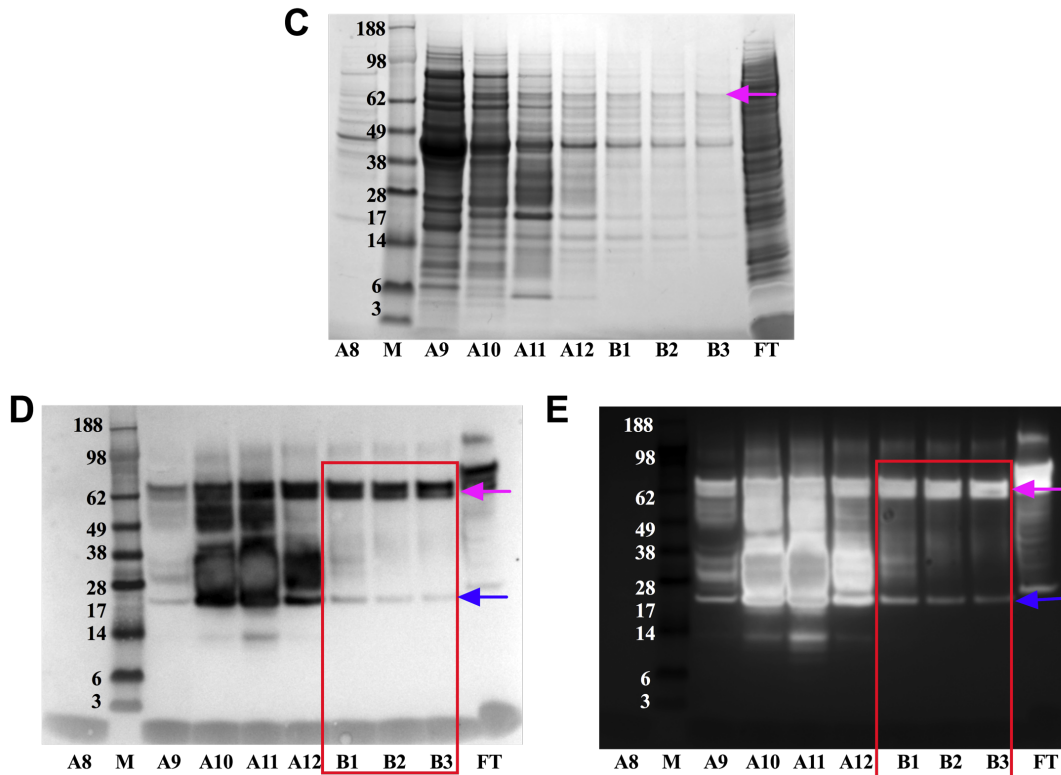


**Figure 4.12: *Bm*-SPN-2-mCherry fusion protein expression and purification.**

(A) Schematic of the *Bm*-SPN-2-mCherry produced, with vector sequences in red and restriction sites used indicated. Sites for *Nde*I (CATATG) in purple and *Xho*I (CTCGAG) in brown. The sequence of *Bm*-SPN-2 in blue and the sequence of mCherry in pink, connected by a *Not*I (GCGGCCGC) site in yellow. A total of 1953 bp should be the size of the PCR product.

(B) The UV trace of purified fractions from mCherry labelled *Bm*-SPN-2. The elution gradient of imidazole is indicated on each trace with a gradient from 0% to 100% of Elution buffer. Fractions are collected by 96 wells plates, then fractions order are shown as A1, A2, ..., A12; B1, B2...B12 and C1, ..., C12.

(C) SDS-PAGE of the purified fractions A8-B3 visualized by instant blue. Samples were pre-heated to 62°C 5mins.

(D) Anti-His western blotting of purified fractions A8-B3 recovered from the chelating chromatography column. Pink arrows point out the *Bm*-SPN-2-mCherry with the size of about 76kDa, the lower band (blue arrow) is an mCherry cleavage product with the size of about 26kDa.

(E) The same anti-His western blotting of purified fractions A8-B3 as (D), photo was captured by Alexa Fluor 488 at 610nm using PXi/PXi Touch Fluorescent & Chemiluminescent Imaging System from SYNGENE.

### 4.3 Discussion

As recombinant *Bm*-SPN-2 had been previously constructed by Zang et al. (Zang et al. 1999) in the Maizels laboratory, this plasmid was used as the starting point of the project. First, its identity was verified by sequencing a single new colony which was then used for expression of soluble recombinant *Bm*-SPN-2. Following nickel chelating chromatography, the purified *Bm*-SPN-2 fractions appeared to be well-expressed and relatively pure, providing ample protein for the studies described in this and accompanying chapters.

A notable point is that *Bm*-SPN-1 and *Bm*-SPN-2 share very low similarity (53.4%, 197/369) and identity (27.9%, 103/369) at the amino acid level. The reason for this might be the very different living environments of the different stages. *Bm*-SPN-1 is secreted by late-vector-stage larvae of *Brugia malayi* from the mosquito (Yenbutr and Scott 1995) whereas *Bm*-SPN-2 is only secreted by the microfilarial stage in the bloodstream of the host (Zang et al. 1999).

Interestingly, a very close homologue is present in the related filarial nematode species *Brugia pahangi* (PRJEB497). Using sequence data available through WormBase ParaSite (<http://parasite.wormbase.org/index.html>) it was found that *Bm*-SPN-2 has very high similarity (99.1%) and identity (96.7%) to *B. pahangi* *Bp*-SPN. However, no information yet exists that *Bp*-SPN is, like *Bm*-SPN-2, expressed solely by the blood-borne microfilarial stage.

Considering that *Bm*-SPN-2 has, compared to both *C. elegans* serpins and *Bm*-SPN-1, gained a short N-terminal extension, and in light of IL-33 cleavage being likely to be an intracellular event, the possibility is raised that *Bm*-SPN-2 may be taken up or otherwise enter target cells (e.g. human neutrophils) to carry out its effect, for example, inhibiting the enzymes activity of neutrophil elastase or cathepsin G. In order to pursue this possibility, it was decided to produce a fusion protein in which the fluorescent protein mCherry is conjugated onto *Bm*-SPN-2. Thus, the coding sequence for mCherry was added at the C-terminus of the *Bm*-SPN-2 pET29 construct. In the first instance, the mCherry sequence was synthesized and flanked with the same restriction enzyme (*Xho*I) at both ends, giving a 50% probability that the mCherry insert is ligated in the correct orientation. However, after trying a wide range of different ratios between insert and vector, no success was found at inserting

mCherry into the r*Bm*-SPN-2 construct. Several reasons might explain this difficulty, for example that single restriction enzyme was not efficient, or that the vector digested by only one restriction enzyme religates too readily.

As a further approach, the whole *Bm*-SPN-2-mCherry coding sequence, flanked with two different restriction enzymes (*Nde*I and *Xho*I) was synthesized, to be inserted directly into the pET29 vector. In this construct, a *Not*I site was placed between the *Bm*-SPN-2 and mCherry sequences so that either could be removed or replaced in future work.

Compared to the vector (~6.5kb), the insert of 1953bp is relatively large and it was decided to increase the ratio of insert to vector as high as 50:1 to complete the ligation successfully. This was accomplished and recombinant fusion protein expressed and purified. After purification, it was interesting to note that following the normal SDS-PAGE protocol of subjecting samples to 95°C heat inactivation caused the fusion protein with the mCherry fragment to separate from the *Bm*-SPN-2, as was also established by the laboratory of Henry McSorley (personal communication). To minimise this, the *Bm*-SPN-2-mCherry protein was treated at a reduced temperature of 62 °C. After Western blotting either visualized by anti-His (Figure 4.4D) or Alexa Fluor 488 (Figure 4.4E), it was shown that compared to 95°C heat shock, only two bands were detected: a more intense band (~76kDa) and a lower mol.wt band with the size of 26kDa representing the mCherry itself. These findings were consistent with the previous work that the cleavage problem could be solved by removing the N-terminal residues 11 amino acids of mCherry, thereby generating a cleavage-resistant fluorescent variant (Huang et al. 2014). At this stage, the newly produced *Bm*-SPN-2-mCherry fusion protein can be used for further research into uptake or entry of *Bm*-SPN-2, and/or *Bm*-SPN-2 at any potential binding site on host cells. In order to investigate whether the N-terminal extension plays such a role, making *Bm*-SPN-2-mCherry fusion proteins with or without this N-terminal sequence would be an important comparison. As *Bm*-SPN-2-mCherry was successfully constructed with the N-terminal, the first ongoing experiment should be tested whether *Bm*-SPN-2-mCherry binds to any human cells such as neutrophils. Next, it would be interesting to test the binding ability of proteins in which there is

truncation of the N-terminal of *Bm*-SPN2-mCherry. Finally, it is worth investigating whether either of them also bind to mouse cells.

A major objective of this chapter was to test the inhibitory function of *Bm*-SPN-2 in the context of IL-33 cleavage. This was done using IL-33 cleavage experiments assayed by western blotting with both human and murine full-length IL-33. Experiments reported in the literature were repeated successfully, for human IL-33, which was processed by human neutrophil cathepsin G (0.025mU/ $\mu$ l), cleaving full-length IL-33<sub>1-270</sub> into two major bands: Hs IL-33<sub>95-270</sub> with mol.wt ~ 21kDa and Hs IL-33<sub>109-270</sub> with mol.wt ~ 18kDa. It was also confirmed that human neutrophil elastase (0.01mU/ $\mu$ l) could cleave full-length IL-33<sub>1-270</sub> into a major product Hs IL-33<sub>99-270</sub> with the size of ~20 kDa. These results are fully consistent with the previous report from Lefrançois et al. (Lefrançois et al. 2012). Murine IL-33, was shown to be digested by 0.025mU/ $\mu$ l of neutrophil Cathepsin G, cleaving murine full-length IL-33<sub>1-266</sub> into a major cleavage product: Mm IL-33<sub>102-266</sub> with the size of ~20 kDa. Similarly, 0.05mU/ $\mu$ l of neutrophil elastase processed full-length murine IL-33<sub>1-266</sub> into a major cleavage product Mm IL-33<sub>102-266</sub> and a second minor product Mm IL-33<sub>109-266</sub>, which is also consistent with the previous finding from Lefrançois et al. (Lefrançois et al. 2012).

With this sensitive assay, it was then shown via western blotting that *Bm*-SPN-2 is able to block human IL-33 cleavage by inhibiting human neutrophil cathepsin G in a dose-dependent manner, which is consistent with the previous finding by Zang et al. (Zang et al. 1999). Notably, however, relatively high concentrations of *Bm*-SPN-2 were required to observe this effect. In addition, as the only a limited quantity of both human and murine full-length IL-33 was available for the cleavage experiment, the Western blotting of different amount of FL-IL-33 was only performed once. Thus, repeat testing the inhibitory function of *Bm*-SPN-2 via Western blotting is an important priority for the future.

*Bm*-SPN-2 is serine protease inhibitor-2 secreted only from *Brugia malayi* microfilariae stage (Zang et al. 1999), as the major and specific secreted product from microfilariae (Hewitson et al. 2008). Mature cleaved IL-33 as an alarmin cytokine could initiate the Type 2 response including TH2 cell, macrophages and innate lymphoid cell recruitment upon helminth infection. It was reported that ILC2s

and TH2 cells interact repeatedly in promoting type 2 immune responses and contributing to helminth expulsion, reflecting an ongoing dialogue between the innate and adaptive arms of the immune system (Oliphant et al. 2014, Huang et al. 2015). Considering that microfilariae live in the bloodstream of the human host and neutrophils are the most numerous type of white blood cells, interaction between these players mediated by *Bm*-SPN-2 represents an attractive model for parasite evasion of host immunity. The major secreted product from *Brugia malayi* microfilariae *Bm*-SPN-2 blocks IL-33 cleavage by inhibiting the enzyme activity of the human neutrophil enzymes cathepsin G and elastase. This results in reduced mature IL-33 production, and blocks initiation of the Type 2 response and parasite killing. Thus, *Bm*-SPN-2, which has the potential for modifying host defense responses, may play an important role in parasite survival during the microfilariae development.

Finally, it is important to note that *Bm*-SPN-2 did not completely inhibit human neutrophil cathepsin G using murine IL-33 cleavage experiment. The reason might be that human neutrophil cathepsin G is specific for cleaving the human full-length IL-33 or that there are subtle differences in the cleavage sites for neutrophil cathepsin G cleaving human and murine full-length IL-33 (Lefrançois et al. 2012). In addition, *Bm*-SPN-2 was also shown to inhibit human neutrophil elastase using murine IL-33 cleavage experiment in a dose dependent manner, but not completely.

Surprisingly, it was not possible to verify the inhibitory function of *Bm*-SPN-2 against human neutrophil cathepsin G by using enzyme activity assay kit with small-molecule chromogenic substrates, which were similarly used by another laboratory (Stanley and Stein 2003). However, the cathepsin G activity colorimetric assay kit used in this study did not reveal the expected substrate. According to the manufacturer, cathepsin G should cleave the substrate and release the dye, pNA (4-Nitroaniline), which is the same dye of the previous two studies (Zang et al. 1999, Stanley and Stein 2003) for cathepsin G, as the substrate was N-succinyl-Ala-Ala-Pro-Phe-p-nitroanilide. This group also expressed the *Bm*-SPN-2 protein in *E. coli*, and characterized its structural and functional properties. While these authors confirmed that *Bm*-SPN-2 shared the conserved tertiary structure of the serpin family, including a reactive centre loop (Irving et al. 2000) they found that the protein had no

effect on the activity of neutrophil cathepsin G on small molecule substrates and did not undergo the characteristic stressed to relaxed transition required for protease inhibition by serpins.

Hence these results remain controversial because it was shown in our hands that *Bm*-SPN-2 could block IL-33 cleavage in a dose dependent manner by inhibiting the activity of human neutrophil cathepsin G. However, it cannot be verified via conventional chromogenic enzyme activity assays, suggesting that *Bm*-SPN-2 may have a significantly different mode of inhibition and/or be closely adapted to interfering with the cleavage of IL-33. As cathepsin G cleaves the human full-length IL-33 at sites F94 and L108 into 95-270 and 109-270 (Lefrancais and Cayrol, 2012), it can be supposed that *Bm*-SPN-2 might block the IL-33 cleavage sites, not giving access to cathepsin G to its enzymatic sites. Thus, it will be meaningful to analyse the structure of *Bm*-SPN-2 and important to further verify this inhibitory function of *Bm*-SPN-2 through in vivo experimentation.



# CHAPTER 5

## *In vivo* studies of the roles of IL-33 and *Bm*-SPN-2 in responses to microfilariae and allergen challenge

### ABSTRACT

Based on the result of the previous chapter, *Bm*-SPN-2 was shown to block human full-length IL-33 cleavage by inhibiting human neutrophil Cathepsin G in a dose-dependent manner, supporting the hypothesis that *Bm*-SPN-2 may act *in vivo* to prevent IL-33 activation and the promotion of the TH2 immune response. Here, several parallel approaches were taken to test this hypothesis *in vivo* in mouse model. Firstly, to directly assess the function of *Bm*-SPN-2 *in vivo*, it was administered to mice in an intranasal allergy model elicited by the *Alternaria alternata* fungal allergen. In this setting, however, eosinophilia and IL-33 production was not affected by *Bm*-SPN-2 intranasal administration. Secondly, the requirement for IL-33 signalling in elimination of filarial parasites was tested. Unexpectedly, it was found that IL-33R (ST2) gene deficiency did not enhance the survival of *B. malayi* microfilariae. Furthermore, in the absence of IL-33R, murine immune responses to microfilariae were not significantly altered compared to wild-type BALB/c mice, other than in a significant increase in IL-33 expression. Finally, an IgG1 monoclonal antibody against *Bm*-SPN-2 was successfully made by fusing myeloma SP2 cells with mouse spleen cells immunized with *Bm*-SPN-2 antigen. The mAb was purified by Protein G affinity chromatography and is available for future experiments to neutralise *Bm*-SPN-2 *in vivo*. In conclusion, while *Bm*-SPN-2 can act *in vitro* to

forestall one of the key events in TH2 induction, this has not yet been shown to be crucial to the immune response to the parasite *in vivo*.

## 5.1 Introduction

*Bm*-SPN-2, as the major secreted product specifically from *Brugia malayi* microfilariae, is also the main component from this stage of the parasite to elicit a strong TH1 response (Zang et al. 2000). This was observed by detecting the high concentration of IFN $\gamma$  cytokine secretion, as well as IL-4 at 14 days post-infection with 300,000 Mf. However, this response may be short-lived, as Kazura's group reported that the initial TH1 response was followed by a mixed TH1/TH2 response from day 21 and obtained contrasting results when Mf were repeatedly injected into the footpad. In this setting of immunization, no IFN $\gamma$  was produced by lymph node cells when restimulated on day 10 (Pearlman et al. 1993, Pearlman et al. 1995). More recently, the TH2 response has been closely linked to IL-33, with, for example, the *in vivo* data of Schmitz et al. demonstrating that IL-33 induces the expression of IL-4, IL-5, and IL-13 and leads to severe pathological changes in mucosal organs (Schmitz et al. 2005).

Considering that *Bm*-SPN-2 drives TH1 responses in mice (Zang et al. 2000) and IL-33 drives TH2 responses (Schmitz et al. 2005), we inferred the possibility that *Bm*-SPN-2 could inhibit TH2 initiation via IL-33 neutralisation. One means to test this would be to investigate whether blockade of *Bm*-SPN-2 could shift the TH1 response to a TH2 profile, and for this purpose a monoclonal antibody against *Bm*-SPN-2 was prepared.

Considering the results of Chapter 4, there remains some controversy whether *Bm*-SPN-2 could inhibit mature IL-33 release requiring cleavage of full-length IL-33. It was concluded from the previous chapter that *Bm*-SPN-2 could indeed impede IL-33 cleavage by inhibiting the enzyme activity of human neutrophil cathepsin G in a dose-dependent manner. However, the inhibitory function of *Bm*-SPN-2 against human neutrophil cathepsin G could not be verified with the Cathepsin G enzyme activity assay kit. It was therefore decided that *in vivo* experiments would be a more direct way to verify this inhibitory function.

In the Maizels lab, a conventional allergic inflammation model has been set up successfully to investigate whether helminths or their soluble products suppress allergy. For example, *H. polygyrus* excretory-secretory products (HES) was shown to inhibit the type 2 innate molecules arginase-1 and RELM- $\alpha$ , as well as eosinophilia and ILC2 activation (McSorley et al. 2012). In particular, it was further reported by

McSorley et al. that HES coadministration with *Alternaria*/OVA suppressed IL-33 release in the first 24 hours of exposure (McSorley et al. 2014). Following fractionation and screening of HES, a novel component responsible for inhibiting IL-33, was identified, initially named Hp42 for its size of 42kDa, and now named Hp-Alarmin Release Inhibitor (Hp-ARI) because IL-33 is recognised as a key innate immune system alarmin (H J McSorley, personal communication).

In addition, it has recently been established that along with soluble proteins and other macromolecules, many parasitic helminths release exosome-like extracellular vesicles (EVs) (Coakley et al. 2015). Notably, it was also reported that EVs are involved in suppression of the IL-33 pathway. Thus, cells exposed to EVs show suppressed levels of ST2 (the IL-33 receptor) protein and mRNA (*illrl1*) (Buck et al. 2014, Coakley et al. 2017). Thus, as the *Alternaria* allergy system is dependent upon IL-33 and sensitive to suppression by HES, it offers an ideal set up for investigating the inhibitory function of *Bm*-SPN-2 *in vivo* in the context of IL-33 activation.

The relationship between IL-33 and helminth infection was summarized in Chapter 1.5.6 that IL-33, shows that this alarmin cytokine plays an important role in developing the initial TH2 response to helminth infections. It was shown that mouse infection with *Nippostrongylus brasiliensis* (Moro and Koyasu 2010), *Schistosoma mansoni* (Townsend et al. 2000) and *Trichuris muris* (Humphreys et al. 2008) each cause IL-33 release and activation of ILC2s and TH2 cytokine production. Utilizing IL-33R-deficient mice (ST2 deficient mice), further studies supported the role for IL-33 in the promotion of TH2 cytokine responses. It was demonstrated that ST2<sup>-/-</sup> mice failed to induce a TH2 response *in vivo* and form granulomas after intravenous injection of *S. mansoni* eggs (Townsend et al. 2000). Mice lacking the IL-33 signalling pathway were observed to have a defect in the induction of type 2 responses to helminth parasites and are more susceptible to infection with *Litomosoides sigmodontis* (Ajendra et al. 2014), *N. brasiliensis* (Hung et al. 2013), and *T. spiralis* (Scalfone et al. 2013). Using *L. sigmodontis* infected mice, the absence of ST2 was proven to lead to significantly increased levels of peripheral blood microfilariae, the filarial progeny, whereas adult worm burdens were not affected (Ajendra et al. 2014).

Based on these findings, in order to further investigate the function of *Bm*-SPN-2 *in vivo*, it would be informative to establish a microfilariae infection model and compare wild type (WT) and IL-33R-deficient mice in our laboratory. For logistical reasons, it was decided to explore this relationship with the parasite *Brugia pahangi*, a closely related filarial nematode that is naturally found in cats, and may also cause clinical infection of humans manifesting as lymphatic filariasis (Tan et al. 2011). The genome of *B. pahangi* was found to have a high similarity to *B. malayi*, with extensive synteny and few genes specific only for one species (Lau et al. 2015). In addition, the life cycle of *B. pahangi* is very similar to *B. malayi* as shown in Figure 1.4. Both *B. pahangi* and *B. malayi* share the same vector mosquito species and can infect the same rodent *Meriones unguiculatus* (the Mongolian jird) in the laboratory (Ash and Riley 1970a, Ash and Riley 1970b). Finally, as stated in Chapter 4, the amino acid alignment between *Bm*-SPN-2 and *Bp*-SPN reveals a very high similarity (99.1%) and identity (96.7%) between the proteins from the two species. Based on this, it is reasonable to utilize *B. pahangi* to study the closely related species *B. malayi*. This enabled the experiments to be undertaken as the life cycle of *B. pahangi* is maintained in Professor Eileen Devaney's laboratory at the University of Glasgow, while IL-33R deficient mice were available from Dr. Henry McSorley at the University of Edinburgh.

## 5.2 Results

### 5.2.1 Making polyclonal and monoclonal antibody against *Bm*-SPN-2

Following the initial finding that mice infected with *B. malayi* microfilariae mount a strong but short-lived *Bm*-SPN-2-specific TH1 response (Zang et al. 2000), *Bm*-SPN-2 was also suggested to play an essential role in neutralizing the immunostimulatory properties of host neutrophil proteases thereby contributing to the longevity of Mf in host bloodstream (Molehin et al. 2012). In order to further understand the *in vivo* function of *Bm*-SPN-2, it may be possible to employ monoclonal antibody blockade to shift the TH1 response to a TH2 response, for which generation of monoclonal antibodies against *Bm*-SPN-2 is necessary.

Prior to administering recombinant protein to mice for the *in vivo* experiments, it was decided to remove any contamination with bacterial Lipopolysaccharide (LPS), as r*Bm*-SPN-2 was expressed by *E. coli*. From 1.5ml of *Bm*-SPN-2, 750µl LPS-depleted *Bm*-SPN-2 (d*Bm*-SPN-2) was obtained with the concentration of 0.79mg/ml. Using the Limulus Amebocyte Lysate (LAL) assay, only 0.023U/ml of LPS was detected in 1µg/ml d*Bm*-SPN-2.

To provide a positive control for the monoclonal antibody screens, polyclonal antiserum was generated followed by the method see section 2.3.3.1. The schedule of antigen injection for making monoclonal antibody is summarized in Figure 5.1A.

In parallel, the mouse myeloma cell line Sp2/0-Ag14 (ATCC® CRL-1581™) (SP2) was cultured for 3 days. For the fusion, immunized spleen cells and SP2 cells were combined at a 1:1 ratio and 1 ml polyethylene glycol (PEG) was added. Cells were then distributed across 96-well plates and supernatants tested 14 days later by an ELISA screen using recombinant *Bm*-SPN-2 ELISA (Results of ELISA screening see Appendix 5.1) and secondary antibody to mouse IgG. Positive wells were re-cultured by two rounds of limiting dilution to select the monoclonal antibody (Procedure of ELISA screen and limiting dilution is shown in Figure 5.1B and details are shown in Section 2.3.3.2).

A total of nine mAb candidates against *Bm*-SPN-2 were chosen from the final ELISA screen, and the isotype of the nine mAb candidates was next determined by

ELISA as IgG1 in all cases by testing with different secondary antibody IgG1-HRP, IgG2a-HRP, IgM-HRP, IgA-HRP or IgE-HRP, with sera from naïve mice as negative control and polyclonal antibody sera as positive control (see Figure 5.2A).

As the *rBm*-SPN-2 construct is tagged by a six-histidine C-terminal tail (His-tag), it was necessary to make sure that the mAb candidate reacts specifically against *Bm*-SPN-2 and not the His-tag. For this purpose, two other proteins in our laboratory (Hp1552 and Hp148) that also include the His-tag were probed by ELISA. ELISA plates coated with either Hp1552 or Hp148 (1µg/ml) and as shown in Figure 5.2B, the mAb candidates were found to be negative against His-tag.

In order to make sure the mAb candidates react specifically against *Bm*-SPN-2, western blotting was performed with *rBm*-SPN-2 together with the mouse polyclonal antibody as positive control and anti-mouse immunoglobulins (P0260 by Dako) as secondary antibody. The western blotting result Figure 5.3A shows that all candidates are positive against *Bm*-SPN-2. In parallel, reactivity of the polyclonal rat antibody sera was verified by western blotting (Figure 5.3B). Next, western blotting was performed on soluble extracts of microfilariae (Mfs) and adult worms that had been stored at -80°C in the Maizels lab. *B. malayi* microfilariae and adult worms extract were prepared, followed the protocol in Section 2.10. and 0.5µg of each extract was loaded onto to SDS-PAGE gel. The western blotting was then performed and shows that mAb candidates only specifically react against Mf extract (Figure 5.3C) and not adult extract (Figure 5.3D). The two bands in Figure 5.3C and three bands in Figure 5.3D seen in the Mf extract may be attributed to some degradation during long term storage prior to the preparation of the extract.

As all mAb candidates were determined to be IgG1 isotype, they were purified using a Protein G column Complete RPMI1640 (cRPMI) medium containing ultra low IgG fetal bovine serum was used to cultivate the hybridoma cells and supernatants harvested when cells were fully confluent. Typically, a total volume 250ml of supernatant was loaded onto a 5ml Protein G column and eluted either manually or using an Akta Prime FPLC. The trace of the purified fractions of mAb candidate 1 is shown in Figure 5.4A. The trace graphs of the rest of the mAb candidates are shown in Appendix 5.2. Measuring the MAb concentrations by Nanodrop, very high concentrations up to 6.221mg/ml were obtained after dialysis,

and the quality of the purification assessed by SDS-PAGE gel. In this analysis, each sample was incubated with or without 2-mercaptoethanol reducing agent to break down into heavy and light chains. As shown in Figure 5.4B, in each case mature IgG mAb is seen ~150kDa (labelled by black arrow) while following reduction with 2-mercaptoethanol, separate heavy and light chains are seen at 49kDa (blue arrow) and 28kDa (red arrow) respectively.

Although the *Bp*-SPN and *Bm*-SPN-2 show very high sequence similarity (99.1%) and identity (96.7%) as discussed in Chapter 4, it would be interesting to test that the mAb antibodies reactive against *Bm*-SPN-2 also react against *B. pahangi* microfilariae extract. *B. pahangi* microfilariae and adult worms were kindly provided by Professor Eileen Devaney's lab. Surprisingly however, it was found that none of the *Bm*-SPN-2 mAb candidates bound to *B. pahangi* microfilariae extract (data not shown), suggesting that the set of mAbs isolated will not be suitable for experiments seeking to interfere with SPN function in *B. pahangi*.

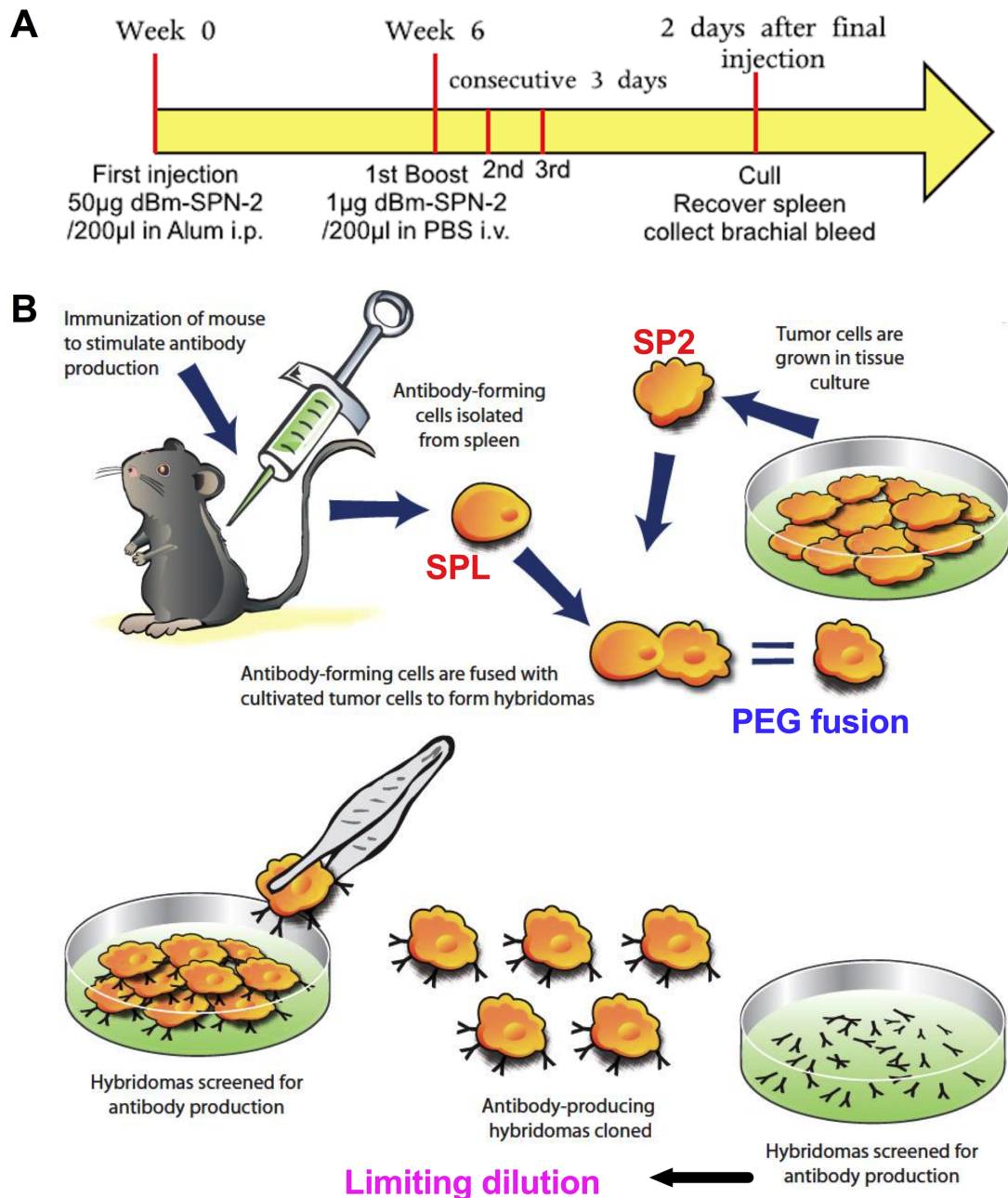


**Figure 5.1: Monoclonal antibody production against *Bm*-SPN-2.**

(A) Schedule of immunizing mice for making monoclonal antibody. BALB/c mice were injected with dBm-SPN-2, boosted three times after 6 weeks. Spleen cells were recovered for making monoclonal antibody and brachial blood harvested for polyclonal antibody.

(B) Protocol of making hybridoma cells. SPL stands for the immunized spleen cells; SP2 is the mouse myeloma cell line Sp2/0-Ag14 (ATCC® CRL-1581™). They were fused in 1:1 ratio by 1 ml polyethylene glycol (PEG). Limiting dilution was followed by the ELISA Screen.

From Alice Ra'anana and Bill Yates, <https://speakingofresearch.com>.

**A**

		Naive mice sera									Polyclonal antibody Sera	
		C2	C4	C6	C1	C3	C5	C7	C8	C9	10	11
		1	2	3	4	5	6	7	8	9	10	11
IgG1	A	1.722	1.469	1.389	1.442	1.481	1.383	1.433	1.390	1.363	0.126	1.375
	B	1.668	1.418	1.426	1.442	1.458	1.492	1.402	1.486	1.380	0.217	1.422
IgG2a	C	0.043	0.045	0.042	0.042	0.042	0.042	0.041	0.043	0.042	0.047	1.081
	D	0.044	0.043	0.044	0.042	0.044	0.044	0.041	0.043	0.045	0.049	1.103
IgM	E	0.045	0.045	0.043	0.043	0.041	0.042	0.043	0.042	0.041	0.098	0.468
	F	0.044	0.044	0.042	0.042	0.042	0.041	0.041	0.043	0.041	0.101	0.493
IgA	G	0.043	0.044	0.041	0.041	0.044	0.043	0.040	0.043	0.044	0.043	0.077
	H	0.044	0.044	0.045	0.043	0.043	0.043	0.045	0.042	0.043	0.041	0.080
IgE	A	0.054	0.060	0.054	0.057	0.054	0.048	0.061	0.061	0.054	0.060	0.169
	B	0.049	0.046	0.048	0.049	0.049	0.046	0.044	0.050	0.048	0.054	0.165

**B**

		C1	C2	C3	C4	C5	C6	C7	C8	C9
		1	2	3	4	5	6	7	8	9
Coated by Hp1552	Triplicates A	0.001	0.005	0.002	0.000	-0.001	0.001	0.001	0.000	0.000
	B	0.005	0.000	0.000	0.001	0.001	0.000	-0.003	0.000	-0.001
	C	-0.001	0.000	0.001	0.001	0.000	0.000	-0.001	-0.001	0.000
	D	Naive	pAb1	pAb2						
Coated by Hp148	control E	0.003	0.608	0.659						
	duplicates F	-0.001	0.000	-0.001	-0.002	0.000	0.000	-0.002	0.007	0.002
	G	-0.001	-0.001	-0.002	0.000	0.001	0.001	-0.001	0.000	0.001

**Figure 5.2: *Bm*-SPN-2 monoclonal antibody candidate isotype determination and specification verification by ELISA**

(A) Isotype determination for monoclonal antibody. The ELISA plate was coated with  $1\mu\text{g/ml}$  of *rBm*-SPN-2, ELISA was performed using mAb candidate as primary antibody and different secondary antibody  $\alpha\text{IgG1-HRP}$ ,  $\alpha\text{IgG2a-HRP}$ ,  $\alpha\text{IgM-HRP}$ ,  $\alpha\text{IgA-HRP}$  or  $\alpha\text{IgE-HRP}$ , with sera from naïve mice as negative control and polyclonal antibody sera as positive control. C1, ..., C9 stand for mAb candidates 1-9.

(B) Verification that mAb candidates are not against His-tag. Hp1552 and Hp148 are proteins including a C-terminal His-tag made in our laboratory. The ELISA plate wells were coated with either Hp1552 or Hp148 ( $1\mu\text{g/ml}$ ). mAb candidates C1-C9 were added as primary antibody, naïve mouse serum was included as negative control, polyclonal antibody against Hp148 was added as the positive control and  $\alpha\text{IgG1-HRP}$  was added as the secondary antibody.

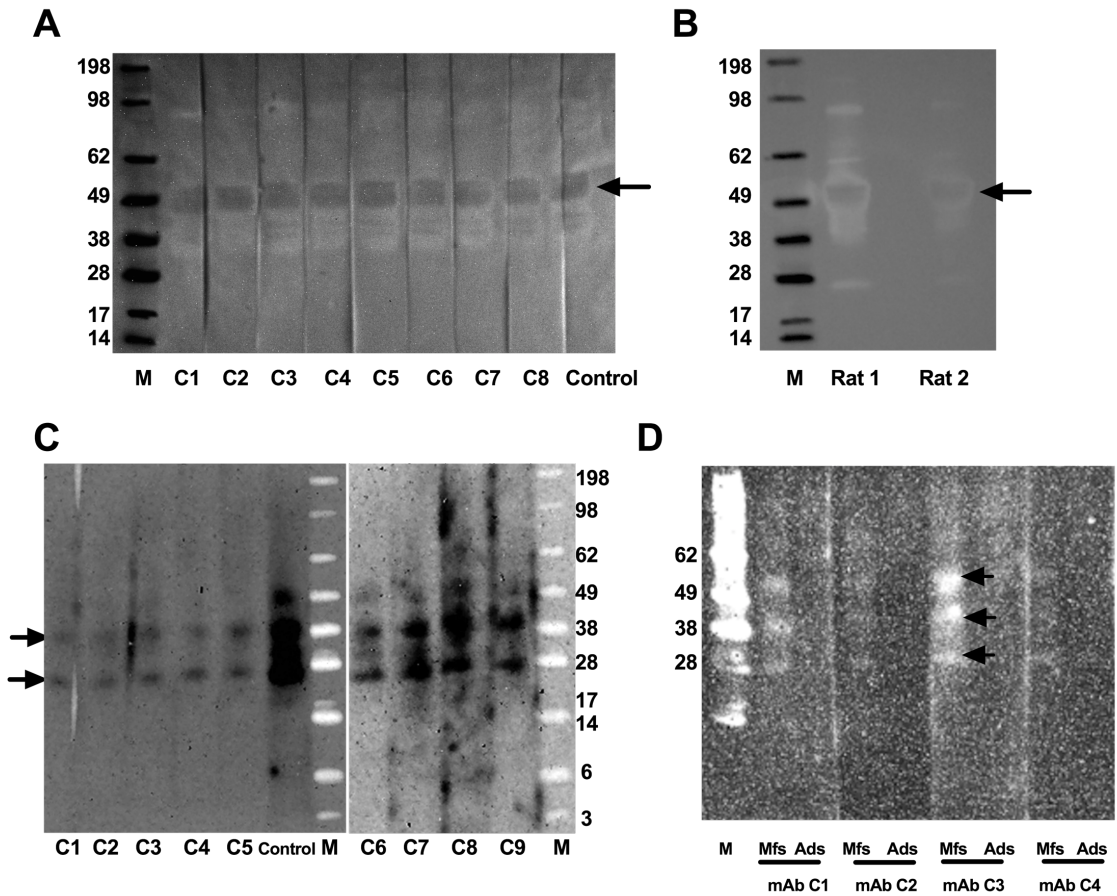


**Figure 5.3: *Bm*-SPN-2 monoclonal and polyclonal antibody candidate verification by Western blotting.**

(A) Verification of mAb candidates against *Bm*-SPN-2 by WB, C1,C2,...C8 stand for Candidate 1, 2,...8.

(B) Verification of polyclonal antibody rat sera against *Bm*-SPN-2 by WB.

(C) Verification of mAb candidates against Mf extract by WB. Two of the black arrows are likely to be the degraded *Bm*-SPN-2.

(D) Specificity of mAb candidates against microfilaria not adult worm extracts. All the western blotting were performed by loading 0.25 $\mu$ g *Bm*-SPN-2 (A and B) or 0.5 $\mu$ g Mf extract (C) or adult extract (C and D) and visualized by each mAb candidate 1:2000 dilution as the primary antibody, polyclonal antibody as positive control and anti-mouse Immunoglobulins (P0260 by Dako) as secondary antibody. The upper arrow is the theoretical size of *Bm*-SPN-2, the two lower bands refer its degradation, as the microfilariae used for extract preparation were frozen in -80  $^{\circ}$ C for years.

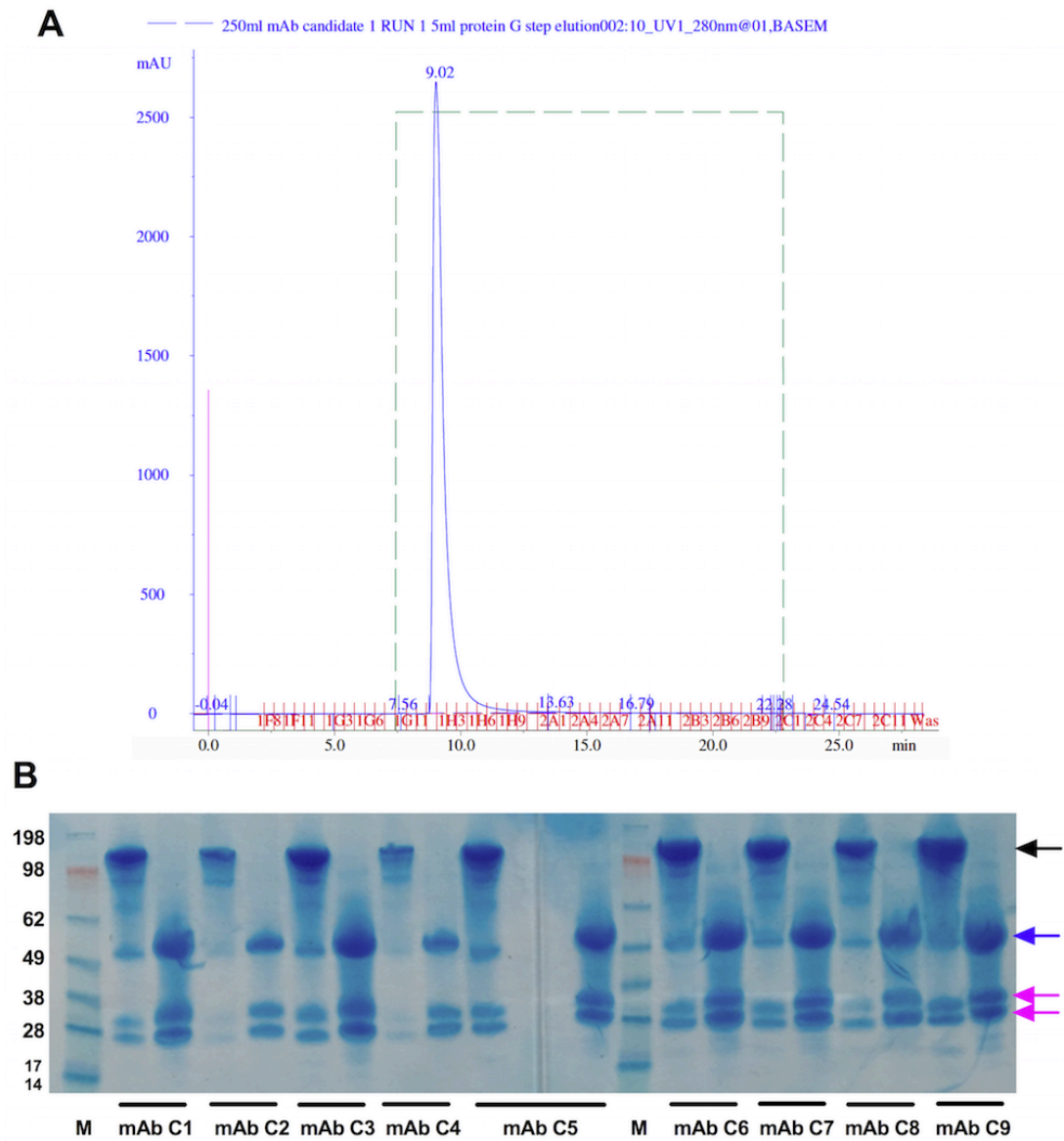


**Figure 5.4: *Bm*-SPN-2 monoclonal antibody candidate purification.**

(A) The UV trace of purified fractions from monoclonal antibody candidate 1. A total of 250ml supernatant of hybridoma cells was loaded onto the 5ml protein G column. 100% Elution buffer 0.1M Glycine-HCl pH2.7 was applied for purification. Fractions are collected into 96 well plates, then fractions order are shown as 1F8, 1F9, ..., 1G3, ..., 2A1, ..., 2C11.

(B) SDS-PAGE gel of purified mAb candidate visualized by Instant blue. mAb C1-C9 are the 9 candidates. The left-hand lane of each mAb candidate was without 2-mercaptoethanol whereas on the right hand side was with 2-ME added. The black arrow is the IgG mAb, the blue arrow is the heavy chain while the pink arrow is the light chain of the mAb.

### 5.2.2 *Alternaria/Bm-SPN-2* intranasal in vivo experiment

In order to test whether *Bm-SPN-2* can suppress IL-33 release after intranasal (i.n.) *Alternaria* administration, an in vivo experiment was set up using a model established in the laboratory (McSorley et al. 2014). The experimental scheme of *Bm-SPN-2* administration was shown in Figure 5.5A. Subsequently, IL-33 was measured from the bronchoalveolar lavage fluid (BAL) and lung homogenate samples (Figure 5.5B and C). Surprisingly, a small increase in IL-33 was seen in the group with *Bm-SPN-2*/PBS administration, for reasons which are as yet not known. However, *Alternaria* elicited very high IL-33 concentrations and although co-administration in the *Bm-SPN-2*/ALT group was slightly lower this did not yield a significant difference (Figure 5.5B). Also, the IL-33 ELISA of the lung homogenate showed no significant difference between the *Bm-SPN-2*/ALT group and PBS/ALT group (Figure 5.5C). In addition, Western blotting was attempted to compare responses in the different groups, using anti-IL-33 to probe BAL and lung homogenate samples. However, no IL-33 was detected in any group, perhaps because there is insufficient IL-33 in a single sample to detect by this method. Unfortunately, no IL-33 was detected even pool 5 lung homogenate sample together (date not shown).

Considering that HES (Excretory and secretory products from *H. polygyrus*) and Hp42 (Alarmin release inhibitor from *H. polygyrus*) are each potentially able to inhibit IL-33 release upon *Alternaria* administration (Osborn et al. 2017), a further experiment was performed with HES and Hp42 as positive controls. The results of this experiment, shown in Figure 5.5D, were that *Bm-SPN-2* could not reduce IL-33 levels in contrast to HES and Hp42 which both significantly reduced IL-33 release. Taken together, these experiments demonstrate that *Bm-SPN-2* is not able to inhibit IL-33 release in the time-frame of 1.5 hours after *Alternaria* administration into the airways of mice.

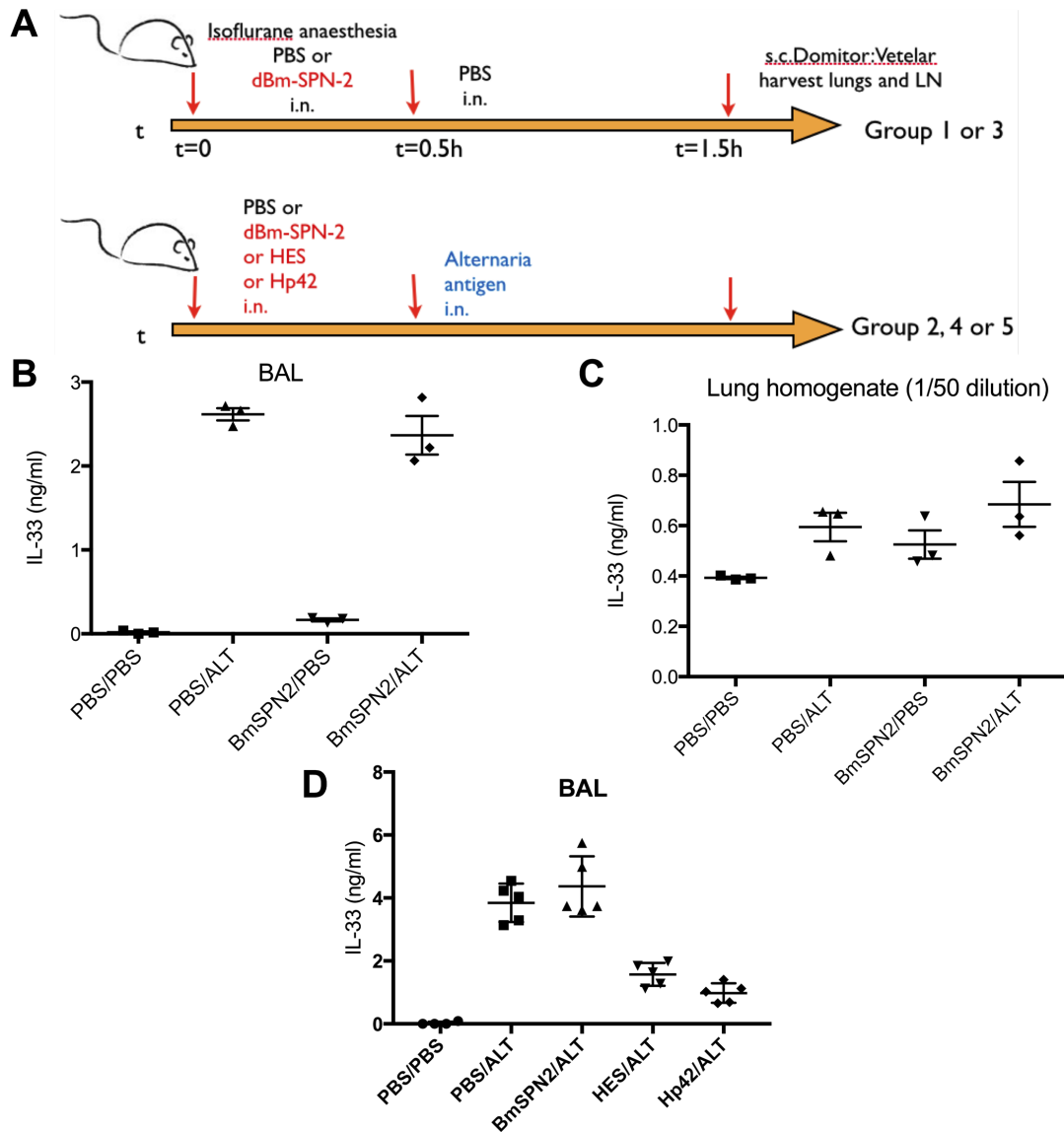


**Figure 5.5: Testing *Bm*-SPN-2 *in vivo* by *Alternaria* intranasal model.**

(A) Workflow of the *Alternaria*/*Bm*-SPN-2 intranasal *in vivo* experiment. Three or five per group of eight-week-old female BALB/c mice were administrated with 50 $\mu$ l PBS or 40 $\mu$ g dBm-SPN-2, or HES or Hp42 (Time 0h) 0.5 hour prior to 50 $\mu$ l PBS or 50  $\mu$ g *Alternaria* i.n. (Time 0.5h), mice were culled at Time 1.5h. The left lung of each mouse was harvested for homogenization. Lungs were homogenized in 0.5 ml of cell lysis buffer with PMSF by magnetic beads. Bronchoalveolar lavage fluid (BAL) was collected after euthanasia by washing the lungs three times with 0.5ml of cold PBS with 0.5% BSA.

(B) IL-33 measurement of the BAL samples by ELISA.

(C) IL-33 measurement for the lung homogenate samples by ELISA.

(D) IL-33 measurement from the BAL samples from a second experiment. Group size: 5. HES: Excretory and Secretory products from *H. polygyrus*; Hp42: alarmin release inhibitor of *H. polygyrus*.

### 5.2.3 *Brugia pahangi* microfilariae infect IL-33R<sup>-/-</sup> mice

With the aim of further understanding the function of *Bm*-SPN-2 *in vivo*, the approach was taken to establish an infection model in the laboratory. It was recently reported that in mice infected with L3 stage of the rodent filarial parasite *Litomosoides sigmodontis*, the absence of ST2 (the IL-33-specific subunit of the IL-33 receptor), led to significantly increased levels of peripheral blood microfilariae, the filarial progeny, whereas adult worm burden was not affected. Based on this finding, an interesting question arose as to how wild type (WT) and IL-33R-deficient mice may differ when infected with *B. malayi*. It is important to note that mice do not develop patent microfilaraemia following infection with L3 stage, and so it was decided to test the outcome of transfer of microfilarial stages alone. In addition, and as discussed above, as *B. pahangi* and *B. malayi* are closely related in genome (Lau et al. 2015), very similar in life cycle (Figure 1.4) (Ash and Riley 1970a, Ash and Riley 1970b) as well as in SPN sequence (Figure 4.11), it was decided to use *B. pahangi* microfilariae (Mff) which were available in sufficient quantity through collaboration with the laboratory of Prof Eileen Devaney.

In this section, the aim is to establish a new experimental model to investigate the importance of IL-33 during *Brugia malayi* Mf infection, including the time points, dose of infection, method of separating Mf and cells from peritoneal lavage as well as choosing the sample for qPCR. Thus, some necessary methodological development is included into the results, to obtain a better understanding of this model.

To assess the effect of lacking IL-33 receptor on Mff infection, *B. pahangi* microfilariae were transferred to wild type BALB/c and ST2-deficient mice. Firstly, a pilot experiment was carried out to determine the optimal time point of infected mice for microfilaria recovery as well as trialing methods for purifying and enumerating the parasites (experimental plan shown in Figure 5.6A). *B. pahangi* microfilariae were kindly provided by Professor Eileen Devaney. The microfilariae were collected from the peritoneal lavage of the infected jird and then purified by Histopaque with the substantial pellet of *B. pahangi* microfilariae shown in Figure 5.6B. The Mff were

resuspended with HBSS for Mff infection by i.p. injection. The detailed protocol of microfilariae purification is described in Section 2.2.1.

Four mice of each mouse strain were infected with 100,000 *B. pahangi* microfilariae by intraperitoneal injection (i.p.) with one mouse of each strain left uninfected. Two infected mice from each mouse strain were culled separately on day 1 and day 6 post-infection, and 3 successive peritoneal lavages performed on each animal (see Figure 5.6C). The great majority of microfilariae were recovered from the 1<sup>st</sup> peritoneal lavage, suggesting that one 5 ml peritoneal lavage will suffice for future experiments.

To both count recovered microfilariae from peritoneal lavage, as well as perform RT-PCR for cytokines from peritoneal lavage cells, a separation method is necessary. Thus, density gradient centrifugation using Histopaque was applied as previously described (Osborne 1997) with separation as shown in Figure 5.6D. Unfortunately, it was found that some microfilariae were trapped by peritoneal cells in the cell layer, as shown in Figure 5.6E. Thus, the cell layer would be contaminated by different numbers of microfilariae, suggesting mesenteric lymph node maybe a more stable source for mRNA expression comparison of cytokines between the two different mouse strains.

The microfilariae recovered from the peritoneal lavages were counted on days 1 and 6 post-infection. Compared to BALB/c mice, the number of microfilariae recovered at day 1 from infected IL-33R KO was higher as shown in Figure 5.7A, but with only 2 mice per group did not reach statistical significance. At day 6 post-infection, it was shown that Mff cannot be detected from the peritoneal lavage of 3 of 4 mice, suggesting a larger initial number of Mff may be needed in this i.p. infection model.

At the immunological level, the spleens of each mouse were collected and weighed immediately after cull. The spleen weights of the infected IL-33R KO and BALB/c mice were significantly greater than the uninfected mice. However, there was no significant difference between two different mice strain (Figure 5.7 C and D). Cytokine ELISAs for IL-4, IL-5, IL-13, IL-33, IFN $\gamma$  and Relm $\alpha$  were then performed on peritoneal lavage supernatants from each infected mouse. Interestingly, only IL-5 was detected in peritoneal lavage of both strains on day 1 post-infection. At this time levels appeared lower in the IL-33R-deficient mice, and by day 6 IL-5 was only

detectable in wild-type hosts (Figure 5.7B). However, IL-5 levels did not show a statistically significant difference between the two mouse strains, suggesting a larger group of mice should be tested to establish if this trend can be robustly replicated.

Based on the trial, another experiment was set up to repeat and extend the study of *B. pahangi* microfilariae infection in IL-33R deficient mice. As shown in Figure 5.8A, group sizes were enlarged to 5 each of BALB/c wild-type and IL-33R KO mice. Ten mice of each mouse strain were infected with 150,000 *B. pahangi* microfilariae per mouse, another five mice from each mouse strain were left uninfected. *B. pahangi* microfilariae were again kindly provided by Professor Eileen Devaney's laboratory. The first 5ml peritoneal lavage was collected for Mff counting and further cytokine ELISA. Immediately after cull, spleen was weighed and mesenteric lymph node was harvested with RNAlater (Qiagen) for subsequent RT-PCR. At day 1 post-infection, the peritoneal lavage of the five BALB/c and IL-33R KO mice were harvested. Before spinning down the peritoneal lavage, 100µl of peritoneal lavage from each mouse was taken for Mff counting (20µl/time). The peritoneal lavage fluid was then centrifuged to yield supernatant for ELISA analysis, and the pellet kept as a backup for Mff counting.

The microfilariae recovered from the peritoneal lavage on days 1 and 6 post-infection showed a broadly similar pattern to the trial experiment, with much higher numbers at the earlier time point. Unexpectedly, the number of microfilariae recovered from peritoneal lavage in BALB/c and IL-33R KO mice showed no significant difference on day 1 post-infection (as shown in Figure 5.8B). By day 6 almost no microfilariae were detected in most animals, but surprisingly, one mouse from each mouse strain had very high numbers of microfilariae (BALB/c mouse #4: 15,367 mff and IL-33R KO mouse #4: 82,387 mff) at that time (Figure 5.8B). Again, the spleen weights of the infected IL-33R KO and wild-type Balb/c mice were significantly greater than the uninfected mice. However, there was no significant difference between two different mouse strains in this respect (Figure 5.8C). As previously, a range of cytokine ELISAs (IL-4, IL-5, IL-13, IL-33, IFN $\gamma$  and Relm $\alpha$ ) were performed on peritoneal lavage supernatants, but unfortunately, none were detected in this experiment (data not shown).

As an alternative to ELISA for released proteins, mRNA expression of IL-4, IL-33, IFN $\gamma$ , Relm $\alpha$  and Arg1 transcripts were measured. RNA extraction was performed by conventional methodology (Section 2.9.1) for each mesenteric lymph node (mLN) sample from Day 1 and Day 6 infected and uninfected IL-33R KO mice and wild-type BALB/c mice. RNA was subjected to DnaseI treatment and purified with an RNeasy® Mini Kit (Qiagen) then measured by Nanodrop. cDNA was made with a Quanta qScript cDNA kit (Section 2.9.2). Then, the mRNA expression of IL-4, IL-33, IFN $\gamma$ , Relm $\alpha$  and Arg1 from mLN was measured by RT-PCR. The details of the protocol for RT-PCR and the primers is described in Section 2.9.3.

From the data obtained, it was found that in the absence of IL-33R, IL-4, IFN $\gamma$ , Relm $\alpha$  and Arg1 responses to microfilariae were not significantly altered compared to wild-type BALB/c mice (Figure 5.9B, C, D and E). There was, however, a significant increase in IL-33 expression especially on day 1 post-infection (Figure 5.9A). Overall, a high level of intra-group variation was found in the mRNA expression of IL-4, IFN $\gamma$ , Relm $\alpha$  and Arg1, making the results inconclusive for these responses.

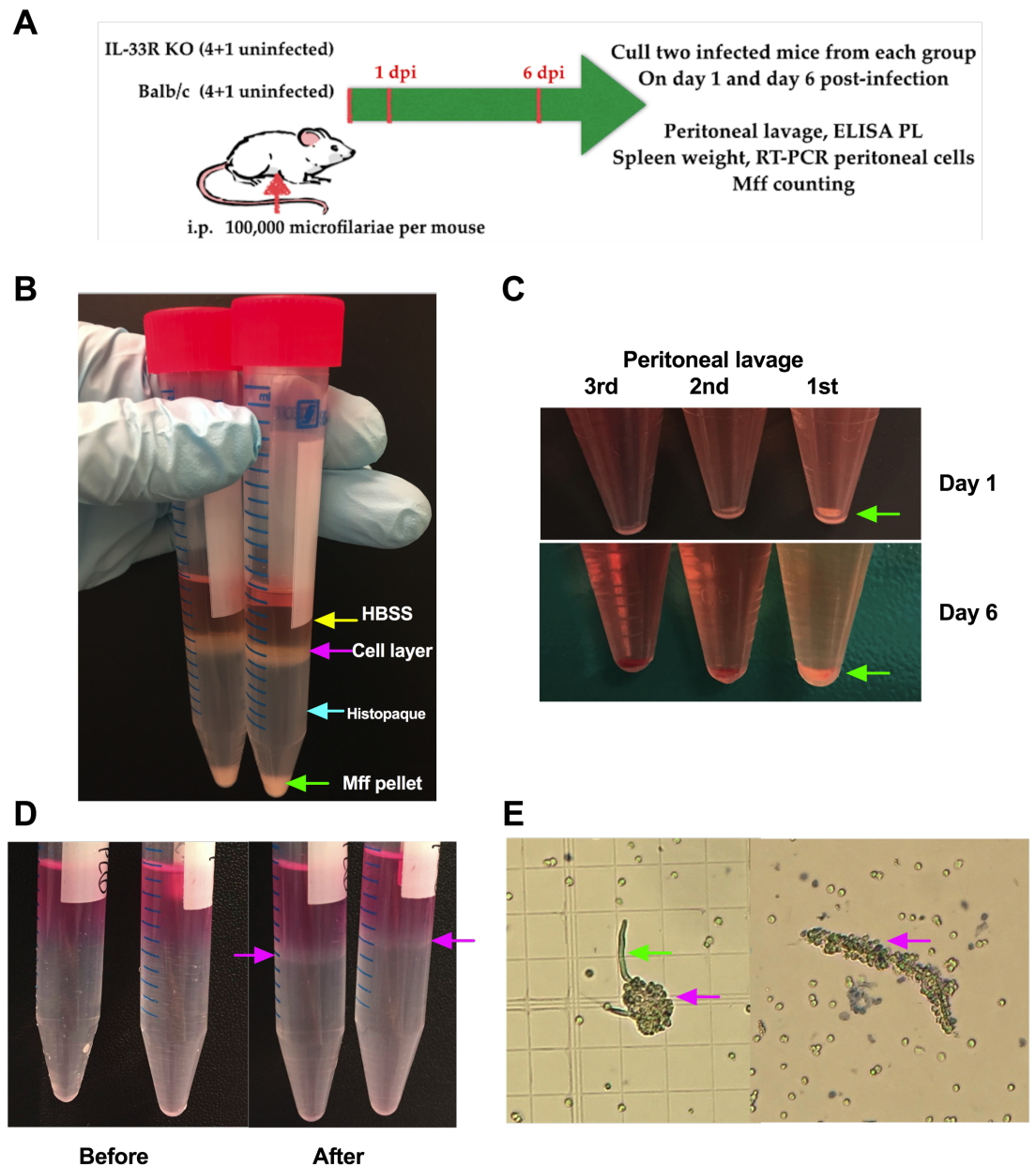


**Figure 5.6: Trial experiment of *Brugia pahangi* microfilariae infection to IL-33R deficient and BALB/c mice.**

(A) Experimental plan for *B. pahangi* microfilariae infection. Four mice of infected IL-33R KO and BALB/c mice were infected with 100,000 *B. pahangi* microfilariae (mff) by i.p. and one mouse of each strain was left uninfected. Two infected mice from each strain were culled on day 1 and day 6 post-infection. Peritoneal lavage was collected for mff counting and ELISA. Spleens were harvested and weighed.

## Chapter 5. In vivo studies

(B) Microfilariae purification from infected gerbil peritoneal lavage by density centrifugation using Histopaque. The layer indicated by the yellow arrow is HBSS, the pink arrow indicates the cell layer, the blue arrow indicates Histopaque and the green arrow indicates the Mff pellet.

(C) Three successive 5 ml peritoneal lavages from the infected mice on day 1 and day 6 post-infection. The pellets were collected after spinning at RCF 1000, 5min.

(D) Cells separation from peritoneal lavage on day 1 post-infection using Histopaque density centrifugation. Pink arrow indicates the cell layer.

(E) The image of cell layer. Pink arrow points the cells whereas green arrow indicates the microfilaria.

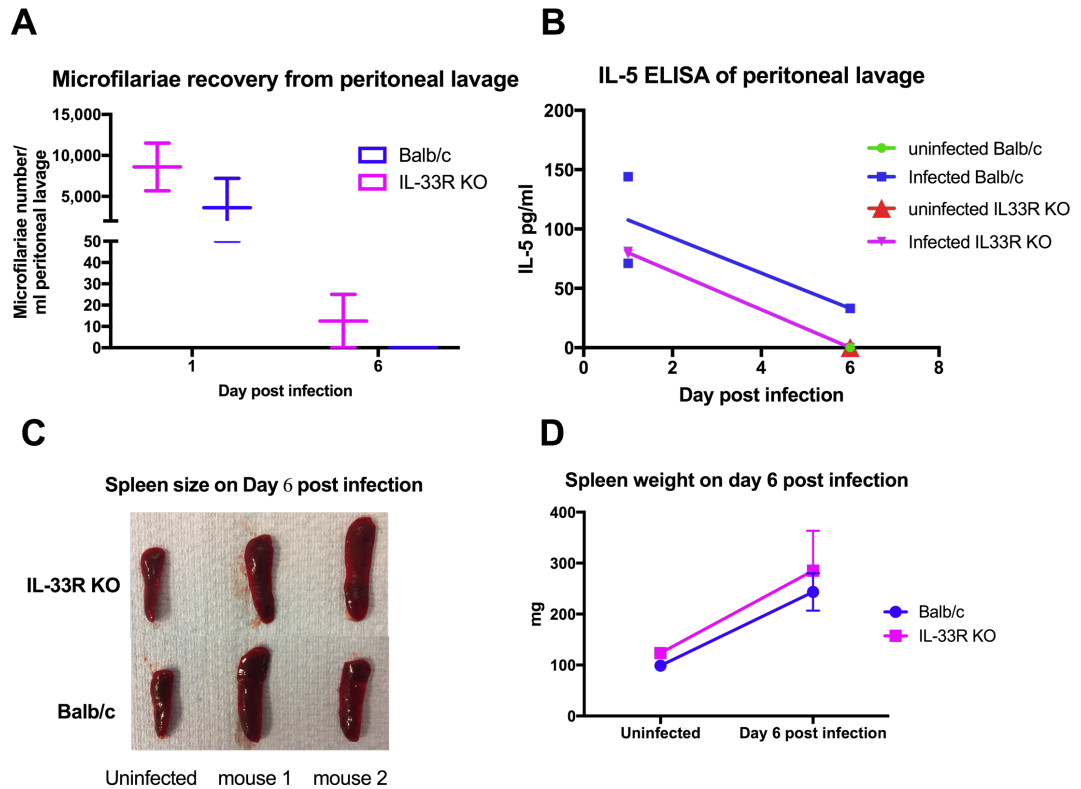


**Figure 5.7: Microfilariae recovery count, IL-5 measurement and spleen weight from the trial infection experiment.**

(A) *B. pahangi* microfilariae recovery from peritoneal lavage of the infected IL-33R KO and BALB/c mice on Day 1 and Day 6 post infection.

(B) IL-5 level of peritoneal lavage of the infected IL-33R KO and BALB/c mice on Day 1 and Day 6 post infection and the uninfected mice.

(C) The spleen harvested from the infected IL-33R KO and BALB/c mice on Day 6 post infection and the uninfected mice.

(D) The spleen weight of the uninfected and infected IL-33R KO and BALB/c mice on day 6 post-infection.

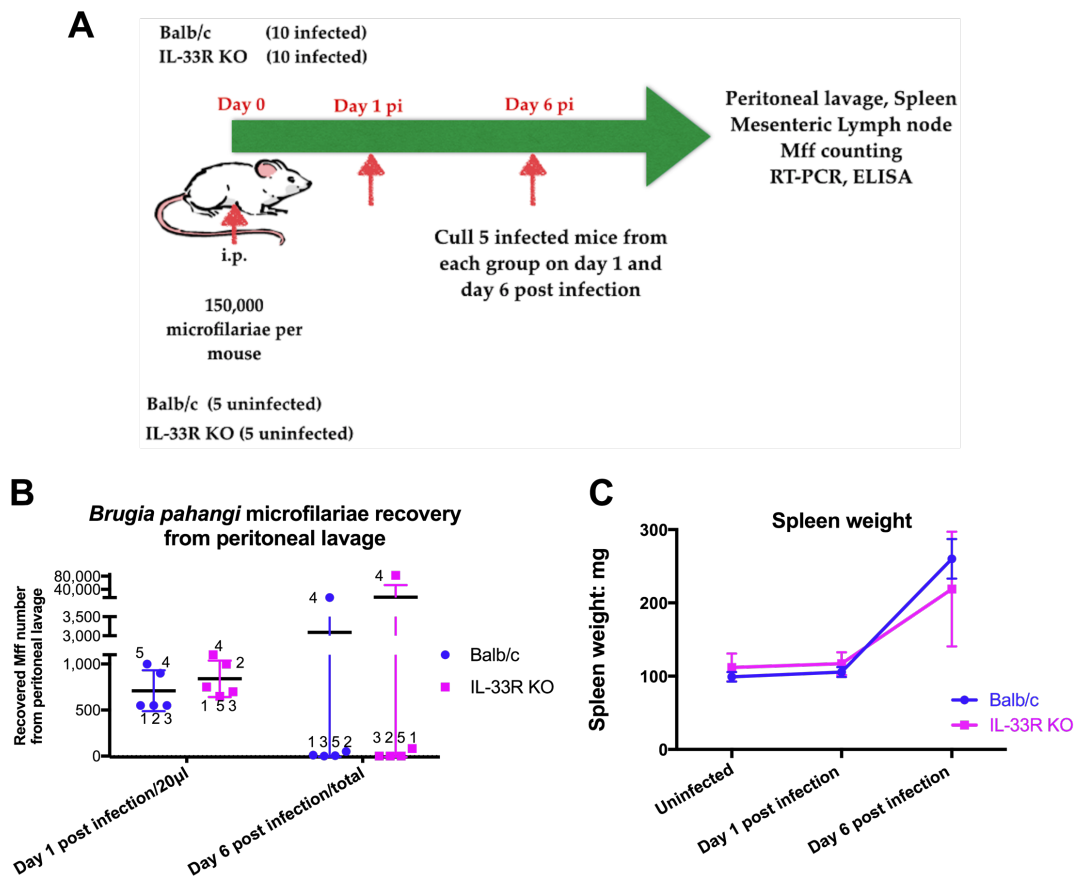


**Figure 5.8: *B. pahangi* microfilariae infect IL-33R deficient and BALB/c mice.**

(A) Experimental plan of the infection experiment to IL-33R deficient and BALB/c mice. Ten mice of each mouse strain were infected by 150,000 *B. pahangi* microfilariae per mouse, another five mice from each mouse strain were left uninfected. Five infected mice from each mouse strain were culled separately on day 1 and day 6 post-infection. Peritoneal lavage was collected for mff counting and ELISA. Spleen was harvested and weighed. Mesenteric lymph node was harvested for RT-PCR.

(B) *B. pahangi* microfilariae recovery from peritoneal lavage of the infected IL-33R KO and BALB/c mice on Day 1 and Day 6 post infection. The number of microfilariae on Day 1 is per 20µl, whereas the number for day 6 is total count. The corresponding numbers of mouse are also labelled on the microfilariae numbers.

(C) The spleen weight of the uninfected and infected IL-33R KO and BALB/c mice on day 1 and day 6 post-infection. As there were extremely large variances, the differences did not attain statistical significance.

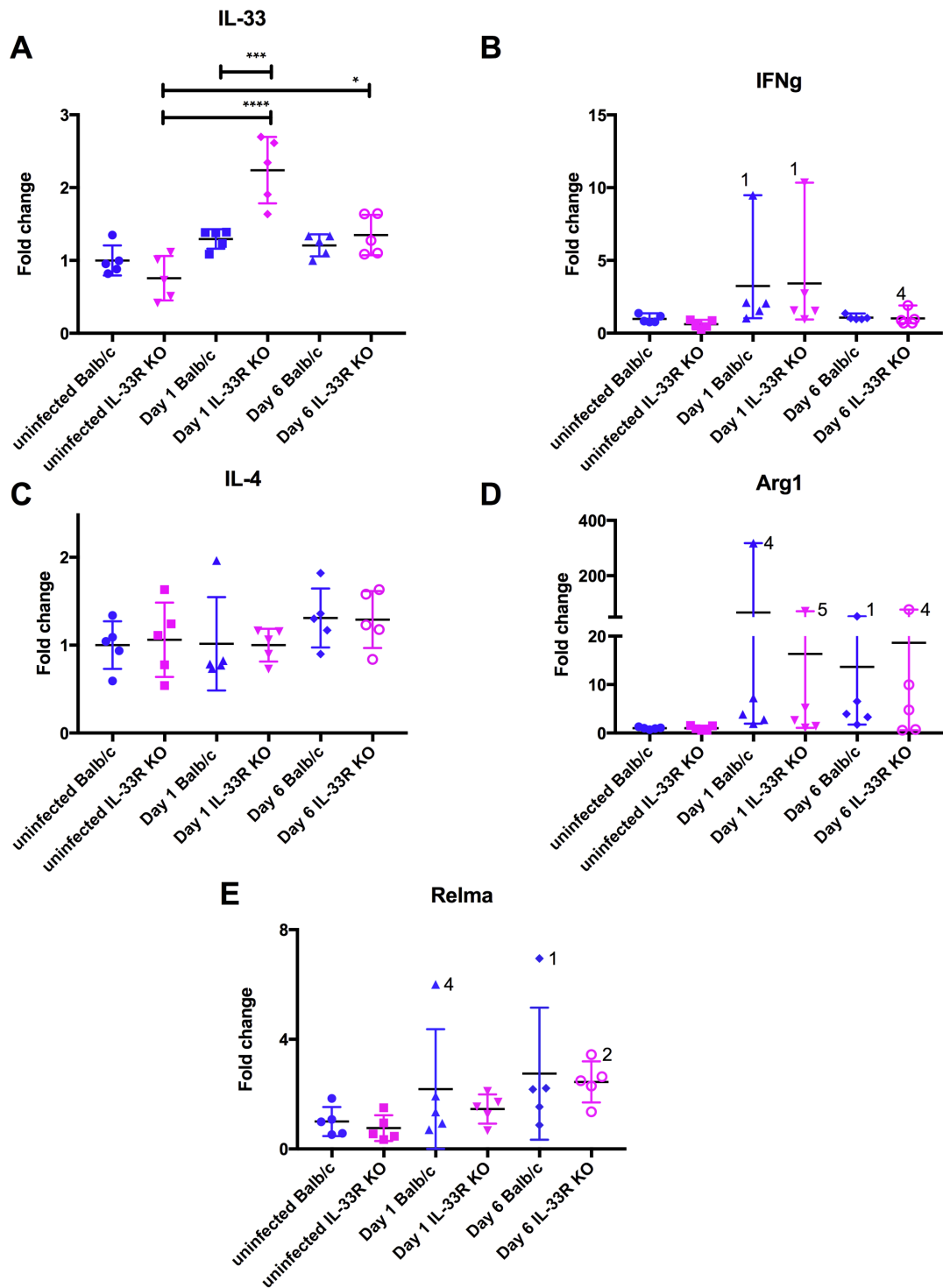


**Figure 5.9: The mRNA expression of cytokines of the mesenteric lymph node of uninfected and infected IL-33R KO and BALB/c mice.**

(A) IL-33, (B) IFN $\gamma$ , (C) IL-4, (D) Arg1 and (E) Relm $\alpha$  expression from mLN of uninfected and infected IL-33R KO and BALB/c mice measured by RT-PCR. As the mRNA expression

## Chapter 5. In vivo studies

of IFN $\gamma$ , IL-4, Arg1 and Relm $\alpha$  (B-E) in each mouse group is very variable, makes it difficult to do the statistics analysis.

### 5.3 Discussion

To further investigate the function of *Bm*-SPN-2 in vivo, three different approaches were adopted. First, it was decided to generate monoclonal antibodies which could be used to neutralise the parasite inhibitor in vivo. Using a conventional method in our laboratory, nine monoclonal antibody candidates against *Bm*-SPN-2 were successfully isolated and their isotypes were all determined to be IgG1. It was confirmed by ELISA that the monoclonal antibodies selected were specific for *Bm*-SPN-2, and they did not react with the C-terminal His-tag encoded by the expression vector. In addition, as *Bm*-SPN-2 is only secreted from *Brugia malayi* microfilarial stage, it was confirmed by western blotting that the mAbs can specifically bind to microfilariae extract and not adult worm extract. Finally, it was confirmed that mAb candidates specifically bind to r*Bm*-SPN-2 by western blotting. All of these three findings establish that the monoclonal antibodies are in fact reactive against *Bm*-SPN-2. Unexpectedly, however, the antibodies did not react with Mff of the closely related species, *Brugia pahangi*. As the intention was to administer anti-SPN-2 mAbs during a *B. pahangi* infection, this finding suggested that further, cross-reactive, mAbs need to be generated before *in vivo* neutralisation experiments can be performed.

In a second approach, it was decided to test whether *Bm*-SPN-2 could suppress IL-33 release induced by *Alternaria* administration into the airways, as release of this cytokine is known to be a rapid and potent response to this allergen. This *in vivo* model was established in our laboratory successfully, by showing that *HpARI* (*H. poly* alarmin release inhibitor) inhibits the IL-33 release within 1 hour of *Alternaria* administration (Osbourn et al. 2017). In the homeostatic state, IL-33 localizes in the nucleus of epithelial cells, with no ST2-dependent cytokine activity and inflammation (Cayrol and Girard 2014). Cell necrosis alerts the immune system to tissue damage or stress, and as an 'alarmin', biologically active full-length IL-33 (the IL-1-like cytokine domain) is released from the nucleus into the extracellular environment followed by the cleavage of IL-33 in the central domain (Miller 2011, Molofsky et al. 2015). Thus, released IL-33 should be theoretically equal to the cleaved IL-33, as only the cleaved bioactive IL-33 is released into the extracellular environment. In this experimental model IL-33 is measured one-hour after *Alternaria*

exposure, and *Bm*-SPN-2 was co-administered intranasally. Unfortunately, by ELISA no reduction in IL-33 was observed. Also, IL-33 was not detected in any BAL samples by western blotting, even after concentrating samples from five mice into a single sample. Thus, from these experiments, no evidence was found to support the primary hypothesis that *Bm*-SPN-2 can reduce IL-33 release. Some caveats may be mentioned; for example, it is possible that the SPN-2 from a human parasite is less effective at inhibiting serine proteases from the mouse.

A second comment relates to the role of neutrophils. As shown in Chapter 4, *Bm*-SPN-2 has the potential to inhibit the enzyme activity of human neutrophil elastase and cathepsin. Loebbermann et al. quantified the total numbers of macrophages, neutrophils, and eosinophils in the BAL using differential cell counting of hematoxylin and eosin-stained cytopsin slides (Loebbermann et al. 2012). It was shown that one hour after *Alternaria* and *Bm*-SPN-2 acute administration, the percentage of neutrophils is very low in the bronchoalveolar lavage fluid, as well as macrophages and eosinophils thus at early time points elastase or cathepsin G may not be involved in the response to *Alternaria*. Instead, serine proteases, chymase and tryptase secreted by activated mast cells are known to cleave the central domain of IL-33 giving rise to potent activation of group-2 innate lymphoid cells (Lefrançois et al. 2014). The fact that neutrophil numbers decreased might be because of the short time-frame of the experiment, which suggests that a longer time point *in vivo* experiment or chronic administration with protein and *Alternaria* should be tested. Hence, the mode of action of *Bm*-SPN-2 may be focussed not on the initial release of IL-33 from epithelial cells but later once more neutrophils are activated, to prevent the continued release of IL-33 in a more chronic setting.

A third strategy employed here was to establish an infection model for analysing whether *Bm*-SPN-2 inhibition of mature IL-33 production is important to expel parasites. As IL-33 is shown to be critically involved in the TH2 response initiation against helminth infection, and peak expression was detected at early time points upon *Trichuris muris* infection (Humphreys et al. 2008). In the experiments described here, timepoints and microfilariae doses were determined in a trial experiment (data not shown), from which relatively early time points day 1 and day 6

were chosen. *B. pahangi* microfilariae were utilized for infecting wild type BALB/c mice and IL-33 receptor deficient mice. A trial infection experiment established the methods, and the limitations, of this system, showing for example that peritoneal lavage cells also trap microfilariae so that mesenteric lymph nodes are a preferable source for measuring mRNA expression of cytokines by RT-PCR. However, this experiment with very small group sizes did indicate a greater susceptibility of the IL-33R deficient mice.

Following *B. pahangi* microfilariae i.p. infection of IL-33R deficient and wild-type BALB/c mice, it was surprising to find no significant differences between the strains. Indeed, one mouse from each mouse strain had very high microfilariae recoveries on day 6 post-infection while the microfilariae of the remaining mice had almost vanished, making the data too variable to analyse. The mice with high density of microfilariae also did not correlate with a high or low mRNA expression of IL-4, IFN $\gamma$ , Relm $\alpha$  and Arg1 as measured by RT-PCR. Compared to wild-type BALB/c mice, it was only found that IL-33 mRNA expression of IL-33 deficient mice is significantly increased on day 1 post-infection. This may be because in the absence of the IL-33 receptor the immune system compensates by producing more IL-33. However, there was also no detectable IL-4, IFN $\gamma$ , Relm $\alpha$  and Arg1 by ELISA, suggesting that the murine immune response had still to initiate the TH1 or TH2 responses very early post-infection.

Unexpectedly, there was also found to be no difference in microfilariae recovery on day 1 post infection between IL-33R/ST2 deficient mice and wild-type BALB/c mice, which is not consistent with the previous finding that microfilaria numbers were enhanced in ST2 deficient mice (Ajendra et al. 2014). The difference between this study and the previous paper is that *L. sigmodontis* microfilariae were inoculated intravenously into the tail vein of the ST2 deficient mice, and peripheral blood were collected for microfilariae comparison, whereas the *B. pahangi* microfilariae were i.p. injected directly into the peritoneal cavity. As noted above, neutrophils are sparse in the peritoneal cavity but are the most numerous leukocyte in the bloodstream. In addition, as the peripheral blood of the host is the physiological niche of the microfilariae, their behaviour or susceptibility may be altered by

infection in the peritoneal cavity. Thus, future experiments should test the fate of microfilariae transferred directly into the peripheral blood by i.v. injection.

As ST2 (IL-33 receptor) deficient mice develop increased microfilaremia following *Litomosoides sigmodontis* infection (Ajendra et al. 2014), it has been demonstrated that the IL-33 receptor plays an important role in the filarial nematode infection. Furthermore, reports in recent years demonstrating the action of IL-33 are not limited to the activation of immune cells involved in type-2 immune responses (Cayrol and Girard 2014). Studies have also uncovered important roles of IL-33 in the activation of immune cells involved in type-1 immunity, infection and chronic inflammation, such as neutrophils, macrophages, Th1 cells, NK cells, CD8+ T cells, B cells and NK T cells (reviewed in (Molofsky et al. 2015, Liew, Girard and Turnquist 2016, Cayrol and Girard 2018)). As 1) it was found in this study that *Bm*-SPN-2 has the potential to inhibit human neutrophil cathepsin G or elastase; and 2) the most abundant product secreted from *Brugia malayi* microfilariae, *Bm*-SPN-2 was found to be able to induce an early and strong Th1 response (Zang et al. 2000), it would be meaningful and interesting to investigate how IL-33 or IL-33 receptor could influence immunity to filarial microfilariae.

# CHAPTER 6

## Final Discussion

Dating back to the 1980s, it has been reported that, by employing a combination of sensitive biochemical and immunochemical techniques, the excretory-secretory products for *Brugia malayi* adult worms could be identified and characterized (Kaushal et al. 1982). A few years later, Lightowers and Rickard summarized the excretory-secretory (ES) products as a variety of molecules that parasitic helminths excrete or secrete into their hosts. It was then proposed that the ES products of parasitic helminths potentially contribute to immune evasion strategies of the parasites through a suite of mechanisms including shedding of surface-bound ligands and cells, alteration of immune cell functions and modulation of complement and other host inflammatory responses (Lightowers and Rickard 1988).

In 1999, it was discovered, by screening the surface secreted antigens of *B. malayi*, a prominent antigen was *Bm*-SPN-2, a serpin which is specifically and exclusively secreted by microfilariae stage. This serpin has the ability to inhibit human neutrophil serine proteinases (Cathepsin G and elastase) (Zang et al. 1999). Further experiments were performed to show that *Bm*-SPN-2, unusually for a helminth antigen could induce a Th1-biased immune response in mice and humans (Zang et al. 2000).

More recently, the stage- and gender-specific ES products of *B. malayi* were identified by three groups using proteomic mass spectrometry (Hewitson et al. 2008, Moreno and Geary 2008, Bennuru et al. 2009). These authors found again that *Bm*-SPN-2 is a major and specific ES product from microfilariae of *B. malayi*, suggesting that *Bm*-SPN-2 might play an important role in immune evasion specifically by the microfilarial stage.

In the meantime, new immunological studies had developed our understanding of IL-33, a key cytokine of innate immune system. These revealed that human and murine full-length IL-33 is processed into mature bioactive IL-33 by human neutrophil Cathepsin G and elastase (Lefrançois et al. 2012). As an alarmin signal, IL-33 plays an important role developing the initial TH2 response to helminth infections. It was shown that mouse infection with the *Nippostrongylus brasiliensis* (Moro and Koyasu 2010), *Schistosoma mansoni* (Townsend et al. 2000) and *Trichuris muris* (Humphreys et al. 2008) each cause IL-33 release and activation of ILC2s and TH2 cytokine production.

Importantly, microfilariae (Mf) are the long-lived blood-dwelling larval stage of *B. malayi*. The ability of the immune response to reduce or eliminate microfilariae in the bloodstream would prevent the spread of parasites to mosquitoes, suggesting that stage specific immunity to microfilariae could be the best strategy to block transmission of *B. malayi*.

Putting these findings together, it was then hypothesised that the major secreted product *Bm*-SPN-2 of the microfilarial stage has the potential to block IL-33 alarmin signals by inhibiting the activity of neutrophil Cathepsin G and elastase. If so, *Bm*-SPN-2 would be a potential drug target or vaccine candidate.

Based on this, the whole PhD project is focused on the functional analysis of *Bm*-SPN-2, the most abundant protein secreted specifically from microfilarial stage of *B. malayi*.

## 6.1 *In vitro* study

The first set of studies investigated the inhibitory function of *Bm*-SPN-2 in blocking full-length human and murine IL-33 cleavage *in vitro*.

Considering that commercially-available human and murine IL-33 are supplied as the cleaved bioactive form of IL-33, it was necessary to make full-length human and murine IL-33 in the laboratory. It was verified that the wild type IL-33 is not secreted into the supernatant of transfected HEK293T cell cultures, as it is retained in the cell nucleus through the chromatin binding motif located in the N-terminal sequence of the IL-33 full-length protein. However, soluble human and mouse full-length IL-33 were successfully purified from the supernatant of

transfected HEK293T cells, after mutating residues 47-49 in the chromatin binding motif of both human and mouse FL-IL-33.

Another clear finding of the IL-33 administration was that cleaved human IL-33<sub>95-270</sub> significantly increased IL-6 secretion by mast cells compared to the full-length protein. Four enzymes including neutrophil elastase, cathepsin G, mast cell chymase and tryptase are each known to cleave human full-length IL-33<sub>1-270</sub> into active fragments such as IL-33<sub>95-270</sub> (Lefrançais et al. 2012, Lefrançais et al. 2014). It was then inferred that the full-length IL-33 is initially cleaved by neutrophil cathepsin G and elastase to IL-33<sub>95-270</sub> which activates mast cells to release their proteases chymase and tryptase, so further amplifying the production of bioactive IL-33 (Figure 3.13), and ensuring the initiation of the TH2 response. This model is consistent with the very recent finding that mast cells play a role as a critical source of IL-33, activating ILC2 responsible for parasite expulsion in the early phase, following infection with the intestinal helminth, *H. polygyrus* (Bouchery and Harris 2017, Shimokawa et al. 2017).

The second objective was to verify the inhibitory function of *Bm*-SPN-2 in the context of IL-33 cleavage, by western blotting and enzyme activity assay kits which were employed *in vitro*.

For western blotting, IL-33 cleavage experiments reported in the literature assayed with both human and murine full-length IL-33 were each repeated successfully. These results of human and murine FL-IL-33 cleavage by neutrophil Cathepsin G and Elastase (see Discussion in Chapter 4) are fully consistent with the previous report from Lefrançais et al. (Lefrançais et al. 2012). It was further verified that via western blotting that *Bm*-SPN-2 is able to block human IL-33 cleavage by inhibiting human neutrophil cathepsin G in a dose-dependent manner, which is consistent with the previous finding by Zang et al. (Zang et al. 1999). Notably, however, relatively high concentrations of *Bm*-SPN-2 were required to observe this effect.

However, it was not possible to verify the inhibitory function of *Bm*-SPN-2 against human neutrophil cathepsin G by using enzyme activity assay kits with small-molecule chromogenic substrates, which were similarly used by another laboratory (Stanley and Stein 2003).

Hence these results remain controversial because it was shown in our hands that *Bm*-SPN-2 could block IL-33 cleavage in a dose dependent manner by inhibiting the activity of human neutrophil cathepsin G. However, it cannot be verified via conventional chromogenic enzyme activity assays, suggesting that *Bm*-SPN-2 may have a significantly different mode of inhibition and/or be closely adapted to interfering with the cleavage of IL-33. Thus, it will be important to further verify this inhibitory function of *Bm*-SPN-2 through *in vivo* experimentation.

## 6.2 In vivo study

Next, further experiments were performed to use an established animal model *in vivo* for functional analysis of *Bm*-SPN-2. In particular, an *in vivo* experiment with *Brugia pahangi* microfilariae infection was set to accomplish two aims:

1) To test if IL-33 receptor deficient mice show enhanced microfilaria survival, which would suggest that IL-33 is important for microfilarial elimination.

2) Based on the result of Chapter 4 that *Bm*-SPN-2 could block mature IL-33 cleavage, as well as the finding that *Bm*-SPN-2 induces a strong Th1 immune response (Zang et al. 2000), the intention would be to use anti-SPN-2 mAb blockade *in vivo* and then measure (a) Th1 and TH2 cytokine responses; and (b) microfilariae recovery.

However, in this study, it was unfortunately found that IL-33R deficient mice do not show enhanced microfilariae recovery in the peritoneal cavity, which is not consistent with the previous study that ST2 deficiency increased microfilaremia in the case of *Litomosoides sigmodontis* (Ajendra et al. 2014).

To establish the reason(s) for this discrepancy, two differences between these two studies have to be mentioned: (1) The data from *B. pahangi* are very variable, including the Mff number and mRNA expression in the mesenteric lymph node, making the comparison difficult to evaluate at this stage. Thus, repeating and optimizing this model is necessary. (2) *B. pahangi* microfilariae were infected by intraperitoneal injection, whereas *L. sigmodontis* microfilariae developed following L3 infection and maturation of adult parasites in Ajendra's study (Ajendra et al. 2014). These authors allowed a time period of parasite to develop in the mice host, which may have developed a more physiological relationship between parasite and

host. Similarly, microfilariae were counted in the bloodstream, the natural niche for this stage, which may make the data more reliable. Thus *B. pahangi* microfilariae intraperitoneal infection might not be the best way to verify the importance of IL-33 signalling in microfilariae elimination. Both points suggest that *B. malayi* microfilariae inoculation intravenously would be the best way to develop this model.

So far, the first hypothesis that IL-33 signalling plays a crucial role in expelling microfilariae cannot be verified in our hands, hence it was not possible to test the second aim at this stage.

Similarly, with respect to the allergic airway model *in vivo*, the short time period (one hour) between allergen administration and measurement of IL-33 release, may not be the appropriate system to test the inhibitory function of *Bm*-SPN-2. Notably, at this time macrophages, eosinophils or neutrophils are all in a very low percentage in the BAL (Loebbermann et al. 2012). However, the experiments have helped define further the setting in which *Bm*-SPN-2 may be active.

### 6.3 Future work

The monoclonal antibody strategy to neutralise SPN-2 *in vivo* remains an attractive route for experimentation. However, stronger evidence is required that an antibody to be administered *in vivo* can block SPN-2 function, which remains a problem as the inhibitor is not active in chromogenic substrate assays. In addition, it appears that surprisingly the mAbs described here do not react with *B. pahangi* Mff, limiting the experimental use of this species.

After mapping the protein sequence of *Bm*-SPN-2 against WormBase ParaSite website, it was shown to have 99.8 % identity with *B. timori* serpin and 96.7% identity with *B. pahangi* serpin. Furthermore, as reported by Zang et al. compared to homologues from other species such as *Caenorhabditis elegans*, *Bm*-SPN-2 has not only acquired a signal peptide but also an extra N-terminal tract (Zang et al. 1999), which might be the crucial for interacting with host cells. In order to investigate whether the N-terminal extension plays such a role, making *Bm*-SPN-2-mCherry fusion proteins with or without this N-terminal sequence is worth trying. As *Bm*-SPN-2-mCherry was successfully constructed with the N-terminal, the first ongoing experiment should be tested whether *Bm*-SPN-2-mCherry bind to any

human cells such as neutrophils. Next, it would be interesting to test the ability of binding to cells for the truncation of the N-terminal of *Bm*-SPN2-mCherry. Finally, it is worth investigating whether both of them also bind to mouse cells.

Recombinant *Bm*-SPN-2 expressed by *E. coli* was employed throughout this study. As *B. malayi* is a human parasite, *Bm*-SPN-2 expressed by human cells such as HEK293T might influence their function. It would also be interesting to test this especially using a conditional system to induce *Bm*-SPN-2 expression by HEK293T cells *in vitro*.

Finally, as the most prominent ES product secreted only by the microfilarial stage, establishing the function of *Bm*-SPN-2 remains an important priority. Although a potential function is now suggested, in neutralizing or evading the host immune response, this is still at a controversial stage and further validation experiments are strongly recommended to further our understanding of this fascinating system.

# References

- Abe, T. & Y. Nawa (1987) Reconstitution of mucosal mast cells in W/W<sup>v</sup> mice by adoptive transfer of bone marrow-derived cultured mast cells and its effects on the protective capacity to *Strongyloides ratti*-infection. *Parasite Immunology*, 9, 31-38.
- Abe, T., H. Sugaya, K. Yoshimura & Y. Nawa (1992) Induction of the expulsion of *Strongyloides ratti* and retention of *Nippostrongylus brasiliensis* in athymic nude mice by repetitive administration of recombinant interleukin-3. *Immunology*, 76, 10.
- Abraham, D., O. Leon, S. Schnyder-Candrian, C. C. Wang, A. M. Galisto, L. A. Kerepesi, J. J. Lee & S. Lustigman (2004) Immunoglobulin E and eosinophil-dependent protective immunity to larval *Onchocerca volvulus* in mice immunized with irradiated larvae. *Infection and Immunity*, 72, 810-817.
- Abreu, M. T. (2010) Toll-like receptor signalling in the intestinal epithelium: how bacterial recognition shapes intestinal function. *Nature Reviews Immunology*, 10, 131.
- Ajendra, J., S. Specht, A.-L. Neumann, F. Gondorf, D. Schmidt, K. Gentil, W. H. Hoffmann, M. J. Taylor, A. Hoerauf & M. P. Hübner (2014) ST2 deficiency does not impair type 2 immune responses during chronic filarial infection but leads to an increased microfilaremia due to an impaired splenic microfilarial clearance. *PLoS One*, 9, e93072.
- Al-Qaoud, K. M., E. Pearlman, T. Hartung, J. Klukowski, B. Fleischer & A. Hoerauf (2000) A new mechanism for IL-5-dependent helminth control: neutrophil accumulation and neutrophil-mediated worm encapsulation in murine filariasis are abolished in the absence of IL-5. *International Immunology*, 12, 899-908.
- Allakhverdi, Z., D. E. Smith, M. R. Comeau & G. Delespesse (2007) Cutting edge: The ST2 ligand IL-33 potently activates and drives maturation of human mast cells. *The Journal of Immunology*, 179, 2051-2054.
- Allen, J. E. & R. M. Maizels (2011) Diversity and dialogue in immunity to helminths. *Nature Reviews Immunology*, 11, 375-388.
- Anthony, R. M., L. I. Rutitzky, J. F. Urban, M. J. Stadecker & W. C. Gause (2007) Protective immune mechanisms in helminth infection. *Nature Reviews Immunology*, 7, 975-87.
- Anthony, R. M., J. F. Urban Jr, F. Alem, H. A. Hamed, C. T. Roza, J.-L. Boucher, N. Van Rooijen & W. C. Gause (2006) Memory TH2 cells induce alternatively activated

- macrophages to mediate protection against nematode parasites. *Nature Medicine*, 12, 955.
- Artis, D., M. L. Wang, S. A. Keilbaugh, W. He, M. Brenes, G. P. Swain, P. A. Knight, D. D. Donaldson, M. A. Lazar & H. R. Miller (2004) RELM $\beta$ /FIZZ2 is a goblet cell-specific immune-effector molecule in the gastrointestinal tract. *Proceedings of the National Academy of Sciences of the United States of America*, 101, 13596-13600.
- Arumugam, S., J. Wei, D. Ward, D. Abraham, S. Lustigman, B. Zhan & T. R. Klei (2014) Vaccination with a genetically modified *Brugia malayi* cysteine protease inhibitor-2 reduces adult parasite numbers and affects the fertility of female worms following a subcutaneous challenge of Mongolian gerbils (*Meriones unguiculatus*) with *B. malayi* infective larvae. *International Journal of Parasitology*, 44, 675-9.
- Ash, L. R. & J. M. Riley (1970a) Development of *Brugia pahangi* in the jird, *Meriones unguiculatus*, with notes on infections in other rodents. *Journal of Parasitology*, 56, 962-8.
- (1970b) Development of subperiodic *Brugia malayi* in the jird, *Meriones unguiculatus*, with notes on infections in other rodents. *Journal of Parasitology*, 56, 969-73.
- Babayan, S. A., A. F. Read, R. A. Lawrence, O. Bain & J. E. Allen (2010) Filarial parasites develop faster and reproduce earlier in response to host immune effectors that determine filarial life expectancy. *PLoS Biology*, 8, e1000525.
- Babu, S., S. Q. Bhat, N. P. Kumar, A. B. Lipira, S. Kumar, C. Karthik, V. Kumaraswami & T. B. Nutman (2009) Filarial lymphedema is characterized by antigen-specific Th1 and th17 proinflammatory responses and a lack of regulatory T cells. *PLoS Neglected Tropical Diseases*, 3, e420.
- Babu, S., C. P. Blauvelt, V. Kumaraswami & T. B. Nutman (2006) Regulatory networks induced by live parasites impair both Th1 and Th2 pathways in patent lymphatic filariasis: implications for parasite persistence. *The Journal of Immunology*, 176, 3248-3256.
- Ballesteros, C., L. Tritten, M. O'Neill, E. Burkman, W. I. Zaky, J. Xia, A. Moorhead, S. A. Williams & T. G. Geary (2016) The effect of in vitro cultivation on the transcriptome of adult *Brugia malayi*. *PLoS neglected tropical diseases*, 10, e0004311.
- Bennuru, S., R. Semnani, Z. Meng, J. M. Ribeiro, T. D. Veenstra & T. B. Nutman (2009) *Brugia malayi* excreted/secreted proteins at the host/parasite interface: stage- and gender-specific proteomic profiling. *PLoS Neglected Tropical Diseases*, 3, e410.

- Bessa, J., C. A. Meyer, M. C. de Vera Mudry, S. Schlicht, S. H. Smith, A. Iglesias & J. Cote-Sierra (2014) Altered subcellular localization of IL-33 leads to non-resolving lethal inflammation. *Journal of Autoimmunity*, 55, 33-41.
- Bethony, J., S. Brooker, M. Albonico, S. M. Geiger, A. Loukas, D. Diemert & P. J. Hotez (2006) Soil-transmitted helminth infections: ascariasis, trichuriasis, and hookworm. *Lancet*, 367, 1521-32.
- Blanton, R. E., L. S. Licate & R. A. Aman (1994) Characterization of a native and recombinant *Schistosoma haematobium* serine protease inhibitor gene product. *Molecular and Biochemical Parasitology*, 63, 1-11.
- Bockarie, M. J., E. M. Pedersen, G. B. White & E. Michael (2009) Role of vector control in the global program to eliminate lymphatic filariasis. *Annual Review of Entomology*, 54, 469-87.
- Bouchery, T. & N. L. Harris (2017) Only two can tango: Mast cells displace epithelial cells to dance with ILC2s. *Immunity*, 46, 766-768.
- Bouchery, T., R. Kyle, M. Camberis, A. Shepherd, K. Filbey, A. Smith, M. Harvie, G. Painter, K. Johnston & P. Ferguson (2015) ILC2s and T cells cooperate to ensure maintenance of M2 macrophages for lung immunity against hookworms. *Nature Communications*, 6, 6970.
- Boussinesq, M., J. Gardon, N. Gardon-Wendel & J. P. Chippaux (2003) Clinical picture, epidemiology and outcome of *Loa*-associated serious adverse events related to mass ivermectin treatment of onchocerciasis in Cameroon. *Filaria Journal*, 2 Suppl 1, S4.
- Branzk, N., A. Lubojemska, S. E. Hardison, Q. Wang, M. G. Gutierrez, G. D. Brown & V. Papayannopoulos (2014) Neutrophils sense microbe size and selectively release neutrophil extracellular traps in response to large pathogens. *Nature Immunology*, 15, 1017-1025.
- Buck, A. H., G. Coakley, F. Simbari, H. J. McSorley, J. F. Quintana, T. Le Bihan, S. Kumar, C. Abreu-Goodger, M. Lear & Y. Harcus (2014) Exosomes secreted by nematode parasites transfer small RNAs to mammalian cells and modulate innate immunity. *Nature Communications*, 5.
- Carriere, V., L. Roussel, N. Ortega, D.-A. Lacorre, L. Americh, L. Aguilar, G. Bouche & J.-P. Girard (2007) IL-33, the IL-1-like cytokine ligand for ST2 receptor, is a chromatin-associated nuclear factor in vivo. *Proceedings of the National Academy of Sciences*, 104, 282-287.
- Cayrol, C. & J.-P. Girard (2009) The IL-1-like cytokine IL-33 is inactivated after maturation by caspase-1. *Proceedings of the National Academy of Sciences*, 106, 9021-9026.

- (2014) IL-33: an alarmin cytokine with crucial roles in innate immunity, inflammation and allergy. *Current Opinion in Immunology*, 31, 31-37.
- Cayrol, C. & J. P. Girard (2018) Interleukin-33 (IL-33): A nuclear cytokine from the IL-1 family. *Immunological Reviews*, 281, 154-168.
- Chen, F., W. Wu, A. Millman, J. F. Craft, E. Chen, N. Patel, J. L. Boucher, J. F. Urban Jr, C. C. Kim & W. C. Gause (2014) Neutrophils prime a long-lived effector macrophage phenotype that mediates accelerated helminth expulsion. *Nature Immunology*, 15, 938-946.
- Chen, G., S. H. Wang, J. C. Jang, J. I. Odegaard & M. G. Nair (2016) Comparison of RELM $\alpha$  and RELM $\beta$  single-and double-gene-deficient mice reveals that RELM $\alpha$  expression dictates inflammation and worm expulsion in hookworm infection. *Infection and Immunity*, 84, 1100-1111.
- Chiu, L.-L., D.-W. Perng, C.-H. Yu, S.-N. Su & L.-P. Chow (2007) Mold allergen, pen C 13, induces IL-8 expression in human airway epithelial cells by activating protease-activated receptor 1 and 2. *The Journal of Immunology*, 178, 5237-5244.
- Clark, C. E., M. P. Fay, M. E. Chico, C. A. Sandoval, M. G. Vaca, A. Boyd, P. J. Cooper & T. B. Nutman (2016) Maternal helminth infection is associated with higher infant immunoglobulin A titers to antigen in orally administered vaccines. *The Journal of Infectious Diseases*, 213, 1996-2004.
- Coakley, G., R. M. Maizels & A. H. Buck (2015) Exosomes and other extracellular vesicles: the new communicators in parasite infections. *Trends in Parasitology*, 31, 477-489.
- Coakley, G., J. L. McCaskill, J. G. Borger, F. Simbari, E. Robertson, M. Millar, Y. Harcus, H. J. McSorley, R. M. Maizels & A. H. Buck (2017) Extracellular vesicles from a helminth parasite suppress macrophage activation and constitute an effective vaccine for protective immunity. *Cell Reports*, 19, 1545-1557.
- Conti, P., D. Kempuraj, M. Di Gioacchino, W. Boucher, R. Letourneau, K. Kandere, R. C. Barbacane, M. Reale, M. Felaco & S. Frydas (2002) Interleukin-6 and mast cells. In *Allergy and Asthma Proceedings*, 331-335.
- Cooper, P., I. Espinel, W. Paredes, R. Guderian & T. Nutman (1998) Impaired tetanus-specific cellular and humoral responses following tetanus vaccination in human onchocerciasis: a possible role for interleukin-10. *The Journal of Infectious Diseases*, 178, 1133-1138.
- Devlin, M. G., R. B. Gasser & T. M. Cocks (2007) Initial support for the hypothesis that PAR2 is involved in the immune response to *Nippostrongylus brasiliensis* in mice. *Parasitology Research*, 101, 105-109.

- Duarte, J., P. Deshpande, V. Guiyedi, S. Mécheri, C. Fesel, P.-A. Cazenave, G. C. Mishra, M. Kombila & S. Pied (2007) Total and functional parasite specific IgE responses in *Plasmodium falciparum*-infected patients exhibiting different clinical status. *Malaria Journal*, 6, 1.
- Duggan, B. M., H. J. Dyson & P. E. Wright (1999) Inherent flexibility in a potent inhibitor of blood coagulation, recombinant nematode anticoagulant protein c2. *The FEBS Journal*, 265, 539-548.
- Elias, D., H. Akuffo, A. Pawlowski, M. Haile, T. Schön & S. Britton (2005) *Schistosoma mansoni* infection reduces the protective efficacy of BCG vaccination against virulent *Mycobacterium tuberculosis*. *Vaccine*, 23, 1326-1334.
- Else, K., F. Finkelman, C. Maliszewski & R. Grencis (1994) Cytokine-mediated regulation of chronic intestinal helminth infection. *Journal of Experimental Medicine*, 179, 347-351.
- Erb, K. J. (2007) Helminths, allergic disorders and IgE-mediated immune responses: Where do we stand? *European Journal of Immunology*, 37, 1170-1173.
- Falcone, F. H., X. Zang, A. S. MacDonald, R. M. Maizels & J. E. Allen (2001) A *Brugia malayi* homolog of macrophage migration inhibitory factor reveals an important link between macrophages and eosinophil recruitment during nematode infection. *The Journal of Immunology*, 167, 5348-5354.
- Fallon, P. G., S. J. Ballantyne, N. E. Mangan, J. L. Barlow, A. Dasvarma, D. R. Hewett, A. McIlgorm, H. E. Jolin & A. N. McKenzie (2006) Identification of an interleukin (IL)-25-dependent cell population that provides IL-4, IL-5, and IL-13 at the onset of helminth expulsion. *Journal of Experimental Medicine*, 203, 1105-1116.
- Faulkner, H., N. Humphreys, J. C. Renauld, J. van Snick & R. Grencis (1997) Interleukin-9 is involved in host protective immunity to intestinal nematode infection. *European Journal of Immunology*, 27, 2536-2540.
- Fitzsimmons, C. M., R. McBeath, S. Joseph, F. M. Jones, K. Walter, K. F. Hoffmann, H. C. Kariuki, J. K. Mwatha, G. Kimani & N. B. Kabatereine (2007) Factors affecting human IgE and IgG responses to allergen-like *Schistosoma mansoni* antigens: Molecular structure and patterns of in vivo exposure. *International Archives of Allergy and Immunology*, 142, 40-50.
- Ford, L., D. B. Guiliano, Y. Oksov, A. K. Debnath, J. Liu, S. A. Williams, M. L. Blaxter & S. Lustigman (2005) Characterization of a novel filarial serine protease inhibitor, Ov-SPI-1, from *Onchocerca volvulus*, with potential multifunctional roles during development of the parasite. *Journal of Biological Chemistry*, 280, 40845-40856.

- Fu, Y., J. Lan, Z. Zhang, R. Hou, X. Wu, D. Yang, R. Zhang, W. Zheng, H. Nie, Y. Xie, N. Yan, Z. Yang, C. Wang, L. Luo, L. Liu, X. Gu, S. Wang, X. Peng & G. Yang (2012) Novel insights into the transcriptome of *Dirofilaria immitis*. *PLoS One*, 7, e41639.
- Fuhrman, J. A., W. S. Lane, R. F. Smith, W. F. Piessens & F. B. Perler (1992) Transmission-blocking antibodies recognize microfilarial chitinase in *brugian* lymphatic filariasis. *Proceedings of the National Academy of Sciences*, 89, 1548-1552.
- Galli, S. J. & M. Tsai (2010) Mast cells in allergy and infection: versatile effector and regulatory cells in innate and adaptive immunity. *European Journal of Immunology*, 40, 1843-1851.
- Gallin, M., K. Edmonds, J. Ellner, K. Erttmann, A. White, H. Newland, H. Taylor & B. Greene (1988) Cell-mediated immune responses in human infection with *Onchocerca volvulus*. *The Journal of Immunology*, 140, 1999-2007.
- Gebreselassie, N. G., A. R. Moorhead, V. Fabre, L. F. Gagliardo, N. A. Lee, J. J. Lee & J. A. Appleton (2012) Eosinophils preserve parasitic nematode larvae by regulating local immunity. *The Journal of Immunology*, 188, 417-425.
- Gerken, S. E., N. M. Vaz & T. A. Mota-Santos (1990) Local anaphylactic reactions to the penetration of cercariae of *Schistosoma mansoni*. *Brazilian Journal of Medical and Biological Research*, 23, 275-81.
- Ghendler, Y., R. Arnon & Z. Fishelson (1994) *Schistosoma mansoni*: isolation and characterization of Smpi56, a novel serine protease inhibitor. *Experimental Parasitology*, 78, 121-131.
- Giard, D. J., S. A. Aaronson, G. J. Todaro, P. Arnstein, J. H. Kersey, H. Dosik & W. P. Parks (1973) In vitro cultivation of human tumors: establishment of cell lines derived from a series of solid tumors 2. *Journal of the National Cancer Institute*, 51, 1417-1423.
- Girard, J.-P., L. Aguilar, M. Erard, G. Haraldsen, E. Baekkevold, M. Veuger & P. Brandtzaeg. 2003. Nf-hev compositions and methods of use. Google Patents.
- Gomez-Escobar, N., C. Bennett, L. Prieto-Lafuente, T. Aebischer, C. C. Blackburn & R. M. Maizels (2005) Heterologous expression of the filarial nematode alt gene products reveals their potential to inhibit immune function. *BMC Biology*, 3, 8.
- Gomez-Escobar, N., W. F. Gregory & R. M. Maizels (2000) Identification of tgh-2, a filarial nematode homolog of *Caenorhabditis elegans* daf-7 and human transforming growth factor  $\beta$ , expressed in microfilarial and adult stages of *Brugia malayi*. *Infection and Immunity*, 68, 6402-6410.

- Gonçalves, M. F., E. S. Umezawa, A. M. Katzin, W. de Souza, M. J. Alves, B. Zingales & W. Colli (1991) *Trypanosoma cruzi*: shedding of surface antigens as membrane vesicles. *Experimental Parasitology*, 72, 43-53.
- Gould, H. J., B. J. Sutton, A. J. Beavil, R. L. Beavil, N. McCloskey, H. A. Coker, D. Fear & L. Smurthwaite (2003) The biology of IGE and the basis of allergic disease. *Annual Review of Immunology*, 21, 579-628.
- Grasberger, B. L., G. M. Clore & A. M. Gronenborn (1994) High-resolution structure of *Ascaris* trypsin inhibitor in solution: direct evidence for a pH-induced conformational transition in the reactive site. *Structure*, 2, 669-678.
- Greenwood, B. (1968) Autoimmune disease and parasitic infections in Nigerians. *The Lancet*, 292, 380-382.
- Greenwood, B., E. M. Herrick & A. Voller (1970) Suppression of autoimmune disease in NZB and (NZB× NZW) F1 hybrid mice by infection with malaria. *Nature*, 226, 266-267.
- Greenwood, B. & A. Voller (1970) Suppression of autoimmune disease in New Zealand mice associated with infection with malaria. I.(NZB× NZW) F1 hybrid mice. *Clinical and Experimental Immunology*, 7, 793.
- Grencis, R. K., K. J. Else, J. F. Huntley & S. I. Nishikawa (1993) The in vivo role of stem cell factor (c-kit ligand) on mastocytosis and host protective immunity to the intestinal nematode *Trichinella spiralis* in mice. *Parasite Immunology*, 15, 55-9.
- Grigoryev, S. A., J. Bednar & C. L. Woodcock (1999) MENT, a heterochromatin protein that mediates higher order chromatin folding, is a new serpin family member. *Journal of Biological Chemistry*, 274, 5626-5636.
- Gyapong, J. O., V. Kumaraswami, G. Biswas & E. A. Ottesen (2005) Treatment strategies underpinning the global programme to eliminate lymphatic filariasis. *Expert Opinion on Pharmacotherapy*, 6, 179-200.
- Haarbrink, M., A. J. Terhell, G. K. Abadi, Y. Mitsui & M. Yazdanbakhsh (1999) Adverse reactions following diethylcarbamazine (DEC) intake in 'endemic normals', microfilaraemics and elephantiasis patients. *Transactions of the Royal Society of Tropical Medicine and Hygiene*, 93, 91-6.
- Hammad, H. & B. N. Lambrecht (2015) Barrier epithelial cells and the control of type 2 immunity. *Immunity*, 43, 29-40.
- Harnett, M., A. Melendez & W. Harnett (2010) The therapeutic potential of the filarial nematode-derived immunomodulator, ES-62 in inflammatory disease. *Clinical & Experimental Immunology*, 159, 256-267.

- Harnett, W., M. R. Deehan, K. M. Houston & M. M. Harnett (1999) Immunomodulatory properties of a phosphorylcholine-containing secreted filarial glycoprotein. *Parasite Immunology*, 21, 601-608.
- Harnett, W. & M. M. Harnett (1999) Phosphorylcholine: friend or foe of the immune system? *Immunology Today*, 20, 125-129.
- Harnett, W., I. B. McInnes & M. M. Harnett (2004) ES-62, a filarial nematode-derived immunomodulator with anti-inflammatory potential. *Immunology Letters*, 94, 27-33.
- Hartmann, S. & R. Lucius (2003) Modulation of host immune responses by nematode cystatins. *International Journal for Parasitology*, 33, 1291-1302.
- Hartmann, W., N. Singh, S. Rathaur, Y. Brenz, E. Liebau, B. Fleischer & M. Breloer (2014) Immunization with *Brugia malayi* Hsp70 protects mice against *Litomosoides sigmodontis* challenge infection. *Parasite Immunology*, 36, 141-9.
- Hasnain, S. Z., C. M. Evans, M. Roy, A. L. Gallagher, K. N. Kindrachuk, L. Barron, B. F. Dickey, M. S. Wilson, T. A. Wynn & R. K. Grencis (2011) Muc5ac: a critical component mediating the rejection of enteric nematodes. *Journal of Experimental Medicine*, 208, 893-900.
- Hayes, K., A. Bancroft, M. Goldrick, C. Portsmouth, I. Roberts & R. Grencis (2010) Exploitation of the intestinal microflora by the parasitic nematode *Trichuris muris*. *Science*, 328, 1391-1394.
- Hepworth, M. R., E. Daniłowicz-Luebert, S. Rausch, M. Metz, C. Klotz, M. Maurer & S. Hartmann (2012a) Mast cells orchestrate type 2 immunity to helminths through regulation of tissue-derived cytokines. *Proceedings of the National Academy of Sciences*, 109, 6644-6649.
- Hepworth, M. R., M. Maurer & S. Hartmann (2012b) Regulation of type 2 immunity to helminths by mast cells. *Gut Microbes*, 3, 476-81.
- Hewitson, J. P., J. R. Grainger & R. M. Maizels (2009) Helminth immunoregulation: the role of parasite secreted proteins in modulating host immunity. *Molecular and Biochemical Parasitology*, 167, 1-11.
- Hewitson, J. P., Y. M. Harcus, R. S. Curwen, A. A. Dowle, A. K. Atmadja, P. D. Ashton, A. Wilson & R. M. Maizels (2008) The secretome of the filarial parasite, *Brugia malayi*: proteomic profile of adult excretory-secretory products. *Molecular and Biochemical Parasitology*, 160, 8-21.
- Hewitson, J. P., D. Ruckerl, Y. Harcus, J. Murray, L. M. Webb, S. A. Babayan, J. E. Allen, A. Kurniawan & R. M. Maizels (2014) The secreted triose phosphate isomerase of

- Brugia malayi* is required to sustain microfilaria production in vivo. *PLoS Pathogens*, 10, e1003930.
- Hoerauf, A., D. W. Büttner, O. Adjei & E. Pearlman (2003) *Onchocerciasis*. *BMJ*, 326, 207-10.
- Hotez, P. J., P. J. Brindley, J. M. Bethony, C. H. King, E. J. Pearce & J. Jacobson (2008) Helminth infections: the great neglected tropical diseases. *Journal of Clinical Investigation*, 118, 1311-21.
- Huang, K., N. C. Strynadka, V. D. Bernard, R. J. Peanasky & M. N. James (1994) The molecular structure of the complex of *Ascaris* chymotrypsin/elastase inhibitor with porcine elastase. *Structure*, 2, 679-689.
- Huang, L., D. Pike, D. E. Sleat, V. Nanda & P. Lobel (2014) Potential pitfalls and solutions for use of fluorescent fusion proteins to study the lysosome. *PloS One*, 9, e88893.
- Huang, Y., L. Guo, J. Qiu, X. Chen, J. Hu-Li, U. Siebenlist, P. R. Williamson, J. F. Urban Jr & W. E. Paul (2015) IL-25-responsive, lineage-negative KLRG1hi cells are multipotential "inflammatory" type 2 innate lymphoid cells. *Nature Immunology*, 16, 161-169.
- Humphreys, N. E., D. Xu, M. R. Hepworth, F. Y. Liew & R. K. Grencis (2008) IL-33, a potent inducer of adaptive immunity to intestinal nematodes. *The Journal of Immunology*, 180, 2443-2449.
- Hung, L.-Y., I. P. Lewkowich, L. A. Dawson, J. Downey, Y. Yang, D. E. Smith & R. H. De'Broski (2013) IL-33 drives biphasic IL-13 production for noncanonical Type 2 immunity against hookworms. *Proceedings of the National Academy of Sciences*, 110, 282-287.
- Huntington, J. A., R. J. Read & R. W. Carrell (2000) Structure of a serpin-protease complex shows inhibition by deformation. *Nature*, 407, 923.
- Hwang, J.-H., W.-G. Lee, B.-K. Na, H.-W. Lee, S.-H. Cho & T.-S. Kim (2009) Identification and characterization of a serine protease inhibitor of *Paragonimus westermani*. *Parasitology Research*, 104, 495-501.
- Hültner, L., C. Druez, J. Moeller, C. Uyttenhove, E. Schmitt, E. Rüde, P. Dörmer & J. van Snick (1990) Mast cell growth-enhancing activity (MEA) is structurally related and functionally identical to the novel mouse T cell growth factor P40/TCGFIII (interleukin 9). *European Journal of Immunology*, 20, 1413-1416.
- Ichimori, K., J. D. King, D. Engels, A. Yajima, A. Mikhailov, P. Lammie & E. A. Ottesen (2014) Global programme to eliminate lymphatic filariasis: the processes underlying programme success. *PLoS Neglected Tropical Diseases*, 8, e3328.

- Iikura, M., H. Suto, N. Kajiwara, K. Oboki, T. Ohno, Y. Okayama, H. Saito, S. J. Galli & S. Nakae (2007) IL-33 can promote survival, adhesion and cytokine production in human mast cells. *Laboratory Investigation*, 87, 971.
- Irving, J. A., R. N. Pike, A. M. Lesk & J. C. Whisstock (2000) Phylogeny of the serpin superfamily: implications of patterns of amino acid conservation for structure and function. *Genome Research*, 10, 1845-1864.
- Johnston, C. J., E. Robertson, Y. Harcus, J. R. Grainger, G. Coakley, D. J. Smyth, H. J. McSorley & R. Maizels (2015) Cultivation of *Heligmosomoides polygyrus*: an immunomodulatory nematode parasite and its secreted products. *Journal of Visualized Experiments: JoVE*.
- Kakkar, R. & R. T. Lee (2008) The IL-33/ST2 pathway: therapeutic target and novel biomarker. *Nature Reviews. Drug Discovery*, 7, 827-40.
- Kang, J.-M., W.-M. Sohn, J.-W. Ju, T.-S. Kim & B.-K. Na (2010) Identification and characterization of a serine protease inhibitor of *Clonorchis sinensis*. *Acta Tropica*, 116, 134-140.
- Kaushal, N., R. Hussain, T. Nash & E. Ottesen (1982) Identification and characterization of excretory-secretory products of *Brugia malayi*, adult filarial parasites. *The Journal of Immunology*, 129, 338-343.
- Khalife, J., D. Dunne, B. Richardson, G. Mazza, K. Thorne, A. Capron & A. Butterworth (1989) Functional role of human IgG subclasses in eosinophil-mediated killing of schistosomula of *Schistosoma mansoni*. *The Journal of Immunology*, 142, 4422-4427.
- Knight, P. A., S. H. Wright, C. E. Lawrence, Y. Y. Paterson & H. R. Miller (2000) Delayed expulsion of the nematode *Trichinella spiralis* in mice lacking the mucosal mast cell-specific granule chymase, mouse mast cell protease-1. *Journal of Experimental Medicine*, 192, 1849-1856.
- Knox, D. (2007) Proteinase inhibitors and helminth parasite infection. *Parasite Immunology*, 29, 57-71.
- Kobayashi, Y., S. Ishizaki, K. Shimakura, Y. Nagashima & K. Shiomi (2007) Molecular cloning and expression of two new allergens from *Anisakis simplex*. *Parasitology Research*, 100, 1233-1241.
- Kurniawan, A., M. Yazdanbakhsh, R. Van Ree, R. Aalberse, M. Selkirk, F. Partono & R. Maizels (1993) Differential expression of IgE and IgG4 specific antibody responses in asymptomatic and chronic human filariasis. *The Journal of Immunology*, 150, 3941-3950.

- L Makepeace, B., C. Martin, J. D Turner & S. Specht (2012) Granulocytes in helminth infection-who is calling the shots? *Current Medicinal Chemistry*, 19, 1567-1586.
- LaBeaud, A. D., I. Malhotra, M. J. King, C. L. King & C. H. King (2009) Do antenatal parasite infections devalue childhood vaccination? *PLoS Neglected Tropical Diseases*, 3, e442.
- Lammie, P. J., J. F. Lindo, W. E. Secor, J. Vasquez, S. K. Ault & M. L. Eberhard (2007) Eliminating lymphatic filariasis, onchocerciasis, and schistosomiasis from the americas: breaking a historical legacy of slavery. *PLoS Neglected Tropical Diseases*, 1, e71.
- Lange, A. M., W. Yutanawiboonchai, P. Scott & D. Abraham (1994) IL-4-and IL-5-dependent protective immunity to *Onchocerca volvulus* infective larvae in BALB/cBYJ mice. *The Journal of Immunology*, 153, 205-211.
- Lantz, C. S., J. Boesiger, C. H. Song & N. Mach (1998) Role for interleukin-3 in mast-cell and basophil development and in immunity to parasites. *Nature*, 392, 90.
- Lau, Y. L., W. C. Lee, J. Xia, G. Zhang, R. Razali, A. Anwar & M. Y. Fong (2015) Draft genome of *Brugia pahangi*: high similarity between *B. pahangi* and *B. malayi*. *Parasite & Vectors*, 8, 451.
- Lawrence, R., J. Allen & C. Gray (2000) Requirements for in vivo IFN $\gamma$ - induction by live microfilariae of the parasitic nematode, *Brugia malayi*. *Parasitology*, 120, 631-640.
- Lawrence, R. A., J. E. Allen, J. Osborne & R. M. Maizels (1994) Adult and microfilarial stages of the filarial parasite *Brugia malayi* stimulate contrasting cytokine and Ig isotype responses in BALB/c mice. *The Journal of Immunology*, 153, 1216-1224.
- Lee, W., J. Hwang, B. Na, J. Cho, H. Lee, S. Cho, Y. Kong, C. Song & T. Kim (2005) Functional expression of a recombinant copper/zinc superoxide dismutase of filarial nematode, *Brugia malayi*. *Journal of Parasitology*, 91, 205-208.
- Lefrançois, E. & C. Cayrol (2012) Mechanisms of IL-33 processing and secretion: differences and similarities between IL-1 family members. *European Cytokine Network*, 23, 120-127.
- Lefrançois, E., A. Duval, E. Mirey, S. Roga, E. Espinosa, C. Cayrol & J.-P. Girard (2014) Central domain of IL-33 is cleaved by mast cell proteases for potent activation of group-2 innate lymphoid cells. *Proceedings of the National Academy of Sciences*, 111, 15502-15507.
- Lefrançois, E., S. Roga, V. Gautier, A. Gonzalez-de-Peredo, B. Monsarrat, J.-P. Girard & C. Cayrol (2012) IL-33 is processed into mature bioactive forms by neutrophil elastase and cathepsin G. *Proceedings of the National Academy of Sciences*, 109, 1673-1678.

- Leitner, J., A. Rieger, W. F. Pickl, G. Zlabinger, K. Grabmeier-Pfistershammer & P. Steinberger (2013) TIM-3 does not act as a receptor for galectin-9. *PLoS Pathogens*, 9, e1003253.
- Leung, J. M. (2013) A role for IL-22 in the relationship between intestinal helminths, gut microbiota and mucosal immunity. *International Journal for Parasitology*, 43, 253-257.
- Levashina, E. A., E. Langley, C. Green, D. Gubb, M. Ashburner, J. A. Hoffmann & J.-M. Reichhart (1999) Constitutive activation of toll-mediated antifungal defense in serpin-deficient *Drosophila*. *Science*, 285, 1917-1919.
- Li, B.-W., Z. Wang, A. C. Rush, M. Mitreva & G. J. Weil (2012) Transcription profiling reveals stage- and function-dependent expression patterns in the filarial nematode *Brugia malayi*. *BMC Genomics*, 13, 184.
- Li, Y., J. Feng, S. Geng, S. Geng, H. Wei, G. Chen, X. Li, L. Wang, R. Wang & H. Peng (2011) The N- and C-terminal carbohydrate recognition domains of galectin-9 contribute differently to its multiple functions in innate immunity and adaptive immunity. *Molecular Immunology*, 48, 670-677.
- Liew, F. Y., J. P. Girard & H. R. Turnquist (2016) Interleukin-33 in health and disease. *Nature Reviews Immunology*, 16, 676-689.
- Lightowers, M. & M. Rickard (1988) Excretory–secretory products of helminth parasites: effects on host immune responses. *Parasitology*, 96, S123-S166.
- Lima, A. W., Z. Medeiros, Z. C. Santos, G. M. Costa & C. Braga (2012) Adverse reactions following mass drug administration with diethylcarbamazine in lymphatic filariasis endemic areas in the Northeast of Brazil. *Revista Da Sociedade Brasileira De Medicina Tropical*, 45, 745-50.
- Liu, S., R. Tobias, S. McClure, G. Styba, Q. Shi & G. Jackowski (1997) Removal of endotoxin from recombinant protein preparations. *Clinical Biochemistry*, 30, 455-463.
- Lizotte-Waniewski, M., W. Tawe, D. B. Guiliano, W. Lu, J. Liu, S. A. Williams & S. Lustigman (2000) Identification of potential vaccine and drug target candidates by expressed sequence tag analysis and immunoscreening of *Onchocerca volvulus* larval cDNA libraries. *Infection and Immunity*, 68, 3491-3501.
- Loebbermann, J., H. Thornton, L. Durant, T. Sparwasser, K. E. Webster, J. Sprent, F. J. Culley, C. Johansson & P. J. Openshaw (2012) Regulatory T cells expressing granzyme B play a critical role in controlling lung inflammation during acute viral infection. *Mucosal Immunology*, 5, 161-72.

- Lu, C.-C., T. Nguyen, S. Morris, D. Hill & J. A. Sakanari (1998) Anisakis simplex: mutational bursts in the reactive site centers of serine protease inhibitors from an ascarid nematode. *Experimental Parasitology*, 89, 257-261.
- Lüthi, A. U., S. P. Cullen, E. A. McNeela, P. J. Duriez, I. S. Afonina, C. Sheridan, G. Brumatti, R. C. Taylor, K. Kersse & P. Vandenabeele (2009) Suppression of interleukin-33 bioactivity through proteolysis by apoptotic caspases. *Immunity*, 31, 84-98.
- Macfarlane, S. R., M. J. Seatter, T. Kanke, G. D. Hunter & R. Plevin (2001) Proteinase-activated receptors. *Pharmacological Reviews*, 53, 245-282.
- MacLennan, K., K. McLean & D. Knox (2005) Serpin expression in the parasitic stages of *Trichostrongylus vitrinus*, an ovine intestinal nematode. *Parasitology*, 130, 349-357.
- Mahmoud, A., K. S. Warren & P. A. Peters (1975) A role for the eosinophil in acquired resistance to *Schistosoma mansoni* infection as determined by antieosinophil serum. *Journal of Experimental Medicine*, 142, 805-813.
- Maizels, R. M., A. Balic, N. Gomez-Escobar, M. Nair, M. D. Taylor & J. E. Allen (2004) Helminth parasites--masters of regulation. *Immunological Reviews*, 201, 89-116.
- Maizels, R. M., D. A. Bundy, M. E. Selkirk, D. F. Smith & R. M. Anderson (1993) Immunological modulation and evasion by helminth parasites in human populations. *Nature*, 365, 797-805.
- Maizels, R. M., N. Gomez-Escobar, W. F. Gregory, J. Murray & X. Zang (2001) Immune evasion genes from filarial nematodes. *International Journal for Parasitology*, 31, 889-898.
- Maizels, R. M., W. F. Gregory, G.-E. Kwan-Lim & M. E. Selkirk (1989) Filarial surface antigens: the major 29 kilodalton glycoprotein and a novel 17–200 kilodalton complex from adult *Brugia malayi* parasites. *Molecular and Biochemical Parasitology*, 32, 213-227.
- Maizels, R. M., J. P. Hewitson & K. A. Smith (2012) Susceptibility and immunity to helminth parasites. *Current Opinion in Immunology*, 24, 459-66.
- Maizels, R. M. & M. J. Holland (1998) Parasite immunity: pathways for expelling intestinal helminths. *Current Biology*, 8, R711-R714.
- Maizels, R. M. & H. J. McSorley (2016) Regulation of the host immune system by helminth parasites. *Journal of Allergy and Clinical Immunology*, 138, 666-75.
- Maizels, R. M., H. J. McSorley & D. J. Smyth (2014) Helminths in the hygiene hypothesis: sooner or later? *Clinical & Experimental Immunology*, 177, 38-46.
- Maizels, R. M. & M. Yazdanbakhsh (2003) Immune regulation by helminth parasites: cellular and molecular mechanisms. *Nature Reviews Immunology*, 3, 733-44.

- Malone, J. B. (1986) Fascioliasis and cestodiasis in cattle. *Veterinary Clinics of North America: Food Animal Practice*, 2, 261-75.
- Manguin, S., M. J. Bangs, J. Pothikasikorn & T. Chareonviriyaphap (2010) Review on global co-transmission of human Plasmodium species and *Wuchereria bancrofti* by Anopheles mosquitoes. *Infection, Genetics and Evolution*, 10, 159-77.
- Manoury, B., W. F. Gregory, R. M. Maizels & C. Watts (2001) Bm-CPI-2, a cystatin homolog secreted by the filarial parasite *Brugia malayi*, inhibits class II MHC-restricted antigen processing. *Current Biology*, 11, 447-451.
- Matsuda, H., N. Watanabe, Y. Kiso, S. Hirota, H. Ushio, Y. Kannan, M. Azuma, H. Koyama & Y. Kitamura (1990) Necessity of IgE antibodies and mast cells for manifestation of resistance against larval *Haemaphysalis longicornis* ticks in mice. *The Journal of Immunology*, 144, 259-262.
- McDermott, J. R., R. E. Bartram, P. A. Knight, H. R. Miller, D. R. Garrod & R. K. Grencis (2003) Mast cells disrupt epithelial barrier function during enteric nematode infection. *Proceedings of the National Academy of Sciences*, 100, 7761-6.
- McSorley, H. J., N. F. Blair, K. A. Smith, A. N. McKenzie & R. M. Maizels (2014) Blockade of IL-33 release and suppression of type 2 innate lymphoid cell responses by helminth secreted products in airway allergy. *Mucosal Immunology*, 7, 1068.
- McSorley, H. J., M. T. O'Gorman, N. Blair, T. E. Sutherland, K. J. Filbey & R. M. Maizels (2012) Suppression of type 2 immunity and allergic airway inflammation by secreted products of the helminth *Heligmosomoides polygyrus*. *European Journal of Immunology*, 42, 2667-2682.
- Merckelbach, A. & A. Ruppel (2007) Biochemical properties of an intracellular serpin from *Echinococcus multilocularis*. *Molecular and Biochemical Parasitology*, 156, 84-88.
- Metenou, S., B. Dembélé, S. Konate, H. Dolo, S. Y. Coulibaly, Y. I. Coulibaly, A. A. Diallo, L. Soumaoro, M. E. Coulibaly & D. Sanogo (2009) Patent filarial infection modulates malaria-specific type 1 cytokine responses in an IL-10-dependent manner in a filaria/malaria-coinfected population. *The Journal of Immunology*, 183, 916-924.
- Miller, A. M. (2011) Role of IL-33 in inflammation and disease. *Journal of Inflammation (London, England)*, 8, 22.
- Miller, B. R. & C. J. Mitchell (1991) Genetic selection of a flavivirus-refractory strain of the yellow fever mosquito *Aedes aegypti*. *The American Journal of Tropical Medicine and Hygiene*, 45, 399-407.
- Mishra, P., M. Palma, D. Bleich, P. Loke & W. Gause (2014) Systemic impact of intestinal helminth infections. *Mucosal Immunology*, 7, 753.

- Modha, J. & M. Doenhoff (1994) *Schistosoma mansoni* host–parasite relationship: interaction of contrapsin with adult worms. *Parasitology*, 109, 487-495.
- Modi, A., S. Gamit, B. S. Jesalpura, G. Kurien & J. K. Kosambiya (2017) Reaching endpoints for lymphatic filariasis elimination- results from mass drug administration and nocturnal blood surveys, South Gujarat, India. *PLoS Neglected Tropical Diseases*, 11, e0005476.
- Molehin, A. J., G. N. Gobert, P. Driguez & D. P. McManus (2014) Characterisation of a secretory serine protease inhibitor (SjB6) from *Schistosoma japonicum*. *Parasites & Vectors*, 7, 330.
- Molehin, A. J., G. N. Gobert & D. P. McManus (2012) Serine protease inhibitors of parasitic helminths. *Parasitology*, 139, 681-95.
- Molofsky, A. B., A. K. Savage & R. M. Locksley (2015) Interleukin-33 in tissue homeostasis, injury, and inflammation. *Immunity*, 42, 1005-1019.
- Moqbel, R. (1980) Histopathological changes following primary, secondary and repeated infections of rats with *Strongyloides ratti*, with special reference to tissue eosinophils. *Parasite Immunology*, 2, 11-27.
- Moreno, Y. & T. G. Geary (2008) Stage- and gender-specific proteomic analysis of *Brugia malayi* excretory-secretory products. *PLoS Neglected Tropical Diseases*, 2, e326.
- Morgan, T. M., I. Sutanto, Purnomo, Sukartono, F. Partono & R. M. Maizels (1986) Antigenic characterization of adult *Wuchereria bancrofti* filarial nematodes. *Parasitology*, 93 (Pt 3), 559-69.
- Moro, K. & S. Koyasu (2010) Innate production of Th2 cytokines by adipose tissue-associated c-Kit<sup>+</sup> Sca-1<sup>+</sup> lymphoid cells. *Nature*, 463, 540-544.
- Mosmann, T. R. & R. Coffman (1989) TH1 and TH2 cells: different patterns of lymphokine secretion lead to different functional properties. *Annual Review of Immunology*, 7, 145-173.
- Moussion, C., N. Ortega & J.-P. Girard (2008) The IL-1-like cytokine IL-33 is constitutively expressed in the nucleus of endothelial cells and epithelial cells in vivo: a novel ‘alarmin’? *PLoS One*, 3, e3331.
- Muller, R. & D. Wakelin (2002) Worms and human disease. New York, *CAB International*.
- Murphy, K. & C. Weaver (2016) Janeway's immunobiology. New York, *Garland Science*.
- Nagano, I., Z. Wu, T. Nakada, A. Matsuo & Y. Takahashi (2001) Molecular cloning and characterization of a serine proteinase inhibitor from *Trichinella spiralis*. *Parasitology*, 123, 77-83.

- Neill, D. R., S. H. Wong, A. Bellosi, R. J. Flynn, M. Daly, T. K. Langford, C. Bucks, C. M. Kane, P. G. Fallon & R. Pannell (2010) Nuocytes represent a new innate effector leukocyte that mediates type-2 immunity. *Nature*, 464, 1367.
- Newlands, G. F., H. R. Miller, A. MacKellar & S. J. Galli (1995) Stem cell factor contributes to intestinal mucosal mast cell hyperplasia in rats infected with *Nippostrongylus brasiliensis* or *Trichinella spiralis*, but anti-stem cell factor treatment decreases parasite egg production during *N. brasiliensis* infection. *Blood*, 86, 1968-76.
- Nguyen, T. T., M. Qasim, S. Morris, C.-C. Lu, D. Hill, M. Laskowski & J. A. Sakanari (1999) Expression and characterization of elastase inhibitors from the ascarid nematodes *Anisakis simplex* and *Ascaris suum*. *Molecular and Biochemical Parasitology*, 102, 79-89.
- Nile, C. J., E. Barksby, P. Jitprasertwong, P. M. Preshaw & J. J. Taylor (2010) Expression and regulation of interleukin-33 in human monocytes. *Immunology*, 130, 172-180.
- Nokes, C., S. M. Grantham-McGregor, A. W. Sawyer, E. S. Cooper, B. A. Robinson & D. A. Bundy (1992) Moderate to heavy infections of *Trichuris trichiura* affect cognitive function in Jamaican school children. *Parasitology*, 104 (Pt 3), 539-47.
- Norões, J., G. Dreyer, A. Santos, V. G. Mendes, Z. Medeiros & D. Addiss (1997) Assessment of the efficacy of diethylcarbamazine on adult *Wuchereria bancrofti* *in vivo*. *Transactions of the Royal Society of Tropical Medicine and Hygiene*, 91, 78-81.
- Nutman, T. & J. W. Kazura (2011) Lymphatic Filariasis. In *Tropical Infection Diseases: Principles, Pathogens and Practice*, <http://www.expertconsult.com/>, 729-734.
- O'Brien, P. J., M. Molino, M. Kahn & L. F. Brass (2001) Protease activated receptors: theme and variations. *Oncogene*, 20, 1570.
- Ohnmacht, C., C. Schwartz, M. Panzer, I. Schiedewitz, R. Naumann & D. Voehringer (2010) Basophils orchestrate chronic allergic dermatitis and protective immunity against helminths. *Immunity*, 33, 364-374.
- Oliphant, C. J., Y. Y. Hwang, J. A. Walker, M. Salimi, S. H. Wong, J. M. Brewer, A. Englezakis, J. L. Barlow, E. Hams & S. T. Scanlon (2014) MHCII-mediated dialog between group 2 innate lymphoid cells and CD4+ T cells potentiates type 2 immunity and promotes parasitic helminth expulsion. *Immunity*, 41, 283-295.
- Osborne, J. 1997. Mechanisms of immunomodulation by *Brugia pahangi* infective larvae and microfilariae. *University of Glasgow*, PhD thesis.
- Osbourn, M., D. C. Soares, F. Vacca, E. S. Cohen, I. C. Scott, W. F. Gregory, D. J. Smyth, M. Toivakka, A. M. Kemter, T. le Bihan, M. Wear, D. Hoving, K. J. Filbey, J. P. Hewitson, H. Henderson, A. González-Ciscar, C. Errington, S. Vermeren, A. L. Astier,

- W. A. Wallace, J. Schwarze, A. C. Ivens, R. M. Maizels & H. J. McSorley (2017) HpARI protein secreted by a helminth parasite suppresses interleukin-33. *Immunity*, 47, 739-751.e5.
- Ou, X., L. Tang, M. McCrossan, K. Henkleduhrsen & M. E. Selkirk (1995) *Brugia malayi*: localisation and differential expression of extracellular and cytoplasmic CuZn superoxide dismutases in adults and microfilariae. *Experimental Parasitology*, 80, 515-529.
- O'Garra, A. & N. Arai (2000) The molecular basis of T helper 1 and T helper 2 cell differentiation. *Trends in Cell Biology*, 10, 542-550.
- Palmieri, J. R., D. H. Connor, Purnomo & H. A. Marwoto (1983) Bancroftian filariasis. *Wuchereria bancrofti* infection in the silvered leaf monkey (*Presbytis cristatus*). *American Journal of Pathology*, 112, 383-6.
- Park, M. K., M. K. Cho, S. A. Kang, H.-K. Park, Y. S. Kim, K. U. Kim, S. C. Ahn, D.-H. Kim & H. S. Yu (2011) Protease-activated receptor 2 is involved in Th2 responses against *Trichinella spiralis* infection. *The Korean Journal of Parasitology*, 49, 235.
- Pearce, E. J. & A. S. MacDonald (2002) The immunobiology of schistosomiasis. *Nature reviews. Immunology*, 2, 499.
- Pearlman, E., F. P. Heinzl, F. Hazlett & J. W. Kazura (1995) IL-12 modulation of T helper responses to the filarial helminth, *Brugia malayi*. *The Journal of Immunology*, 154, 4658-4664.
- Pearlman, E., W. Kroeze, F. Hazlett, S. Chen, S. Mawhorter, W. H. Boom & J. W. Kazura (1993) *Brugia malayi*: acquired resistance to microfilariae in BALB/c mice correlates with local Th2 responses. *Experimental Parasitology*, 76, 200-208.
- Pennock, J. L. & R. K. Grencis (2006) The mast cell and gut nematodes: damage and defence. *Chemical Immunology and Allergy*, 90, 128-40.
- Perera, M., M. Whitehead, D. Molyneux, M. Weerasooriya & G. Gunatilleke (2007) Neglected patients with a neglected disease? A qualitative study of lymphatic filariasis. *PLOS Neglected Tropical Diseases*, 1, e128.
- Pfister, K., K. Turner, A. Currie, E. Hall & E. Jarrett (1983) IgE production in rat fascioliasis. *Parasite Immunology*, 5, 587-593.
- Pichery, M., E. Mirey, P. Mercier, E. Lefrancais, A. Dujardin, N. Ortega & J.-P. Girard (2012) Endogenous IL-33 is highly expressed in mouse epithelial barrier tissues, lymphoid organs, brain, embryos, and inflamed tissues: in situ analysis using a novel IL-33-LacZ gene trap reporter strain. *The Journal of Immunology*, 188, 3488-3495.

- Piessens, W. F., S. Ratiwayanto, S. Tuti, J. H. Palmieri, P. W. Piessens, I. Koiman & D. T. Dennis (1980) Antigen-specific suppressor cells and suppressor factors in human filariasis with *Brugia malayi*. *New England Journal of Medicine*, 302, 833-837.
- Pineda, M. A., D. T. Rodgers, L. Al-Riyami, W. Harnett & M. M. Harnett (2014) ES-62 protects against collagen-induced arthritis by resetting interleukin-22 toward resolution of inflammation in the joints. *Arthritis & Rheumatology*, 66, 1492-1503.
- Potempa, J., E. Korzus & J. Travis (1994) The serpin superfamily of proteinase inhibitors: structure, function, and regulation. *Journal of Biological Chemistry-Paper Edition*, 269, 15957-15960.
- Price, A. E., H.-E. Liang, B. M. Sullivan, R. L. Reinhardt, C. J. Eisley, D. J. Erle & R. M. Locksley (2010) Systemically dispersed innate IL-13-expressing cells in type 2 immunity. *Proceedings of the National Academy of Sciences*, 107, 11489-11494.
- Prieto-Lafuente, L., W. F. Gregory, J. E. Allen & R. M. Maizels (2009) MIF homologues from a filarial nematode parasite synergize with IL-4 to induce alternative activation of host macrophages. *Journal of Leukocyte Biology*, 85, 844-854.
- Rabinovich, G. A., L. G. Baum, N. Tinari, R. Paganelli, C. Natoli, F.-T. Liu & S. Iacobelli (2002a) Galectins and their ligands: amplifiers, silencers or tuners of the inflammatory response? *Trends in Immunology*, 23, 313-320.
- Rabinovich, G. A., N. Rubinstein & M. A. Toscano (2002b) Role of galectins in inflammatory and immunomodulatory processes. *Biochimica et Biophysica Acta (BBA)-General Subjects*, 1572, 274-284.
- Raghavan, N., D. O. Freedman, P. C. Fitzgerald, T. R. Unnasch, E. A. Ottesen & T. B. Nutman (1994) Cloning and characterization of a potentially protective chitinase-like recombinant antigen from *Wuchereria bancrofti*. *Infection and Immunity*, 62, 1901-1908.
- Rhoads, M., R. Fetterer, D. Hill & J. Urban (2000a) *Trichuris suis*: a secretory chymotrypsin/elastase inhibitor with potential as an immunomodulator. *Experimental Parasitology*, 95, 36-44.
- Rhoads, M. L., R. H. Fetterer & D. E. Hill (2000b) *Trichuris suis*: a secretory serine protease inhibitor. *Experimental Parasitology*, 94, 1-7.
- Roussel, L., M. Erard, C. Cayrol & J. P. Girard (2008) Molecular mimicry between IL-33 and KSHV for attachment to chromatin through the H2A-H2B acidic pocket. *EMBO reports*, 9, 1006-1012.

- Sabin, E. A., M. I. Araujo, E. M. Carvalho & E. J. Pearce (1996) Impairment of tetanus toxoid-specific Th1-like immune responses in humans infected with *Schistosoma mansoni*. *The Journal of Infectious Diseases*, 173, 269-272.
- Saenz, S. A., M. Noti & D. Artis (2010) Innate immune cell populations function as initiators and effectors in Th2 cytokine responses. *Trends in Immunology*, 31, 407-413.
- Salimi, M., J. L. Barlow, S. P. Saunders, L. Xue, D. Gutowska-Owsiak, X. Wang, L.-C. Huang, D. Johnson, S. T. Scanlon & A. N. McKenzie (2013) A role for IL-25 and IL-33-driven type-2 innate lymphoid cells in atopic dermatitis. *Journal of Experimental Medicine*, 210, 2939-2950.
- Sambrook, J., E. F. Fritsch & T. Maniatis. 1989. Molecular cloning: a laboratory manual. *Cold Spring Harbor Laboratory press*.
- Scalfone, L. K., H. J. Nel, L. F. Gagliardo, J. L. Cameron, S. Al-Shokri, C. A. Leifer, P. G. Fallon & J. A. Appleton (2013) Participation of MyD88 and interleukin-33 as innate drivers of Th2 immunity to *Trichinella spiralis*. *Infection and Immunity*, 81, 1354-1363.
- Schmitz, J., A. Owyang, E. Oldham, Y. Song, E. Murphy, T. K. McClanahan, G. Zurawski, M. Moshrefi, J. Qin & X. Li (2005) IL-33, an interleukin-1-like cytokine that signals via the IL-1 receptor-related protein ST2 and induces T helper type 2-associated cytokines. *Immunity*, 23, 479-490.
- Seki, M., S. Oomizu, K.-m. Sakata, A. Sakata, T. Arikawa, K. Watanabe, K. Ito, K. Takeshita, T. Niki & N. Saita (2008) Galectin-9 suppresses the generation of Th17, promotes the induction of regulatory T cells, and regulates experimental autoimmune arthritis. *Clinical Immunology*, 127, 78-88.
- Semnani, R. T., P. G. Venugopal, C. A. Leifer, S. Mostböck, H. Sabzevari & T. B. Nutman (2008) Inhibition of TLR3 and TLR4 function and expression in human dendritic cells by helminth parasites. *Blood*, 112, 1290-8.
- Shaner, N. C., R. E. Campbell, P. A. Steinbach, B. N. Giepmans, A. E. Palmer & R. Y. Tsien (2004) Improved monomeric red, orange and yellow fluorescent proteins derived from *Discosoma sp.* red fluorescent protein. *Nature Biotechnology*, 22, 1567.
- Shepherd, J. C., A. Aitken & D. P. McManus (1991) A protein secreted in vivo by *Echinococcus granulosus* inhibits elastase activity and neutrophil chemotaxis. *Molecular and Biochemical Parasitology*, 44, 81-90.
- Shimokawa, C., T. Kanaya, M. Hachisuka, K. Ishiwata, H. Hisaeda, Y. Kurashima, H. Kiyono, T. Yoshimoto, T. Kaisho & H. Ohno (2017) Mast cells are crucial for induction of group 2 innate lymphoid cells and clearance of helminth infections. *Immunity*, 46, 863-874. e4.

- Silverman, G. A., P. I. Bird, R. W. Carrell, P. B. Coughlin, P. G. Gettins, J. I. Irving, D. A. Lomas, C. J. Luke, R. W. Moyer & P. A. Pemberton (2001) The serpins are an expanding superfamily of structurally similar but functionally diverse proteins: Evolution, mechanism of inhibition, novel functions, and a revised nomenclature. *Journal of Biological Chemistry*, 276(36), 33293-6.
- Silverman, J. M., J. Clos, E. Horakova, A. Y. Wang, M. Wiesgigl, I. Kelly, M. A. Lynn, W. R. McMaster, L. J. Foster, M. K. Levings & N. E. Reiner (2010) *Leishmania* exosomes modulate innate and adaptive immune responses through effects on monocytes and dendritic cells. *The Journal of Immunology*, 185, 5011-22.
- Smith, K. A. & R. M. Maizels (2014) IL-6 controls susceptibility to helminth infection by impeding Th2 responsiveness and altering the Treg phenotype in vivo. *European Journal of Immunology*, 44, 150-61.
- Stanley, P. & P. E. Stein (2003) BmSPN2, a serpin secreted by the filarial nematode *Brugia malayi*, does not inhibit human neutrophil proteinases but plays a noninhibitory role. *Biochemistry*, 42, 6241-6248.
- Stassens, P., P. W. Bergum, Y. Gansemans, L. Jespers, Y. Laroche, S. Huang, S. Maki, J. Messens, M. Lauwereys & M. Cappello (1996) Anticoagulant repertoire of the hookworm *Ancylostoma caninum*. *Proceedings of the National Academy of Sciences*, 93, 2149-2154.
- Strachan, D. P. (1989) Hay fever, hygiene, and household size. *BMJ: British Medical Journal*, 299, 1259.
- (2000) Family size, infection and atopy: the first decade of the 'hygiene hypothesis'. *Thorax*, 55, S2.
- Sutherland, T. E., N. Logan, D. Ruckerl, A. A. Humbles, S. M. Allan, V. Papayannopoulos, B. Stockinger, R. M. Maizels & J. E. Allen (2014) Chitinase-like proteins promote IL-17-mediated neutrophilia in a tradeoff between nematode killing and host damage. *Nature Immunology*, 15, 1116-1125.
- Szempruch, A. J., S. E. Sykes, R. Kieft, L. Dennison, A. C. Becker, A. Gartrell, W. J. Martin, E. S. Nakayasu, I. C. Almeida, S. L. Hajduk & J. M. Harrington (2016) Extracellular vesicles from *Trypanosoma brucei* mediate virulence factor transfer and cause host anemia. *Cell*, 164, 246-257.
- Tachu, B., S. Pillai, R. Lucius & T. Pogonka (2008) Essential role of chitinase in the development of the filarial nematode *Acanthocheilonema viteae*. *Infection and Immunity*, 76, 221-228.

- Tan, L. H., M. Y. Fong, R. Mahmud, A. Muslim, Y. L. Lau & A. Kamarulzaman (2011) Zoonotic *Brugia pahangi* filariasis in a suburbia of Kuala Lumpur City, Malaysia. *Parasitology International*, 60, 111-3.
- Taylor, M. D., A. Harris, S. A. Babayan, O. Bain, A. Culshaw, J. E. Allen & R. M. Maizels (2007) CTLA-4 and CD4<sup>+</sup> CD25<sup>+</sup> regulatory T cells inhibit protective immunity to filarial parasites *in vivo*. *The Journal of Immunology*, 179, 4626-4634.
- Taylor, M. D., L. LeGoff, A. Harris, E. Malone, J. E. Allen & R. M. Maizels (2005) Removal of regulatory T cell activity reverses hyporesponsiveness and leads to filarial parasite clearance *in vivo*. *The Journal of Immunology*, 174, 4924-4933.
- Taylor, M. D., N. van der Werf, A. Harris, A. L. Graham, O. Bain, J. E. Allen & R. M. Maizels (2009) Early recruitment of natural CD4<sup>+</sup> Foxp3<sup>+</sup> Treg cells by infective larvae determines the outcome of filarial infection. *European Journal of Immunology*, 39, 192-206.
- Taylor, M. D., N. van der Werf & R. M. Maizels (2012) T cells in helminth infection: the regulators and the regulated. *Trends Immunol*, 33, 181-9.
- Taylor, M. J., A. Hoerauf & M. Bockarie (2010) Lymphatic filariasis and onchocerciasis. *Lancet*, 376, 1175-85.
- Townsend, M. J., P. G. Fallon, D. J. Matthews, H. E. Jolin & A. N. McKenzie (2000) T1/ST2-deficient mice demonstrate the importance of T1/ST2 in developing primary T helper cell type 2 responses. *Journal of Experimental Medicine*, 191, 1069-1076.
- Twu, O., N. de Miguel, G. Lustig, G. C. Stevens, A. A. Vashisht, J. A. Wohlschlegel & P. J. Johnson (2013) *Trichomonas vaginalis* exosomes deliver cargo to host cells and mediate host: parasite interactions. *PLoS Pathogen*, 9, e1003482.
- Ullrich, A., J. Shine, J. Chirgwin, R. Pictet, E. Tischer, W. Rutter & H. Goodman (1977). Rat insulin genes: construction of plasmids containing the coding sequences. *Science*, 196(4296), 1313-9.
- van den Biggelaar, A. H., L. C. Rodrigues, R. van Ree, J. S. van der Zee, Y. C. Hoeksma-Kruize, J. H. Souverijn, M. A. Missinou, S. Borrmann, P. G. Kremsner & M. Yazdanbakhsh (2004) Long-term treatment of intestinal helminths increases mite skin-test reactivity in Gabonese schoolchildren. *Journal of Infectious Diseases*, 189, 892-900.
- van den Biggelaar, A. H., R. van Ree, L. C. Rodrigues, B. Lell, A. M. Deelder, P. G. Kremsner & M. Yazdanbakhsh (2000) Decreased atopy in children infected with *Schistosoma haematobium*: a role for parasite-induced interleukin-10. *The Lancet*, 356, 1723-1727.

- van Gent, D., P. Sharp, K. Morgan & N. Kalsheker (2003) Serpins: structure, function and molecular evolution. *The International Journal of Biochemistry & Cell Biology*, 35, 1536-1547.
- Vandenabeele, P., L. Galluzzi, T. V. Berghe & G. Kroemer (2010) Molecular mechanisms of necroptosis: an ordered cellular explosion. *Nature reviews. Molecular Cell Biology*, 11, 700.
- Versini, M., P.-Y. Jeandel, T. Bashi, G. Bizzaro, M. Blank & Y. Shoenfeld (2015) Unraveling the hygiene hypothesis of helminthes and autoimmunity: origins, pathophysiology, and clinical applications. *BMC Medicine*, 13, 81.
- Walk, S. T., A. M. Blum, S. A. S. Ewing, J. V. Weinstock & V. B. Young (2010) Alteration of the murine gut microbiota during infection with the parasitic helminth *Heligmosomoides polygyrus*. *Inflammatory Bowel Diseases*, 16, 1841-1849.
- Wammes, L. J., F. Hamid, A. E. Wiria, H. Wibowo, E. Sartono, R. M. Maizels, H. H. Smits, T. Supali & M. Yazdanbakhsh (2012) Regulatory T cells in human lymphatic filariasis: stronger functional activity in microfilaremics. *PLoS Neglected Tropical Diseases*, 6, e1655.
- Watanabe, N., F. Bruschi & M. Korenaga (2005) IgE: a question of protective immunity in *Trichinella spiralis* infection. *Trends in Parasitology*, 21, 175-178.
- Xu, D., W. L. Chan, B. P. Leung, F.-p. Huang, R. Wheeler, D. Piedrafita, J. H. Robinson & F. Y. Liew (1998) Selective expression of a stable cell surface molecule on type 2 but not type 1 helper T cells. *Journal of Experimental Medicine*, 187, 787-794.
- Xu, Z., H. Zan, E. J. Pone, T. Mai & P. Casali (2012) Immunoglobulin class switch DNA recombination: induction, targeting and beyond. *Nature reviews. Immunology*, 12, 517.
- Yakob, L. & T. Walker (2016) Zika virus outbreak in the Americas: the need for novel mosquito control methods. *Lancet Glob Health*, 4, e148-9.
- Yan, Y., S. Liu, G. Song, Y. Xu & C. Dissous (2005) Characterization of a novel vaccine candidate and serine proteinase inhibitor from *Schistosoma japonicum* (Sj serpin). *Veterinary Parasitology*, 131, 53-60.
- Yang, Y., D. Hu, L. Wang, C. Liang, X. Hu, X. Wang, J. Chen, J. Xu & X. Yu (2009) Molecular cloning and characterization of a novel serpin gene of *Clonorchis sinensis*, highly expressed in the stage of metacercaria. *Parasitology Research*, 106, 221-225.
- Yang, Z., V. Grinchuk, J. F. Urban Jr, J. Bohl, R. Sun, L. Notari, S. Yan, T. Ramalingam, A. D. Keegan & T. A. Wynn (2013) Macrophages as IL-25/IL-33-responsive cells play an important role in the induction of type 2 immunity. *PLoS One*, 8, e59441.

- Yasuda, K., T. Muto, T. Kawagoe, M. Matsumoto, Y. Sasaki, K. Matsushita, Y. Taki, S. Futatsugi-Yumikura, H. Tsutsui & K. J. Ishii (2012) Contribution of IL-33-activated type II innate lymphoid cells to pulmonary eosinophilia in intestinal nematode-infected mice. *Proceedings of the National Academy of Sciences*, 109, 3451-3456.
- Yenbutr, P. & A. L. Scott (1995) Molecular cloning of a serine proteinase inhibitor from *Brugia malayi*. *Infection and Immunity*, 63, 1745-1753.
- Yi, D., L. Xu, R. Yan & X. Li (2010) *Haemonchus contortus*: cloning and characterization of serpin. *Experimental Parasitology*, 125, 363-370.
- Zang, X., A. K. Atmadja, P. Gray, J. E. Allen, C. A. Gray, R. A. Lawrence, M. Yazdanbakhsh & R. M. Maizels (2000) The serpin secreted by *Brugia malayi* microfilariae, Bm-SPN-2, elicits strong, but short-lived, immune responses in mice and humans. *The Journal of Immunology*, 165, 5161-5169.
- Zang, X. & R. M. Maizels (2001) Serine proteinase inhibitors from nematodes and the arms race between host and pathogen. *Trends in Biochemical Sciences*, 26, 191-197.
- Zang, X., P. Taylor, J. M. Wang, D. J. Meyer, A. L. Scott, M. D. Walkinshaw & R. M. Maizels (2002) Homologues of human macrophage migration inhibitory factor from a parasitic nematode. Gene cloning, protein activity, and crystal structure. *Journal of Biological Chemistry*, 277, 44261-44267.
- Zang, X., M. Yazdanbakhsh, H. Jiang, M. R. Kanost & R. M. Maizels (1999) A novel serpin expressed by blood-borne microfilariae of the parasitic nematode *Brugia malayi* inhibits human neutrophil serine proteinases. *Blood*, 94, 1418-1428.
- Zhu, C., A. C. Anderson & V. K. Kuchroo. 2011. TIM-3 and its regulatory role in immune responses. In *Negative Co-Receptors and Ligands*, 1-15. Springer.
- Zhu, C., A. C. Anderson, A. Schubart, H. Xiong, J. Imitola, S. J. Khoury, X. X. Zheng, T. B. Strom & V. K. Kuchroo (2005) The Tim-3 ligand galectin-9 negatively regulates T helper type 1 immunity. *Nature Immunology*, 6, 1245-1252.



# Appendices

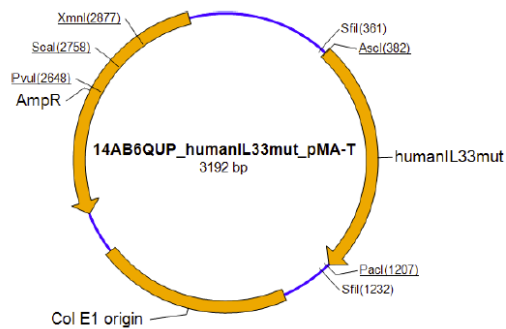
## 1. Human and murine mutant IL-33 gene synthesis

### 1.1 Human mutant IL-33

#### Plasmid DNA Description:

The synthetic gene humanIL33mut was assembled from synthetic oligonucleotides and/or PCR products. The fragment was cloned into pMA-T using SfiI and SfiI cloning sites. The plasmid DNA was purified from transformed bacteria and concentration determined by UV spectroscopy. The final construct was verified by sequencing. The sequence congruence within the used restriction sites was 100%. See the accompanying data sheets for sequences and find the original ABI trace files as well as the assembled sequences electronically on disk. 5 µg of the plasmid preparation were lyophilized for shipping.

#### Plasmid Map:



#### Quality Assurance Documentation: 14AB6QUP

Ref. No.: 1569693

**Designation:** E.coli K12 (dam+ dcm+ tonA)  
**Gene name:** humanIL33mut  
**Gene size:** 821 bp  
**Vector backbone:** pMA-T  
**Cloning sites:** SfiI / SfiI  
**Quantity:** ~5 µg Plasmid DNA  
**Note:** Please dissolve lyophilized DNA in 50 µl distilled water or 10 mM Tris-HCl (pH 8.0). We recommend sequence verification after each transformation step.  
**Date:** 23 August 2014

Carmen Billerbeck  
Quality control

GeneArt AG [www.lifetechnologies.com](http://www.lifetechnologies.com) [GeneArtSupport@lifetech.com](mailto:GeneArtSupport@lifetech.com)

ID Construct           **14AB6QUP**           **Map**  
 Customer               **EDINBURGH UNIV, Henry McSorley**  
 Name of the gene       **humanIL33mut**  
 optimized for           Non optimized

23.08.2014 15:49:43

*BssHII*  
*AscI*

CGAATTGGCGGAAGGCCGTC AAGGCCACGTGCTTGTCCAGGCGGCCAAGCCCAAGATG  
 1 -----+-----+-----+-----+-----+  
 GCTTAACCGCCTTCCGGCAGTTCCGGTGCACAGAACAGGTCCGCGCGGTTCCGGTCTAC

AAGTACAGCACCAACAAGATCAGCACCGCCAAGTGAAGAACACCGCCAGCAAGGCCCTG  
 61 -----+-----+-----+-----+-----+  
 TTCATGTCGTGGTTGTTCTAGTCGTGGCGGTTACCTTCTTGTGGCGGTCGTTCCGGGAC

TGCTTCAAGCTGGGCAAGAGCCAGCAGAAAGCCAAAGAAGTGTGCCCATGTACTTTATG  
 121 -----+-----+-----+-----+-----+  
 ACGAAGTTCGACCCGTTCTCGGTCGTCTTTCGGTTTCTTACACGGGTACATGAAATAC

*BclI*           *StuI*

AAGGCCGCTGCCGGCCTGATGATCAAGAAAGAGGCCTGCTACTTCCGGCGGAAACCACC  
 181 -----+-----+-----+-----+-----+  
 TTCCGGCGACGGCCGGACTACTAGTTCTTCTCCGGACGATGAAGGCCGCCCTTTGGTGG

*EagI*

AAGCGCCCAGCCTGAAAACCGGCCGGAAGCACAAGAGACACCTGGTGTGGCCGCCTGC  
 241 -----+-----+-----+-----+-----+  
 TTCGCCGGTGGACTTTTGGCCGGCCTTCGTGTTCTCTGTGGACCACGACCGGCGGACG

CAGCAGCAGAGCACCGTGAATGCTTCGCCCTTCGGCATCAGCGGCGTGCAGAAGTACACC  
 301 -----+-----+-----+-----+-----+  
 GTCGTCGTCTCGTGGCACCTTACGAAGCGGAAGCCGTAGTCGCCGCACGTCTTCATGTGG

AGAGCCCTGCACGACAGCAGCATCACCGGCATCTCCCCATCACCGAGTACCTGGCCAGC  
361 -----+-----+-----+-----+-----+-----+  
TCTCGGGACGTGCTGTCGTAGTGGCCGTAGAGGGGTAGTGGCTCATGGACCGGTG

*BglII*

CTGAGCACCTACAACGACCAGTCCATCACCTTCGCCCTGGAAGATGAGAGCTACGAGATC  
421 -----+-----+-----+-----+-----+-----+  
GACTCGTGGATGTTGCTGGTCAGGTAGTGAAGCGGGACCTTCTACTCTCGATGCTCTAG

*BglII*

TACGTGGAAGATCTGAAGAAGGACGAGAAGAAAGACAAGGTGCTGCTGAGCTACTACGAG  
481 -----+-----+-----+-----+-----+-----+  
ATGCACCTTCTAGACTTCTTCCTGCTCTTCTTTCTGTTCCACGACGACTCGATGATGCTC

*BstEII*

TCCCAGCACCCCAGCAACGAGTCTGGGGATGGCGTGGACGGCAAGATGCTGATGGTCACC  
541 -----+-----+-----+-----+-----+-----+  
AGGGTCGTGGGGTCGTTGCTCAGACCCCTACCGCACCTGCCGTTCTACGACTACCAGTGG

CTGAGCCCCACCAAGGATTTCTGGCTGCACGCCAACAAAGAACACAGCGTGGAACTG  
601 -----+-----+-----+-----+-----+-----+  
GACTCGGGGTGGTTCCTAAAGACCGACGTGCGGTTGTTGTTTCTTGTGTCGCACCTTGAC

*StuI*

CACAAGTGCAGAGAAGCCCCTGCCCGACCAGGCCTTCTTCGTGCTGCACAACATGCACAGC  
661 -----+-----+-----+-----+-----+-----+  
GTGTTACAGCTCTTCGGGGACGGGCTGGTCCGGAAGAAGCACGACGTGTTGTACGTGTCG

AACTGCGTGTCTTCGAGTGCAAGACCGACCCCGGCGTGTTCATCGGCGTGAAGACAAT  
721 -----+-----+-----+-----+-----+-----+  
TTGACGCACAGGAAGCTCACGTTCTGGCTGGGGCCGCACAAGTAGCCGCACCTCCTGTTA

*BclI*

CACCTGGCCCTGATCAAGGTGGACAGCAGCGAGAACCTGTGCACCGAGAACATCCTGTTC  
781 -----+-----+-----+-----+-----+-----+  
GTGGACCGGGACTAGTTCACCTGTCTGCTGCTCTTGGACACGTGGCTCTTGTAGGACAAG

*ApaI* *PacI*

AAGCTGAGCGAGACAGGGCCATTAATTAATGGAGCACAAGACTGGCCTCATGGGCCTTC  
841 -----+-----+-----+-----+-----+-----+  
TTCGACTCGCTCTGTCCCGGTAATTAATTACCTCGTGTCTGACCGGAGTACCCGGAAG

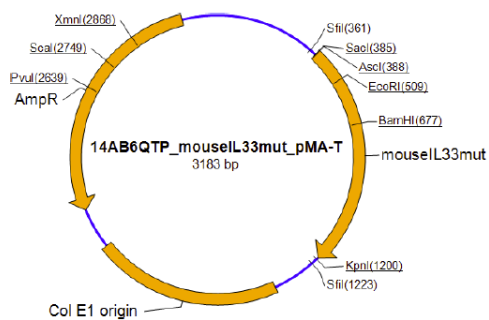
CGCTCACTGC  
901 -----+  
GCGAGTGACG

## 1.2 Murine mutant IL-33

### Plasmid DNA Description:

The synthetic gene mouseIL33mut was assembled from synthetic oligonucleotides and/or PCR products. The fragment was cloned into pMA-T using SfiI and SfiI cloning sites. The plasmid DNA was purified from transformed bacteria and concentration determined by UV spectroscopy. The final construct was verified by sequencing. The sequence congruence within the used restriction sites was 100%. See the accompanying data sheets for sequences and find the original ABI trace files as well as the assembled sequences electronically on disk. 5 µg of the plasmid preparation were lyophilized for shipping.

### Plasmid Map:



### Quality Assurance Documentation: 14AB6QTP

Ref. No.: 1569692

**Designation:** E.coli K12 (dam+ dcm+ tonA)

**Gene name:** mouseIL33mut

**Gene size:** 809 bp

**Vector backbone:** pMA-T

**Cloning sites:** SfiI / SfiI

**Quantity:** ~5 µg Plasmid DNA

**Note:** Please dissolve lyophilized DNA in 50 µl distilled water or 10 mM Tris-HCl (pH 8.0). We recommend sequence verification after each transformation step.

**Date:** 22 August 2014

**Carmen Billerbeck**

Quality control

**GeneArt AG** [www.lifetechnologies.com](http://www.lifetechnologies.com) [GeneArtSupport@lifetech.com](mailto:GeneArtSupport@lifetech.com)

ID Construct           **14AB6QTP**           **Map**  
 Customer               **EDINBURGH UNIV, Henry McSorley**  
 Name of the gene       **mouseL33mut**  
 optimized for           Non optimized

22.08.2014 16:51:02

*BssHII*

*SacI AscI*

CGAATTGGCGGAAGGCCGTCAAGGCCACGTGCTTGTCCAGAGCTCGGCGGCCAGACCC  
 1 -----+-----+-----+-----+-----+-----+  
 GCTTAACCGCCTTCCGGCAGTTCCGGTGCACAGAACAGGTCTCGAGCCGCGCGGTCTGGG

AGAATGAAGTACAGCAACAGCAAGATCAGCCCCGCCAAGTTCAGCAGCACAGCCGGCGAA  
 61 -----+-----+-----+-----+-----+-----+  
 TCTTACTTCATGTCGTTGTCGTTCTAGTCGGGGCGGTTCAAGTCGTCGTGTCGGCCGCTT

*EcoRI*

GCTCTGGTGCCCCCTGCAAGATTCGGCGGAGCCAGCAGAAAACAAAAGAAATTCGCCAC  
 121 -----+-----+-----+-----+-----+-----+  
 CGAGACCACGGGGGACGTTCTAAGCCGCCTCGGTCGTCTTTGTTTCTTAAGACGGTG

GTGTACTGCATGAGAGCCGCGCTGGCCTGACCATCCGAAAGAGACAAGCTACTTCAGA  
 181 -----+-----+-----+-----+-----+-----+  
 CACATGACGTACTCTCGGCGGCGACCGGACTGGTAGGCCTTCTCTGTTTCGATGAAGTCT

AAAGAGCCCACCAAGCGGTACAGCCTGAAGTCCGGCACCAAGCACGAGGAAAACCTCAGC  
 241 -----+-----+-----+-----+-----+-----+  
 TTTCTCGGGTGGTTCGCCATGTCGGACTTCAGGCCGTGGTTCGTGCTCCTTTGAAGTCG

*SmaI*

*BamHI*

*StuI*

GCCTACCCCGGGACAGCCGGAAGAGAAGTCTGCTGGGATCCATCCAGGCCCTTCGCCGCC  
 301 -----+-----+-----+-----+-----+-----+  
 CGGATGGGGGCCCTGTCCGCCTTCTCTTCAGACGACCCTAGGTAGGTCCGGAAGCGGCGG

TCTGTGGACACCCCTGAGCATCCAGGGCACCAGCCTGCTGACACAGTCTCCAGCCAGCCTG  
361 -----+-----+-----+-----+-----+-----+  
AGACACCTGTGGGACTCGTAGGTCCCCTGGTCCGACGACTGTGTTCAGAGGTCGGTCCGGAC

*BclI*

AGCACCTACAACGACCAGAGCGTGTCTTCGTGCTGGAAAACGGCTGCTACGTGATCAAC  
421 -----+-----+-----+-----+-----+-----+  
TCGTGGATGTTGCTGGTCTCGCACAGGAAGCACGACCTTTTGCCGACGATGCAC TAGTTG

GTGGACGACAGCGGCAAGGACCAGGAACAGGACCAGGTGCTGCTGCGGTACTACGAGAGC  
481 -----+-----+-----+-----+-----+-----+  
CACCTGCTGTCGCCGTTCCCTGGTCTTGTCTGGTCCACGACGACGCCATGATGCTCTCG

*HincII*

CCTTGTCTGCCAGCCAGTCTGGGGATGGCGTGGACGGCAAGAACTGATGGTCAACATG  
541 -----+-----+-----+-----+-----+-----+  
GGAACAGGACGGTCGGTCAGACCCCTACCGCACCTGCCGTTCTTTGACTACCAGTTGTAC

AGCCCCATCAAGGACACCGACATCTGGCTGCACGCCAACGACAAGGACTACAGCGTGGAA  
601 -----+-----+-----+-----+-----+-----+  
TCGGGGTAGTTCTCTGTGGCTGTAGACCGACGTGCCGTTGCTGTTCTGATGTGCGCACCTT

*PstI*

*StuI*

CTGCAGCGGGGGCAGTGTCCCCACCTGAGCAGGCCTTTTTTCGTGCTGCACAAGAAAAGC  
661 -----+-----+-----+-----+-----+-----+  
GACGTCGCCCCGCTGCACAGGGGTGGACTCGTCCGAAAAGCACGACGTGTTCTTTTCG

*BspMI*

AGCGACTTCGTGTCTTTGAGTGCAAGAACCCTGCCCGGCACCTACATCGGCGTGAAGGAC  
721 -----+-----+-----+-----+-----+-----+  
TCGCTGAAGCACAGGAACTCACGTTCTTGGACGGGCCGTGGATGTAGCCGCACTTCCTG

*PvuII*

AATCAGCTGGCCCTGGTGGAAAGAGAAAAGACGAGAGCTGCAACAACATCATGTTCAAGCTG  
781 -----+-----+-----+-----+-----+-----+  
TTAGTCGACCGGGACCACCTTCTCTTTCTGCTCTCGACGTTGTTGTAGTACAAGTTCGAC

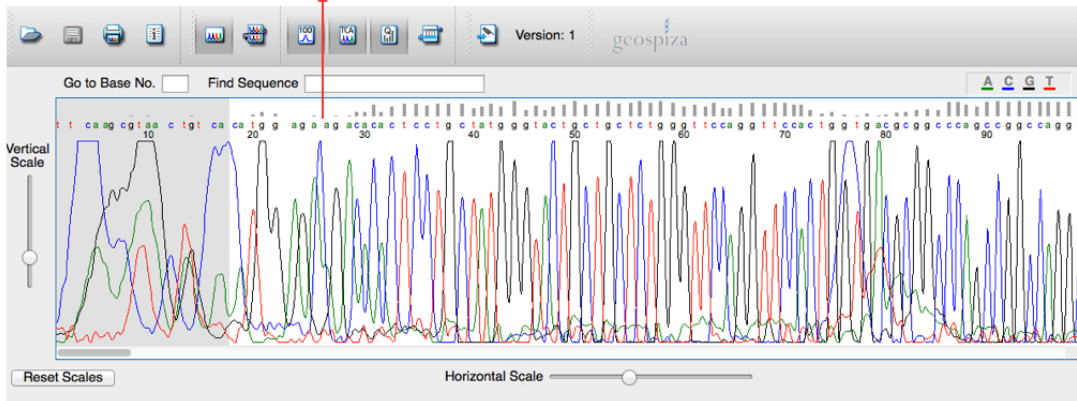
*ApaI KpnI*

AGCAAGATCGGGCCCGGTACCTGGAGCACAAGACTGGCCTCATGGGCCCTCCGCTCACTG  
841 -----+-----+-----+-----+-----+-----+  
TCGTTCTAGCCCGGCCATGGACCTCGTGTTCTGACCGGAGTACCCGGAAGGCGAGTGAC

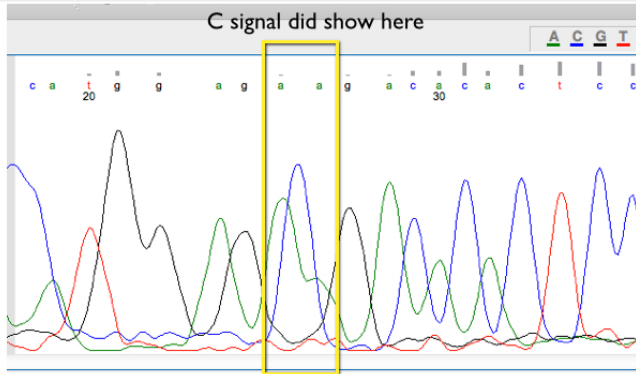
C  
901 -  
G



missed a C here



C signal did show here



mouse IL-33 mut  
Sequence ID: Icll9489 Length: 954 Number of Matches: 1

Range 1: 112 to 944 [Graphics](#)

Score	Expect	Identities	Gaps
1533 bits(830)	0.0	832/833(99%)	0/833(0%)

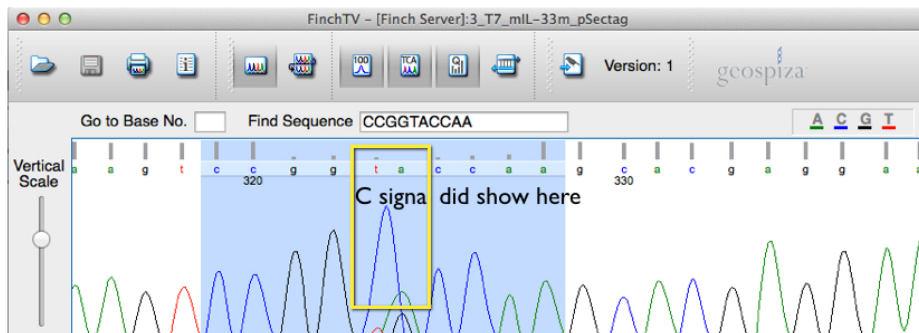
```

Query 1  AGCAAGATCAGCCCGCCAAAGTTCAGCAGCAGAGCCGCGAAGCTCTGTGTGCCDCTCG 60
Sbjct 112  AGCAAGATCAGCCCGCCAAAGTTCAGCAGCAGAGCCGCGAAGCTCTGTGTGCCDCTCG 171
Query 61  AAGATTGGCGGAGCCAGCAGAAAACAAAAGATTCTGCCAGTGTACTGCATGAGAGCC 120
Sbjct 172  AAGATTGGCGGAGCCAGCAGAAAACAAAAGATTCTGCCAGTGTACTGCATGAGAGCC 231
Query 121  GCGCTGGCTGACATCCCGAAGAGACAAAGCTACTTCAGAAAAGAGCCACCAAGAGCG 180
Sbjct 232  GCGCTGGCTGACATCCCGAAGAGACAAAGCTACTTCAGAAAAGAGCCACCAAGAGCG 291
Query 181  TACAGCTGAAGTCTGTACCAAGCAGCAGAAAATTCAGCGCTTACDCCGGGACAG 240
Sbjct 292  TACAGCTGAAGTCTGTACCAAGCAGCAGAAAATTCAGCGCTTACDCCGGGACAG 351
Query 241  CGGAAGAGAAGTCTGCGGATCCATCCAGGCTTCCGCGCTCTGTGGACACDCTGAGC 300
Sbjct 352  CGGAAGAGAAGTCTGCGGATCCATCCAGGCTTCCGCGCTCTGTGGACACDCTGAGC 411
Query 301  ATCCAGGGCCAGCCTGTGACACAGTCTCCAGCCAGCCTGAGCAGCTACAAAGACCCAG 360
Sbjct 412  ATCCAGGGCCAGCCTGTGACACAGTCTCCAGCCAGCCTGAGCAGCTACAAAGACCCAG 471
Query 361  AGCGTGTCTTCTGCTGAAAACGGCTGCTAGTGATCAAGCTGGAGACAGCGGCAAG 420
Sbjct 472  AGCGTGTCTTCTGCTGAAAACGGCTGCTAGTGATCAAGCTGGAGACAGCGGCAAG 531
Query 421  GACCAGGAACAGGACAGGTGCTGCTCGGTAAGTACAGAGAGCCCTGTGCTGCCAGCCAG 480
Sbjct 532  GACCAGGAACAGGACAGGTGCTGCTCGGTAAGTACAGAGAGCCCTGTGCTGCCAGCCAG 591
  
```

mouse IL-33 mutant colony 4 (DNA binding domain depleted)

```

Query 481  TCTGGGATGGCTGGAGGGCAAGAAACTGATGGTCAACATGAGCCCATCAAGGACACC 540
Sbjct 592  TCTGGGATGGCTGGAGGGCAAGAAACTGATGGTCAACATGAGCCCATCAAGGACACC 651
Query 541  GACATCTGGCTGCAGCCCAAGCAAGGACTACAGGTGGAATGCAGCGGGGCGACTG 600
Sbjct 652  GACATCTGGCTGCAGCCCAAGCAAGGACTACAGGTGGAATGCAGCGGGGCGACTG 711
Query 601  TCCCACCTGAGCAGGCTTTTTGCTGCTGCACAAGAAAAGCAGCGACTTCGTCTCTT 660
Sbjct 712  TCCCACCTGAGCAGGCTTTTTGCTGCTGCACAAGAAAAGCAGCGACTTCGTCTCTT 771
Query 661  GAGTCAAGAACTGCCGGCCCTACATCGCGCTGAAGGACAACTAGCTGGCCCTGGTG 720
Sbjct 772  GAGTCAAGAACTGCCGGCCCTACATCGCGCTGAAGGACAACTAGCTGGCCCTGGTG 831
Query 721  GAAGAGAAAAGCAGAGCTGCAACAACTATGTTCAAGCTGAGCAAGATCGGCCGAA 780
Sbjct 832  GAAGAGAAAAGCAGAGCTGCAACAACTATGTTCAAGCTGAGCAAGATCGGCCGAA 891
Query 781  CAAAACTCATCTCAGAAAGGATCTGAATAGCGCCGTCACCATCATCATCA 833
Sbjct 892  CAAAACTCATCTCAGAAAGGATCTGAATAGCGCCGTCACCATCATCATCA 944
  
```



### 3. Sequencing result of Mini prep product of Bm-SPN-2

```
#####
# Program: matcher
# Rundate: Thu 13 Jul 2017 14:59:08
# Commandline: matcher
# -auto
# -stdout
# -asequence emboss_matcher-I20170713-145907-0059-3741926-pg.asequence
# -bsequence emboss_matcher-I20170713-145907-0059-3741926-pg.bsequence
# -datafile EDNAFULL
# -gapopen 16
# -gapextend 4
# -alternatives 1
# -aformat3 pair
# -snucleotide1
# -snucleotide2
# Align_format: pair
# Report_file: stdout
#####

#-----
#
# Aligned_sequences: 2
# 1: AF009825_without_signal
# 2: sequencing_BmSPN2_A_1486bp
# Matrix: EDNAFULL
# Gap_penalty: 16
# Extend_penalty: 4
#
# Length: 1224
# Identity: 1224/1224 (100.0%)
# Similarity: 1224/1224 (100.0%)
# Gaps: 0/1224 ( 0.0%)
# Score: 6120
#
#
#-----

AF009825_with 1 AACAGTACTTTAAACCATTGTTCTGAAAACAATGATGATCAAACAAGCT 50
|
sequencing_Bm 150 AACAGTACTTTAAACCATTGTTCTGAAAACAATGATGATCAAACAAGCT 199
|

AF009825_with 51 ACTGATAACTAAGGCGCAAATGAATTCGCATTGGAACATTGCGCTATT 100
|
sequencing_Bm 200 ACTGATAACTAAGGCGCAAATGAATTCGCATTGGAACATTGCGCTATT 249
|

AF009825_with 101 CTTGCAAGCTGATGAAACCTCGCTATTATCGCCATTGCAATCGCTTCC 150
|
sequencing_Bm 250 CTTGCAAGCTGATGAAACCTCGCTATTATCGCCATTGCAATCGCTTCC 299
|

AF009825_with 151 GTAATGTCATTATTATATGAAGGAGCCAGAGGTGAACTGAGCGTGAGAT 200
|
sequencing_Bm 300 GTAATGTCATTATTATATGAAGGAGCCAGAGGTGAACTGAGCGTGAGAT 349
|

AF009825_with 201 GGGGAGGGTGCTTTCAGCAGATCAACCAAAAAATGCATTGGAGCTTACA 250
|
sequencing_Bm 350 GGGGAGGGTGCTTTCAGCAGATCAACCAAAAAATGCATTGGAGCTTACA 399
|

AF009825_with 251 TAGAGTGCCTATCAAAAATATTCACAAGCAATCAAAGCGAAATGATTAT 300
|
sequencing_Bm 400 TAGAGTGCCTATCAAAAATATTCACAAGCAATCAAAGCGAAATGATTAT 449
|
```

AF009825_with	301	TCTTTGTACTATTTAACCAAATTTTTGTGCAACAAAATCCTTTGAAGTC	350
sequencing_Bm	450		499
AF009825_with	351	TGATTTTAAAGATATTACTCGTCGACGATATCCTTATGAGTTGACACAAA	400
sequencing_Bm	500		549
AF009825_with	401	TCAATTTTCGCTTCACCTCTGCAAGTGAAGAGTATAAGAGAAAATTTTATT	450
sequencing_Bm	550		599
AF009825_with	451	AAATGGATAAAGAAAAGTATGAATTATGGAGCCCGTAATATCGCTAGCAT	500
sequencing_Bm	600		649
AF009825_with	501	CACTTCCACTCAGTCATTAACCTTATTTAATGGAATACATTTCACTGATG	550
sequencing_Bm	650		699
AF009825_with	551	ATTGGATGTACGAATTTCTTCCGCTCAATCACATATTACCGTTCTATTCA	600
sequencing_Bm	700		749
AF009825_with	601	CCACGGCTACGTGTAAGTATGATGCAATGATGAAAGAACGGCCAAATT	650
sequencing_Bm	750		799
AF009825_with	651	TCCTTACTATGAAAACCAACACATGCAAGCGGTGTCGCTACCGTTCAAAG	700
sequencing_Bm	800		849
AF009825_with	701	ATTCCGAAATGCAAAATGTTAATTATTTGCCCCAAAAAACCTTTGATCTA	750
sequencing_Bm	850		899
AF009825_with	751	GCAAAGTTTGAAGATAAACTTACGGGAGAGAACTATTCAGTTATATTAG	800
sequencing_Bm	900		949
AF009825_with	801	TGCACTTGACTCATCTCACGAAATTACCGTTACAATTCAAAAATTTAAGT	850
sequencing_Bm	950		999
AF009825_with	851	ACGAAAATCAAATATGTTTGTAAATGGATTGAAGAGGATGGGAGTGCAA	900
sequencing_Bm	1000		1049
AF009825_with	901	TCAATGTTCCACGAATCGAATGATTTTCCGGCATTTTTGAGCAGCGGTT	950
sequencing_Bm	1050		1099
AF009825_with	951	ATTTACAATGGATGATATCAGAAATCATGCTTATATCAAAATTTGATGAGA	1000
sequencing_Bm	1100		1149
AF009825_with	1001	AAGGAATCAATAACGAAAATTCAGTATGCCAGTAAGAAATGATATGGTA	1050
sequencing_Bm	1150		1199

```

AF009825_with 1051 ATGGATAAAGGAGAAGCATTTCGTGCTAATCATCCCTTCCTTTATGCAAT 1100
                |||
sequencing_Bm 1200 ATGGATAAAGGAGAAGCATTTCGTGCTAATCATCCCTTCCTTTATGCAAT 1249
                |||
AF009825_with 1101 CATTGATAACCACGGGACTGTACTATGGATTGGTCGTTTCACCGGAAAAA 1150
                |||
sequencing_Bm 1250 CATTGATAACCACGGGACTGTACTATGGATTGGTCGTTTCACCGGAAAAA 1299
                |||
AF009825_with 1151 ACAGAGAAACAATTGTCGAAAACTCGGATGACTCTATGCAATGTGAGGAA 1200
                |||
sequencing_Bm 1300 ACAGAGAAACAATTGTCGAAAACTCGGATGACTCTATGCAATGTGAGGAA 1349
                |||
AF009825_with 1201 ACACCGAAAAAAGACAAAGGTTA 1224
                |||
sequencing_Bm 1350 ACACCGAAAAAAGACAAAGGTTA 1373
                |||

```

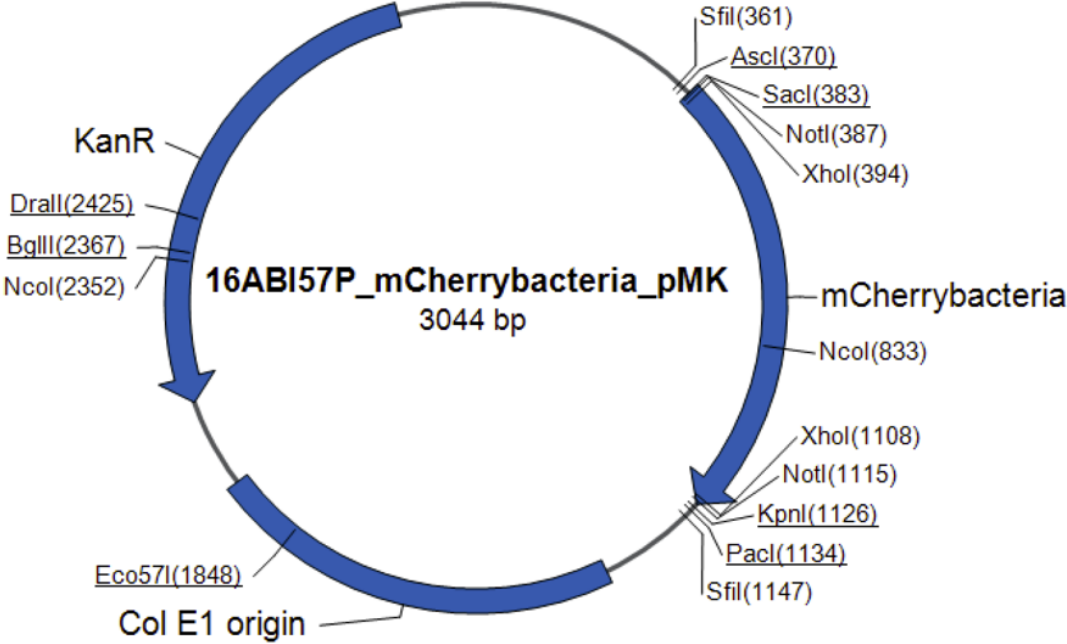
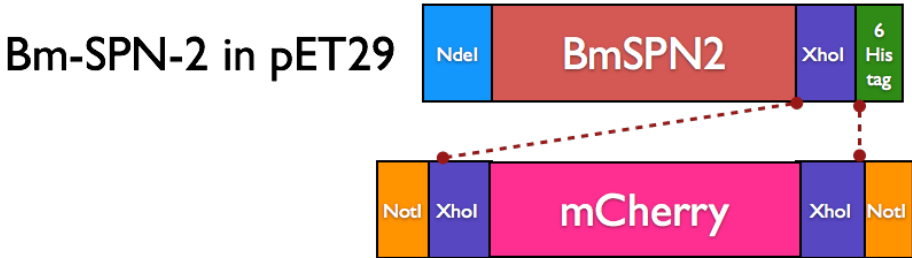
```

#-----
#-----

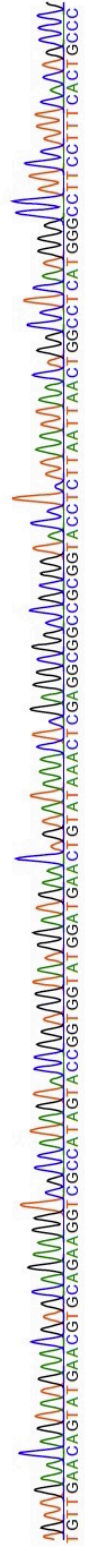
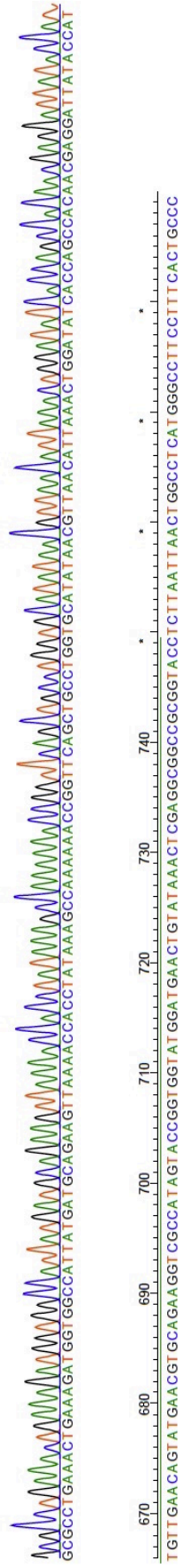
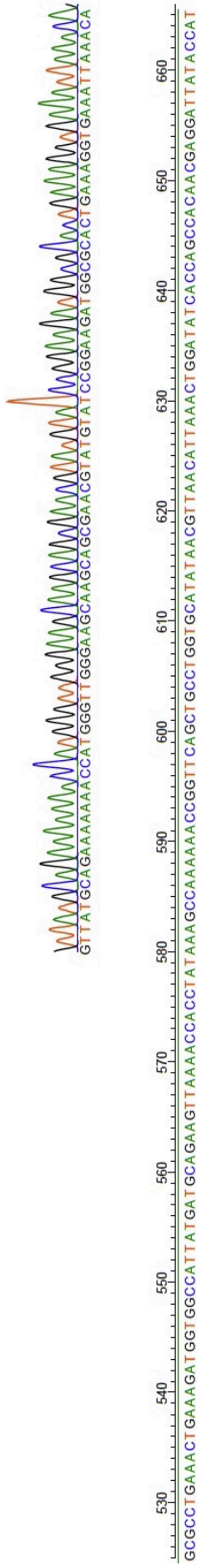
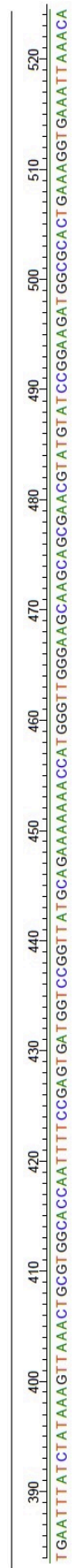
```

# 4.1 Gene synthesis for mCherry

T7 promotor, NdeI [CATATG] sequence, Signal peptide deleted Bm-SPN-2 sequence, XhoI [CTCGAG] sequence, 6His tag, Stop







## 4.2 Gene synthesis for Bm-SPN-2-mCherry

### Fusion sequence (BmSPN2 signal peptide removed and codon optimised)

**NdeI [CATATG] sequence, BmSPN2, NotI [GCGGCCGC] sequence, mCherry sequence, XhoI [CTCGAG] sequence**

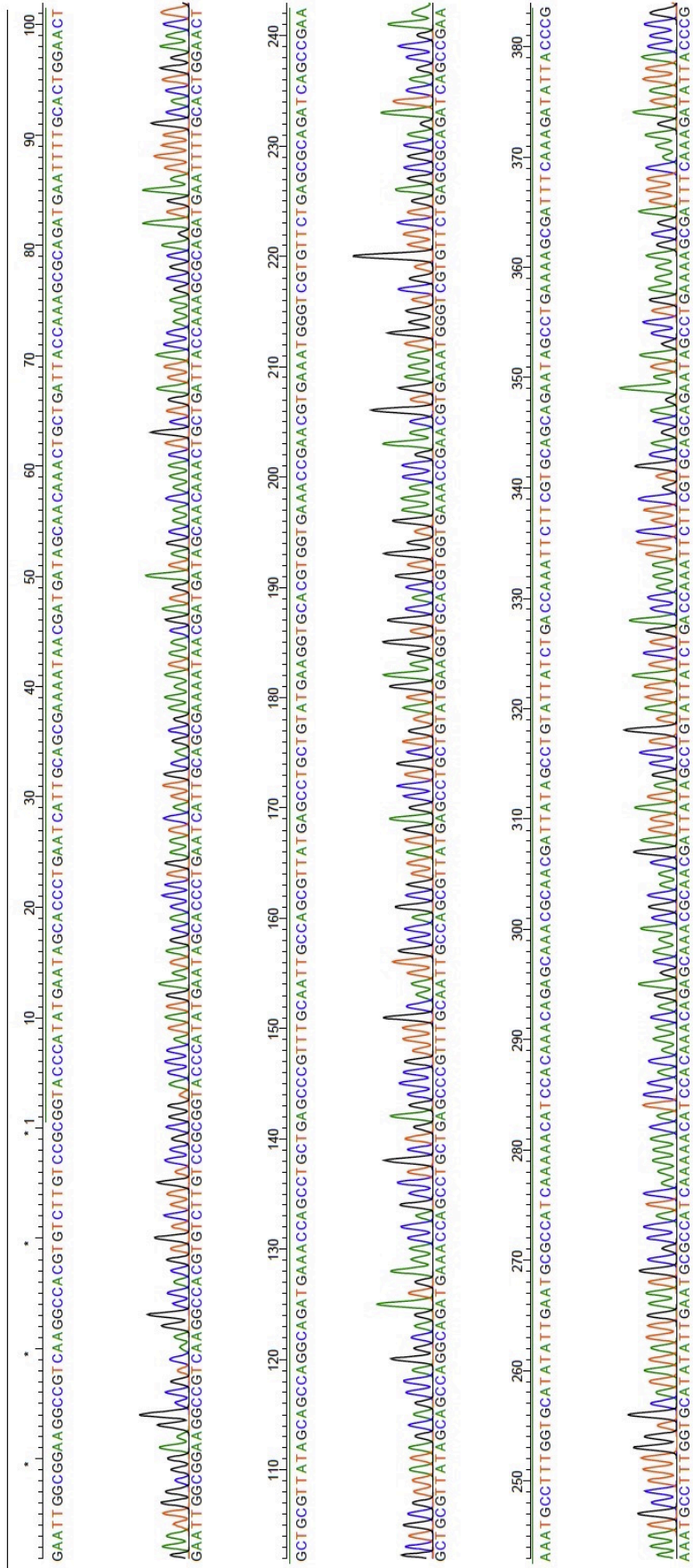
```
CATATGAACAGTACTTTAAACCATTGTTCTGAAAAAATGATGATTCAAACAAGCTACTGATAACTAAGGCGCAAA
TGAATTCGCATTGGAACTATTGCGCTATTCTTCGCAAGCTGATGAAACCTCGCTATTATCGCCATTTGCAATCGC
TTCCGTAATGTCATTATTATATGAAGGAGCCAGAGGTGAAACTGAGCGTGAGATGGGGAGGGTGCTTTTCAGCAG
ATCAACCAAAAAATGCATTTGGAGCTTACATAGAGTGCCTATCAAAAATATTACAAGCAATCAAAGCGAAATG
ATTATTCTTTGACTATTTAACCAATTTTTGTGCAACAAAATCTTTGAAGTCTGATTTTAAAGATATTACTCGTCG
ACGATATCCTTATGAGTTGACACAAAATCAATTCGCTTCACTCTGCAAGTGAAGAGTATAAGAGAAAATTTTATT
AAATGGATAAAGAAAAGTATGAATTATGGAGCCCGTAATATCTGCTAGCATCACTCCACTCATTAAACTTAT
TTAATGGAATACATTTCACTGATGATTGGATGTACGAATTTCTTCCGCTCAATCACATATTACCGTTCTATTCACCA
CGGCTACGTGTAAGTATGATGCCAATGATGGAAAGAACGGCCAAATTTCTTACTATGAAAACCAACACATGCAA
GCGGTGTCGCTACCGTTCAAAGATTCCGAAATGCAAATGTTAATTTTTGCCAAAAAACCTTTGATCTAGCAA
AGTTTGAAGATAAACTACGGGAGAGGAACTATTCAGTTATATTAGTGCCTTGACTCATCTCACGAAATTACCGT
TACAATCCAAAATTAAGTACGAAAATCAAATATGTTTGTAAATGGATTGAAGAGGATGGGAGTGAATCAATG
TTCCACGAATCGAATGATTTTTCCGGCATTTCGAGCAGCGTTATTTACAATGGATGATATCAGAAATCATGCTT
ATATCAAAATGATGAGAAAAGGAATCAATAACGAAAATCAAGTATGCCAGTAAGAAAATGATATGGTAATGGATA
AAGGAGAAGCATTTCGTGCTAATCATCCCTTCCTTATGCAATCATTGATAACCACGGGACTGTACTATGGATTGG
TCGTTTACCAGGAAAAAACAGAGAAAACAATTCGAAAACCTGGATGACTCTATGCAATGTGAGGAAACACCGA
AAAAAAGACAAAGGTTAGGCGGCCGCATGGTTTCAAAGGTTGAAGAAGATAATATGGCTATTATTAAGAATTTA
TGAGATTTAAAGTTCATATGGAAGGTTCAAGTTAATGGTTCATGAATTTGAAATGAAGGTGAAGGTGAAGGTAGAC
CATATGAAGGTAAGTCAAACTGCTAAATGAAAGTTACTAAAGGTGGTCCATTACCATTGCTTGGGATATTTGTC
ACCACAATTTATGTATGGTTCAAAGCTTATGTTAAACATCCAGCTGATATCCAGATTATTTAAAATTGTCATTTT
CAGAAGGTTTTAAATGGGAAAGAGTTATGAATTTGAAGATGGTGGTGTGTTACTGTTACTCAAGATTCATCATT
ACAAGATGGTGAATTTATTTATAAAGTTAAATGAGAGGTTACTAATTTCCATCAGATGGTCCAGTTATGCAAAAA
AAAATATGGGTTGGGAAGCTTCATCAGAAAGAATGATCCAGAAGATGGTGTCTTTAAAAGGTGAAATTAACAA
AGATTGAAATTAAGATGGTGGTCAATATGATGCTGAAGTTAAAACACTTATAAAGCTAAAAAACAGTTCAAT
TACCAGGTGCTTATAATGTTAATTAATTAATTTGGATATTACTTCACATAATGAAGATTATACTATTGTTGAACAATATG
AAAGAGCTGAAGGTAGACATTCAACTGGTGGTATGGATGAATTATATAAACTCGAG
```

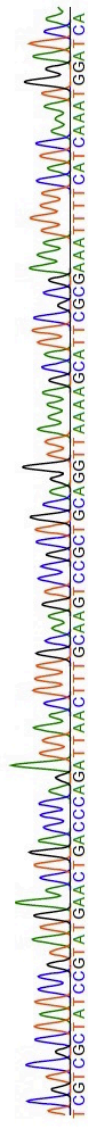
### Fusion protein (+3 frame translated)

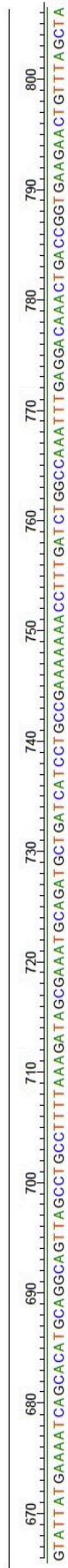
**NdeI [CATATG] sequence, SPN2, NotI sequence, mCherry sequence, XhoI [CTCGAG] sequence**

```
HMNSTLNHCSENNDSDNKLITKAQMNFALELLRYSSOADETSLSPFAIASVMSLLYEGARGETEREMGRV
LSADQPKNAFGAYIECAIKNIHKQSKRNDYSLYYLTKFFVQQNSLKSDFKDIRRRYPYELTQINFASPLQVKS
REIFIKWIKSMNYGARNIASITSTQSLNLFNGIHFDDWMEFLPLNHILPFYSPRLRVTDMPMmertakfpy
YENQHMQAVSLPFKDSEMQLIILPKKTFDLAKFEDKLTGEELFSYISALDSSHEITVTPKFYENQICLLNGL
KRMGVQSMFHESNDFSGIFEQRLFTMDDIRNHAYIKIDEKINNENSSMPVRNDMVMMDKGEAFRANHPFL
YAIIDNHGTVLWIGRFTGKNRETIVENSDDSMQCEETPKKRQRLGGRMVSKGEEDNMAIIKEFMRFKVHME
GSVNGHEFEIEGEGEGRPYEGTQTAKLKVTKGGPLPFAWDILSPQFMYGSKAYVKHPADIPDYLKLSFPEGF
KWERMVNFEDGGVVTVDSSLDGFEFYKVKLRGTNFPDGPVMQKKTMGWEASSERMYPEDGALKGE
IKQRLKLDGGHYDAEVKTTYKAKKPVLPGAYNVNIKLDITSHNEDYIVEQYERAEGRHSTGGMDELYKL
```

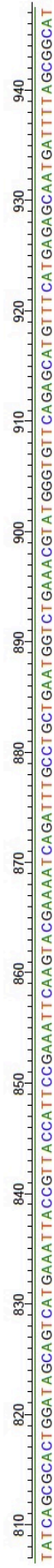
E







AAGAACTGTTTAGCTA

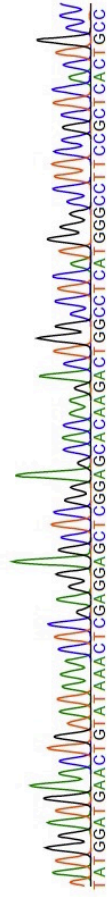
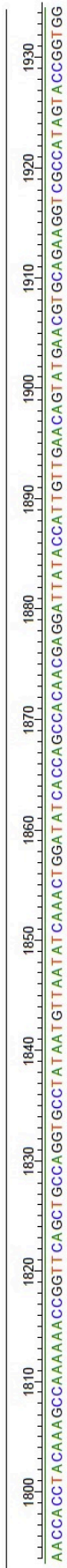


TATCAGCGCACTGGATAGCAGTCATGAAATACCGTTACCATCCGAAATCAAAGTACGAAAAACAGATGGCTGCTGAAATGGTCTGAAAACGATGGGTCTCAGAGCATGTTTCATGAGAGCAATGATTTTAGCGGCAT











TTGATATTAACATTATAGGCACCTGGCAGCTGAACCGGTTTTTTGGCTTT  
GTAGGTGGTTTTAACTTCTGCATCATAATGACCGCCATCTTTCAGCTTCA  
GGCGCTGTTTAATTTACCTTTTCAGTGCGCCATCTTCCGGATACATACG  
TTCGCTGCTTGCTTCCCAACCCATTGTTTTTTTTCTGCATAACCGGACCAT  
CACTCGGAAAATTCGTGCCACGCAGTTTAACTTTATAGATAAATTCACCA  
TCCTGCAGGCTGCTATCCTGGGTAAGTGTAAACAACACCACCATCTTCGA  
AATTCATCACGCGTTCCCATTTAAAACCTTCCGGAAGCTCAGTTTCAGA  
TAATCCGGGATATCTGCCGGATGTTTAAACATAGGCTTTGCTACCATACAT  
AAACTGCGGACTCAGAATATCCCATGCAAACGGCAGCGGACCACCTTT  
GGTAACTTTCAGTTTTGCGGTCTGGGTGCCTTCATAAGGACGACCTTCG  
CCTTCACCTTCAATTTCAAATTCGTGGCCATTAACGCTACCTTCCATGTG  
AACTTTGAAGCGCATGAATTCTTTGATGATGGCCATATTATCCTCTTCGC  
CTTTGCTAACCATGCGGCCGCCTAACGCTGACGTTTTTTTCGGGGTTTC  
TTCACACTGCATGCTATCGTCTGAATTTTCCACAATGGTTTCACGATTTT  
TGCCGGTAAAACGACCAATCCACAGAACGGTGCCATGATTATCAATGAT  
GGCATAACAGAAACGGATGATTTGCACGAAAGGCTTCACCTTTATCCATA  
ACCATATCATTACGAACCGGCATGCTGCTATTTCTCGT

T7t F RC

ACGAGAAATAGCAGCATGCCGGTTCGTAATGATATGGTTATGGATAAAG  
GTGAAGCCTTTTCGTGCAAATCATCCGTTTCTGTATGCCATCATTGATAAT  
CATGGCACCGTTCTGTGGATTGGTCGTTTTACCGGCAAAAATCGTGAAA  
CCATTGTGGAAAATTCAGACGATAGCATGCAGTGTGAAGAAACCCCGAA  
AAAACGTCAGCGTTTAGGCGGCCGCATGGTTAGCAAAGGCGAAGAGGA  
TAATATGGCCATCATCAAAGAATTCATGCGCTTCAAAGTTCACATGGAAG  
GTAGCGTTAATGGCCACGAATTTGAAATTGAAGGTGAAGGCGAAGGTC  
GTCCTTATGAAGGCACCCAGACCGCAAAACTGAAAGTTACCAAAGGTG  
GTCCGCTGCCGTTTGCATGGGATATTCTGAGTCCGCAGTTTATGTATGG  
TAGCAAAGCCTATGTTAAACATCCGGCAGATATCCCGGATTATCTGAAA  
CTGAGCTTTCCGGAAGGTTTTAAATGGGAACGCGTGATGAATTTGAAG  
ATGGTGGTGTGTTACAGTTACCCAGGATAGCAGCCTGCAGGATGGTG  
AATTTATCTATAAAGTTAAACTGCGTGGCACGAATTTTCCGAGTGATGGT  
CCGTTATGCAGAAAAAACAATGGGTTGGGAAGCAAGCAGCGAACGT  
ATGTATCCGGAAGATGGCGCACTGAAAGGTGAAATTAACAGCGCCTG  
AAGCTGAAAGATGGCGGTTCATTATGATGCAGAAGTTAAAACACCTACA  
AAGCCAAAAACCGGTTTCAGCTGCCAGGTGCCTATAATGTTAATATCAA  
ACTGGATATCACCAGCCACAACGAGGATTATACCATTGTTGAACAGTAT  
GAACGTGCAGAAGGTGCCATAGTACCGGTGGTATGGATGAACTGTAT  
AAA**CTCGAG**CACCACCACCACCACCTGAGATCCGGCTGCTAACAAA  
GC

## Sequenced T7 miniprep F VS designed Bm-SPN-2-mCherry

EMBOSS_001	1	CATATGAATAGCACCCCTGAATCATTTGCAGCGAAAAATAACGATGATAGCAA	50
EMBOSS_001	1	CATATGAATAGCACCCCTGAATCATTTGCAGCGAAAAATAACGATGATAGCAA	50
EMBOSS_001	51	CAAACCTGCTGATTACCAAAGCGCAGATGAATTTTGCCTGGAACCTGCTGC	100
EMBOSS_001	51	CAAACCTGCTGATTACCAAAGCGCAGATGAATTTTGCCTGGAACCTGCTGC	100
EMBOSS_001	101	GTTATAGCAGCCAGGCAGATGAAACCAGCCTGCTGAGCCCGTTTGC AATT	150
EMBOSS_001	101	GTTATAGCAGCCAGGCAGATGAAACCAGCCTGCTGAGCCCGTTTGC AATT	150
EMBOSS_001	151	GCCAGCGTTATGAGCCTGCTGTATGAAGGTGCACGTGGTGA AACCGAACG	200
EMBOSS_001	151	GCCAGCGTTATGAGCCTGCTGTATGAAGGTGCACGTGGTGA AACCGAACG	200
EMBOSS_001	201	TGAAATGGGTCGTGTTCTGAGCGCAGATCAGCCGAAAAATGCCTTTGGTG	250
EMBOSS_001	201	TGAAATGGGTCGTGTTCTGAGCGCAGATCAGCCGAAAAATGCCTTTGGTG	250
EMBOSS_001	251	CATATATTGAATGCGCCATCAAAAACATCCACAAAACAGAGCAAACGCAAC	300
EMBOSS_001	251	CATATATTGAATGCGCCATCAAAAACATCCACAAAACAGAGCAAACGCAAC	300
EMBOSS_001	301	GATTATAGCCTGTATTATCTGACCAAATTCCTCGTGCAGCAGAAATAGCCT	350
EMBOSS_001	301	GATTATAGCCTGTATTATCTGACCAAATTCCTCGTGCAGCAGAAATAGCCT	350
EMBOSS_001	351	GAAAAGCGATTTCAAAGATATTACCCGTCGTCGCTATCCGTATGAACTGA	400
EMBOSS_001	351	GAAAAGCGATTTCAAAGATATTACCCGTCGTCGCTATCCGTATGAACTGA	400
EMBOSS_001	401	CCCAGATTAACCTTTGCAAGTCCGCTGCAGGTTAAAAGCATTCGCGAAATT	450
EMBOSS_001	401	CCCAGATTAACCTTTGCAAGTCCGCTGCAGGTTAAAAGCATTCGCGAAATT	450
EMBOSS_001	451	TTCATCAAATGGATCAAAAAAGCATGAACTATGGCGCACGTAACATTGC	500
EMBOSS_001	451	TTCATCAAATGGATCAAAAAAGCATGAACTATGGCGCACGTAACATTGC	500
EMBOSS_001	501	AAGCATTACCAGCACACAGAGCCTGAACCTGTTTAAATGGTATTCACTTTA	550
EMBOSS_001	501	AAGCATTACCAGCACACAGAGCCTGAACCTGTTTAAATGGTATTCACTTTA	550
EMBOSS_001	551	CCGATGACTGGATGTATGAATTTCTGCCGCTGAATCATATCCTGCCGTTT	600
EMBOSS_001	551	CCGATGACTGGATGTATGAATTTCTGCCGCTGAATCATATCCTGCCGTTT	600
EMBOSS_001	601	TATAGTCCGCGTCTGCGTGTACCGATATGCCGATGATGGAACGTACCGC	650
EMBOSS_001	601	TATAGTCCGCGTCTGCGTGTACCGATATGCCGATGATGGAACGTACCGC	650
EMBOSS_001	651	AAAAATTCGCTATTATGAAAATCAGCACATGCAGGCAGTTAGCCTGCCTT	700
EMBOSS_001	651	AAAAATTCGCTATTATGAAAATCAGCACATGCAGGCAGTTAGCCTGCCTT	700
EMBOSS_001	701	TTAAAGATAGCGAAATGCAGATGCTGATCATCCTGCCGAAAAAACCTTT	750
EMBOSS_001	701	TTAAAGATAGCGAAATGCAGATGCTGATCATCCTGCCGAAAAAACCTTT	750
EMBOSS_001	751	GATCTGGCCAAATTTGAGGACAAACTGACCGGTGAAGAAGTGTATTAGCTA	800
EMBOSS_001	751	GATCTGGCCAAATTTGAGGACAAACTGACCGGTGAAGAAGTGTATTAGCTA	800
EMBOSS_001	801	TATCAGCGCACTGGATAGCAGTCATGAAATACCGGTACCATTCCGAAAT	850
EMBOSS_001	801	TATCAGCGCACTGGATAGCAGTCATGAAATACCGGTACCATTCCGAAAT	850
EMBOSS_001	851	TC-AGTACGAAAATCAGATTTGCCTGCTGAATGGTCTGAAACGTCATGGG	899
EMBOSS_001	851	TCAAGTACGAAAATCAGATTTGCCTGCTGAATGGTCTGAAACGTCATGGG	899
EMBOSS_001	900	TG-TCAGAGCATGTTTCATGAAAGCAATGATTTTAGCCGCATTTTGA-	947
EMBOSS_001	900	TGTTACAGAGCATGTTTCATGAGAGCAATGATTTTAGCCGCATTTTGAAC	949

## sequenced T7t miniprep F VS mCherry BmSPN2

```

# Length: 930
# Identity: 930/930 (100.0%)
# Similarity: 930/930 (100.0%)
# Gaps: 0/930 ( 0.0%)
# Score: 4650.0
#
#-----
EMBOSS_001      1 AATAGCAGCATGCCGGTTCGTAATGATATGGTTATGGATAAAGGTGAAGC   50
|||
EMBOSS_001      1 AATAGCAGCATGCCGGTTCGTAATGATATGGTTATGGATAAAGGTGAAGC   50
|||
EMBOSS_001     51 CTTTCGTGCAAAATCATCCGTTTCTGTATGCCATCATGATAATCATGGCA  100
|||
EMBOSS_001     51 CTTTCGTGCAAAATCATCCGTTTCTGTATGCCATCATGATAATCATGGCA  100
|||
EMBOSS_001    101 CCGTTCGTGGATTGGTCGTTTACCGGCCAAAATCGTGAACCATTGTG    150
|||
EMBOSS_001    101 CCGTTCGTGGATTGGTCGTTTACCGGCCAAAATCGTGAACCATTGTG    150
|||
EMBOSS_001    151 GAAAATTCAGACGATAGCATGCAGTGTGAAGAAACCCGAAAAACGTCA  200
|||
EMBOSS_001    151 GAAAATTCAGACGATAGCATGCAGTGTGAAGAAACCCGAAAAACGTCA  200
|||
EMBOSS_001    201 GCGTTTAGCGGCCGCATGGTTAGCAAAGGCGAAGAGGATAATATGGCCA  250
|||
EMBOSS_001    201 GCGTTTAGCGGCCGCATGGTTAGCAAAGGCGAAGAGGATAATATGGCCA  250
|||
EMBOSS_001    251 TCATCAAAGAAATTCATGCGCTTCAAAGTTCACATGGAAGGTAGCGTAA  300
|||
EMBOSS_001    251 TCATCAAAGAAATTCATGCGCTTCAAAGTTCACATGGAAGGTAGCGTAA  300
|||
EMBOSS_001    301 GGCCACGAATTTGAAATGAAAGGTGAAGGCGAAGGTCGTCCTTATGAAG  350
|||
EMBOSS_001    301 GGCCACGAATTTGAAATGAAAGGTGAAGGCGAAGGTCGTCCTTATGAAG  350
|||
EMBOSS_001    351 CACCCAGACCGCAAACGAAAGTTACCAAAGGTGGTCCGCTGCCGTTG   400
|||
EMBOSS_001    351 CACCCAGACCGCAAACGAAAGTTACCAAAGGTGGTCCGCTGCCGTTG   400
|||
EMBOSS_001    401 CATGGGATATCTGAGTCCGCAGTTTATGTATGGTAGCAAAGCCTATGTT  450
|||
EMBOSS_001    401 CATGGGATATCTGAGTCCGCAGTTTATGTATGGTAGCAAAGCCTATGTT  450
|||
EMBOSS_001    451 AAACATCCGGCAGATATCCCGATTATCTGAAACTGAGCTTCCGGAAGG   500
|||
EMBOSS_001    451 AAACATCCGGCAGATATCCCGATTATCTGAAACTGAGCTTCCGGAAGG   500
|||
EMBOSS_001    501 TTTTAAATGGGAACCGGTGATGAATTTGAAAGTGGTGGTGTGTACAG   550
|||
EMBOSS_001    501 TTTTAAATGGGAACCGGTGATGAATTTGAAAGTGGTGGTGTGTACAG   550
|||
EMBOSS_001    551 TTACCCAGGATAGCAGCCTGCAGGATGGTGAATTTATCTATAAAGTAAA  600
|||
EMBOSS_001    551 TTACCCAGGATAGCAGCCTGCAGGATGGTGAATTTATCTATAAAGTAAA  600
|||
EMBOSS_001    601 CTGCGTGGCAGCAATTTCCGAGTGTGGTCCGGTTATGCAGAAAAAAC  650
|||
EMBOSS_001    601 CTGCGTGGCAGCAATTTCCGAGTGTGGTCCGGTTATGCAGAAAAAAC  650
|||
EMBOSS_001    651 AATGGGTGGGAAGCAAGCAGCGAACGTATGTATCCGGAAGATGGCGCAC  700
|||
EMBOSS_001    651 AATGGGTGGGAAGCAAGCAGCGAACGTATGTATCCGGAAGATGGCGCAC  700
|||
EMBOSS_001    701 TGAAGGTGAAATTAACAGCCCTGAAAGCTGAAAGATGGCGGTCATTAT  750
|||
EMBOSS_001    701 TGAAGGTGAAATTAACAGCCCTGAAAGCTGAAAGATGGCGGTCATTAT  750
|||
EMBOSS_001    751 GATGCAGAAGTTAAAACACCTACAAAGCCAAAAAACCGGTCAGCTGCC  800
|||
EMBOSS_001    751 GATGCAGAAGTTAAAACACCTACAAAGCCAAAAAACCGGTCAGCTGCC  800
|||
EMBOSS_001    801 AGGTGCCATATAATGTTAATATCAAACTGGATATCACCAGCCACAACGAG  850
|||
EMBOSS_001    801 AGGTGCCATATAATGTTAATATCAAACTGGATATCACCAGCCACAACGAG  850
|||
EMBOSS_001    851 APTATACCATGTTGAACAGTATGAACGTGCAGAAGGTCGCCATAGTACC  900
|||
EMBOSS_001    851 APTATACCATGTTGAACAGTATGAACGTGCAGAAGGTCGCCATAGTACC  900
|||
EMBOSS_001    901 GGTGGTATGGATGAACTGTATAAACTCGAG   930
|||
EMBOSS_001    901 GGTGGTATGGATGAACTGTATAAACTCGAG   930

```





## Sequenced mCherry and gene synthesized mCherry

```

π
# Length: 708
# Identity: 708/708 (100.0%)
# Similarity: 708/708 (100.0%)
# Gaps: 0/708 ( 0.0%)
# Score: 3540.0
#
#
#=====
EMBOSS_001      1  ATGGTTAGCAAAGGCCGAAGAGGATAATATGGCCATCATCAAAGAATTCAT      50
   |||
EMBOSS_001      1  ATGGTTAGCAAAGGCCGAAGAGGATAATATGGCCATCATCAAAGAATTCAT      50
   |||
EMBOSS_001     51  GCGCTTCAAAGTTCACATGGAAGGTAGCGTTAATGGCCACGAATTTGAAA     100
   |||
EMBOSS_001     51  GCGCTTCAAAGTTCACATGGAAGGTAGCGTTAATGGCCACGAATTTGAAA     100
   |||
EMBOSS_001    101  TTGAAGGTGAAGGCGAAGGTTCGTCCTTATGAAGGCACCCAGACCGCAAAA    150
   |||
EMBOSS_001    101  TTGAAGGTGAAGGCGAAGGTTCGTCCTTATGAAGGCACCCAGACCGCAAAA    150
   |||
EMBOSS_001    151  CTGAAAGTTACCAAAGGTGGTCCGCTGCCGTTTGCATGGGATATTCTGAG     200
   |||
EMBOSS_001    151  CTGAAAGTTACCAAAGGTGGTCCGCTGCCGTTTGCATGGGATATTCTGAG     200
   |||
EMBOSS_001    201  TCCGCAGTTTATGTATGGTAGCAAAGCCTATGTTAAACATCCGGCAGATA     250
   |||
EMBOSS_001    201  TCCGCAGTTTATGTATGGTAGCAAAGCCTATGTTAAACATCCGGCAGATA     250
   |||
EMBOSS_001    251  TCCCGGATTATCTGAAACTGAGCTTCCGGAAGGTTTAAATGGGAACGC      300
   |||
EMBOSS_001    251  TCCCGGATTATCTGAAACTGAGCTTCCGGAAGGTTTAAATGGGAACGC      300
   |||
EMBOSS_001    301  GTGATGAATTTCGAAGATGGTGGTGTGTTACAGTTACCCAGGATAGCAG     350
   |||
EMBOSS_001    301  GTGATGAATTTCGAAGATGGTGGTGTGTTACAGTTACCCAGGATAGCAG     350
   |||
EMBOSS_001    351  CCTGCAGGATGGTGAATTTATCTATAAAGTTAAACTGCGTGGCAGCAATT     400
   |||
EMBOSS_001    351  CCTGCAGGATGGTGAATTTATCTATAAAGTTAAACTGCGTGGCAGCAATT     400
   |||
EMBOSS_001    401  TTCCGAGTGATGGTCCGGTTATGCAGAAAAAACAATGGGTTGGGAAGCA     450
   |||
EMBOSS_001    401  TTCCGAGTGATGGTCCGGTTATGCAGAAAAAACAATGGGTTGGGAAGCA     450
   |||
EMBOSS_001    451  AGCAGCGAACGTATGTATCCGGAAGATGGCGCACTGAAAGGTGAAATTAA     500
   |||
EMBOSS_001    451  AGCAGCGAACGTATGTATCCGGAAGATGGCGCACTGAAAGGTGAAATTAA     500
   |||
EMBOSS_001    501  ACAGCGCCTGAAGCTGAAAGATGGCGGTCATTATGATGCAGAAGTTAAAA     550
   |||
EMBOSS_001    501  ACAGCGCCTGAAGCTGAAAGATGGCGGTCATTATGATGCAGAAGTTAAAA     550
   |||
EMBOSS_001    551  CCACCTACAAAGCCAAAAAACCAGTTCAGCTGCCAGGTGCCTATAATGTT     600
   |||
EMBOSS_001    551  CCACCTACAAAGCCAAAAAACCAGTTCAGCTGCCAGGTGCCTATAATGTT     600
   |||
EMBOSS_001    601  AATATCAAACGGATATCACCAGCCACAACGAGGATTATACCATTGTTGA     650
   |||
EMBOSS_001    601  AATATCAAACGGATATCACCAGCCACAACGAGGATTATACCATTGTTGA     650
   |||
EMBOSS_001    651  ACAGTATGAACGTGCAGAAGGTGCCATAGTACCGTGGTATGGATGAAC     700
   |||
EMBOSS_001    651  ACAGTATGAACGTGCAGAAGGTGCCATAGTACCGTGGTATGGATGAAC     700
   |||
EMBOSS_001    701  TGTATAAA      708
   |||
EMBOSS_001    701  TGTATAAA      708
   |||
#-----
#-----

```

## 5.1 Result of ELISA screening for selecting Bm-SPN-2 monoclonal antibody

### Making monoclonal antibody against Bm-SPN-2

#### 1st ELISA screen against Bm-SPN-2

Naive mouse serum	Mouse 1 serum	Mouse 2 serum												
serum	polyclonal	polyclonal	1	2	3	4	5	6	7	8	9	10	11	12
A	-0.004	-0.009	0.919	0.876	0.843	0.921								
B	0.003	-0.003	0.904	0.825	0.725	0.765								
C	-0.008	-0.008	0.834	0.792	0.564	0.564								
D	-0.008	-0.007	0.734	0.645	0.436	0.420								
E	-0.001	-0.007	0.591	0.525	0.281	0.265								
F	-0.000	-0.005	0.434	0.360	0.171	0.170								
G	-0.005	-0.007	0.288	0.248	0.093	0.104								
H	-0.002	-0.001	0.001	0.002	-0.003	0.004								

Endpoint  
Lm1 405  
Automix: Off  
Calibrate: On  
Start Read:  
16:06 30/4/15

Wavelength Combination: lLm1  
Mean Temperature: 0.0  
Data Type: Absorbance  
Plate Blank: Used Lm1 = 0.054  
Reader: Emax ROM v--

Control

	1	2	3	4	5	6	7	8	9	10	11	12
A	0.045	0.054	0.049	0.044	0.044	0.046	0.052	0.045	0.053	0.050	0.052	0.054
B	0.060	0.045	0.045	0.055	0.054	0.049	0.044	0.053	0.055	0.045	0.048	0.054
C	0.072	0.047	0.046	0.058	0.050	0.044	0.058	0.082	0.045	0.052	0.048	0.065
D	0.047	0.064	0.050	0.051	0.043	0.064	0.074	0.057	0.058	0.049	0.063	0.056
E	0.076	0.079	0.055	0.077	0.043	0.048	0.049	0.063	0.045	0.042	0.047	0.049
F	0.069	0.048	0.050	0.044	0.044	0.044	0.053	0.063	0.052	0.056	0.046	0.056
G	0.658	0.046	0.046	0.064	0.049	0.046	0.052	0.045	0.047	0.052	0.046	0.062
H	0.061	0.050	0.052	0.037	0.051	0.046	0.064	0.046	0.056	0.070	0.058	0.055

Endpoint  
Lm1 405  
Automix: Off  
Calibrate: On  
Start Read:  
16:12 30/4/15

Wavelength Combination: lLm1  
Mean Temperature: 0.0  
Data Type: Absorbance  
Reader: Emax ROM v--

Plate 4 G1 was chosen for limiting dilution

# 2nd ELISA screen against Bm-SPN-2

2 weeks after the 1st limiting dilution of plate4 G1

	Naive mouse serum		Mouse 1 serum polyclonal				Mouse 2 serum polyclonal				Endpoint			
	1	2	3	4	5	6	7	8	9	10		11	12	
A	-0.003	-0.004	1.062	0.982	1.105	1.058								Lm1 405 Automix: Off Calibrate: On Start Read: 18:03 14/5/15
B	0.011	-0.001	1.024	0.971	1.026	0.965								
C	0.010	-0.005	1.051	0.868	0.857	0.772								
D	0.004	-0.006	0.954	0.935	0.679	0.534								
E	0.009	-0.001	0.832	0.801	0.470	0.332								
F	0.003	-0.003	0.597	0.576	0.267	0.173								
G	-0.001	-0.006	0.415	0.399	0.149	0.105								
H	-0.003	-0.004	0.002	0.000	0.002	0.003								

Control

	1	2	3	4	5	6	7	8	9	10	11	12	Endpoint
A	0.918	1.049	1.057	1.077	0.990	0.501	0.620	0.381	0.205	0.059	0.057	0.051	Lm1 405 Automix: Off Calibrate: On Start Read: 18:08 14/5/15
B	0.993	1.040	1.107	1.133	1.042	0.759	0.208	0.092	0.063	0.254	0.055	0.123	
C	1.082	1.111	1.089	0.977	0.756	0.275	0.367	0.762	0.057	0.050	0.049	0.050	
D	1.188	1.015	0.678	0.256	0.373	0.568	0.100	0.057	0.053	0.451	0.050	0.048	
E	1.175	1.094	0.749	0.662	0.152	0.070	0.058	0.061	0.048	0.045	0.047	0.053	
F	1.058	0.938	0.496	0.118	0.072	0.057	0.055	0.049	0.047	0.046	0.047	0.050	
G	0.477	0.168	0.285	0.079	0.059	0.054	0.050	0.049	0.049	0.046	0.049	0.047	
H	0.308	0.215	0.070	0.065	0.055	0.054	0.052	0.047	0.049	0.043	0.048	0.050	

A7  
B6  
B10  
B12  
C8  
D6  
D10  
E4

were chosen for 2nd Limiting dilution

dilution plate 4G1

## 3rd screen against Bm-SPN-2

	Naive mouse serum		Mouse 1 serum polyclonal				Mouse 2 serum polyclonal				Endpoint		
	1	2	3	4	5	6	7	8	9	10		11	12
A	-0.012	-0.013	0.744	0.679	0.723	0.718							Lm1 405 Automix: Off Calibrate: On Start Read: 16:51 28/5/15
B	-0.001	-0.002	0.657	0.655	0.603	0.587							
C	-0.008	0.002	0.606	0.649	0.453	0.470							
D	-0.008	-0.013	0.578	0.546	0.386	0.337							
E	0.006	-0.005	0.454	0.436	0.209	0.246							
F	-0.009	-0.009	0.520	0.319	0.139	0.154							
G	-0.010	0.003	0.218	0.220	0.070	0.094							
H	0.012	-0.010	-0.007	0.003	-0.003	0.006							

Control

	1	2	3	4	5	6	7	8	9	10	11	12	Endpoint
A	0.505	0.599	0.632	0.322	0.628	0.106	0.057	0.476	0.055	0.050	0.051	0.050	Lm1 405 Automix: Off Calibrate: On Start Read: 17:05 28/5/15
B	0.673	0.716	0.770	0.745	0.691	0.440	0.049	0.457	0.048	0.050	0.053	0.055	
C	0.726	0.711	0.694	0.694	0.425	0.048	0.046	0.049	0.053	0.057	0.050	0.050	
D	0.587	0.786	0.427	0.319	0.060	0.051	0.044	0.048	0.018	0.053	0.047	0.049	
E	0.395	0.443	0.055	0.049	0.048	0.050	0.047	0.046	0.044	0.045	0.047	0.052	
F	0.065	0.098	0.052	0.047	0.048	0.045	0.043	0.045	0.045	0.046	0.049	0.050	
G	0.058	0.544	0.046	0.045	0.045	0.046	0.044	0.048	0.047	0.050	0.047	0.045	
H	0.052	0.047	0.048	0.044	0.444	0.045	0.045	0.046	0.045	0.042	0.047	0.046	

C8

	1	2	3	4	5	6	7	8	9	10	11	12	Endpoint
A	0.573	0.750	0.642	0.624	0.647	0.243	0.272	0.046	0.037	0.046	0.046	0.046	Lm1 405 Automix: Off Calibrate: On Start Read: 17:08 28/5/15
B	0.701	0.700	0.613	0.062	0.150	0.439	0.095	0.047	0.048	0.046	0.046	0.049	
C	0.713	0.730	0.744	0.058	0.053	0.053	0.048	0.047	0.045	0.047	0.050	0.047	
D	0.653	0.772	0.592	0.051	0.050	0.051	0.044	0.050	0.047	0.050	0.051	0.049	
E	0.223	0.059	0.055	0.045	0.052	0.050	0.049	0.045	0.044	0.049	0.047	0.046	
F	0.087	0.710	0.053	0.046	0.049	0.047	0.044	0.045	0.045	0.044	0.044	0.048	
G	0.254	0.048	0.053	0.051	0.544	0.048	0.045	0.047	0.047	0.046	0.044	0.046	
H	0.065	0.046	0.051	0.044	0.057	0.046	0.045	0.046	0.046	0.042	0.044	0.049	

B6

	1	2	3	4	5	6	7	8	9	10	11	12	Endpoint
A	0.515	0.695	0.419	0.398	0.122	0.050	0.059	0.047	0.046	0.048	0.048	0.046	Lm1 405 Automix: Off Calibrate: On Start Read: 17:00 28/5/15
B	0.618	0.746	0.381	0.075	0.517	0.045	0.045	0.046	0.045	0.043	0.047	0.048	
C	0.253	0.056	0.052	0.062	0.047	0.045	0.042	0.044	0.042	0.042	0.043	0.047	
D	0.447	0.540	0.119	0.202	0.046	0.047	0.047	0.042	0.045	0.043	0.046	0.044	
E	0.147	0.050	0.047	0.042	0.042	0.045	0.046	0.042	0.044	0.042	0.043	0.045	
F	0.048	0.046	0.045	0.046	0.043	0.044	0.041	0.042	0.042	0.042	0.043	0.044	
G	0.045	0.044	0.044	0.044	0.042	0.043	0.042	0.046	0.045	0.045	0.043	0.045	
H	0.073	0.042	0.046	0.042	0.041	0.043	0.043	0.042	0.044	0.040	0.045	0.049	

D10

	1	2	3	4	5	6	7	8	9	10	11	12	Endpoint
A	0.267	0.534	0.462	0.069	0.082	0.115	0.051	0.052	0.048	0.053	0.050	0.044	Lm1 405 Automix: Off Calibrate: On Start Read: 17:05 28/5/15
B	0.367	0.694	0.607	0.402	0.566	0.051	0.046	0.046	0.046	0.047	0.046	0.050	
C	0.493	0.414	0.059	0.109	0.046	0.045	0.045	0.045	0.044	0.044	0.054	0.052	
D	0.193	0.053	0.049	0.047	0.046	0.046	0.042	0.045	0.046	0.046	0.049	0.061	
E	0.056	0.051	0.047	0.044	0.045	0.049	0.046	0.046	0.047	0.055	0.053	0.054	
F	0.051	0.052	0.044	0.045	0.045	0.389	0.048	0.047	0.047	0.046	0.064	0.060	
G	0.051	0.048	0.044	0.044	0.045	0.052	0.050	0.049	0.052	0.070	0.055	0.057	
H	0.047	0.049	0.047	0.046	0.055	0.048	0.054	0.062	0.062	0.050	0.061	0.062	

E4

	1	2	3	4	5	6	7	8	9	10	11	12	Endpoint
A	0.377	0.517	0.701	0.221	0.519	0.154	0.078	0.050	0.056	0.059	0.050	0.050	Lm1 405 Automix: Off Calibrate: On Start Read: 17:11 28/5/15
B	0.325	0.591	0.690	0.088	0.117	0.108	0.073	0.089	0.076	0.074	0.072	0.053	
C	0.099	0.099	0.355	0.056	0.057	0.050	0.051	0.072	0.094	0.056	0.067	0.074	
D	0.111	0.060	0.054	0.047	0.047	0.048	0.046	0.047	0.058	0.058	0.066	0.054	
E	0.371	0.502	0.358	0.048	0.048	0.051	0.049	0.047	0.041	0.055	0.062	0.052	
F	0.190	0.056	0.048	0.047	0.051	0.059	0.050	0.053	0.049	0.046	0.063	0.047	
G	0.345	0.047	0.045	0.045	0.046	0.060	0.060	0.052	0.066	0.054	0.069	0.057	
H	0.054	0.049	0.050	0.045	0.047	0.080	0.079	0.054	0.056	0.046	0.058	0.051	

A7

	1	2	3	4	5	6	7	8	9	10	11	12	Endpoint
A	0.472	0.601	0.191	0.351	0.067	0.052	0.136	0.050	0.061	0.053	0.046	0.044	Lm1 405 Automix: Off Calibrate: On Start Read: 17:08 28/5/15
B	0.553	0.295	0.418	0.400	0.117	0.050	0.049	0.047	0.052	0.054	0.045	0.048	
C	0.577	0.074	0.302	0.042	0.049	0.053	0.050	0.048	0.054	0.051	0.046	0.048	
D	0.538	0.061	0.174	0.132	0.054	0.052	0.052	0.047	0.052	0.050	0.050	0.047	
E	0.425	0.061	0.051	0.061	0.050	0.059	0.052	0.052	0.048	0.051	0.046	0.045	
F	0.051	0.053	0.209	0.061	0.048	0.054	0.055	0.047	0.054	0.044	0.047	0.046	
G	0.054	0.050	0.044	0.054	0.058	0.046	0.055	0.049	0.057	0.047			

## Final ELISA against Bm-SPN-2 of the hybridoma candidate cells

	1	2	3	4	5	6	7	8	9	10	11	12
A	-0.014	-0.013	0.595	0.506	0.548	0.545		0.091	0.223	0.295		
B	-0.016	-0.019	0.467	0.453	0.383	0.394		0.172	0.228	0.032		
C	-0.019	-0.017	0.415	0.358	0.281	0.278		0.031	0.228	0.305		
D	-0.014	-0.017	0.331	0.297	0.208	0.178		0.275	0.253	0.090		
E	-0.016	-0.016	0.199	0.196	0.093	0.096						
F	-0.016	-0.017	0.144	0.146	0.048	0.049		0.158	0.223	0.122		
G	-0.017	-0.018	0.085	0.076	0.019	0.021		0.050	-0.008	0.014		
H	-0.013	-0.008	-0.012	0.006	-0.013	0.040		-0.006	0.037	0.029		

Endpoint
Lm1 405
Automix: Off
Calibrate: On

Start Read:  
18:48 11/6/15

Control

21 candidates

10 from 21 candidates were chosen for verification and purification

## 5.2 Monoclonal antibody candidate purification trace.

